2012

c-ABL AND ARG DRIVE CANCER CHEMORESISTANCE VIA ACTIVATION OF MULTIPLE SIGNALING PATHWAYS

Jonathan Thomas Sims
University of Kentucky, jonathan.t.sims@gmail.com

STUDENT AGREEMENT:

I represent that my thesis or dissertation and abstract are my original work. Proper attribution has been given to all outside sources. I understand that I am solely responsible for obtaining any needed copyright permissions. I have obtained and attached hereto needed written permission statements(s) from the owner(s) of each third-party copyrighted matter to be included in my work, allowing electronic distribution (if such use is not permitted by the fair use doctrine).

I hereby grant to The University of Kentucky and its agents the non-exclusive license to archive and make accessible my work in whole or in part in all forms of media, now or hereafter known. I agree that the document mentioned above may be made available immediately for worldwide access unless a preapproved embargo applies.

I retain all other ownership rights to the copyright of my work. I also retain the right to use in future works (such as articles or books) all or part of my work. I understand that I am free to register the copyright to my work.

REVIEW, APPROVAL AND ACCEPTANCE

The document mentioned above has been reviewed and accepted by the student's advisor, on behalf of the advisory committee, and by the Director of Graduate Studies (DGS), on behalf of the program; we verify that this is the final, approved version of the student's dissertation including all changes required by the advisory committee. The undersigned agree to abide by the statements above.

Jonathan Thomas Sims, Student

Dr. Rina Plattner, Major Professor

Dr. Robert Hadley, Director of Graduate Studies

ABSTRACT OF DISSERTATION

Jonathan Thomas Sims

The Graduate School

University of Kentucky

2012

c-ABL AND ARG DRIVE CANCER CHEMORESISTANCE VIA ACTIVATION OF MULTIPLE SIGNALING PATHWAYS

ABSTRACT OF DISSERTATION

A dissertation submitted in partial fulfillment of the requirements for the degree of Doctor of Philosophy in the College of Medicine at the University of Kentucky

By

Jonathan Thomas Sims

Director: Dr. Rina Plattner, Associate Professor

Department of Molecular and Biomedical Pharmacology

Lexington, KY

2012

c-ABL AND ARG DRIVE CANCER CHEMORESISTANCE VIA ACTIVATION OF MULTIPLE SIGNALING PATHWAYS

ABSTRACT OF DISSERTATION

A dissertation submitted in partial fulfillment of the requirements for the degree of Doctor of Philosophy in the College of Medicine at the University of Kentucky

By

Jonathan Thomas Sims

Co-Director: Dr. David Kaetzel, Professor

Department of Molecular and Biomedical Pharmacology

Lexington, KY

2012

ABSTRACT OF DISSERTATION

c-ABL AND ARG DRIVE CANCER CHEMORESISTANCE VIA ACTIVATION OF MULTIPLE SIGNALING PATHWAYS

Despite 35 years of clinical trials, there has been little improvement in one-year survival rates with any chemotherapeutic regimen for the treatment of metastatic melanoma due to resistance to all known agents. Regardless of advances in detection and prevention, diagnosis of metastatic disease remains a death sentence. Resistance mechanisms, including aberrant kinase signaling and drug transport pumps, indicate a need for identification of other therapeutic targets that impinge upon multiple signaling pathways. The Abl family of non-receptor tyrosine kinases (c-Abl, Arg) has been indicted as a causative force in leukemia for more than three decades; however, their role in solid tumors has only recently been described. We first demonstrated that activated Abl family kinases promote breast cancer development and progression, and recently identified them to be novel therapeutic targets in metastatic melanoma cells by demonstrating that they promote proliferation, survival, invasion, and metastasis. We now present evidence that inhibitors of Abl family kinases abrogate resistance to a number of commonly used chemotherapeutics (i.e., 5-fluorouracil, cisplatin, paclitaxel, camptothecin) in a panel of breast cancer cells. We proceed to show that inhibitors of Abl family kinases, likewise, sensitize both breast cancer and melanoma cells to doxorubicin by blocking cell proliferation and dramatically inducing apoptosis. These findings were extended to advanced multi-drug resistant melanoma cells, in which we show for the first time that c-Abl promotes expression of the drug transporter, ABCB1, during acquired resistance, and drugs that inhibit c-Abl/Arg prevent ABCB1 expression and function. Moreover, c-Abl/Arg also promote acquired chemoresistance independent of ABCB1 by modulating multiple survival pathways. We demonstrate that c-Abl/Arg promote chemoresistance by upregulating STAT3, preventing doxorubicin-mediated conversion of NF-κB into a transcriptional repressor, activating an HSP27/p38/Akt survival pathway, and modulating ERK signaling. Therefore, c-Abl/Arg promote chemoresistance in highly resistant melanoma cells by impinging on drug transporter and cell survival pathways. Taken together, these data indicate that c-Abl/Arg inhibitors are likely to reverse acquired resistance in metastatic melanomas harboring activated c-Abl/Arg, and thus, may be effective in a combination regimen.

Keywords: c-Abl, Arg, chemoresistance, breast cancer, melanoma

Jonathan Thomas Sims
Student's signature

4/17/12
Date

c-ABL AND ARG DRIVE CANCER CHEMORESISTANCE VIA ACTIVATION OF MULTIPLE SIGNALING PATHWAYS

By

Jonathan Thomas Sims

Rina Plattner, Ph.D.
Director of Dissertation

Robert Hadley, Ph.D.
Director of Graduate Studies

4/17/12
Date

c-ABL AND ARG DRIVE CANCER CHEMORESISTANCE VIA ACTIVATION OF MULTIPLE SIGNALING PATHWAYS

By

Jonathan Thomas Sims

David Kaetzel, Ph.D.
Co-Director of Dissertation

Robert Hadley, Ph.D.
Director of Graduate Studies

4/17/12
Date

RULES FOR THE USE OF DISSERTATIONS

Unpublished dissertations submitted for the Doctor's degree and deposited in the University of Kentucky Library are as a rule open for inspection, but are to be used only with due regard to the rights of the authors. Bibliographical references may be noted, but quotations or summaries of parts may be published only with the permission of the author, and with the usual scholarly acknowledgments.

Extensive copying or publication of the dissertation in whole or in part also requires the consent of the Dean of the Graduate School of the University of Kentucky.

A library that borrows this dissertation for use by its patrons is expected to secure the signature of each user.

Name	Date

DISSERTATION

Jonathan Thomas Sims

The Graduate School

University of Kentucky

2012

c-ABL AND ARG DRIVE CANCER CHEMORESISTANCE VIA ACTIVATION OF MULTIPLE SIGNALING PATHWAYS

DISSERTATION

A dissertation submitted in partial fulfillment of the
requirements for the degree of Doctor of Philosophy in the
College of Medicine at the University of Kentucky

By

Jonathan Thomas Sims

Director: Dr. Rina Plattner, Associate Professor

Department of Molecular and Biomedical Pharmacology

Lexington, KY

2012

Dedicated to Amy, my Dad, Mom, and Rebecca

ACKNOWLEDGEMENTS

I would like to especially thank my mentor, Dr. Rina Plattner, for her guidance throughout my graduate career. I would like to thank my committee members (Dr. David Kaetzel, Dr. Rolf Craven, Dr. Vivek Rangnekar, and my outside examiner, Dr. Kenneth Campbell) for their knowledgeable insights and suggestions related to this work. I would like to thank all present and former members of the Plattner lab for their contributions, both intellectually in lab meetings and hands-on with experiments, and their support for my project: Dr. Divyamani Srinivasan, Dr. Sayan Mitra, Sourik Ganguly, Leann Fiore, Woodrow Friend, Aruna Visavadiya, and Holly Bennett. I especially want to recognize those who contributed to my scientific publications: most importantly, Dr. Rina Plattner, for insights and formative ideas related to the entirety of this work; Sourik Ganguly, Leann Fiore, Eun-sil Park, and Chris Holler, for work referenced in chapter 2; Holly Bennett and Jessica Tepe for work referenced in chapter 3; and Woodrow Friend, for work referenced in chapters 5 and 6.

Table of Contents

List of Tables

List of Figures

CHAPTER ONE
INTRODUCTION

1.1 Abelson family kinases

1.1.1 Regulation

The Abelson family of non-receptor tyrosine kinases (Abl family kinases) includes two proteins, c-Abl and Arg (Abl-Related-Gene), which are encoded by *Abl1* and *Abl2* genes, respectively (Figure 1.1A) [1]. Both genes can give rise to one of two alternatively spliced isoforms (i.e., 1a or 1b), with the 1a isoforms lacking a myristic acid residue at their N(amino)-termini [2]. c-Abl and Arg are highly homologous in their N-termini, where they contain SH3, SH2, and kinase domains, but are more divergent in their C(carboxy)-termini (Figure 1.1A) [1]. Abl family kinases are activated via phosphorylation of tyrosine residue Y245, Y89, and Y276, which are located in the SH2/kinase domain interlinker region, and Y412, located in the activation loop [3-5].

c-Abl and Arg are ubiquitously expressed in all tissues, but these two proteins vary in their subcellular localization [4]. Whereas most tyrosine kinases are predominantly localized near the plasma membrane, c-Abl uniquely possesses three nuclear localization signals in its C-terminus, allowing it to also shuttle between the cytoplasm and nucleus (Figure 1.1A) [6-8]. Cytoplasmic and membrane-localized c-Abl and Arg respond to growth factor signals, promoting cell proliferation and motility [3, 9]. Upon activation in the nucleus, c-Abl can promote genotoxic stress-induced apoptosis [10]. Another unique property of Abl family kinases, relative to most other tyrosine kinases, is the ability to directly bind cytoskeletal components and influence and respond to changes in cell movement and shape [11].

Autoinhibition of c-Abl/Arg prevents aberrant activation of these kinases, and is regulated via intramolecular interactions between myristic acid residues on the N-termini and the kinase domains of c-Abl and Arg, as well as the interaction of SH3 domains and proline residues within the interlinker region [1, 12, 13]. In addition to autoinhibition, several molecules have been discovered to act as inhibitors of Abl family kinases, including RB, PRDX1, PIP_2, AAP1, Fus1, and PCNA. RB (retinoblastoma protein) binds and prevents c-Abl-mediated cell cycle regulation and activation of transcription [14]. PRDX1 (Peroxiredoxin 1) inhibits c-Abl kinase activity via interaction with its SH3 domain [15]. Autoinhibition of membrane-bound c-Abl/Arg is disrupted due to insertion of the myristic acid tail into the phospholipid bilayer, and in these instances, PIP_2 prevents

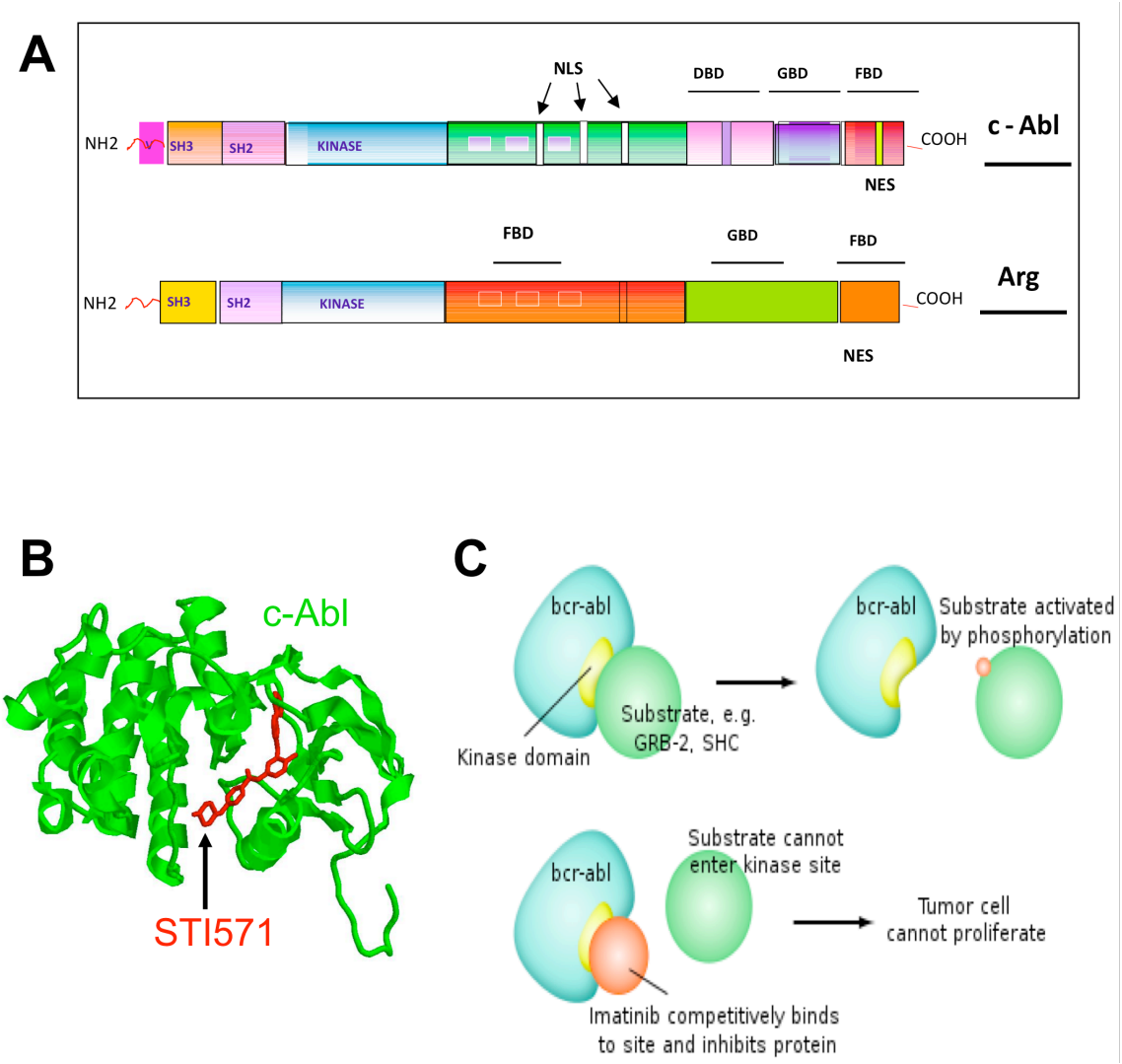

Figure 1.1. c-Abl and Arg structure and function. (A) c-Abl and Arg possess very high homology in their N-terminal region, due to highly conserved SH3, SH2, and kinase domains. The C-terminal region is variable since c-Abl, but not Arg, possesses a DNA binding domain (DBD) and three nuclear localization signals (NLS). Both contain an F-actin binding domain (FBD) and G-actin binding domain (GBD). Figure provided by Dr. Plattner. Adapted from Pendergast, Adv Cancer Research (2002);85:51-100. **(B)** Protein crystallography demonstrating the interaction of STI571 with the kinase domain of c-Abl. STI571 binds the kinase domain of Abl family kinases and stabilizes the inactive confirmation. Figure adapted from Nagar, et al, Cancer Research (2002) Aug 1;62(15):4236-43. **(C)** STI571 (imatinib) binds the kinase domain of Abl family kinases (BCR-Abl is shown), preventing substrate binding and subsequent phosphorylation. Figure attributed to Sodium at the English language Wikipedia.

kinase activity by directly binding to the kinase domain [16, 17]. AAP1 (Abl-associated protein 1) binds the SH3 domain of c-Abl, preventing substrate phosphorylation, and, importantly, loss of AAP1 correlates with increased expression of oncogenic forms of c-Abl [18]. Fus1 is a negative regulator of Abl family kinases, preventing their full activation and subsequent tumorigenic signaling [19]. PCNA (proliferating cell nuclear antigen) promotes the degradation of c-Abl in response to genotoxic stress, thereby attenuating the pro-apoptotic function of nuclear c-Abl [20]. Importantly, the loss of regulation of Abl family kinase activity, either by disruption of autoinhibition or disruption of inhibitory interactions with other proteins, is directly correlated with disease progression, both in hematopoietic cancer and solid tumors.

1.1.2 Role in hematopoietic cancer

Abl family kinases (c-Abl, Arg) were first characterized for their involvement in human leukemia, where a chromosomal translocation event causes the translocation of the *Abl1* gene next to the *BCR* gene [21]. This results in a constitutively active BCR-Abl fusion protein that drives the development of chronic myelogenous leukemia (CML) [21]. BCR-Abl$^+$ CML cells possess an increased capability to survive, proliferate, migrate, and invade [22, 23]. This chromosomal abnormality was identified to be a reciprocal translocation between chromosomes 9 and 22, resulting in an elongated chromosome 9 and a severely truncated chromosome 22 [24]. 95% of CML patients were found to harbor this abnormality in chromosome 22, which was referred to as the Philadelphia chromosome due to the discovery of the phenotype by scientists at the University of Pennsylvania and Fox Chase Cancer Center (Philadelphia, PA) [24]. Depending on the specific site where the chromosomal fusion occurs, three variants of the BCR-Abl fusion protein have been shown to be of clinical importance. These variants, p190, p210, and p230, have been shown to promote specific forms of hematopoietic disease: acute lymphoblastic leukemia (ALL), CML, and chronic neutrophilic leukemia (CNL), respectively [25]. In addition, novel *FOXP1-Abl1*, *SNX2-Abl1*, and *NUP214-Abl1* fusion genes have recently been observed in a small cohort of ALL patients [5, 26]. Other leukemogenic c-Abl and Arg fusion genes arise due to translocations with the *ETV6*, *EML1*, *RCSD1*, and *Tel* genes in a number of leukemias [5, 27-29]. In summary, constitutively active, mutant forms of Abl family kinases, arising from chromosomal translocations, drive malignant transformation in a variety of leukemias.

STI571 (Gleevec; imatinib) was developed to specifically inhibit BCR-Abl, and is FDA-approved to treat CML [30]. STI571 competitively binds the kinase domain of active Abl family kinases, preventing subsequent phosphorylation of target substrates (Figure 1.1B, C) [30]. Nilotinib, a second-generation c-Abl/Arg inhibitor, has shown effectiveness in CML patients that develop resistance to STI571 [31]. In addition to inhibiting constitutively active Abl family kinases (i.e., BCR-Abl), accumulating evidence has revealed other cellular targets for nilotinib and STI571, including c-Abl/Arg, DDR1 (Discoidin domain receptor 1), c-Kit, PDGFR, and CSF1R (colony stimulating factor 1 receptor) [32-36].

1.1.3 Role in solid tumors

We showed that endogenous Abl family kinases are activated by growth factors (PDGF, platelet-derived growth factor; EGF, epidermal growth factor receptor), and promote proliferation, membrane ruffling, and migration in fibroblasts [16, 37]. Significantly, our lab recently demonstrated that Abl family kinases are also activated downstream of deregulated growth factor receptors (PDGFR, EGFR, IGF-1R, ErbB2/Her2) and Src family kinases in invasive breast cancer cells, and promote invasion, survival in response to nutrient deprivation, and proliferation [38, 39]. We demonstrated that PDGFR-mediated activation of Abl family kinases requires both PLC-γ1 and Src, and that Src can independently activate c-Abl/Arg [37, 40]. Our lab was first to demonstrate that activated Abl family kinases drive the proliferation, invasion, cell survival, and anchorage-independent growth of aggressive breast cancer cells [38, 39]; however, others have demonstrated a role for activated Abl family kinases in breast cancer cells as well, implicating c-Abl/Arg in Src-mediated transformation and invadopodia formation [41-43].

We also demonstrated that activation of Abl family kinases in glioblastoma occurs in a PDGFR-dependent manner [44]. Activated c-Abl and Arg have also been implicated in non-small cell lung cancer cells, and drive progression of gastric carcinoma cells in response to c-Met [19, 45]. c-Abl is strongly expressed in chondrosarcoma and liposarcoma, and is coexpressed with EGFR in colon cancer specimens, but kinase activity has not been measured in these cancer types [46, 47]. Recent work has also demonstrated a potential role of Abl family kinases in prostate cancer cell motility [48, 49]. We also were the first to demonstrate that c-Abl and Arg are highly activated in invasive melanoma cells (Figure 1.2), and promote proliferation, invasion, and

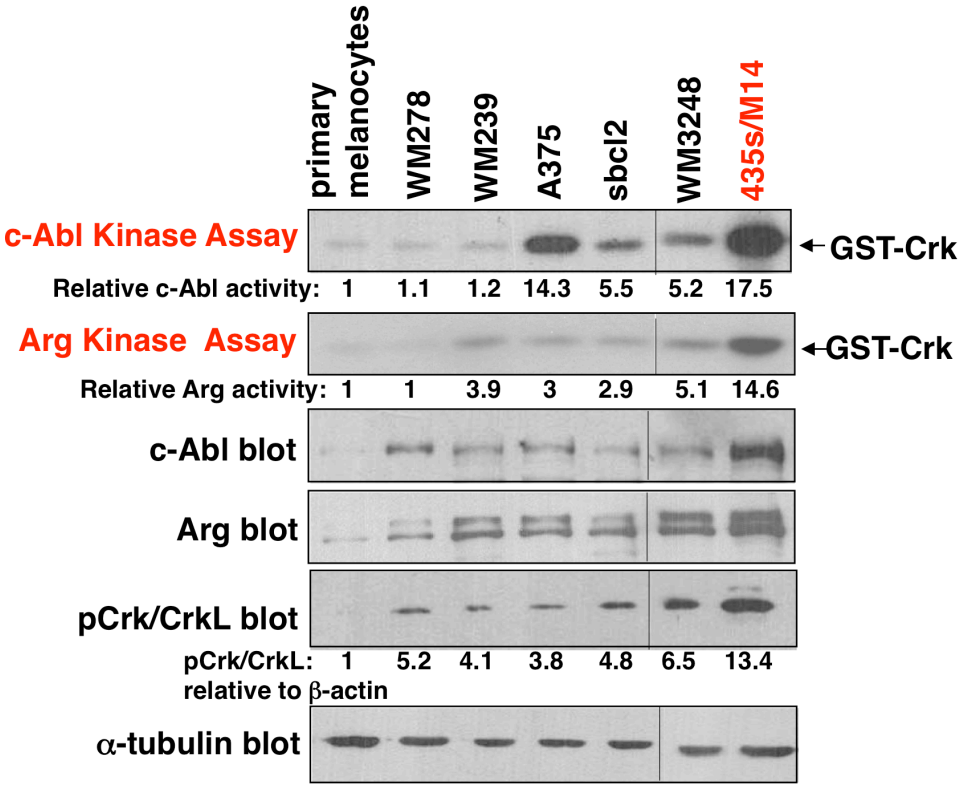

Figure 1.2. c-Abl and Arg are highly activated in melanoma cells. Melanoma cells were serum-starved, lysed, and c-Abl and Arg were immunoprecipitated. Kinase activities were determined by *in vitro* kinase assay using GST-Crk as the substrate. Lysates were also blotted with indicated antibodies. Figure adapted from Ganguly, et al, Oncogene (2011) Sep 5. doi: 10.1038/onc.2011.361.

metastasis of melanoma cells [50]. Taken together, these data explicitly demonstrate the integral role of Abl family kinases in many facets of cancer progression to metastasis.

1.2 Deregulated proliferation and survival pathways in cancer

1.2.1 STAT3 pathway

The STAT (signal transducer and activator of transcription) family of transcription factors is composed of seven members that possess a DNA binding domain, SH2 domain, and a C-terminal transactivation domain [51]. The transcription factor, STAT3, is primarily activated via phosphorylation downstream of cytokines and receptor and non-receptor tyrosine kinases, and is responsible for transferring signals from the plasma membrane to the nucleus [52]. Upon phosphorylation on tyrosine residue Y705, STAT3 dimerizes, translocates to the nucleus, binds specific sites in a gene's promoter region, and induces transcription of genes that control cell development, survival, and proliferation (Figure 1.3) [51, 53].

STAT3 activation has been observed in numerous human cancers, including breast cancer and melanoma, and promotes cellular transformation *in vitro* [51]. STAT3 mediates survival by increasing expression of anti-apoptotic proteins (i.e., Bcl-2 family members), and is crucial for G1→S cell cycle transition via activation of cyclin D1/cyclin-dependent kinase 4 (cdk4) complexes, and inactivation of p27 [54-56]. Non-receptor tyrosine kinases, such as Src and constitutively active Abl family kinases, have been shown to promote STAT3 phosphorylation [53]. Importantly, we observed that Abl family kinases promote STAT3 phosphorylation in breast cancer and melanoma cells, and promote melanoma invasion in a STAT3-dependent manner [39, 50]. STAT3 has been linked to chemoresistance of tumor cells, and downregulation of this transcription factor sensitizes cells to undergo chemotherapy-induced apoptosis [51].

1.2.2 PI3K/Akt pathway

The PI3K (phosphoinositide 3-kinase)/Akt pathway is commonly activated in an abundance of tumor types [57]. PI3K/Akt signaling is activated by growth factor receptors and G protein-coupled receptors (GPCR) and promotes cell proliferation and survival [58]. After receptor-mediated activation, PI3K phosphorylates the membrane phospholipid PIP_2 (phosphatidylinositol (3,4)-bisphosphate), generating PIP_3 (phosphatidylinositol (3,4,5)-triphosphate), and PTEN negatively regulates this process by dephosphorylating PIP_3 [59, 60]. PDK1 localizes to the membrane, where upon

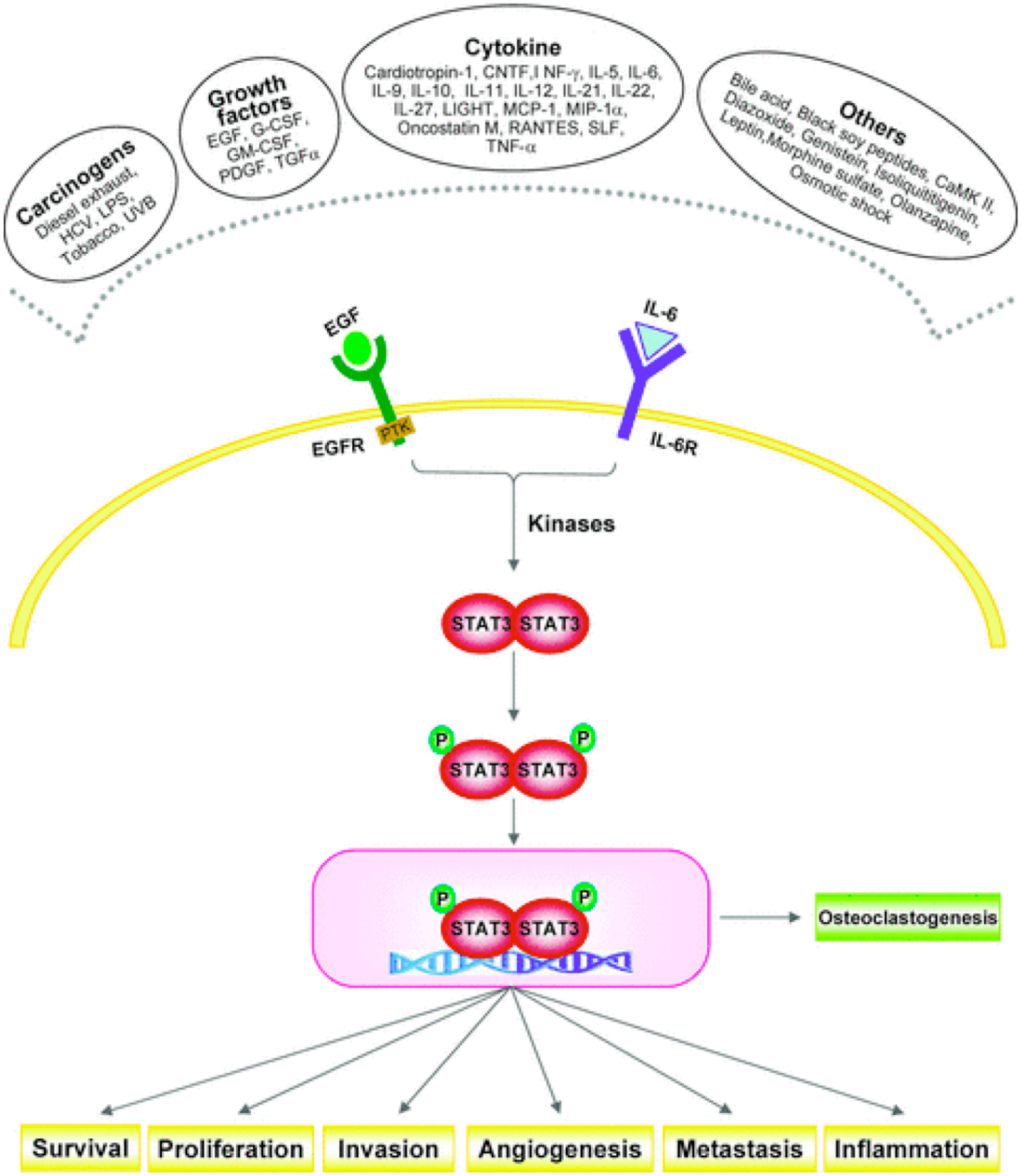

Figure 1.3. STAT3 signaling in cancer cells. STAT3 is activated by growth factor receptors (e.g., EGFR) or cytokines (e.g., IL-6R) in response to a wide array of stimuli. Phosphorylated STAT3 localizes to the nucleus and binds in a site-specific manner to the promoter regions of genes responsible for promoting many processes involved in cancer progression. Figure adapted from Aggarwal, et al., Ann NY Acad Sci **(**2009) Aug;1171:59-76.

activation by PIP_3, it phosphorylates Akt on its T308 residue [61]. In order to fully activate Akt, phosphorylation on a second residue, S473, is also required. Akt is activated by a diverse number of stimuli leading to enhanced cell growth (Figure 1.4) [58, 62]. In response to growth factors, Akt is activated by PDK1, leading to phosphorylation of T308, and mTORC2, which acts as a PDK2 and phosphorylates S473. In response to DNA damage, DNA-PK acts as a PDK2 and activates Akt signaling, and, in certain cell types, in response to cell stress, such as DNA damage and reactive oxygen species, Akt is activated by phosphorylation of S473 via a complex comprised of HSP27, p38, and MK2 [62-68]. HSP27 expression is induced by cell stress and it regulates cell survival in response to cell stress, resulting in cancer cell progression. HSP27 is upregulated transcriptionally by STAT3 in response to stress, and further regulated by p38 [69]. HSP27 expression is crucial for Akt activation in response to stress due to its scaffolding function, and disruption of HSP27/Akt interaction induces apoptosis in neutrophils [64]. Activation of the PI3K/Akt pathway promotes cell proliferation and survival by driving cell cycle progression via cyclin D1 and c-Myc, and upregulating a variety of anti-apoptotic proteins [60, 70-72].

1.2.3 NF-κB pathway

The NF-κB pathway is known to promote cancer progression, and various components of this pathway are overexpressed in advanced cancer types [73, 74]. The NF-κB pathway consists of numerous binding partners (i.e., p65/RelA, RelB, c-Rel, p50, p52) that share a common Rel homology domain, with p65/RelA as the major component of most NF-κB-mediated signaling events [75]. Canonical NF-κB activation occurs in response to growth factors and cytokine stimulation, and this results in IKKβ phosphorylation of the NF-κB inhibitor, IκBα (Figure 1.5) [76]. This promotes IκB degredation, allowing p65/RelA to localize to the nucleus, and allows translocation of the NF-κB dimer (i.e., p65-p50) to the nucleus [76]. NF-κB dimers are phosphorylated on two serine residues (S536 and S276) by IKK1/2 and PKA, respectively [77], and can be further modified via acetylation by histone acetyltransferases (HATs) such as p300, to promote interaction with various coactivators [76, 78]. Once in the nucleus, NF-κB binds DNA binding sites and promotes transcription of target genes, many of which are responsible for cancer cell survival [77]. Non-canonical activation of NF-κB signaling

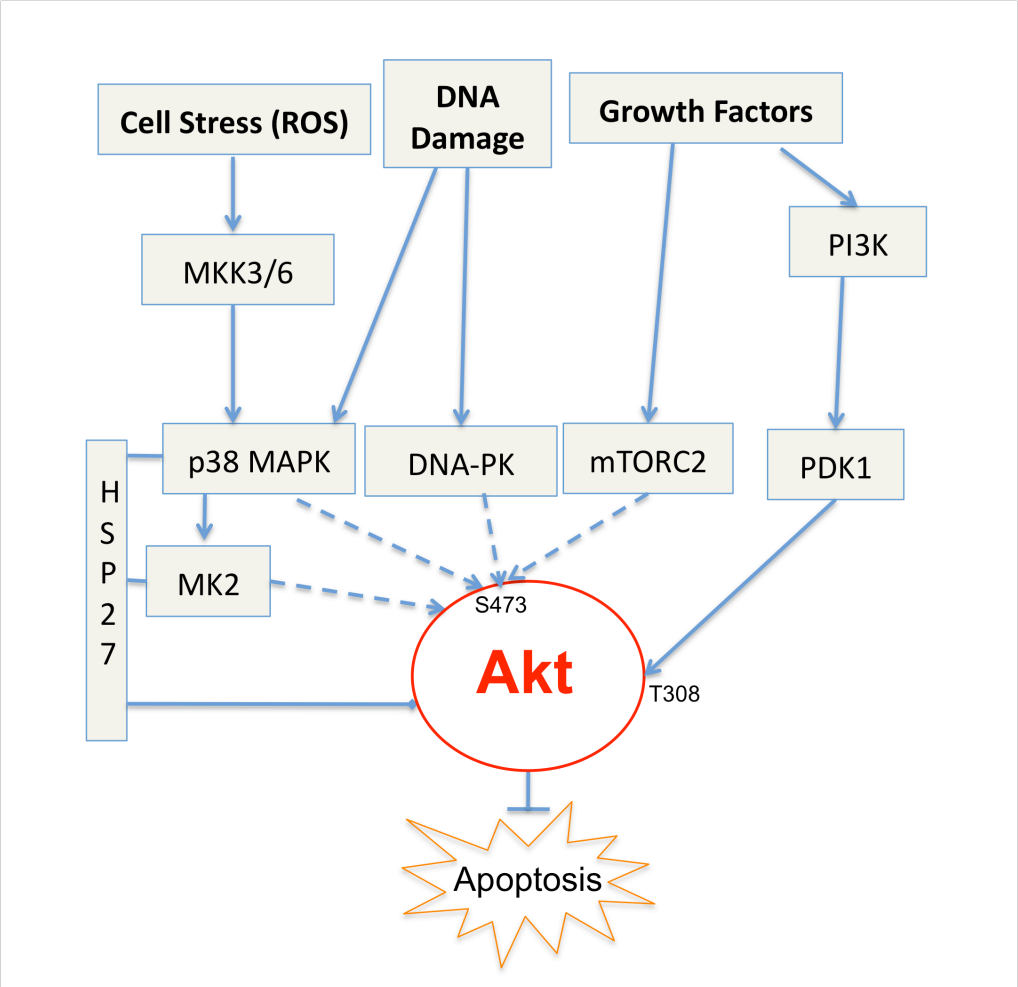

Figure 1.4. Akt promotes cell survival following activation by diverse stimuli. Activation of Akt signaling is dependent on PI3K/PDK1-dependent phosphorylation of T308, as well as phosphorylation of S473. The protein responsible for phosphorylating S473 varies depending on the stimulus (i.e., growth factor stimulation, DNA damage, or cell stress resulting from deleterious cellular insults, such as reactive oxygen species (ROS)). Figure references data from: Rane, et al, J Biol Chem (2001) Feb 2;276(5):3517-23; Rane, et al, J Biol Chem (2003) Jul 25;278(30):27828-35; Zheng, et al, J Biol Chem (2006) Dec 1;281(48):37215-26; Wu, et al, J Biol Chem (2007) Jul 27;282(30):21598-608; Shi, et al, Mol Cell Biol (2011) May;31(10):1938-48; Dowling, et al, Biochim Biophys Acta (2010) Mar;1804(3):433-9; Bozulic, et al, Mol Cell (2008) Apr 25;30(2):203-13.

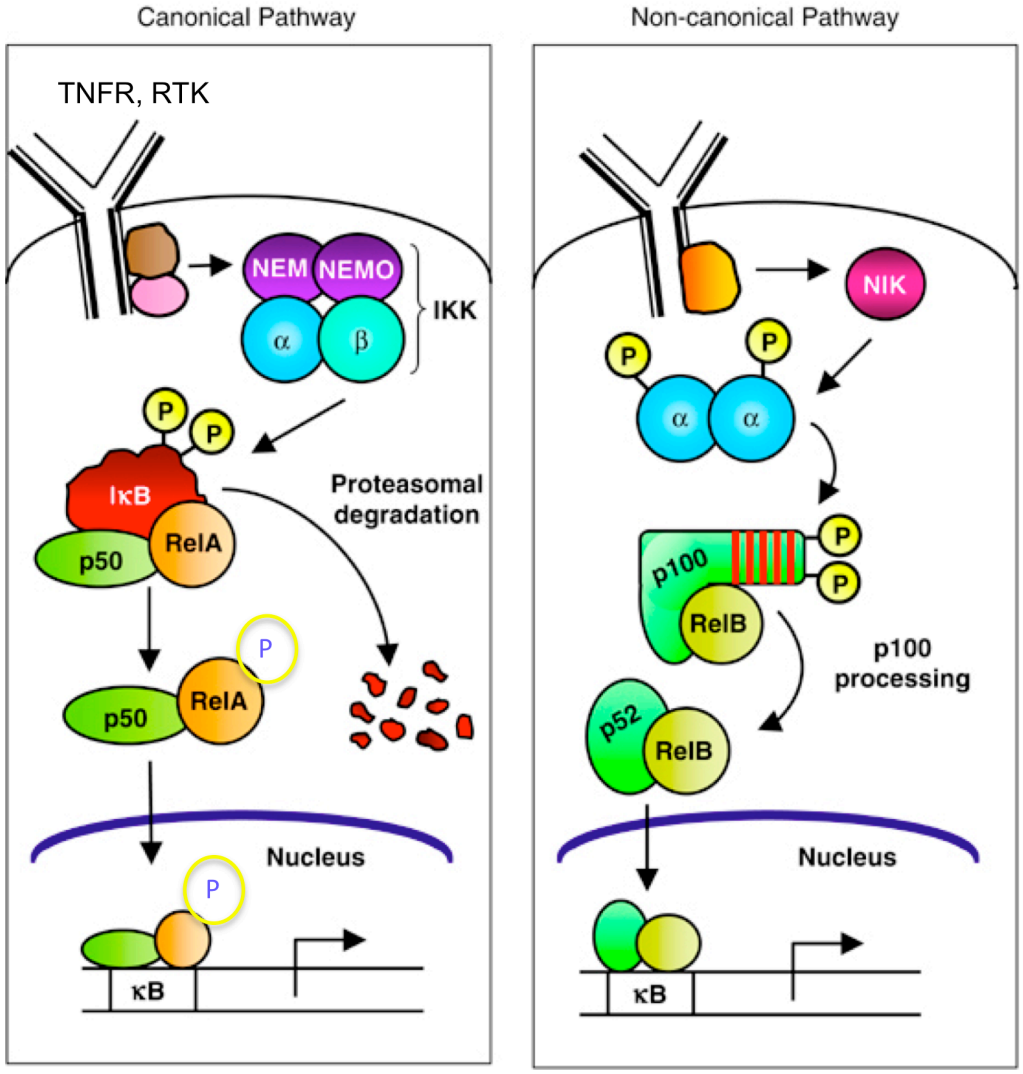

Figure 1.5. Mechanisms of NF-κB activation in cancer cells. NF-κB signaling occurs via a canonical or non-canonical pathway. In the canonical pathway, IKKβ phosphorylates IκB, targeting it for degradation. The p65/RelA-p50 dimer is released, further modified via phosphorylation and acetylation, and translocates to the nucleus where it binds in a site-specific manner to the promoter regions of genes, inducing transcription. In the non-canonical pathway, IKKα phosphorylates p100, inducing processing of p100 to p52. The RelB-p52 dimer translocates to the nucleus and induces gene transcription. Figure adapted from Gilmore, Oncogene (2006) Oct 30;25(51):6887-99.

involves IKKα-mediated phosphorylation of the inhibitory protein, p100 (Figure 1.5) [76]. Unlike IκB, which is degraded, p100 is processed to p52 and the resulting RelB-p52 dimer then translocates to the nucleus to promote transcription of target genes [76].

NF-κB signaling is activated by STAT3 and PI3K/Akt and promotes cancer cell progression and survival in the presence of chemotherapeutic agents [79-81]. Specifically, STAT3 has been shown to promote phosphorylation and acetylation of p65/RelA, increasing the duration of transactivation [78]. The NF-κB pathway is a master regulator of anti-apoptotic IAP (inhibitor of apoptosis protein) expression [82]. The IAP family inhibits caspases-3, -7, and -9, and are inhibited themselves by Smac/DIABLO (Figure 1.6), and this balance critically determines cellular response to therapy in numerous cancer types [83, 84]. There is some controversy regarding the role of NF-κB in response to chemotherapeutics such as doxorubicin. Some reports indicate that NF-κB activity is induced in response to doxorubicin, while others show that NF-κB promotes doxorubicin-induced death via transcriptional repression of anti-apoptotic genes [85-87]. This is likely to be tightly governed by cell type-specific responses to various stimuli, and determining how cellular milieu regulates NF-κB activation in response to therapy will be critical for designing future therapeutic agents.

1.3 Breast Cancer

1.3.1 Clinical stages and progression

Breast cancer is one of the most commonly diagnosed diseases in U.S. women [88]. As with other epithelial-derived malignancies, progression to metastasis is responsible for 90% of cancer-related deaths [89]. Cells progress to an invasive, metastatic state via a process defined as epithelial-to-mesenchymal transition (EMT) [90]. During this process, cells undergo remodeling of their actin cytoskeleton, lose apical-basal polarity and adhesion, and gain the ability to migrate and infiltrate the extracellular matrix [90]. Epithelial cancers of glandular origin arise due to enhanced localized cell proliferation, giving rise to a benign tumor called an adenoma [90]. As the disease progresses towards malignancy, this cell mass, now defined as an adenocarcinoma, acquires the ability to invade surrounding tissues and potentially intravasate into the bloodstream, extravasate to secondary sites, and establish colonies in distant organs to form metastases (Figure 1.7) [90].

Proliferation is a strong prognostic index for response to breast cancer therapy, since enhanced proliferation drives tumor development and increases the likelihood of

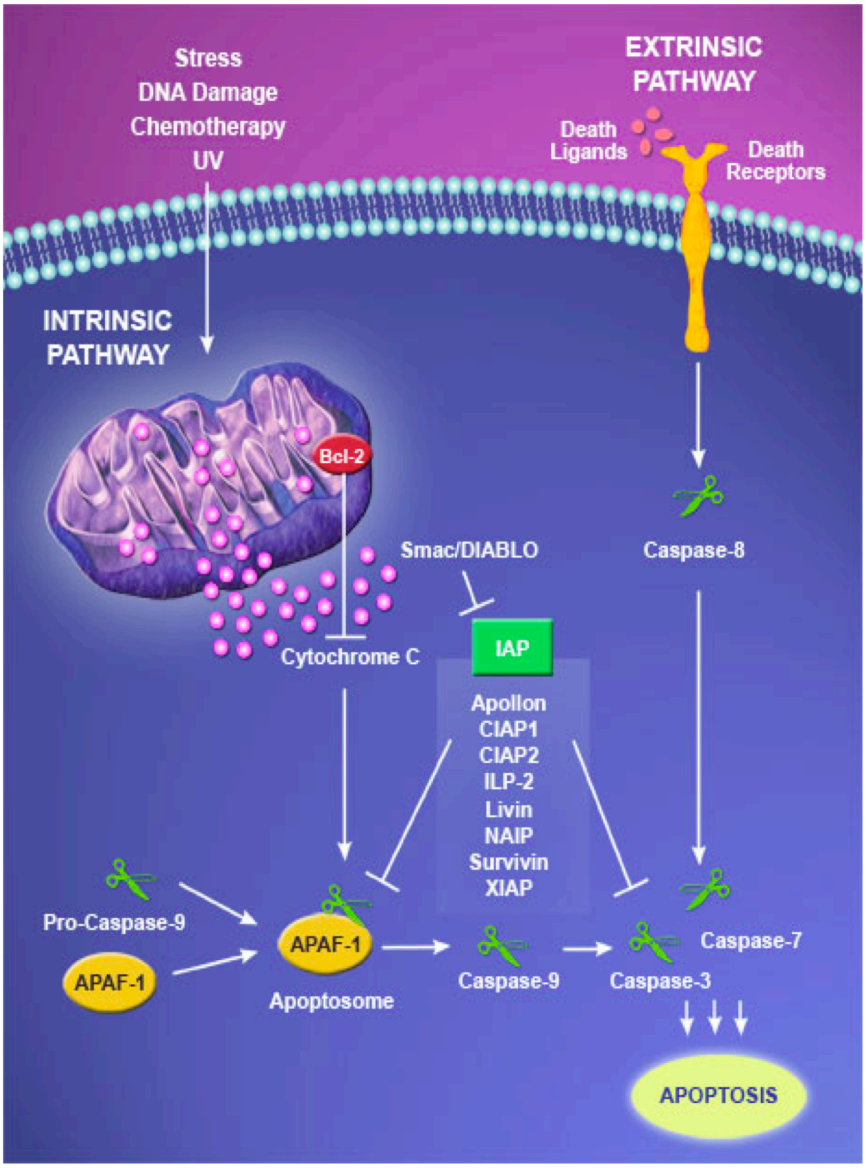

Figure 1.6. Inhibitors of Apoptosis Proteins (IAPs) inhibit caspase activation. Apoptosis can be induced by either an intrinsic or extrinsic pathway. In the extrinsic pathway, death receptors activate caspase-8, leading to caspase-3/7 activation. In the intrinsic pathway, cell stress/damage leads to cytochrome c release from the mitochondria and formation of the apoptosome, which is composed of cytochrome c, APAF-1, and caspase-9, and this leads to caspase-3/7 activation. IAPs inhibit caspases-3, -7, and -9, and are inhibited by Smac/DIABLO. Adapted from: Arnt, et al., J Biol Chem (2002) Nov 15;277(46):44236-43; Abe, et al, Exp Mol Path (2007) Dec;83(3):405-12; Lopes, et al., Int J Cancer (2007) Jun 1;120(11):2344-52; Wright, et al, J Clin Invest (2005) Oct;115(10):2673-8.

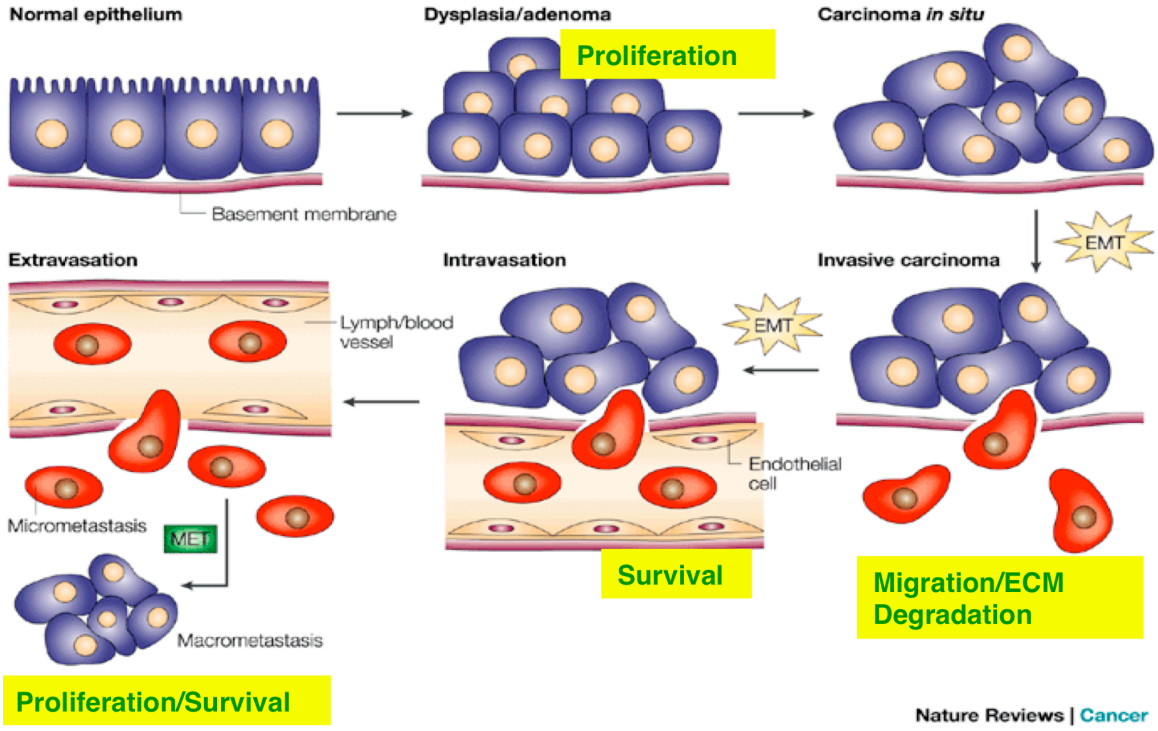

Figure 1.7. The stages of epithelial cancer progression. Cellular dysplasia and unchecked proliferation results in the formation of an adenoma. As cells develop into a carcinoma and become more malignant, they undergo epithelial-to-mesenchymal transition (EMT) and acquire the ability to invade surrounding tissues, intravasate into the bloodstream, and extravasate out at secondary sites to form metastases. Figure adapted from Thiery, JP, Nat Rev Cancer (2002) Jun;2(6):442-54.

metastasis, resulting in a poor prognosis for the patient [91, 92]. MAPK, PI3K/Akt, & STAT have all been shown to drive breast cancer proliferation and progression [93-95]. Akt signaling promotes breast cancer cell survival in the presence of chemotherapeutic agents, with Akt2 having specifically been shown to promote chemoresistance [71]. Moreover, primary breast tumor samples possess elevated levels of pAkt [57]. The NF-κB pathway is known to promote breast cancer progression, and various components of this pathway are significantly overexpressed in breast cancer cells [73, 74]. Tyrosine kinases have a pivotal role in breast cancer progression, including the ErbB family (i.e., EGFR, Her2), IGFR, PDGFR, Src, and Abl family kinases [38, 39, 96]. Previously, we showed that Abl family kinases promote STAT3 activation in breast cancer cells [39], and elevated STAT3 activity promotes proliferation, survival, and chemoresistance of invasive breast cancer cells [97-99].

1.3.2 Current breast cancer treatment options

Invasive, aggressively growing breast tumors are less amenable to currently used treatments; therefore, new therapeutic targets are required to specifically combat highly aggressive breast cancer [92, 100, 101]. Doxorubicin is one of the most successful chemotherapeutic agents for treating epithelial cancers [101, 102]. Doxorubicin-induced DNA damage stalls the progression of cells through the cell cycle [103]. Doxorubicin has many different mechanisms of action, including inhibition of topoisomerase II, DNA intercalation, and free radical generation [104, 105]. Chemotherapy, such as doxorubicin, improves survival, but causes harmful side effects due to a lack of target specificity; therefore targeted agents are routinely used in combination regimens to increase antitumor effects without increasing systemic toxicity [101, 106, 107]. Targeted therapies, focused on inhibition of specific deregulated signaling pathways, as in the case of trastuzumab or erlotinib for treatment of $Her2^+$ or ER^+ breast cancers, respectively, have generated some exciting clinical data both as single agents and in combination regimens [108]. However, these therapies are not effective in $Her2^-$ or ER^- tumors, and advanced metastatic disease has proven refractory to these targeted therapies as well [108]. Patient-specific, diagnostic therapies must be developed to eradicate this difficult to treat disease.

1.4 Melanoma

1.4.1 Clinical stages and progression

Melanoma, the most frequently diagnosed skin cancer type, can arise from exposure to the sun that is both chronic and intermittent; however, cases are diagnosed in mucosal/unexposed areas as well [109, 110]. Half of all cases arise from dysplastic nevi (i.e., atypical moles) [111, 112]. Though melanoma represents a small proportion of all diagnosed skin malignancies (~7%), it is responsible for the majority of skin cancer-related deaths (~75%) [109].

Melanoma spreads by first exhibiting the ability to grow within the epidermal layer in a process known as radial growth phase (RGP) (Figure 1.8). This is followed by transition into vertical growth phase (VGP), where cells invade the dermal layer, and finally metastasis to distant organs (Figure 1.8) [111]. Akt is activated in primary melanoma samples, and activated Akt converts RGP→VGP melanoma [113]. Progression from RGP to VGP to metastasis also requires activation of various transcription factors (i.e., STAT3 & NF-κB) [111, 114]. A majority of the critical markers of melanoma progression and invasion are direct transcriptional targets of these factors [114, 115]. Importantly, we showed in melanoma cells that c-Abl-mediated invasion occurs in a STAT3-dependent manner, whereas Arg-mediated invasion is STAT3-independent [50]. Therefore, we propose that Abl family kinases could represent novel therapeutic targets in melanoma, allowing for direct inhibition of signaling mechanisms that are critical for chemoresistance.

1.4.2 Current melanoma treatment options

Only 5% of patients with advanced disease survive longer than one year and melanoma diagnoses are more common than any other cancer [116]. Currently metastatic melanoma essentially represents an untreatable disease, with little to no improvement having been observed in one-year survival rates. Due to resistance to currently used chemotherapeutics, surgery is the only viable therapeutic option [88, 116]. Past clinical trials for melanoma have tested a gamut of chemotherapeutic options: Alkylating agents, nitroureas, vinca alkaloids, platinums, taxanes, topoisomerase inhibitors, and anthracyclines. These all had little impact on patient survival [116]. One such chemotherapeutic drug, doxorubicin, is currently the focus of six clinical trials based on data obtained from the ClinicalTrials.gov database.

One of the more common genetic phenotypes associated with malignant,

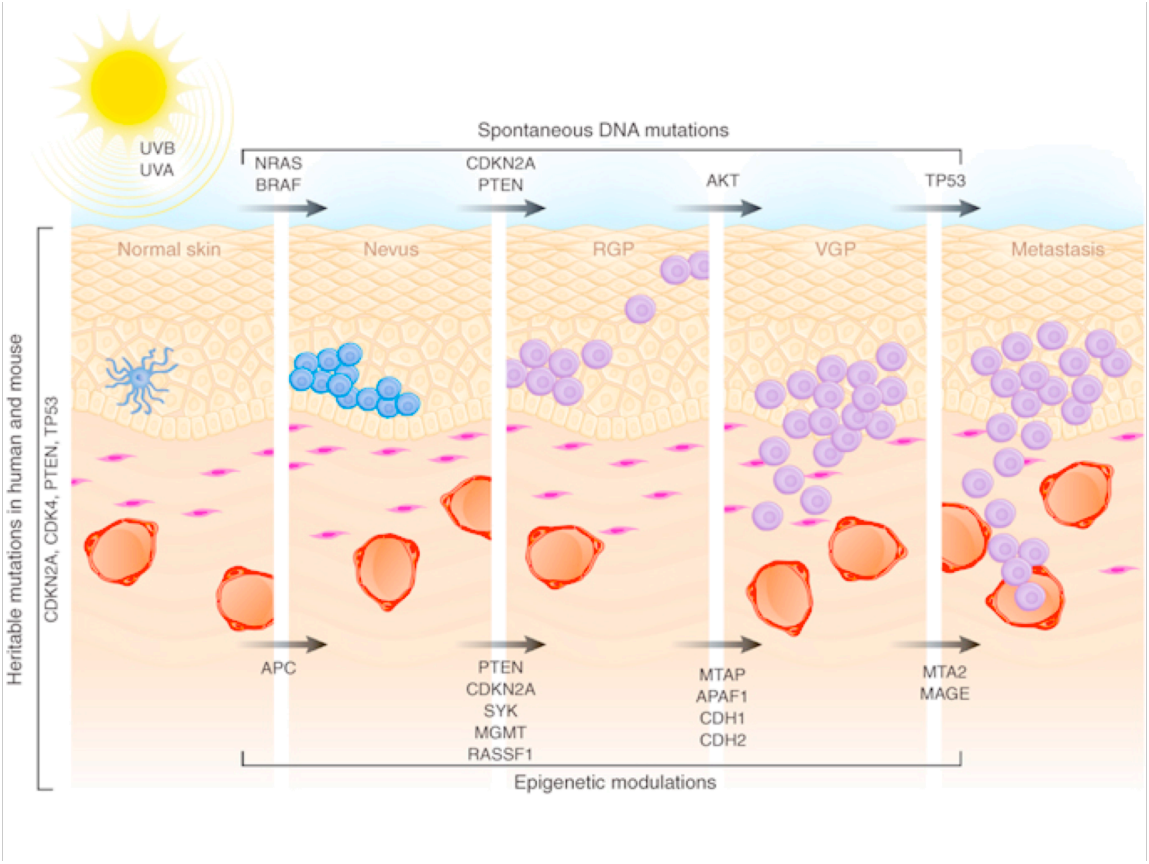

Figure 1.8. Proposed molecular changes for the initiation and progression of metastatic melanoma. Abnormal cells within the epidermal layer arise from either heritable mutations or from cellular insults such as sun exposure. These cells form a nevus, and, via additional DNA mutations and epigenetic modifications, eventually expand within the epidermal layer to form a RGP (radial growth phase) melanoma. Tumors with the acquired ability to invade the dermal layer are known as VGP (vertical growth phase) melanomas. The progression from RGP to VGP to metastasis requires gain of function of various transcription factors (i.e., STAT3 and NF-kB). Figure adapted from: Zaidi, et al., J Invest Dermatol (2008) Oct;128(10):2381-91.

chemoresistant melanoma is oncogenic mutation of B-Raf [117, 118]. Although B-Raf mutations are rare across all cancers (~7%), they are present in nearly 60-70% of malignant melanomas [119]. B-Raf inhibitors show promise for treating metastatic melanoma; however, some melanomas do not contain B-Raf mutations, others acquire resistance by activating receptor tyrosine kinase signaling pathways [120, 121], and still others (10%) are intrinsically resistant [122]. c-Kit mutations are more commonly observed in melanomas from mucosal and minimal exposure areas (i.e. hands and feet) [110, 123]. Some melanomas containing activated c-Kit respond to STI571; however, there are other cases in which they do not [110, 123, 124].

Treatment regimens are limited, in part, because approximately 80% of melanomas express an ABC transporter [125]. Studies indicate that ABCC1 and ABCB1 are commonly expressed in melanoma, positively correlating with progression to metastasis, and contribute to the invasive potential of melanoma cells [125, 126]. Studies have shown promising data in regards to malignant melanoma therapy with drugs that target c-Kit or B-Raf [122, 124], although no therapy to date has extended survival longer than 10 months [127].

1.5 Drug Resistance

1.5.1 Types of resistance mechanisms

Resistance to chemotherapy is a constant obstacle in treating cancer patients, which highlights the need to understand mechanisms that drive resistance. Multidrug resistance occurs via three primary mechanisms: 1) decreased influx of water soluble compounds that require transport mechanisms to enter cells; 2) increased efflux of hydrophobic drugs that diffuse through cell membranes; and 3) upregulation of DNA repair processes, anti-apoptotic and proliferative factors, or metabolic enzymes [128]. Overexpression of anti-apoptotic proteins (e.g., Bcl-2, Bcl-X_L) and induction of transcription factors (e.g., STAT3, NF-κB) have a definitive role in chemotherapeutic resistance.

Doxorubicin activates pro-apoptotic proteins (i.e. Bak, Bax), and this process is counteracted by anti-apoptotic proteins (i.e. Bcl-2, Bcl-X_L) that prevent Bak/Bax from triggering cytochrome c release and the mitochondrial cell death pathway [129]. STAT3 signaling induces expression of anti-apoptotic proteins (i.e., Survivin, Bcl-2, and Mcl-1), and XIAP/cIAP1 are upregulated transcriptionally by NF-κB [130, 131]. IAP expression correlates with resistance to doxorubicin and chemo-resistant cells potentially lack

mechanisms for down-regulating IAPs & up-regulating Smac/DIABLO [83, 130, 132]. However, although a plethora of intrinsic resistance mechanisms exist, the most common mechanism of resistance is via increased efflux mediated by ATP Binding Cassette (ABC) transporter family members [128, 133].

1.5.2 ATP Binding Cassette (ABC) transporters

The ATP Binding Cassette (ABC) transporter family consists of a multitude of membrane spanning proteins responsible for ATP-dependent transport of substances across both intra- and extracellular membranes [134]. Members of this superfamily possess two highly conserved nucleotide (ATP) binding domains and two transmembrane domains (Figure 1.9) [135]. Although substrate specificities vary between members, transporter activity is dependent on ATP [135]. Researchers have identified approximately fifty human ABC transporters in a variety of tissue types [136]. Three ABC transporters (i.e., ABCB1, ABCC1, and ABCG2) account for an overwhelming majority of the multidrug resistance observed in mammalian cells *in vitro* [137].

ABCB1, or P-glycoprotein, is highly elevated within many cancer types and possesses the broadest substrate specificity of all known transporters [128]. It transports hydrophobic compounds that are neutral to slightly positive in charge; therefore, encapsulating most commonly used chemotherapeutic drugs [138]. It is widely associated with resistance to anthracyclines, taxanes, and vinca alkaloids, among many other classes of chemotherapeutics across a multitude of cell types [135].

ABCG2 was originally named BCRP (breast cancer resistance protein), due to the fact that it was cloned from a doxorubicin-resistant breast cancer cell line [139]. This transporter recognizes both positively and negatively charged molecules, organic anions, and substrates possessing sulfate conjugates. There is a great deal of similarity in tissue distribution and substrate specificity between ABCG2 and ABCB1 [137]. ABCG2 differs from other members of the ABC transporter family in that it only contains one ATP-binding domain, one transmembrane domain, and typically functions as either a homodimer or a tetramer [137, 140]. It primarily confers resistance to anthracyclines, mitoxantrone, and topotecan [135].

ABCC1, also called MRP1, is expressed ubiquitously as well, and primarily effluxes negatively charged molecules and compounds that have undergone phase II metabolism [134, 141]. It shares substrate specificity with ABCB1 for a number of

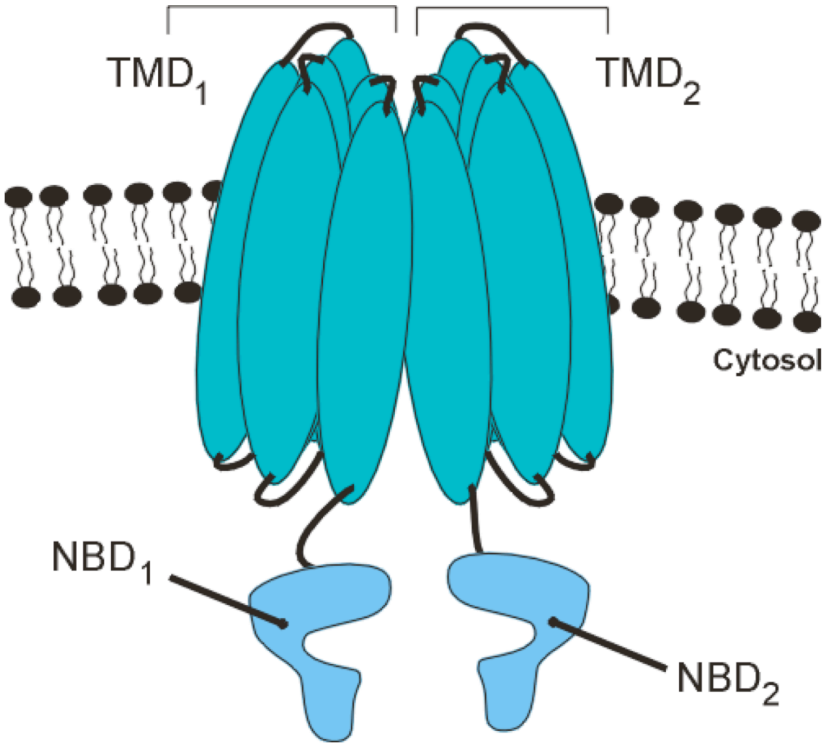

Figure 1.9. Basic structure of ABC transporters. Family members of the ATP binding cassette (ABC) transporter family contain transmembrane domains (TMD) and nucleotide binding domains (NBD). The NBDs of ABC transporters bind ATP, resulting in active transport of substrates across cellular membranes. Figure adapted from: http://www-dsv.cea.fr/art/images/devm_lems/abc3d.gif

hydrophobic compounds and primarily confers resistance to doxorubicin, etoposide, vincristine, and methotrexate [128, 135].

1.5.3 Role of ABC transporters in disease

Studies have shown that ABCB5 and ABCB8, structural paralogs of ABCB1, promote melanoma resistance to doxorubicin [142, 143], and ABCB1 expression and function is induced in melanoma cells following drug treatment [144]. Breast cancer stem cells bypass chemotherapy-induced cell death, in part, by upregulating the drug transporter, ABCG2, a stem cell marker [145]. Interestingly, BCR-Abl increases ABCG2 expression in hematopoietic cells [146]. ABCB1 has been shown to induce efflux of doxorubicin in BCR-Abl$^+$ hematopoietic cells [147], and STI571 and nilotinib have been shown to interact with both ABCB1 and ABCG2 [148].

1.5.4 Use of ABC transporter inhibitors for cancer treatment

While a number of inhibitors are well suited for laboratory-based pharmacological studies, there are abundant limitations preventing the clinical usefulness of these compounds. Fumitremorgin C (FTC), a mycotoxin derived from *A. fumigatus*, and its many analogs, reverses ABCG2-mediated drug resistance, but is highly neurotoxic *in vivo* [137, 149]. Ko143, another potent BCRP inhibitor, is currently undergoing analysis, and has produced a promisingly low degree of *in vivo* toxicity in preliminary tests [150]. ABCB1 inhibitors, such as cyclosporine A and verapamil, increase intracellular drug accumulation and cytotoxic effects; however, it appears that the effectiveness of these inhibitors varies across different cell types [151]. Despite three decades of study, all attempts to therapeutically target ABCB1 have failed due to systemic toxicity [135]. Targeting resistant cancers has proved difficult due to intrinsic (anti-apoptotic signaling) and acquired (ABC transporter) resistance mechanisms. Current treatment options have not provided the necessary therapeutic value required to adequately combat chemoresistant tumors; therefore, novel druggable targets which influence multiple mechanisms of resistance must be identified in order to make headway against these most difficult to treat forms of disease.

1.6 Project Objectives

Our previous observations have indicted Abl family kinases as causative agents in melanoma and breast cancer cell proliferation, invasion, survival to nutrient

deprivation, and metastasis [38, 39, 50]. As cancer cells progress, they notoriously become more resistant to therapy that may have effectively killed cells at an earlier stage of the disease. Due to the critical nature of Abl family kinases in promotion of melanoma and breast cancer cell progression, we hypothesize that c-Abl/Arg may be critical mediators of the resistant phenotype required for survival of advanced disease. The goal of this work is to identify whether c-Abl and Arg promote chemoresistance of invasive/metastatic cancer cells, and identify the mechanisms by which this occurs.

We will determine whether c-Abl/Arg promote viability, proliferation and prevent apoptosis in response to various chemotherapeutics used in the treatment of breast cancer and melanoma cells (chapters 2 and 3). Furthermore, we will identify mechanisms by which c-Abl/Arg inhibitors sensitize highly resistant melanoma cells to doxorubicin (chapter 4). Finally, we will ascertain the mechanism by which c-Abl/Arg promote resistance to doxorubicin-induced apoptosis (chapter 5), and postulate a mechanism by which c-Abl/Arg promote proliferation in the presence of doxorubicin (chapter 6).

CHAPTER TWO

ABL FAMILY KINASES PROMOTE BREAST CANCER CHEMORESISTANCE

2.1 Introduction

Breast cancer is the second leading cause of cancer-related deaths in U.S. women, and accounts for a quarter of new cancer diagnoses each year [152]. Her2-positive breast cancers are treated with Herceptin; however, many tumors develop resistance and others are Her2-negative. Taxanes (e.g. paclitaxel; taxol), 5-fluorouracil (5-FU), camptothecins, and cyclophosphamide, which metabolizes to mechloroethamine, are currently used for treatment of patients with ER^- (estrogen receptor-negative), PR^- (progesterone receptor-negative) tumors, and platinum (e.g. cisplatin) regimens are in preclinical trials [153-156]. Conventional chemotherapeutic approaches for treating patients with hormone-negative, Her2-negative tumors are far from optimal, as the treatments often are not effective due to resistance, and the drugs have significant side effects. Thus, the development of new combinations to treat this class of patients is critical. The use of targeted agents together with conventional chemotherapeutic drugs may increase the effectiveness of the drugs, allowing doses to be decreased, thereby decreasing toxicity.

We showed that Abl family kinases have dramatically increased activities in invasive breast cancer cells as compared to non-invasive MCF-7 breast cancer cells [38]. Interestingly, the mechanism of c-Abl/Arg activation in breast cancer cells is unique from their activation in leukemia. In leukemia, chromosomal translocation activates the Abl family kinases, whereas in ER^-, PR^- breast cancer cells, Abl family kinases are activated downstream of deregulated growth factor receptors such as EGFR, ErbB2/Her2, and IGF-1R, as well as by activated Src family kinases [38, 39]. Using STI571 and siRNA approaches, we showed that activation of c-Abl/Arg in breast cancer cells has dramatic consequences as they promote proliferation, G1→S transition in response to IGF-1, survival in response to nutrient deprivation, and invasion [38, 39]. In this chapter, we demonstrate that STI571 synergizes with conventional chemotherapeutic agents to inhibit proliferation and increase apoptosis of breast cancer cells. Interestingly, the effects of the drug combinations are cell type-specific, as STI571 synergizes with cisplatin in BT-549 cells, camptothecin in MDA-MB-231 cells, and 5-FU in MDA-MB-468 cells, whereas mechloroethamine has antagonistic effects with STI571 in all cell lines. Therefore, although all the cell lines are equally sensitive to the effects of

STI571 alone [39], there are cell type-specific differences, which affect the ability of STI571 to synergize with conventional chemotherapeutic agents.

2.2 Materials and Methods

2.2.1 Cell Lines and Reagents

Cell lines were purchased from the University of North Carolina Tissue Culture Facility. BT-549 cells were grown in RPMI/10% FBS (fetal bovine serum), and MDA-MB-231 and MDA-MB-468 cells were cultured in MEM/10% FBS/1mM sodium pyruvate. STI571, kindly provided by Novartis (Basel, Switzerland), was dissolved in water at a concentration of 10mM and stored at −80°C. Doxorubicin, paclitaxel, cisplatin, camptothecin, 5-fluorouracil, and mechlorethamine were purchased from Sigma (St. Louis, MO). Antibodies to PARP (Poly (ADP-ribose) polymerase; sc-8007), pan-ERK1/2 (sc-94), IκB (sc-371), and α-tubulin were obtained from Santa Cruz Biotechnologies (Santa Cruz Biotechnology; Santa Cruz, CA), Lamin A/C was obtained from Milllipore (Temecula, CA), GAPDH, c-Abl (8E9), and STAT3 antibodies were obtained from BD Biosciences (Chicago, IL), phospho-Akt, Akt, and phospho-STAT3 (Y705) antibodies were from Cell Signaling Technology (Danvers, MA), and phospho-ERK1/2 antibody was from Promega (Madison, WI). Western blots were performed according to manufacturers' protocols.

2.2.2 Viability Assays

CellTiter-Glo Assay (Promega; Madison, WI). Cells were plated in triplicate in 96-well dishes such that the vehicle-treated population was subconfluent at the end of the assay. The day after plating, the media was replaced with media containing drugs, and viability was assessed 72 hours later using the CellTiter-Glo Assay. For 5-FU experiments, viability was assessed after 96 hours. An equal volume of CellTiter-Glo reagent (at room temperature) was added to each well, the plate was rocked, incubated at room temperature for 10 minutes, half of the mixture from each well was transferred to an opaque 96-well plate, and luminescence (all wavelengths of light emitted for 10 seconds) was measured on a Synergy 2 plate reader (Biotek; Winooski, VT). MTT Assay (Sigma; St. Louis, MO). Cells were plated in triplicate in 96-well plates at a density of 2500 cells/well, and the next day the media was replaced with media containing STI571. After 72 hours, the media was replaced with 3-(4, 5-methylthiazol-2-yl)-2, 5-diphenyl-tetrazolium bromide (MTT)-containing media (0.5mg/ml), incubated at 37°C for 4 hours,

an equal volume of solubilization solution (10% SDS, 0.01M HCl) was added, and the plate was incubated at 37°C overnight to solubilize formazon crystals. Absorbance was measured at 570nm in a Biotek Synergy 2 plate reader (Biotek; Winooski, VT).

2.2.3 Proliferation Assays

Cells were plated in triplicate in 24-well dishes so that vehicle-treated cells were subconfluent on the day of harvest. The day after plating, the media was replaced with media containing drugs, and 72 hours later (96 hours for low dose 5-FU experiments) tritiated thymidine was added (2.5μCi) for 2 hours. Cells were harvested by washing with PBS, 10% trichloroacetic acid (TCA), incubating in 10% TCA for 45 minutes, solubilizing radioactivity in 0.2N NaOH, and reading on a scintillation counter.

2.2.4 Apoptosis Assays

PARP Assay. Cells were plated in 60mm dishes, the media was replaced with media containing drugs the next day, and 40 hours later, detached and attached cells were lysed in RIPA buffer (50mM Tris pH 7.5, 150mM NaCl, 1% triton-X 100, 0.1% SDS, 1% sodium deoxycholate, 1mM PMSF, 1mM sodium orthovanadate, 25mM sodium fluoride, 10μg/ml leupeptin, aprotinin, pepstatin). Total protein was quantitated with a Lowry DC kit (BioRad; Hercules, CA), equal protein was loaded on SDS-PAGE gels, and blots were incubated with antibodies to PARP and GAPDH. Caspase-Glo-3/7 Assay (Promega; Madison, WI). Cells were plated as described above, lysed in caspase lysis buffer (50mM HEPES pH 7.4, 5mM CHAPS, 5mM DTT), clarified by centrifugation, 15μl of the supernatant or buffer (blank) and 35μl of buffer were added to wells in an opaque 96-well plate, and an equal volume (50μl) of room temperature Caspase-Glo substrate was added to each well. The plate was rocked, and luminescence (all wavelengths of light emitted) from each well was read 40–60 minutes after addition of Caspase-Glo using the Synergy 2 plate reader. Luminescent values were normalized to protein concentration using the Bradford protein assay (BioRad; Hercules, CA). Fluorescent Caspase-3/7 Assay (Sigma; St. Louis, MO). Cells were plated in 6-well dishes (60,000 cells/well), treated for 40hours with STI571, and lysed in 1X lysis buffer. Lysate (5μl) was added to an opaque 96-well plate, incubated with 200μl of substrate (diluted 1:3), and fluorescence was assessed at 360nm (excitation)/460nm (emission) using a Biotek Synergy 2 plate reader. Relative Fluorescence Units (RFUs) were divided by the protein concentration of each sample as determined by Bradford assay (Biorad; Hercules, CA).

2.2.5 Subcellular Fractionation

Cells were plated in 60mm dishes, and cytoplasmic/membrane and nuclear fractions were isolated using the NE-PER kit (Pierce; Rockford, IL) according to the manufacturer's protocol.

2.2.6 Statistics/Determination of Combination Indices

Statistics were performed using SigmaStat for Windows (Systat Software, Inc.; San Jose, CA). Combination Index (CI) values were determined using CalcuSyn software (Biosoft; Cambridge, UK) utilizing STI571 and chemotherapeutic drug dose response curves.

2.3 Results

2.3.1 MTT viability assays cannot be utilized to study effects of STI571 on solid tumor cell lines.

We previously showed that STI571 inhibits many cellular processes associated with cancer progression in a variety of breast cancer and melanoma cell lines [39, 50]. For instance, we demonstrated that treatment of breast cancer and 435s/M14 melanoma cells, which possess active Abl family kinases, with the c-Abl/Arg inhibitor, STI571 (Gleevec), dramatically inhibits cell growth [39]. MDA-MB-435s cells were originally believed to be of breast cancer origin, but, in fact, are identical to M14 melanoma cells and will be referred to as 435s/M14 [50, 157]. To determine if the aforementioned decrease in growth in these cells was due to proliferation, we performed tritiated thymidine assays and observed a dose-dependent decrease in cell proliferation (Figure 2.1A). To determine whether STI571 induces apoptosis of solid tumor cells grown in serum conditions, we performed fluorescent caspase-3/7 assays. Significantly, treatment of 435s/M14 and MDA-MB-468 cells with STI571 increased caspase activity (Figure 2.1B). Therefore, STI571 reduces the growth of cells in serum by inhibiting proliferation and inducing apoptosis. A dose of 10μM STI571 was used for these assays because we previously showed that 10μM was required to effectively (65–75%) reduce phosphorylation/activities of active endogenous c-Abl and/or Arg [38]. Since our studies are focused on chemotherapeutic resistance, we decided to focus primarily on STI571's overall effect on cell viability.

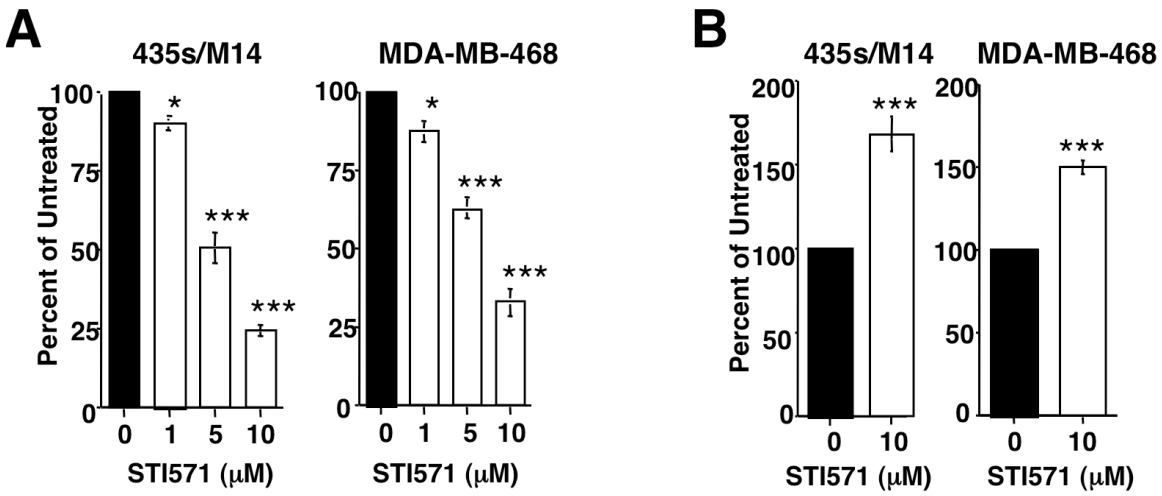

Figure 2.1. STI571 inhibits proliferation and induces apoptosis of cells containing highly active Abl family kinases. (A) Cell lines were plated in triplicate in 12-well dishes, the media was replaced the next day with media containing STI571, and tritiated thymidine incorporation was measured 72h later. Experiments shown are mean±SEM of three independent experiments. **(B)** Cells were plated in 6-well dishes, the media was replaced with media containing STI571 the next day, and caspase-3/7 activity was detected 40h after treatment in detached and attached cells by fluorescent caspase assay. Mean±SEM of three independent experiments. Values were normalized to values obtained in untreated wells and expressed as a percentage of untreated. *p<0.05, ***p<0.001 using a Student t-test.

Since both proliferation and apoptosis are affected by STI571, viability assays should demonstrate a decrease in viability in the presence of STI571. To test this hypothesis, we utilized the MTT assay (Sigma; St. Louis, MO). 435s/M14 and MDA-MB-468 cells were grown in the absence or presence of STI571 in serum, and MTT was added 72 hours later (the same timepoint used for tritiated thymidine assays). Surprisingly, although there was a noticeable decrease in cell number in wells treated with STI571, there was *increased* rather than decreased MTT reduction to formazan in STI571-treated 435s/M14 and MDA-MB-468 cells, and the increase in formazan formation was dependent on the STI571 dose, which was observed with as little as 1μM STI571 (Figure 2.2A, data not shown). These data were clearly inconsistent with growth kinetics, tritiated thymidine, and caspase assays, and also were inconsistent with what was observed by eye (Figure 2.1, data not shown) [39]. To be certain that the MTT assay was working in our hands, we treated 435s/M14 cells with increasing doses of doxorubicin, a drug known to inhibit cell viability, and observed that doxorubicin induced decreased MTT reduction, demonstrating that the MTT assay accurately assesses the ability of doxorubicin to inhibit viability (Figure 2.2B).

To determine whether the effect of STI571 on viability was specific to the tetrazolium-based assay, we assessed the effect of STI571 treatment on the viability of 435s/M14 and MDA-MB-468 cells using a different assay, CellTiter-Glo (CTG; Promega; Fitchburg, WI). CellTiter-Glo is a luminescent assay that quantitates the amount of cellular ATP present, which reflects the number of metabolically active, viable cells. Luciferase enzymatic activity requires ATP; therefore, the amount of luminescent signal is proportional to the amount of ATP present in the lysate. Treatment of 435s/M14 and MDA-MB-468 cells with STI571 resulted in a decrease in CellTiter-Glo luminescence (Figure 2.2C) consistent with tritiated thymidine and caspase assays (Figure 2.1), although the decrease in luminescence was not as great as one would expect given the large effect of STI571 on proliferation and apoptosis. However, the CellTiter-Glo assay *did* detect a decrease in viability that was not observed with the MTT assay.

2.3.2 STI571 sensitizes MDA-MB-468 cells to paclitaxel.

We previously showed that a variety of breast cancer cell lines containing highly active Abl family kinases are sensitive to STI571, which inhibits cell proliferation in serum and serum-free conditions [39]. In this chapter, we utilized three of the cell lines that we previously characterized: BT-549, which has highly active c-Abl and Arg, MDA-

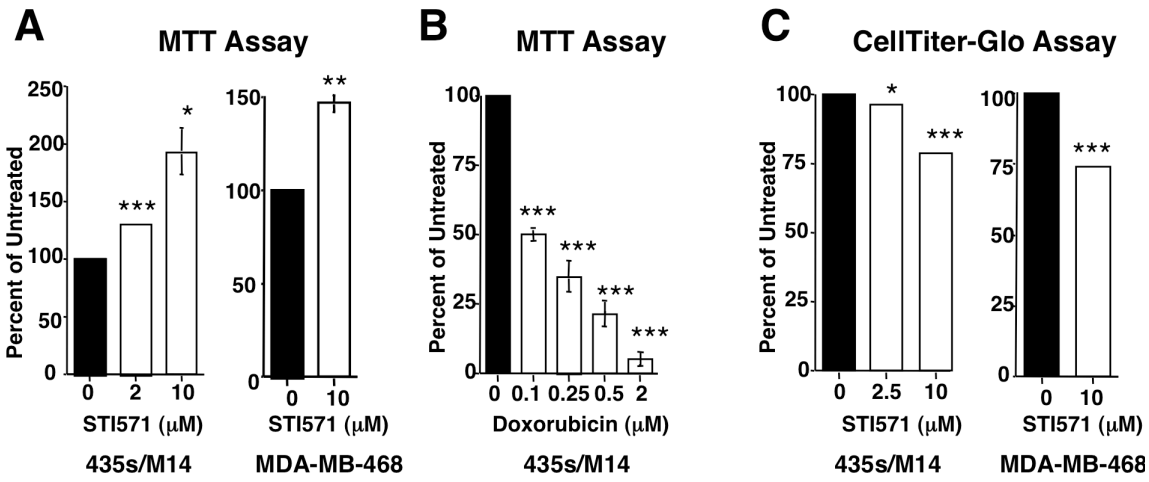

Fig. 2.2. STI571 interferes with the ability of the MTT assay to measure cell viability. 435s/M14 melanoma cells and MDA-MB-468 breast cancer cells were plated in 96-well dishes in triplicate, the media was replaced the next day with media containing STI571 **(A,C)** or doxorubicin **(B)**, and 72h later the cells were used either in MTT **(A,B)** or CellTiter-Glo **(C)** viability assays. Experiments shown are mean±SEM for three independent experiments. Some error bars are too small to be visualized. *p<0.05, **p<0.005, ***p<0.001 using Student t-tests.

MB-231, which has highly active c-Abl, and MDA-MB-468, which has highly active Arg and also expresses another STI571 target, c-Kit [38]. To determine whether STI571 sensitizes breast cancer cells to conventional chemotherapeutic agents, we treated the above cell lines with vehicle, STI571, chemotherapeutic drug, or STI571+chemotherapeutic drug, and assessed the effect on viability, proliferation, and apoptosis. First, we tested the taxane, paclitaxel, a frequently used breast cancer drug, which promotes assembly of microtubules from tubulin dimers, leading to hyperstabilization and decreased depolymerization, thereby preventing microtubule reorganization, which is essential for interphase and mitotic cellular functions [153]. Breast cancer cells were treated with STI571 and paclitaxel alone or in combination, and viability was assessed using the CellTiter-Glo assay, which quantitates ATP, a measure of metabolically active cells. Combination indices (CI), a measure of how well the drugs act together, were determined with CalcuSyn software, using STI571 and paclitaxel dose response curves (Table 2.1; data not shown). CI values that are greater than one indicate drug antagonism, values equal to one indicate that the drugs act in an additive fashion, and values that are less than one indicate drug synergism.

In MDA-MB-231 and BT-549 cells, treatment with STI571 antagonized the effects of paclitaxel on viability (Figure 2.3A, B; Table 2.1), whereas in MDA-MB-468 cells, STI571 slightly sensitized the cells to paclitaxel in an additive→synergistic manner (Figure 2.3C; Table 2.1). To determine whether STI571 sensitized MDA-MB-468 cells to paclitaxel by inhibiting proliferation, we performed tritiated thymidine assays. Since tritiated thymidine assays are extremely sensitive, low doses of the drugs have a very dramatic effect, and thus low doses were utilized in order to accurately assess IC_{50} values. We observed a dose-dependent decrease in proliferation mediated by STI571 and paclitaxel alone in MDA-MB-468 cells, and the combination of the two drugs produced additive effects (Figure 2.3D; Table 2.1). To determine whether apoptosis contributed to the additive→synergistic effects on viability, we measured two outcomes indicative of apoptosis: cleavage of PARP, a nuclear polymerase that is cleaved from 115 kDa to 89 kDa during apoptosis [158]; and quantitation of caspase-3/7 activities using a luminescent caspase assay, Caspase-Glo (Promega; Madison, WI). The caspase-3/7 proluminescent substrate contains the signature DEVD peptide sequence. Lysed cells release active caspase-3 or -7, which cleaves the DEVD substrate from aminoluciferin, and the oxidation of luciferin by luciferase produces light. The amount of light produced is proportional to the amount of caspase activity. STI571 had no effect on

Table 2.1. Combination indices for STI571/chemotherapeutic combinations. Combination indices were determined using CalcuSyn software and dose response curves for STI571 and chemotherapeutic drugs (data not shown). Values shown are representative of three independent experiments. Values greater than one indicate antagonism; values equal to one indicate additivity; and values less than one indicate synergism. MCE=mechlorethamine.

Drug	Cell Line	Drug Dose	STI571 Dose	Viability CI	Proliferation CI
Paclitaxel	MDA-MB-231	5nM, 10nM	10μM	1.1, 1.4	
	BT-549	10nM, 30nM	"	1.8, 2.4	
	MDA-MB-468	10nM, 50nM	"	0.99, 0.64	
	MDA-MB-468	2.5nM	1,5,10μM		1.0, 1.3, 1.1
	"	5nM	"		1.2, 1.1, 1.1
Cisplatin	MDA-MB-468	1,5μM	10μM	0.9, 0.72	
	BT-549	10, 15μM	"	0.73, 0.47	
	MDA-MB-231	25, 50μM	"	1.3, 1.3	
	BT-549	0.5μM	2,5,10μM		0.8, 0.7, 0.6
	"	1μM	"		0.5, 0.4, 0.3
	MDA-MB-468	0.125μM	"		0.6, 0.9, 0.8
	"	0.5μM	"		0.7, 0.8, 0.9
Camptothecin	MDA-MB-468	0.5, 1μM	10μM	1.1, 1.1	
	BT-549	0.01, 0.025	"	0.92, 1.2	
	MDA-MB-231	0.5, 0.75μM	"	1.5, 1.2	
	MDA-MB-231-Alt. dose	0.5, 0.75μM	"	0.34, 0.64	
	MDA-MB-231-Alt. dose	0.0025μM	2,5,10μM		1.1, 0.7, 0.9
	"	0.01μM	"		1.2, 0.9, 0.9
	MDA-MB-468	0.0125μM	"		1.0, 1.3, 0.94
	"	0.035μM	"		0.85, 0.95, 0.79
5-FU	MDA-MB-468	100, 500μM	10μM	0.44, 0.09	
	BT-549	10, 500μM	"	1.6, 1.9	
	MDA-MB-231	50, 500μM	"	2.0, 1.4	
	MDA-MB-468	1.25μM	2,5,10μM		2.1, 2.9, 1.8
	"	3.5μM	"		1.5, 2.4, 1.5
	"	100μM	"		0.9, 1.1, 1.1
	"	250μM	"		1.0, 0.9, 0.5
	"	500μM	"		0.7, 0.6, 0.4
MCE	MDA-MB-468	1.5, 30μM	10μM	5.1, 2.9	
	BT-549	1, 10μM	"	3.1, 3.4	
	MDA-MB-231	20, 50μM	"	2.5, 3.6	

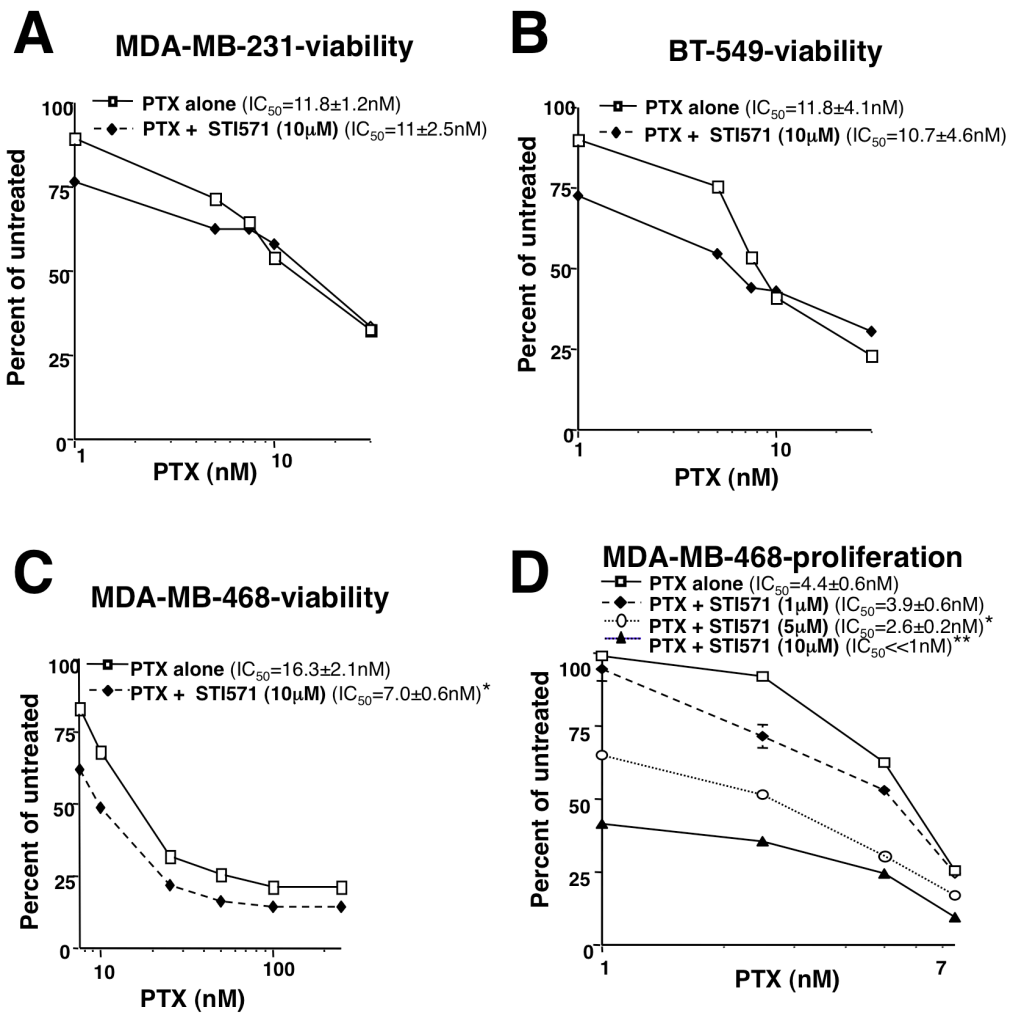

Figure 2.3. Paclitaxel has additive or antagonistic effects with STI571 in breast cancer cells. (A-C) Cells were plated in triplicate in 96-well dishes, the media was replaced the next day with media containing drugs, and three days later viability was assessed by CellTiter-Glo Assay. Experiments were performed three times in triplicate, and representative experiments are shown. Data are expressed as a percentage of values obtained from vehicle-treated cells. Mean±SEM. Some error bars are too small to be visualized. IC_{50} values are mean±SEM for three independent experiments. **(D)** MDA-MB-468 cells were plated in 24-well dishes in triplicate, drug treated the next day, and proliferation was assessed 72h later by tritiated thymidine assay. Experiments were performed in triplicate three times, and a representative experiment is shown. Mean±SEM. Some error bars are too small to be visualized. IC_{50} values are mean±SEM for three independent experiments. *p<0.05, **p<0.005 using Student's t-tests.

the ability of paclitaxel to induce PARP cleavage or activate caspase-3/7 (Figure 2.4A, B). Taken together, these data indicate that STI571 produces additive→synergistic effects with paclitaxel in MDA-MB-468 cells by decreasing proliferation, whereas STI571 antagonizes the effects of paclitaxel in BT-549 and MDA-MB-231 cells. To identify the mechanism by which STI571 reduces proliferation of MDA-MB-468 cells treated with paclitaxel, we blotted lysates with antibodies to Akt, ERK1/2 (Extracellular Signal-Regulated Kinase 1, 2), STAT3, and IκB, in order to assess whether activation of PI3K/Akt, Ras/ERK, STAT3, or NF-κB signaling pathways, which are involved in breast cancer cell proliferation and survival [93-95, 159, 160], are altered in the presence of STI571. IκB stability was not altered by STI571 and/or paclitaxel treatment (Figure 2.4B). Moreover, Akt phosphorylation was increased by paclitaxel treatment, which may be a mechanism by which cells resist the effects of paclitaxel; however STI571 had no effect on this upregulation (Figure 2.4B). Interestingly, STI571 induced phosphorylation of ERK1/2 and STAT3 (Figure 2.4B), which may be a mechanism by which cells resist STI571. Interestingly, treatment of cells with paclitaxel reduced the STI571-dependent induction of STAT3 and ERK1/2 phosphorylation (Figure 2.4B), indicating that paclitaxel may sensitize cells to STI571 by inhibiting STI571-dependent activation of STAT3 and ERK1/2.

2.3.3 STI571 acts synergistically with cisplatin in BT-549 and MDA-MB-468 breast cancer cells to inhibit viability, proliferation, and survival.

Cisplatin is not commonly used to treat breast cancer; however, there are a number of preclinical and clinical studies underway to test whether cisplatin may be efficacious [156]. Cisplatin, a DNA damaging agent, crosslinks guanine bases in DNA strands, which inhibits the ability of the strands to uncoil and separate, thereby blocking cell division [156]. DNA damaging agents such MMS (methyl methanesulfonate), mitomycin C, and cisplatin induce apoptosis of non-transformed fibroblasts by activating the nuclear pool of c-Abl [161]. Since cisplatin induces apoptosis by activating nuclear c-Abl in fibroblasts, we hypothesized that STI571 treatment will inhibit cisplatin-induced activation of nuclear c-Abl, thereby antagonizing the effects of cisplatin. To our surprise, STI571 treatment of MDA-MB-468 cells reduced the cisplatin viability IC_{50} nearly 3-fold, and STI571 demonstrated synergism with cisplatin at multiple doses (Figure 2.5A; Table 2.1; data not shown). STI571 sensitized BT-549 to cisplatin and moderately lowered the

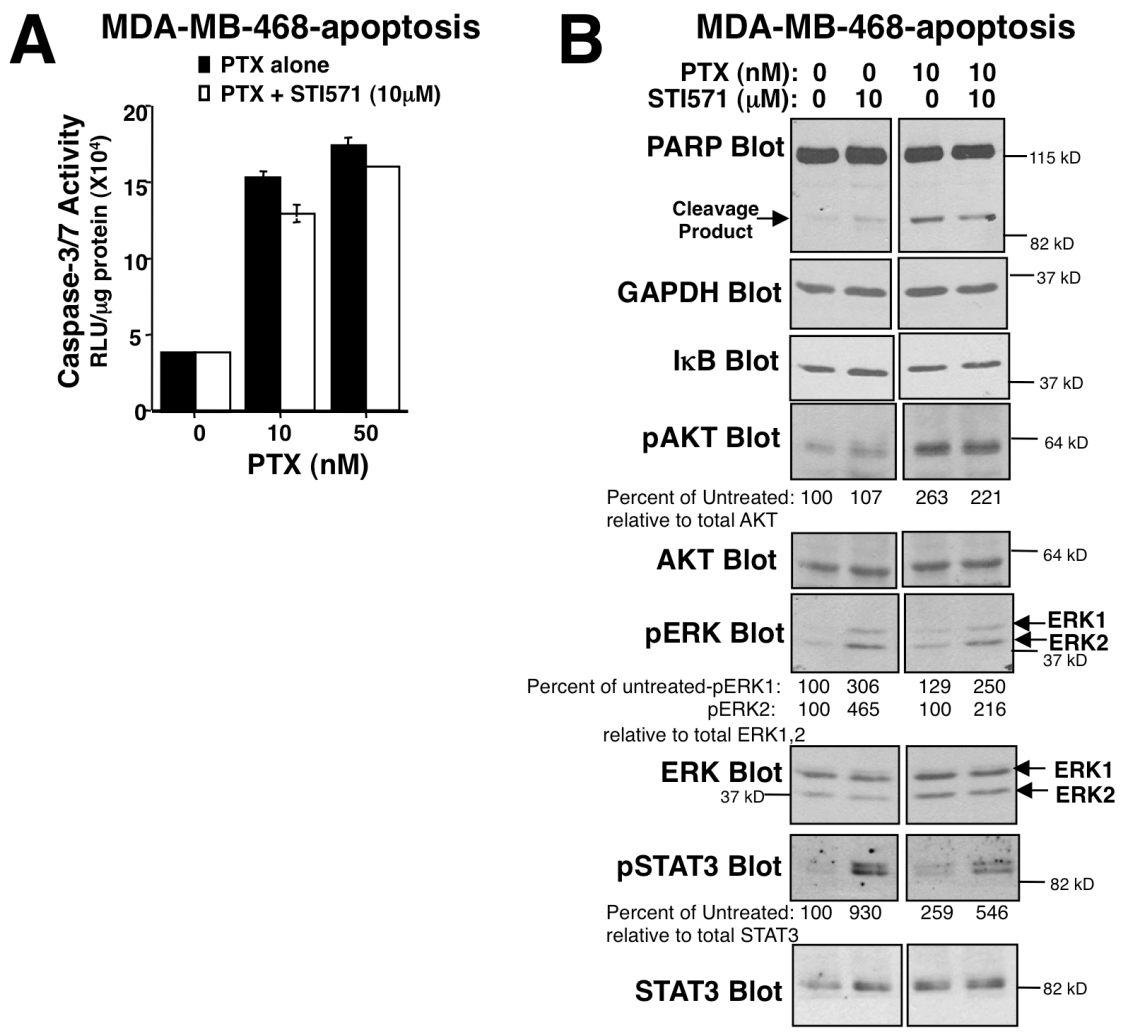

Figure 2.4. Paclitaxel inhibits STI571-induced phosphorylation of STAT3 and ERK1/2 in MDA-MB-468 cells. MDA-MB-468 cells were plated in 60mm dishes, treated with STI571 and/or paclitaxel the next day, and 40h later, detached and attached cells were lysed and apoptosis assessed by Caspase-Glo assay **(A)**, or by Western blot with PARP and GAPDH antibodies **(B)**. Mean±SEM from three independent experiments. Some error bars are too small to be visualized **(A).** PARP and GAPDH blots were stripped and probed with other antibodies **(B).** (A) Done in collaboration with S. Ganguly.

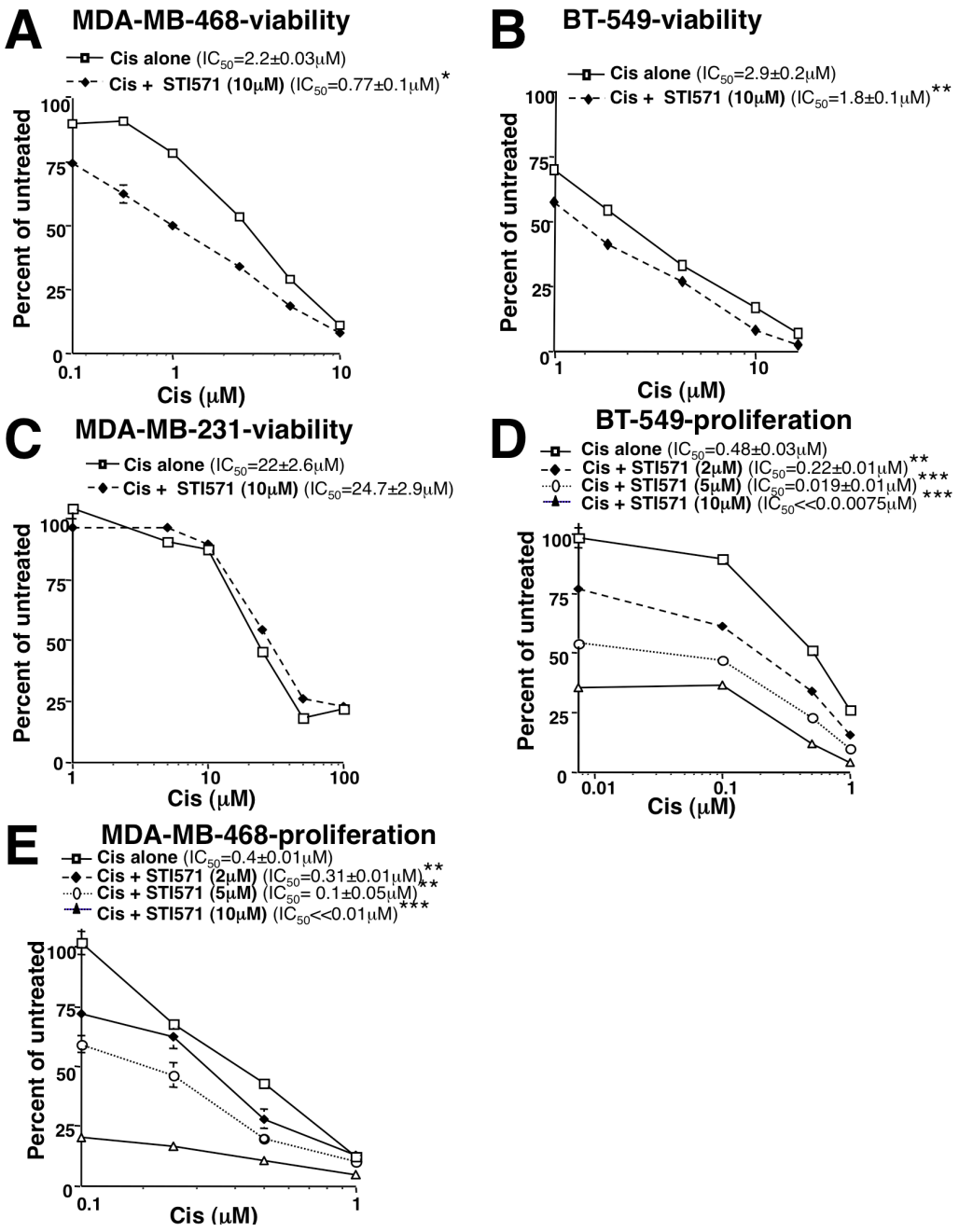

Figure 2.5. STI571 synergistically sensitizes MDA-MB-468 and BT-549 breast cancer cells to cisplatin. (A-C) Cells were plated, treated, and viability assessed as in Fig. 2.3A–C. Experiments were performed in triplicate 3 times, and representative experiments are shown. Mean±SEM. IC_{50} values are mean±SEM for 3 independent experiments. **(D, E)** Proliferation was assessed by tritiated thymidine assay as in Fig. 2.3D. Graphs shown are representative of 3 experiments. Mean±SEM. IC_{50} values are mean±SEM for 3 independent experiments. (A-E) Done in collaboration with L. Fiore. *p<0.05, **p<0.005, ***p<0.001 using Student's t-tests.

IC_{50}; however, at certain cisplatin doses (10μM, 15μM), strong synergy was observed (Figure 2.5B; Table 2.1). In contrast to BT-549 and MDA-MB-468 cells, STI571 slightly antagonized cisplatin in MDA-MB-231 cells (Figure 2.5C; Table 2.1).

To determine the mechanism by which STI571 sensitizes BT-549 and MDA-MB-468 cells to cisplatin, we assessed the effect of combination treatment on proliferation and apoptosis. In both BT-549 and MDA-MB-468 cells, STI571 synergized with cisplatin to inhibit proliferation (Figure 2.5D, E). In BT-549 cells, STI571 also dramatically sensitized cisplatin-treated cells to apoptosis, as seen by increased PARP cleavage and caspase-3/7 activity (Figure 2.6A, B), whereas in MDA-MB-468 cells, STI571 treatment did not increase cisplatin-mediated PARP cleavage or caspase-3/7 activity (Figure 2.6C, D). Taken together, these data indicate that although cisplatin induces apoptosis by activating nuclear c-Abl in non-transformed cells, inhibition of Abl family kinases using STI571 in BT-549 and MDA-MB-468 breast cancer cells does not prevent cisplatin from inhibiting viability, but rather sensitizes cells to cisplatin. In BT-549 cells, STI571 synergizes with cisplatin to inhibit cell viability by affecting both proliferation and apoptosis, whereas in MDA-MB-468 cells, the synergistic effect of STI571+cisplatin on viability is due to decreased proliferation. In contrast, in MDA-MB-231 cells, STI571 antagonized the effects of cisplatin (Figure 2.5C; Table 2.1), which suggests that there is something intrinsically different about the MDA-MB-231 cell line, which prevents STI571 from sensitizing the cells to cisplatin.

To determine the mechanism by which STI571 synergistically inhibits proliferation and induces apoptosis in cisplatin-treated BT-549 cells, we analyzed PI3K/Akt, ERK1/2, STAT3, and NF-κB signaling pathways. Interestingly, STI571 and cisplatin independently increased the stability of IκB (Figure 2.6A), which negatively regulates NF-κB signaling. However, STI571+cisplatin combination treatment did increase IκB stabilization (Figure 2.6A), suggesting that inhibition of NF-κB signaling is not a likely mechanism by which STI571 sensitizes BT-549 cells to cisplatin. Similarly, cisplatin treatment resulted in a significant reduction in STAT3 phosphorylation; however, addition of STI571 had no additional effect (Figure 2.6A). Significantly, STI571 increased the ability of cisplatin to inhibit constitutive Akt phosphorylation (Figure 2.6A), which indicates that STI571 is likely to increase apoptosis by inhibiting activation of the PI3K/Akt pathway. STI571 treatment also increased phosphorylation of ERK2, and cotreatment with cisplatin further increased ERK2 phosphorylation (Figure 2.6A). Activation of ERK2 by STI571 and cisplatin could be a mechanism by which BT-549

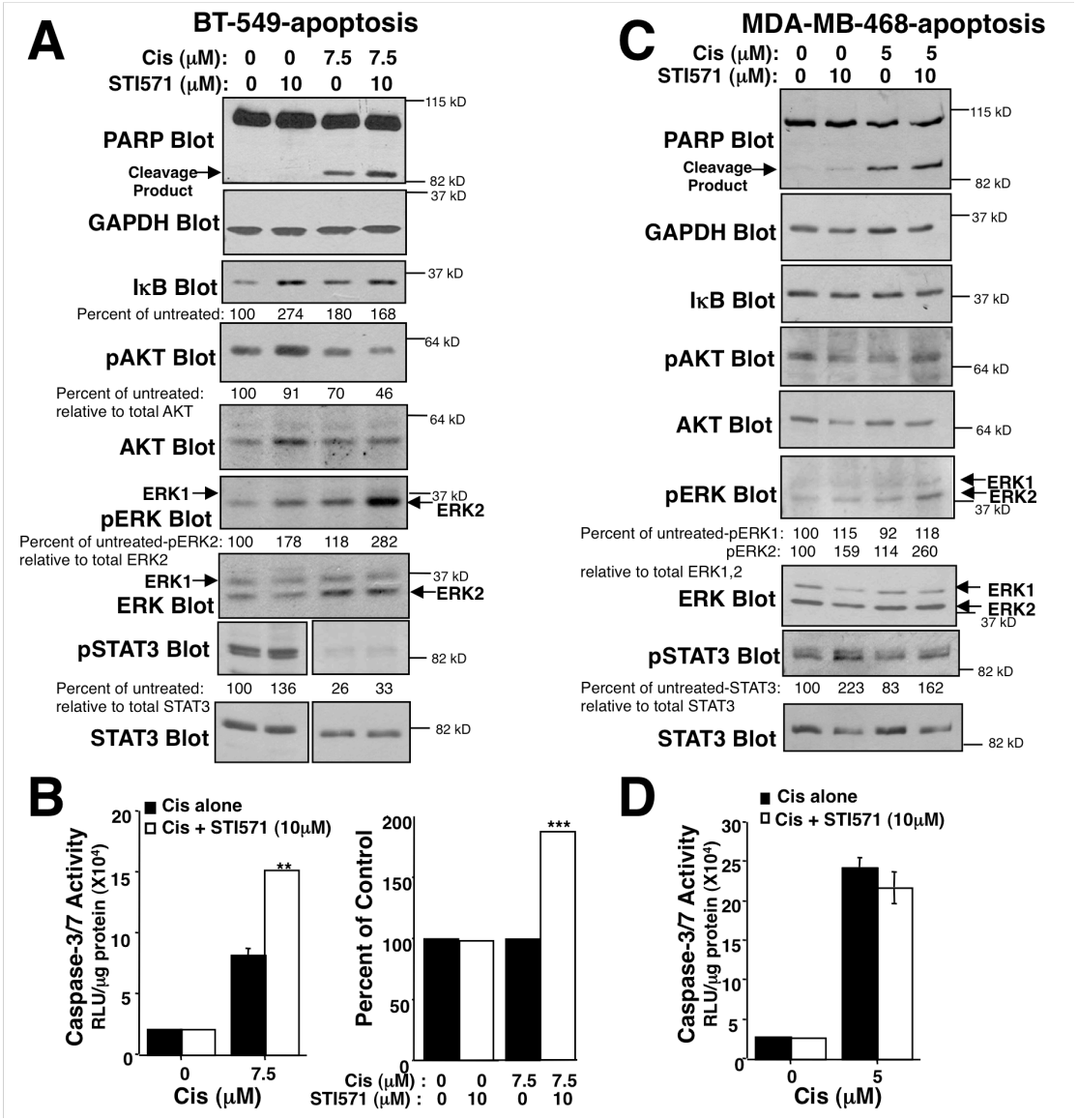

Figure 2.6. Cisplatin and STI571 synergize to induce apoptosis in BT-549 cells. BT-549 and MDA-MB-468 cells were plated in 60mm dishes, treated with STI571 and/or cisplatin the next day, and 40h later, detached and attached cells were lysed and blotted with antibodies to PARP and GAPDH **(A, C)** or caspase-3/7 activity was assessed by Caspase-Glo assay from duplicate samples **(B, D).** PARP and GAPDH blots were stripped and reprobed with other antibodies **(A, C).** Experiments shown are representative of three independent experiments. Mean±SEM. **(B-left, D)**. Mean±SEM of three independent experiments where STI571 alone is normalized to untreated, and Cis+STI571 is normalized to cisplatin alone **(B-right).** Some error bars are too small to be seen. (A, C, D) Done in collaboration with S. Ganguly. **p<0.01, ***p<0.001 using a Student's t-test.

cells resist the effects of STI571 and cisplatin. However, it is also possible that ERK2 upregulation is a mechanism by which both drugs inhibit proliferation and induce apoptosis, since STI571 treatment of BCR-Abl$^+$ CML cells increases ERK1/2 activity, and treatment with a MEK1/2 inhibitor increases suppression of CML progenitors, and sensitizes cells to STI571-dependent apoptosis [162, 163]. Interestingly, in MDA-MB-468 cells, STI571 and cisplatin had no effect on IκB stability or Akt phosphorylation, and similar to BT-549 cells, STI571 increased ERK2 activation in a synergistic manner with cisplatin (Figure 2.6C). In addition, STI571 increased STAT3 phosphorylation, and cisplatin treatment decreased the STI571-dependent effect (Figure 2.6C). Therefore, cisplatin may synergize with STI571 in MDA-MB-468 cells by inhibiting the STI571-dependent increase in STAT3 phosphorylation and/or by increasing ERK2 phosphorylation.

2.3.4 STI571 chemosensitizes MDA-MB-231 cells to camptothecin.

Camptothecin binds topisomerase I, and prevents it from religating DNA, which results in single strand breaks in DNA, and camptothecin also stabilizes the topoisomerase I/DNA complex so that single strand nicks result in double strand breaks [154]. STI571 sensitized MDA-MB-468 and BT-549 cells to camptothecin in an additive fashion, and there was a 2-fold reduction in the IC_{50} in the presence of STI571 (Figure 2.7A, B; Table 2.1). In MDA-MB-231 cells, STI571 had an additive→antagonistic effect with camptothecin, when camptothecin was added at the same time as STI571 (Figure 2.7C; Table 2.1). However, when MDA-MB-231 cells were treated with camptothecin 24 hours prior to addition of STI571 (alternate dosing), STI571 synergistically sensitized cells to camptothecin, reducing the camptothecin IC_{50} 5-fold (Figure 2.7D; Table 2.1). An alternate dosing regimen also was tested with STI571 and other chemotherapeutic agents in MDA-MB-231 cells, and a similar response was not noted (data not shown), indicating that the effect of alternate dosing is specific for the STI571+camptothecin combination. Similarly, synergistic effects of STI571 and camptothecin were observed on the proliferation of MDA-MB-231 cells, using an alternate dosing regimen (Figure 2.7E; Table 2.1). In MDA-MB-468 cells, STI571 also sensitized the cells to the anti-proliferative effects of camptothecin, and synergized with camptothecin at higher doses (0.035μM) (Figure 2.7F; Table 2.1).

To determine whether STI571 increases the ability of camptothecin to induce apoptosis, PARP and caspase-3/7 assays were performed. In MDA-MB-231 cells,

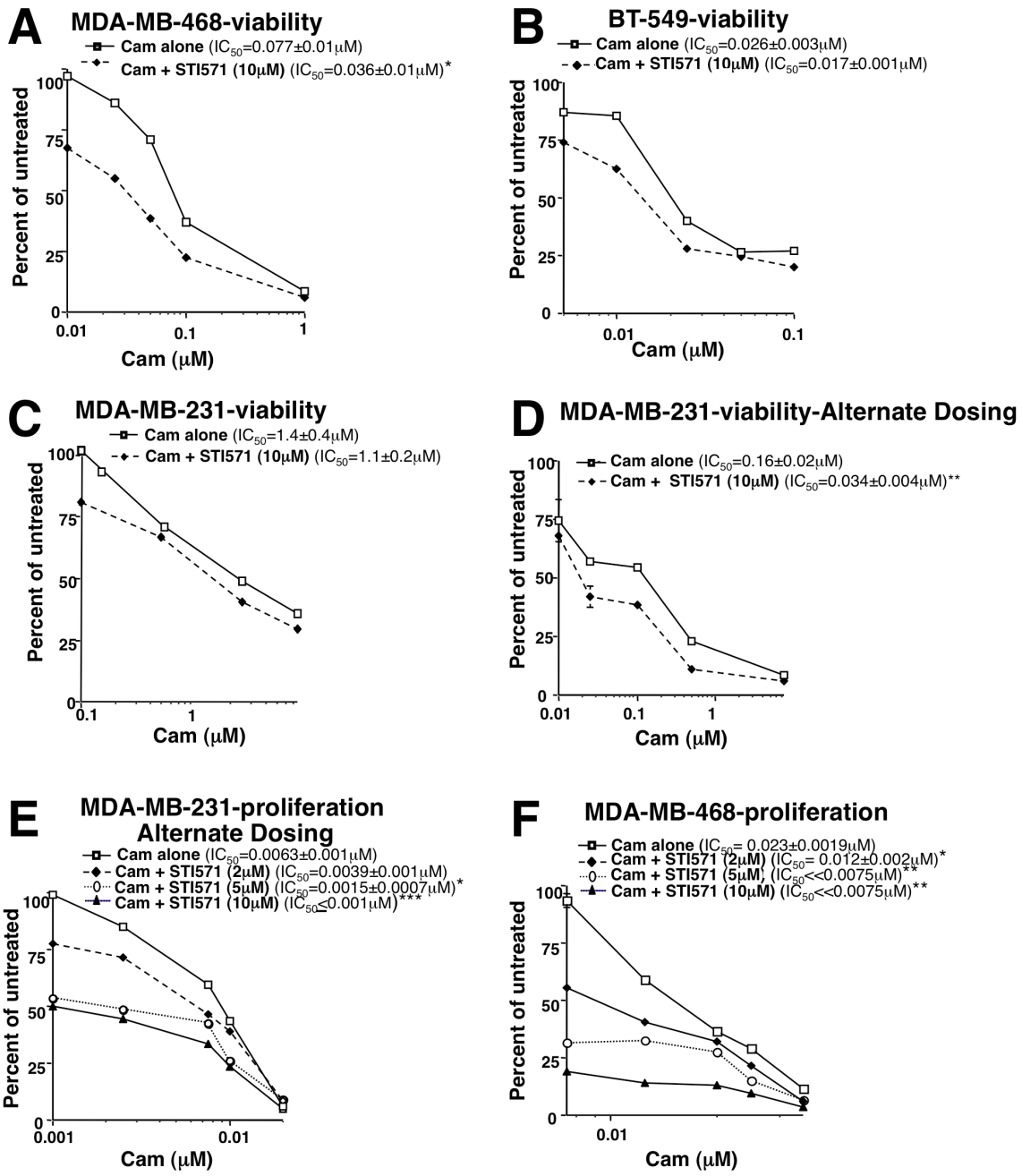
A
MDA-MB-468-viability
Cam alone (IC50=0.077±0.01μM)
Cam + STI571 (10μM) (IC50=0.036±0.01μM)*
Percent of untreated
Cam (μM)
B
BT-549-viability
Cam alone (IC50=0.026±0.003μM)
Cam + STI571 (10μM) (IC50=0.017±0.001μM)
Percent of untreated
Cam (μM)
C
MDA-MB-231-viability
Cam alone (IC50=1.4±0.4μM)
Cam + STI571 (10μM) (IC50=1.1±0.2μM)
Percent of untreated
Cam (μM)
D
MDA-MB-231-viability-Alternate Dosing
Cam alone (IC50=0.16±0.02μM)
Cam + STI571 (10μM) (IC50=0.034±0.004μM)**
Percent of untreated
Cam (μM)
E
MDA-MB-231-proliferation
Alternate Dosing
Cam alone (IC50=0.0063±0.001μM)
Cam + STI571 (2μM) (IC50=0.0039±0.001μM)
Cam + STI571 (5μM) (IC50=0.0015±0.0007μM)*
Cam + STI571 (10μM) (IC50≤0.001μM)***
Percent of untreated
Cam (μM)
F
MDA-MB-468-proliferation
Cam alone (IC50= 0.023±0.0019μM)
Cam + STI571 (2μM) (IC50= 0.012±0.002μM)*
Cam + STI571 (5μM) (IC50<<0.0075μM)**
Cam + STI571 (10μM) (IC50<<0.0075μM)**
Percent of untreated
Cam (μM)

Figure 2.7. STI571 and camptothecin synergize to inhibit the viability and proliferation of MDA-MB-231 cells when utilizing an alternate dosing schedule. (A-D) MDA-MB-468, BT-549, and MDA-MB-231 cells were plated, treated as described in Fig. 2.3A–C, and viability assessed. For alternate dosing experiments, MDA-MB-231 cells were plated in triplicate in 96-well dishes, camptothecin was added the next day, and the following day, the media was changed and camptothecin and STI571 were added. Cells were harvested for the CellTiter-Glo assay 72h later **(D).** Experiments were repeated three times, and representative experiments are shown. Mean±SEM IC_{50} values are mean±SEM for three independent experiments. **(E)** MDA-MB-231 cells were plated in 24-well dishes, and treated for 24h with camptothecin alone, followed by 72h of STI571+camptothecin, and tritiated thymidine incorporation was measured. **(F)** MDA-MB-468 cells were set-up and treated as described in Fig. 2.3D, and tritiated thymidine incorporation assessed. Experiments were repeated three times, and representative experiments are shown. Mean±SEM. IC_{50} values are mean±SEM for three independent experiments. *$p<0.05$, **$p<0.01$ using Student's t-tests.

STI571 had no effect on the ability of camptothecin to induce apoptosis (Figure 2.8A, B), whereas in MDA-MB-468 cells, STI571 antagonized the apoptotic effects of camptothecin (Figure 2.8C, D). Thus, in MDA-MB-468 cells, STI571 synergistically increases the ability of camptothecin to inhibit proliferation, while it only has additive effects on viability. This is likely due to the fact that STI571 antagonizes the ability of camptothecin to induce apoptosis, resulting in a decreased overall effect on viability. In MDA-MB-231 cells, synergistic effects of STI571 and camptothecin were observed both in proliferation and viability assays, whereas STI571 had no effect on apoptosis, indicating that camptothecin inhibits the viability of MDA-MB-231 cells solely by affecting cell proliferation.

In MDA-MB-231 cells, STI571 and camptothecin had little effect on STAT3 phosphorylation, Akt was not constitutively phosphorylated in this cell type, as a band the correct size was not detected, and ERK1/2 phosphorylation was decreased by camptothecin treatment, but this inhibition was not enhanced by STI571 (Figure 2.8A). Conversely, the stability of IκB was enhanced in MDA-MB-231 cells treated with STI571 or camptothecin, and the combination regimen further increased IκB stability (Figure 2.8A). These data indicate that inhibition of NF-κB signaling is a likely mechanism by which STI571 sensitizes MDA-MB-231 cells to the anti-proliferative effects of camptothecin. In MDA-MB-468 cells, STI571 induced a modest decrease in Akt phosphorylation; however, this inhibition was not reproducible and camptothecin had no additional effect on Akt phosphorylation (Figure 2.8C). Interestingly, STAT3 phosphorylation was induced by STI571, and treatment with camptothecin prevented this upregulation (Figure 2.8C), similar to what was observed in MDA-MB-468 cells treated with paclitaxel (Figure 2.4B). These data indicate that camptothecin may synergize with STI571 to inhibit proliferation in MDA-MB-468 cells by preventing STI571-dependent upregulation of STAT3. ERK1/2 also was upregulated by STI571 treatment and addition of camptothecin increased this upregulation (Figure 2.8C), similar to what was observed in BT-549 cells treated with STI571 and cisplatin (Figure 2.6A).

2.3.5 STI571 synergistically sensitizes MDA-MB-468 cells to 5-fluorouracil.

5-fluorouracil (5-FU) is an anti-metabolite; FUTP incorporates into RNA, FdUTP incorporates into DNA, and FdUMP forms a complex with thymidylate synthase [155]. 5-FU is incorporated in the place of purines or pyrimidines, and prevents purine/pyrimidine incorporation into DNA during S-phase, inhibiting cell division [155]. 5-FU also inhibits

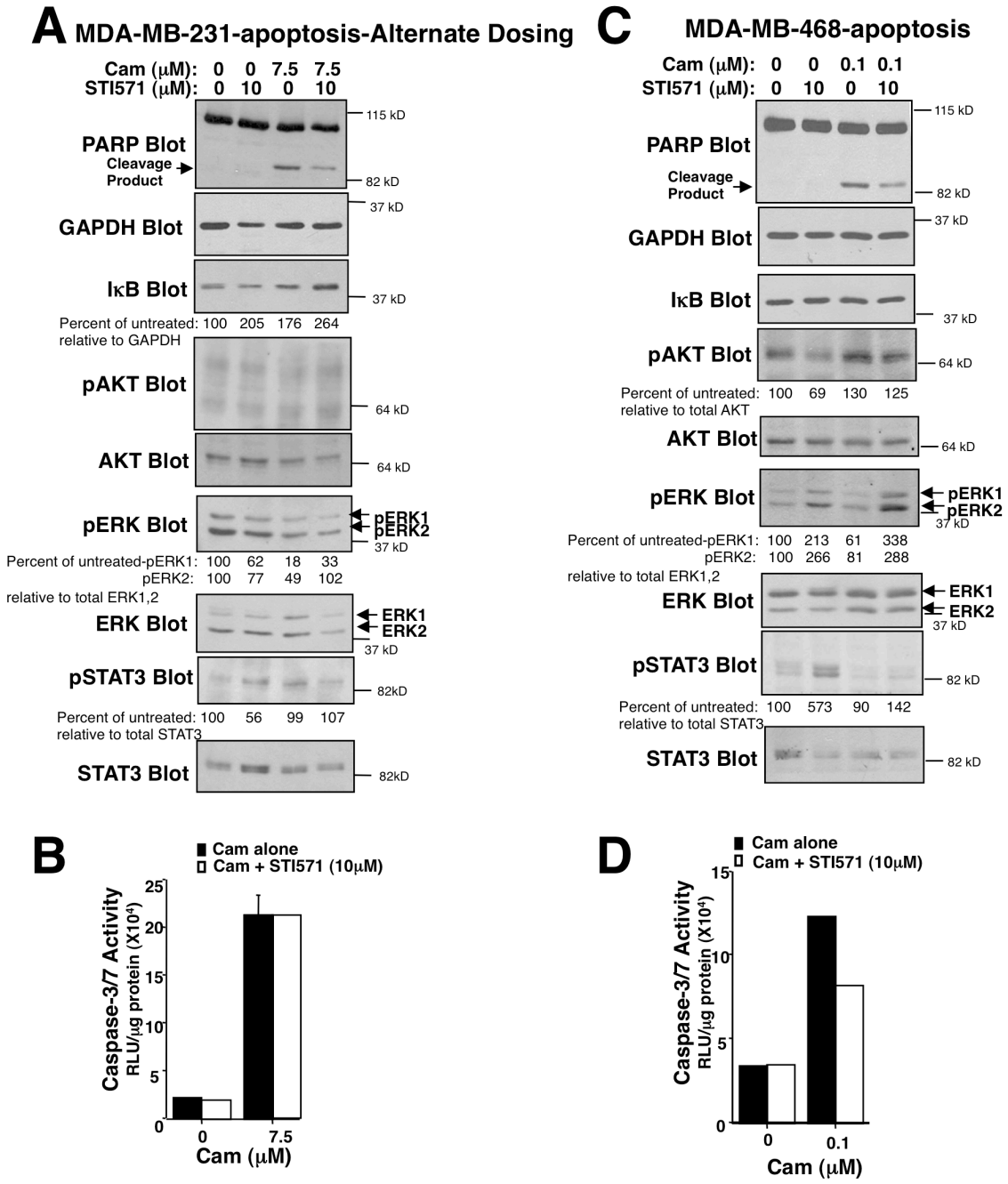

Figure 2.8. STI571 synergizes with camptothecin to increase the stability of IκB in MDA-MB-231 cells, but STI571 has no effect on the ability of camptothecin to induce apoptosis. Cells were plated in 60mm dishes, treated with STI571 and/or camptothecin the next day, and 40h later, detached and attached cells were lysed and blotted with antibodies to PARP and GAPDH **(A, C)** or caspase-3/7 activity was assessed by Caspase-Glo assay **(B, D).** Mean±SEM for three independent experiments. (D) Done in collaboration with S. Ganguly.

thymidine incorporation into DNA, which inhibits DNA/RNA synthesis [155]. STI571 sensitized MDA-MB-468 cells to 5-FU in a synergistic manner only at higher doses of 5-FU (100–500μM), but had additive/antagonistic effects at lower doses (Figure 2.9A; Table 2.1). These data indicate that STI571 may kill or prevent the proliferation of a small population of MDA-MB-468 cells that are intrinsically resistant to 5-FU and survive high doses of the drug. In contrast, in BT-549 and MDA-MB-231 cells, STI571 antagonized the effects of 5-FU on cell viability (Figure 2.9B, C; Table 2.1). Interestingly, although STI571 reduced the viability of 5-FU-treated MDA-MB-468 cells in a synergistic manner, synergism was not observed in proliferation assays, and in fact STI571 actually antagonized the effect of 5-FU on proliferation at several 5-FU doses (e.g. 1.25μM, 3.5μM; Figure 2.9D; Table 2.1). This may be due to the fact that lower doses of 5-FU were utilized in proliferation assays. To test this hypothesis, we repeated the proliferation assays using high doses of 5-FU, and indeed, STI571 synergized with high doses of 5-FU to inhibit proliferation (Figure 2.9E; Table 2.1). These data confirm that STI571 induces synergism by preventing the proliferation of cells that survive high doses of 5-FU. We performed PARP and caspase-3/7 assays to determine whether STI571 also reduces the viability of MDA-MB-468 cells by increasing apoptosis. Significantly, STI571 dramatically sensitized MDA-MB-468 cells to apoptotic death induced by high doses of 5-FU (Figure 2.10A, B). Thus, STI571 sensitizes MDA-MB-468 cells to 5-FU by increasing its ability to induce apoptosis as well as by inhibiting proliferation, and STI571 may specifically target residual cells that are resistant to 5-FU.

STI571 did not increase IκB stability in MDA-MB-468 cells treated with 5-FU (Figure 2.10A) nor did STI571 alter Akt phosphorylation, indicating that STI571 does not increase apoptosis or reduce proliferation by inhibiting NF-κB or PI3K/Akt signaling. However, as was observed in MDA-MB-468 cells treated with cisplatin (Figure 2.6C), STI571 increased STAT3 phosphorylation (Figure 2.10A), and addition of 5-FU prevented STI571-dependent STAT3 upregulation (Figure 2.10A), indicating that this may be a mechanism by which the combination treatment inhibits proliferation. In addition, ERK1/2 phosphorylation was dramatically increased in the combination treatment regimen, which indicates that the Ras/ERK signaling may also be involved in the antiproliferative response (Figure 2.10A).

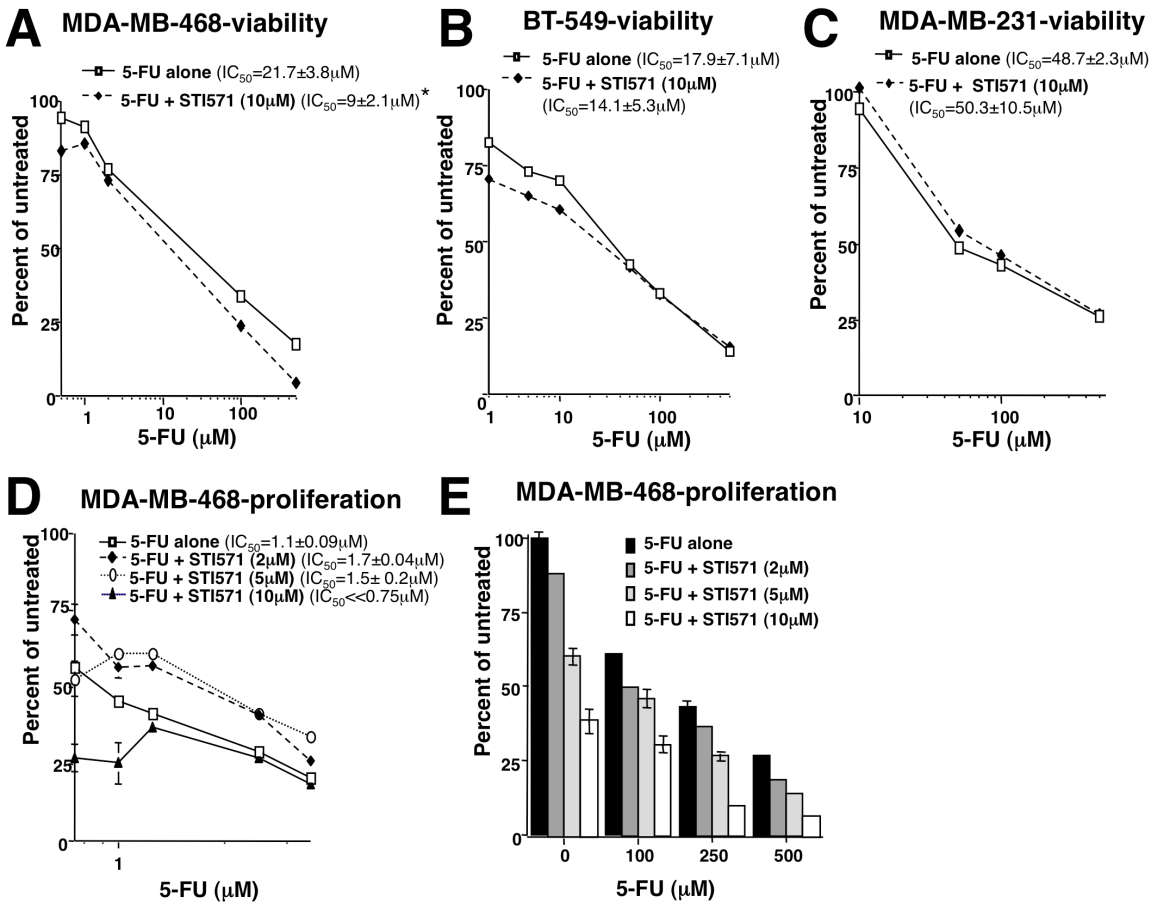

Figure 2.9. STI571 synergizes with high doses of 5-fluorouracil in MDA-MB-468 cells, while STI571 antagonizes the effects of 5-fluorouracil in BT-549 and MDA-MB-231 cells. (A-C) Cells were plated, treated with STI571 and/or 5-fluorouracil for 96h, and viability assessed as in Fig. 2.3A. Experiments were repeated three times, and representative experiments are shown. Mean±SEM. IC_{50} values are mean±SEM for three independent experiments. **(D,E)** MDA-MB-468 cells were set-up and treated with STI571 and/or 5-FU for 72 **(E)** or 96h **(D),** and tritiated thymidine incorporation assessed. Experiments were repeated three times, and representative experiments are shown. Mean±SEM. IC_{50} values are mean±SEM for three independent experiments. (A) Done in collaboration with C. Holler and L. Fiore. (C) Done in collaboration with E. Park. (D) Done in collaboration with S. Ganguly. *$p<0.05$ using a Student's t-test.

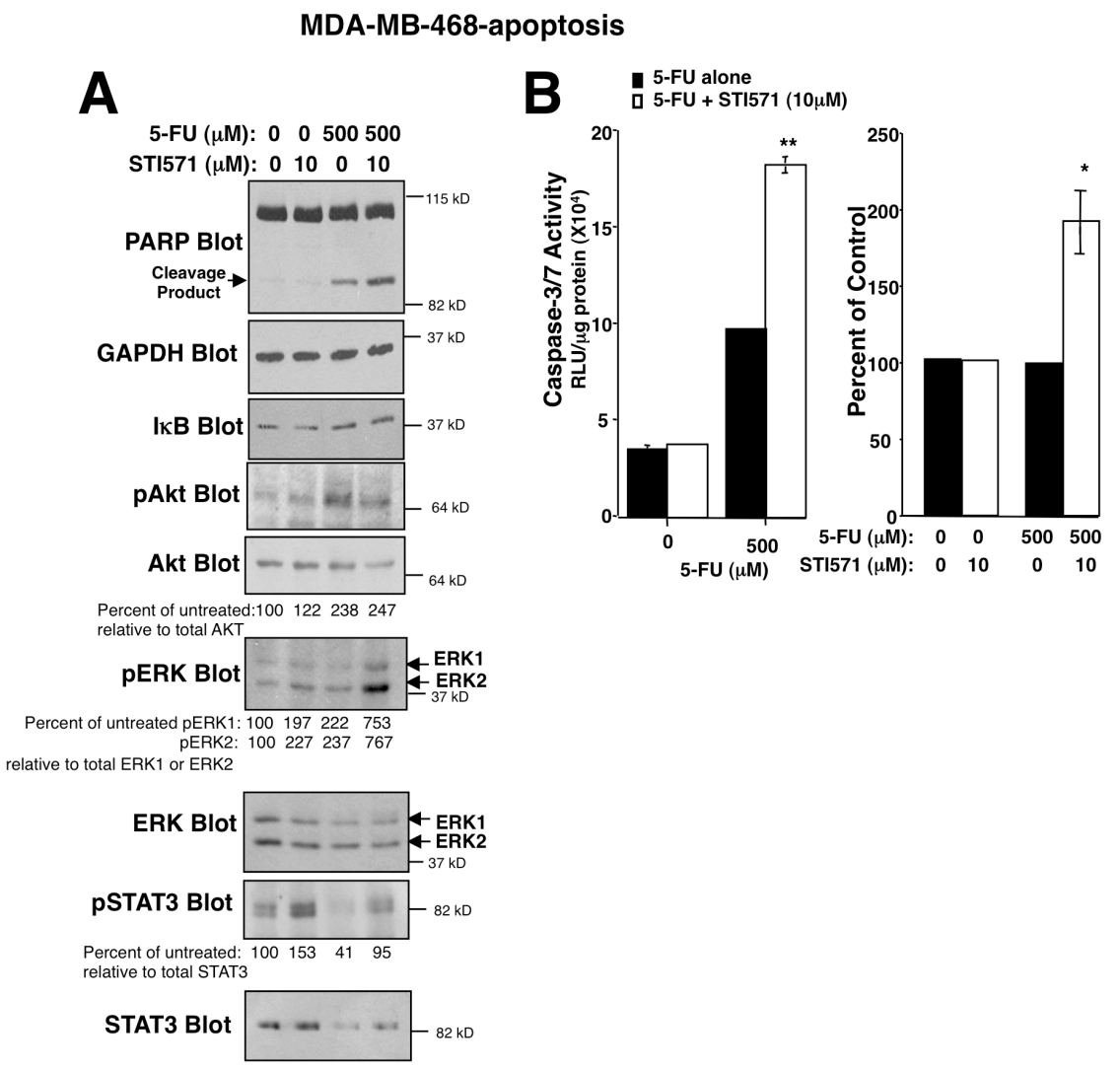

Figure 2.10. STI571 increases the ability of 5-FU to induce apoptosis. (A) PARP cleavage, western blots, and **(B)** caspase-3/7 activity were assessed as described in Fig. 2.4. Mean±SEM for three independent experiments. **(B-left)**. Mean of three independent experiments where STI571 alone is normalized to untreated, and 5-FU+STI571 is normalized to 5-FU alone **(B-right)**. Some error bars are too small to be seen. (A, B) Done in collaboration with S. Ganguly. *p<0.05, **p<0.01 using a Student's t-test.

2.3.6 STI571 strongly antagonizes the effects of mechloroethamine in all breast cancer cell lines.

Mechlorethamine, a metabolite of cyclophosphamide, is an alkylating agent that: 1) attaches alkyl groups to DNA bases, which results in DNA fragmentation; 2) induces DNA damage by forming crosslinks that prevent DNA strands from separating; and 3) induces mispairing of nucleotides, which leads to mutations [164]. Interestingly, STI571 strongly antagonized the effects of mechloroethamine on viability in all breast cancer cell lines examined (Figure 2.11; Table 2.1), which indicates that Abl family kinases or another STI571 target is likely to be required for the action of mechloroethamine in breast cancer cells.

2.3.7 MDA-MB-468 and MDA-MB-231 cells have similar levels of nuclear and cytoplasmic c-Abl.

In MDA-MB-231 cells, STI571 had antagonistic effects with all chemotherapeutic agents examined except for camptothecin. In contrast, in MDA-MB-468 cells, STI571 had either additive or synergistic effects with all the chemotherapeutic agents examined, except for mechloroethamine. DNA damaging agents induce apoptosis in non-transformed fibroblasts by activating the nuclear pool of c-Abl [161]. Thus, STI571, which is likely to inhibit nuclear c-Abl, could antagonize the effects of chemotherapeutic agents if there is large pool of c-Abl localized in the nucleus. To determine whether MDA-MB-231 cells have higher levels of nuclear c-Abl than MDA-MB-468 cells, we performed subcellular fractionation. Both cell lines contained high levels of c-Abl in the cytoplasm, and lower levels of c-Abl in the nucleus (Figure 2.12A). These data indicate that increased expression of nuclear c-Abl is not likely to be the reason that MDA-MB-231 cells are more resistant to the effects of STI571 in combination with chemotherapeutic agents than MDA-MB-468 cells (Figure 2.12A).

2.4 Discussion

In this chapter, we demonstrate for the first time that STI571 sensitizes breast cancer cells containing highly active Abl family kinases to several conventional chemotherapeutic agents. Interestingly, sensitization is cell type-specific in that STI571 synergizes with paclitaxel, cisplatin, and 5-FU in MDA-MB-468 cells, while STI571 only synergizes with cisplatin in BT-549 cells, and with camptothecin in MDA-MB-231 cells. These data indicate that there are intrinsic differences between the three cell lines,

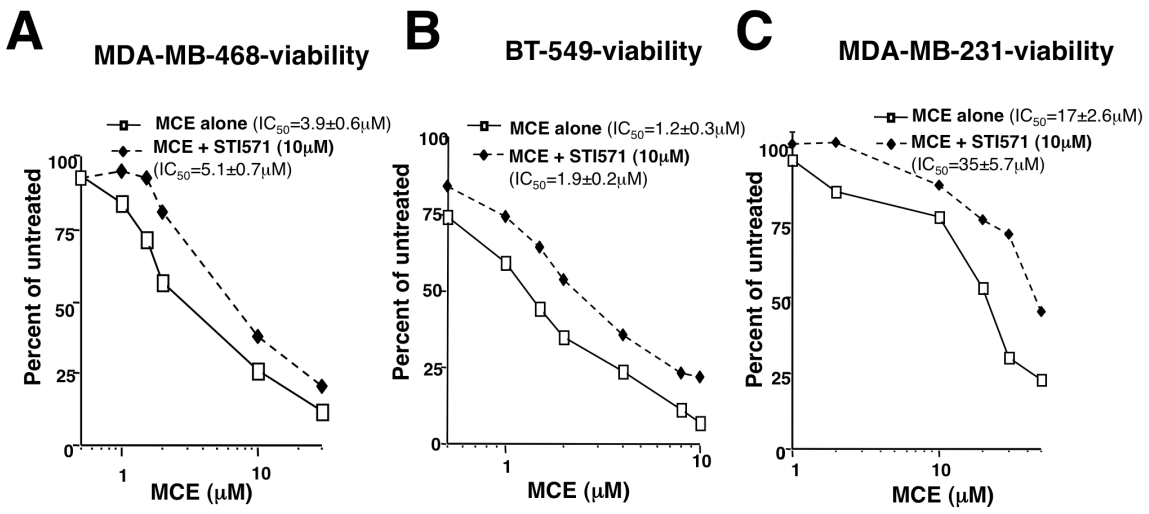

Figure 2.11. STI571 and mechloroethamine are antagonistic in all breast cancer cell lines. Cells were plated, treated, and viability assessed as in Fig. 2.3A. Experiments were repeated three times, and representative experiments are shown. Mean±SEM. IC_{50} values are mean±SEM for three independent experiments. (A-C) Done in collaboration with C. Holler.

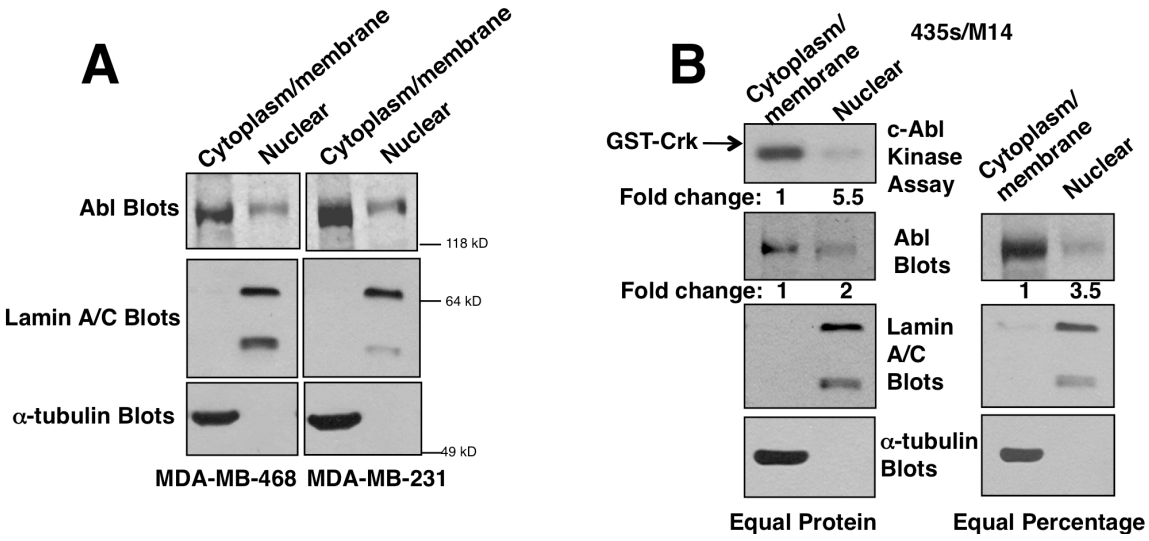

Figure 2.12. Abl kinases are preferentially activated and reside primarily in the cytoplasm. (A, B) Cells were fractionated using NE-PER (Pierce; Rockford, IL) into cytoplasmic/membrane and nuclear fractions. Equal percentages of the fractions were loaded on an SDS-PAGE gel, and blotted with c-Abl antibody (A, B) or analyzed by *in vitro* kinase assay (B). Lysates also were blotted with antibodies to α-tubulin to assess the purity of the cytoplasmic fractions, and lamin A/C to assess nuclear fraction purity.

which govern their susceptibility to STI571/conventional chemotherapy combination regimens. Interestingly, the three cell lines all have fairly equal sensitivities to the effect of STI571 alone on viability (data not shown). When tritiated thymidine incorporation and growth kinetic assays are used to measure the sensitivity of the cell lines to STI571, BT-549 and MDA-MB-468 cells are equally sensitive, while STI571 takes more time to inhibit the growth of MDA-MB-231 cells [39]. However, the overall effect after 4–5 days of STI571 treatment is similar between the three cell lines [39]. Activation of particular signaling pathways or increased expression of drug transporters may explain the differential sensitivity of the cell lines to different STI571/chemotherapeutic combination regimens. However, regardless of the mechanism, our data are significant because they indicate that STI571 may be effective in certain combination regimens.

Tetrazolium salt assays (MTT, MTS, XTT) are often used to screen cell lines for sensitivity to drugs, due to the fact that they are relatively inexpensive, are quick, easy, and quantitative. However, our data clearly show that STI571 cannot reliably be used in MTT assays when utilizing doses of 1−10μM (Figure 2.2; data not shown), as it interferes with the assay. MTT assays have frequently been used to study the effects of STI571. In leukemic cells, BCR-Abl is much more sensitive to STI571, and doses of 0.1−1μM inhibit BCR-Abl phosphorylation and/activity [32]. At these doses, STI571 may not affect the MTT assay or may not affect it to as great an extent as when higher doses are used. However, we and others have shown that higher doses of STI571 (5−10μM) are required to inhibit the activity of endogenous Abl family kinases in nontransformed cells and in solid tumor cell lines [38, 165]. Therefore, MTT assays cannot reliably be utilized to determine the effect of STI571 on the viability of solid tumor cells if doses >1 μM are utilized, as STI571 interferes with the assay, which may lead to erroneous conclusions.

Previously, we showed that the effects of STI571 on proliferation, survival, anchorage-independent growth, and invasion of breast cancer cells containing highly active Abl family kinases were c-Abl/Arg-dependent as siRNA produced similar results [38, 39]. In addition, except for MDA-MB-468 cells, cell lines containing high c-Abl/Arg activities were sensitive to STI571 even though they did not express other STI571 targets (c-Kit or PDGF (platelet-derived-growth factor) receptors) [38]. To determine whether STI571 synergizes with chemotherapeutic agents specifically by inhibiting Abl family kinases, we attempted to test whether silencing Abl family kinases sensitizes cells to the chemotherapeutic drugs. Since cells must be transfected with siRNAs or shRNAs

prior to being treated with chemotherapeutic agents, these experiments were unsuccessful, as silencing Abl family kinases significantly slowed cell growth, thereby decreasing the effectiveness of the chemotherapeutic drugs, which act on highly proliferating cells (data not shown). These data highlight the importance of inhibiting Abl family kinases at the same time or after chemotherapeutic drug administration. In order to inhibit Abl family kinases during this time frame, cell lines expressing inducible shRNAs must be obtained; a laborious process which often results in inefficient silencing. Regardless of whether or not STI571 targets Abl family kinases to sensitize breast cancer cells to chemotherapeutic agents, the data we obtained are still significant, as they indicate that use of STI571 with some chemotherapeutic agents may be a viable treatment option for some STI571-sensitive breast cancers. Clearly, the treatment combinations will require individualization since some cells are responsive to certain combinations and others are not. STI571 also has been shown to synergize with camptothecin in small cell lung cancer cells [166], cisplatin in head and neck cancer [167] and lung cancer cells [168], carboplatin in ovarian [169], paclitaxel in ovarian [169], and 5-FU in colon cancer cells [170]. The target of STI571 in these cell lines also has not been proven, most likely due to the difficulty in using siRNA/shRNA approaches.

Interestingly, although STI571 synergizes with both cisplatin and 5-FU in MDA-MB-468 cells, it does so by different mechanisms. STI571 sensitizes MDA-MB-468 cells to cisplatin by increasing its ability to inhibit proliferation. In contrast, STI571 sensitizes MDA-MB-468 cells to high doses of 5-FU by dramatically increasing its ability to induce apoptosis, and by targeting cells that are resistant to high doses of 5-FU. These data demonstrate that STI571 acts not only as a cytostatic agent but also as a cytotoxic agent in breast cancer cells. The different mechanisms of action of the chemotherapeutic drugs are likely to affect the ability of STI571 to synergize with the chemotherapeutic agents. Previously, we showed that STI571 slows serum-induced G1→S progression of breast cancer cells containing highly active Abl family kinases [38, 39]. Thus, by slowing S-phase progression, STI571 may prevent incorporation of 5-FU into DNA in S-phase resulting in drug antagonism at low 5-FU doses. Such an effect may not be observed at high doses, as STI571 may specifically target cells that are resistant to high doses of 5-FU, perhaps by inhibiting a drug transporter which effluxes 5-FU. Indeed, STI571 inhibits and/or is a substrate for ABCB1 and ABCG2/BCRP [148, 171-175], and 5-FU is a substrate of ABCG2 [176] and ABCC5 [177].

Significantly, STI571 synergizes with cisplatin in both MDA-MB-468 and BT-549

cells. In MDA-MB-468 cells, STI571 increases the ability of cisplatin to inhibit proliferation, whereas in BT-549 cells, STI571 enhances both the anti-proliferative and pro-apoptotic effects of cisplatin. These data are interesting because previous data indicated that cisplatin induces apoptosis of non-transformed fibroblasts by activating the nuclear pool of c-Abl [161]. Clearly, cisplatin does not induce apoptosis of BT-549 breast cancer cells via this mechanism, as STI571 would be predicted to prevent cisplatin-induced apoptosis. However, unlike fibroblasts, breast cancer cells have highly active Abl family kinases. Preliminary data in another solid tumor cell line, 435s/M14, which also contains highly active Abl family kinases [38, 39], show that the pool of c-Abl that is highly active is primarily the cytoplasmic/membrane pool and not the nuclear pool (Figure 2.12B). These data are not particularly surprising given that activation of nuclear c-Abl is associated with apoptosis rather than proliferation, and that c-Abl is activated by cytoplasmic/membrane receptor tyrosine kinases and Src kinases in breast cancer cells [38, 39]. Thus, STI571 treatment of breast cancer cells may preferentially inhibit the highly active cytoplasmic/membrane c-Abl pool as opposed to the smaller, less-active nuclear pool. In addition, Arg is not located in the nucleus, Arg is the only Abl family kinase that is highly active in MDA-MB-468 cells, and in BT-549 cells, although both c-Abl and Arg have elevated activities, Arg activity is much higher than c-Abl [38, 39]. Therefore, it is possible that STI571 synergizes with cisplatin in these two cell lines by targeting Arg. In contrast, cisplatin has less of an effect in MDA-MB-231 cells, which have more highly active c-Abl than Arg. MDA-MB-231 cells, in general, are more resistant to STI571/chemotherapeutic combination regimens, and this could be due to the fact that c-Abl, rather than Arg, is the main Abl family kinase activated in these cells [38, 39].

Although STI571 has cytotoxic effects in combination with cisplatin in BT-549 cells and 5-FU in MDA-MB-468 cells, the molecular mechanisms are different. In BT-549 cells, STI571 increases the ability of cisplatin to inhibit constitutive Akt phosphorylation, while in MDA-MB-468 cells treated with 5-FU, STI571 does not alter Akt phosphorylation. As mentioned earlier, STI571 may inhibit a 5-FU transporter in MDA-MB-468 cells, thereby sensitizing resistant cells to 5-FU. Future experiments will address this possibility. In MDA-MB-231 cells, STI571 sensitizes cells to camptothecin most likely by increasing the stability of IκB, thereby inhibiting NF-κB signaling which promotes proliferation. In MDA-MB-468 cells, STI571 treatment causes increased phosphorylation of STAT3, and treatment with paclitaxel, cisplatin, camptothecin or 5-FU inhibits the

STI571-dependent STAT3 activation. Since STAT3 induces proliferation of breast cancer cells, MDA-MB-468 cells may resist the effects of STI571 by activating STAT3, and treatment with conventional chemotherapeutic agents, which prevents this upregulation, may prevent resistance. Thus, inhibition of STAT3 activation may be a common mechanism by which STI571 synergizes with chemotherapeutic agents to inhibit the proliferation of MDA-MB-468 cells. Taken together, these data indicate that the mechanisms by which STI571 potentiates the effects of chemotherapeutic agents are not only cell type-specific but also are specific for particular STI571/chemotherapeutic combinations.

In summary, our data demonstrate that STI571 cooperates with several conventional chemotherapeutic agents to inhibit viability by decreasing proliferation and/or increasing apoptosis. These data indicate that STI571 may be an effective agent in combination chemotherapy for treating breast cancer patients with ER^-, PR^- tumors that have active Abl family kinases. However, our data indicate that the cellular milieu dictates which cells will be sensitive to particular therapeutic combinations, which emphasizes the need to determine empirically, which patients will respond to particular STI571/chemotherapeutic combinations.

CHAPTER THREE

ABL FAMILY KINASES PROMOTE CHEMORESISTANCE TO DOXORUBICIN

3.1 Introduction

The Abl family of non-receptor tyrosine kinases (c-Abl/Arg) has been indicted as a causative force in leukemia for more than three decades; however, their role in solid tumors has only recently been described. We previously demonstrated that activated Abl family kinases drive the proliferation, invasion, cell survival, and anchorage-independent growth of aggressive breast cancer cells [38, 39]. Breast cancer is responsible for 26% of newly diagnosed cancer cases for women each year, and is the most common fatal cancer for women age 20-59 [88]. Treatment options for the most aggressive forms of breast cancer, labeled as "triple negative" status (ER^- (estrogen receptor), PR^- (progesterone receptor), and $Her2^-$), are limited due to a lack of efficacious targets and development of chemoresistance [178, 179]. We demonstrated in chapter 2 that inhibitors of Abl family kinases abrogate resistance to a number of commonly used chemotherapeutics (i.e., 5-fluoruracil, cisplatin, paclitaxel, camptothecin) in a panel of breast cancer cells [180]; however, the anthracycline, doxorubicin, which is considered front-line therapy for breast cancer, was not tested in that study. Though doxorubicin is initially highly effective in a majority of patients, resistance arises in advanced, metastatic cases [179, 181]; therefore, it is imperative to identify new therapeutic targets in these difficult to treat patients.

Recently, we also provided the first evidence that Abl family non-receptor tyrosine kinases (c-Abl, Arg) are activated in a subset of primary melanomas and in some melanoma cell lines, and promote many processes involved in melanoma progression such as proliferation, invasion, survival, and metastasis [50]. There has been virtually no change in one-year survival rates for patients with metastatic melanoma, and the number of newly diagnosed cases is increasing faster than with any other cancer [88]. Melanomas are highly resistant to all known chemotherapeutic agents; complete responses are observed in less than 5% of patients; and cells refractory to treatment are highly metastatic [182]. Chemotherapeutic agents spanning almost every class have been tested in clinical trials; however, none of these agents significantly impacts patient survival [116, 183]. Anthracyclines (i.e., doxorubicin, daunorubicin) are not routinely used to treat metastatic melanoma due to intrinsic resistance [142]. However, current treatment regimens (dacarbazine-DTIC or temozolamide-TMZ) are

also ineffective [182]. Chemotherapeutic resistance occurs via expression of multi-drug resistance transporters and by upregulation of anti-apoptotic signaling pathways [133, 182]. Therapeutic strategies tailored to individuals and targeting multiple signaling pathways are likely to provide maximal therapeutic efficacy.

Recurrent, metastatic disease occurs due to aberrant proliferation, invasion, and survival of cells at secondary sites. Melanoma progression is driven by transcription factors such as NF-κB and STAT3, which have major roles in melanoma survival and chemoresistance [114], and inhibiting expression of the anti-apoptotic proteins, XIAP and cIAP1, targets of NF-κB, promotes chemotherapy-induced cell death [84, 130]. Intrinsic resistance of malignant melanomas to DNA damage-inducing therapies also has been tied to activation of PI3K/Akt and B-Raf/ERK signaling pathways [68, 117], and co-targeting these pathways has been a major therapeutic focus for melanoma treatment [72]. This is especially important since Akt is a key promoter of melanoma progression [184].

Based on our data in both breast cancer and melanoma cells, demonstrating that activated c-Abl/Arg promote proliferation, invasion, and survival [38, 39, 50], we focused this chapter on testing whether c-Abl/Arg promote resistance to doxorubicin. Understanding the mechanisms underlying melanoma and breast cancer drug resistance is critical for developing new therapies to treat resistant/disseminated disease. We demonstrate that c-Abl/Arg inhibitors dramatically sensitize breast cancer and melanoma cells to doxorubicin, halting cell proliferation and dramatically inducing apoptosis. These data indicate that, in addition to inhibiting metastatic disease [50], c-Abl/Arg inhibitors also are likely to prevent chemotherapeutic resistance.

3.2 Materials and Methods

3.2.1 Cell Lines and Reagents

MDA-MB-435s cells were obtained from the University of North Carolina Tissue Culture Facility, and are a spindle-shaped, highly metastatic variant of MDA-MB-435 cells (Chapel Hill, NC). Genetic analysis confirmed that these cells are identical to melanoma M14, and therefore, are referred to as 435s/M14 [50, 157]. A drug-resistant variant of 435s/M14 (435s/M14-DR) was created via step-wise treatment with increasing concentrations of doxorubicin (using a maximum dose of 100nM) [185]. 435s/M14 and 435s/M14-DR cells were cultured in DMEM/10% FBS (fetal bovine serum), + insulin (10μg/ml). WM3248 cells were obtained from Dr. Meenhard Herlyn (Wistar Institute,

Philadephia, PA). WM3248 cells were cultured in MCDB153 + L-15 (80:20 mixture, respectively)/2% FBS, + insulin (5μg/ml) + calcium chloride (1.68mM). BT-549 cells were cultured in DMEM/10% FBS. MDA-MB-468 cells were cultured in MEM/10% FBS, + sodium pyruvate (10μg/ml). STI571-resistant c-Abl/Arg constructs, in which the Threonine 315 residue was mutated to Isoleucine (AblT/ArgT; T315I) [186, 187], were purchased from GenScript.

STI571 (Gleevec; imatinib mesylate) and nilotinib were obtained from Novartis (Basal, Switzerland). STI571 was dissolved in water (10mM) and stored at -80^{o}C, while nilotinib (10mM) was dissolved in DMSO, and stored at 4^{o}C. Doxorubicin was purchased from Sigma (St. Louis, MO). PARP (poly(ADP-ribose) polymerase; sc-8007) and α-tubulin antibodies were purchased from Santa Cruz Biotechnologies (Santa Cruz, CA); phospho-Crk/CrkL (Y221/Y207) was purchased from Cell Signaling Technology (Danvers, MA); and GAPDH antibody was obtained from BD Biosciences (Chicago, IL). Western blots were performed as described in the manufacturers' protocols.

3.2.2 CellTiter-Glo Viability Assay (Promega; Madison, WI) [180]

Cells were plated in 96-well plates in triplicate in 100μl of medium, refreshed with media containing drugs the following day when cells were 30-40% confluent, and harvested 72h later. CellTiter-Glo reagent (100μl) was added to each well, the plates were rocked for 2', incubated at room temperature for 10', 100μl was removed from each well and transferred to an opaque 96-well plate, and luminescence (total light emitted, 10"/well) measured with a Synergy 2 microplate reader (Biotek; Winooski, VT).

3.2.3 Proliferation Assays

Tritiated thymidine assays [180]. Cells were plated in 24-well plates in triplicate, drug-treated the following day when cells were 30-40% confluent, and harvested after 72h. Cells were pulsed with tritiated thymidine (2.5μCi; 2h), washed with PBS, incubated in 10% trichloroacetic acid, radioactivity was solubilized in 0.2N NaOH, and analyzed on a scintillation counter. Cell cycle analysis. Cells were plated in 100mm dishes, refreshed with media containing drugs the following day when cells were 30-40% confluent, and harvested after 72h. Cells were labeled with bromodeoxyuridine (BrdU, 10μM) for 1h at 37°C, trypsinized, washed and permeabilized with ethanol (70%), stained with fluorescein isothiocyanate (FITC)-conjugated anti-BrdU antibody and propidium iodide (PI; 5μg/ml), and analyzed by fluorescence-activated cell sorting (FACS) using Cell

Quest software (BD Biosciences) and Modfit analysis (Verity Software House, Topsham, ME).

3.2.4 Apoptosis Assays

PARP cleavage [180]. Cells were plated in 60mm dishes, and treated with drugs the following day when cells were 30-40% confluent. After 40h, attached and detached cells were lysed in RIPA buffer (50mM Tris pH 7.5, 150mM NaCl, 1% Triton-X 100, 0.1% SDS, 1% sodium deoxycholate), protein was quantitated by Lowry DC (Bio-Rad; Hercules, CA), equal protein was loaded on SDS-PAGE gels, and blots were incubated with antibodies for PARP and GAPDH. Fluorescent Caspase-3/7 assay (Sigma; St. Louis, MO) [188]**.** Cells were plated in 6-well dishes in triplicate, drug-treated the following day when cells were 30-40% confluent, and attached and detached cells were lysed 40h later in 1X lysis buffer. Lysate (5μl) was incubated with substrate (200μl, diluted 1:3), and fluorescence detected at 360nm/460nm (excitation/emission) with a Synergy 2 microplate reader (Biotek; Winooski, VT). Annexin-V FACS analysis. Cells were plated in 100mm dishes, and treated with drugs the following day when cells were 30-40% confluent. After 40h, cells were trypsinized, washed in DMEM (-phenol red, $+Ca^{2+}$)/5% FBS, counted, and $1x10^5$ cells were incubated with Annexin-V-APC (5μl) + propidium iodide (50μg/ml) for 15min before analysis by FACS.

3.2.5 Statistics

Statistical analyses were performed using Sigma Stat for Windows (Systat Software, Inc.; San Jose, CA). Combination Index (CI) values were calculated with CalcuSyn software (Biosoft; Cambridge, UK) using single drug and drug combination dose response curves.

3.3 Results

3.3.1 c-Abl/Arg promote melanoma and breast cancer cell viability in the presence of doxorubicin.

We previously demonstrated that c-Abl and Arg are highly active in a wide array of aggressive melanoma and breast cancer cell lines, and drive proliferation, invasion, survival to nutrient deprivation and metastasis [38, 39, 50]. We further demonstrated that inhibitors of Abl family kinases abrogate resistance to a number of commonly used chemotherapeutics in a panel of breast cancer cells [180]. In this chapter, we wanted to

determine whether inhibition of Abl family kinases sensitizes invasive breast cancer and melanoma cells to doxorubicin and identify the mechanism by which this occurs. Doxorubicin acts primarily as a topoisomerase II inhibitor and induces DNA damage by stabilizing topoisomerase II, preventing religation of DNA following strand breakage [101]. Doxorubicin also induces DNA damage by intercalating into DNA, and has been shown to induce free radical formation [101].

To test our hypothesis, we first treated cells with the c-Abl/Arg inhibitor, STI571, and doxorubicin, alone or in combination, and measured cell viability using the CellTiter-Glo assay, which quantitates ATP, a measure of metabolically active cells [180]. We observed that STI571+doxorubicin dramatically decreased viability of 435s/M14 and WM3248 melanoma (Figure 3.1A, C) and BT-549 and MDA-MB-468 breast cancer (Figure 3.1B, D) cells, all of which express highly active c-Abl/Arg [38, 50]. A dose of 10μM STI571 was used for these studies because this physiologically relevant dose is required to effectively inhibit c-Abl/Arg kinase activities [38]. Of the cell lines tested, only MDA-MB-468 cells possess c-Kit, another target of the c-Abl inhibitors STI571 and nilotinib [38, 50]. This demonstrates that selective targeting of cell populations containing highly active c-Abl/Arg may yield dramatic clinical benefit to numerous aggressive cell types. Interestingly, melanoma cells were more resistant to doxorubicin than breast cancer cells; however, STI571 dramatically sensitized both cell types to doxorubicin (Figure 3.1A-435s/M14, IC_{50}=0.41μM; Figure 3.1B-BT-549, IC_{50}=0.066μM). CalcuSyn software was utilized to calculate combination indices (CI), which indicate whether the effect of the two drugs together is greater than either alone using the dose response curves for each drug and the combination (Figure 3.2A, B) [180]. A CI value less than one denotes drug synergism, equal to one signifies additivity, and greater than one indicates antagonism. Likewise, nilotinib, a second-generation c-Abl/Arg inhibitor that is more potent and more specific for c-Abl/Arg, sensitized 435s/M14 cells to doxorubicin (Figure 3.2A, C). We proceeded to demonstrate conclusively that STI571 specifically targets c-Abl and Arg in these cells and that inhibition of these kinases is responsible for the observed synergism of STI571 with doxorubicin. We expressed STI571-resistant mutant forms of c-Abl and Arg (AblT/ArgT) in 293T cells, treated with STI571, and observed no decrease in phosphorylation of Crk/CrkL, a c-Abl/Arg substrate (Figure 3.3A). We proceeded to stably express AblT/ArgT constructs in 435s/M14 cells, treated with STI571+doxorubicin, and observed that AblT/ArgT expression rescued the synergistic decrease in cell viability observed with STI571+doxorubicin (Figure 3.3B).

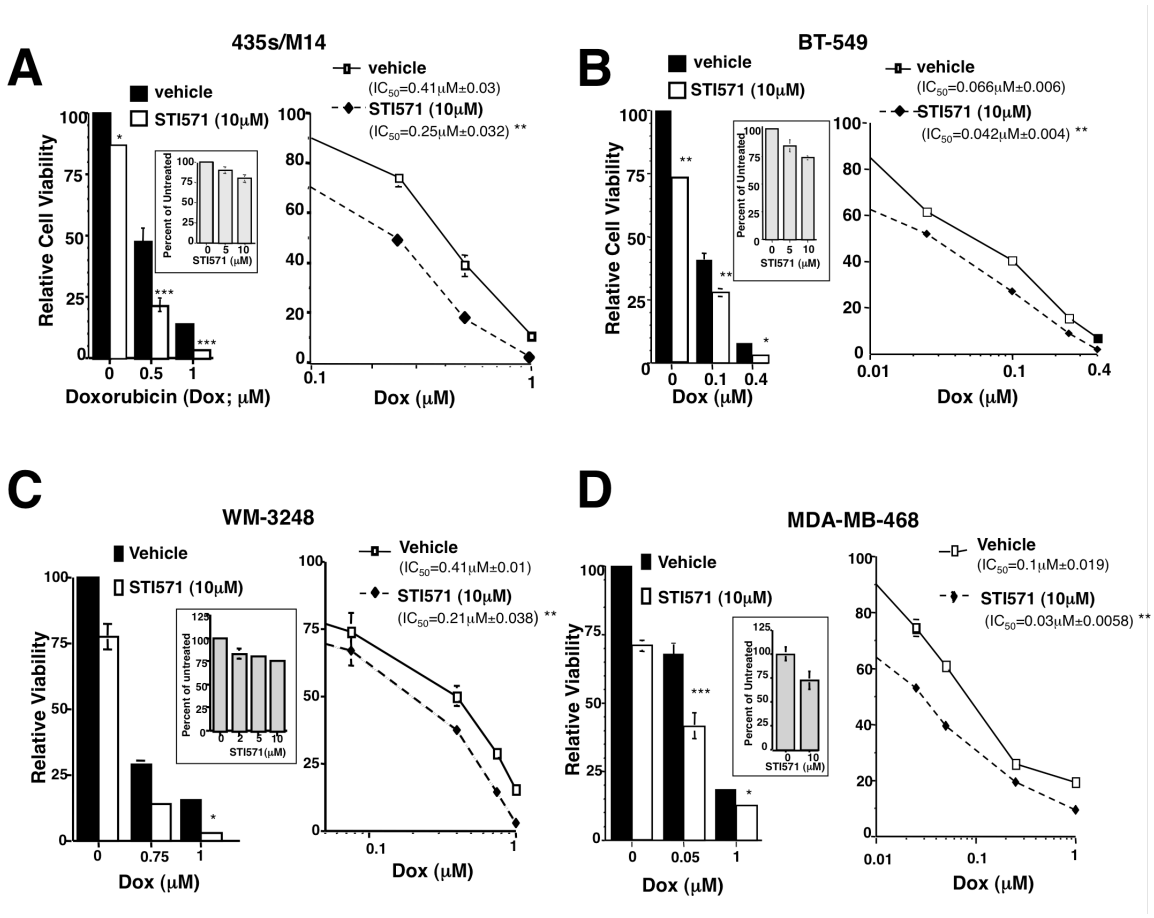

Figure 3.1. c-Abl/Arg inhibitors sensitize breast cancer and melanoma cells to doxorubicin by inhibiting viability. (A) 435s/M14, **(B)** BT549, **(C)** WM3248, and **(D)** MDA-MB-468 cells were were plated in triplicate, treated with doxorubicin and STI571 for 72h, and viability assessed by CellTiter-Glo. Mean±SEM for 3 independent experiments (left). Representative dose response curve (right). (C) Done in collaboration with J. Tepe. *$0.01 \leq p < 0.05$, **$0.001 \leq p < 0.01$, ***$p < 0.001$.

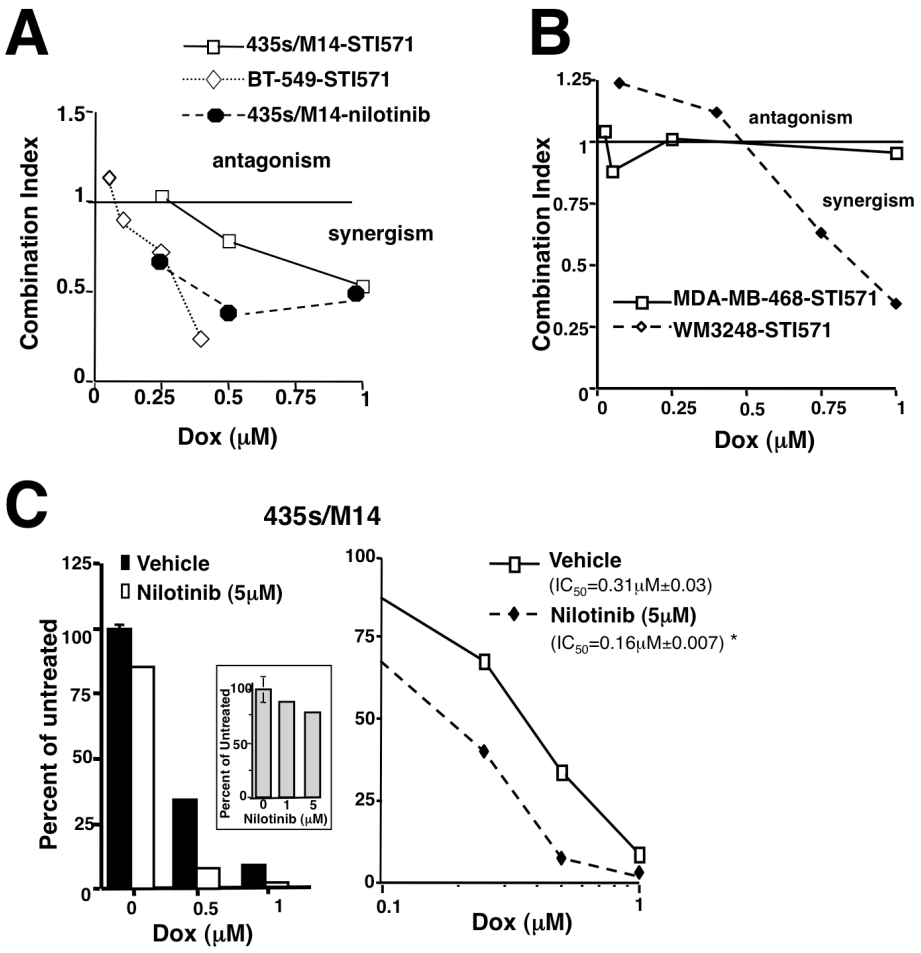

Figure 3.2. c-Abl/Arg inhibitors dramatically sensitize breast cancer and melanoma cells to doxorubicin. (A, B) Graphical representation of combination indices obtained with CalcuSyn software (>1-antagonism; =1-additive; <1-synergism). Graph shown is representative of 3 independent experiments. **(C)** Parental (435s/M14) cells were treated with nilotinib and/or doxorubicin for 72h, and viability assessed by CellTiter-Glo (Promega). Mean±SEM for 3 independent experiments is shown (left). Dose response curve is representative of 3 independent experiments (right). *p<0.05.

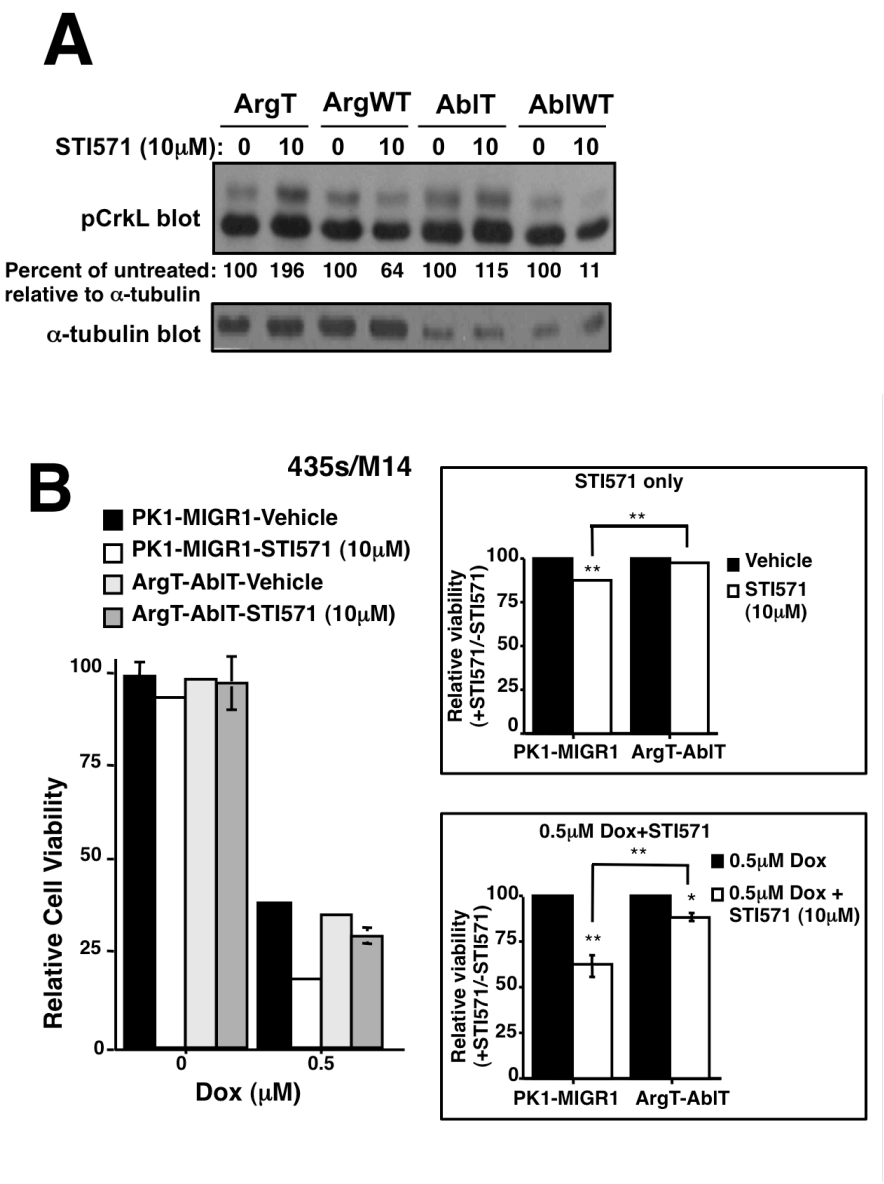

Figure 3.3. c-Abl/Arg specifically promote resistance to doxorubicin. (A) Functionality of STI571-resistant c-Abl (AblT) and Arg (ArgT) was analyzed in 293T cells following 72h treatment with STI571 via Western blotting for pCrkL, a c-Abl/Arg subrate. **(B)** Cells expressing STI571-resistant mutant c-Abl (AblT) and Arg (ArgT) were treated with doxorubicin and/or STI571 (48h), and viability assessed. Representative experiment (left). Mean±SEM of 3 independent experiments: STI571 alone (right, top) and STI571+doxorubicin (right, bottom). (A) Performed by H. Bennett. **p*<0.05, ***p*<0.01.

3.3.2 c-Abl/Arg inhibitors sensitize doxorubicin-resistant melanoma cells to doxorubicin.

Although chemotherapeutic agents sometimes kill the majority of cells, residual, highly resistant cells often remain, which are very aggressive and metastatic. In order to mimic outgrowth of highly resistant, metastatic cells following treatment with chemotherapeutic agents, we cultured 435s/M14 melanoma cells with increasing concentrations of the chemotherapeutic drug, doxorubicin, over the course of 8 months (435s/M14-DR). 435s/M14-DR cells were highly resistant to doxorubicin (1μM reduced viability by 15% as compared to 80% in parental cells; Figure 3.4A). To determine whether c-Abl/Arg promote chemoresistance in 435s/M14-DR cells, cells were treated with doxorubicin and the c-Abl/Arg inhibitor, STI571, alone or in combination, and cell viability measured using the CellTiter-Glo assay. STI571 dramatically decreased the viability of highly resistant 435s/M14-DR cells treated with doxorubicin (Figure 3.4A, C). Nilotinib also dramatically sensitized 435s/M14-DR cells to doxorubicin, reducing cell viability (Figure 3.4B, C). Remarkably, the use of these two c-Abl/Arg inhibitors rendered acquired chemoresistant cells equally sensitive with parental cells to doxorubicin treatment (Figure 3.4A, data not shown).

3.3.3 c-Abl/Arg promote proliferation and prevent apoptosis in melanoma and breast cancer cells exposed to doxorubicin.

Since STI571+doxorubicin decreased cell viability, and viability is a balance of proliferation and apoptosis, we performed tritiated thymidine assays to determine the extent to which cell proliferation in the presence of doxorubicin was affected by Abl family kinase inhibition. We observed that STI571 synergized with doxorubicin to completely halt proliferation of melanoma (435s/M14 and WM3248; Figure 3.5A, C, E) and breast cancer (BT-549 and MDA-MB-468; Figure 3.5B, C, D) cell lines, as well as cells that had acquired advanced chemoresistance (Figure 3.5F). We wanted to determine exactly how STI571 was synergizing with doxorubicin to decrease cell proliferation so we performed BrdU/PI cell cycle analysis on asynchronous parental 435s/M14 cells and 435s/M14-DR cells to accurately assess the phases of the cell cycle in response to combination treatment. We observed a dramatic induction of G2/M arrest following treatment with doxorubicin and the c-Abl/Arg inhibitor, STI571 (Figure 3.6A, B). Notably, STI571 or low dose doxorubicin had little effect on the cell cycle of 435s/M14-DR cells; however, STI571+doxorubicin induced a dramatic blockade of cells in G2/M,

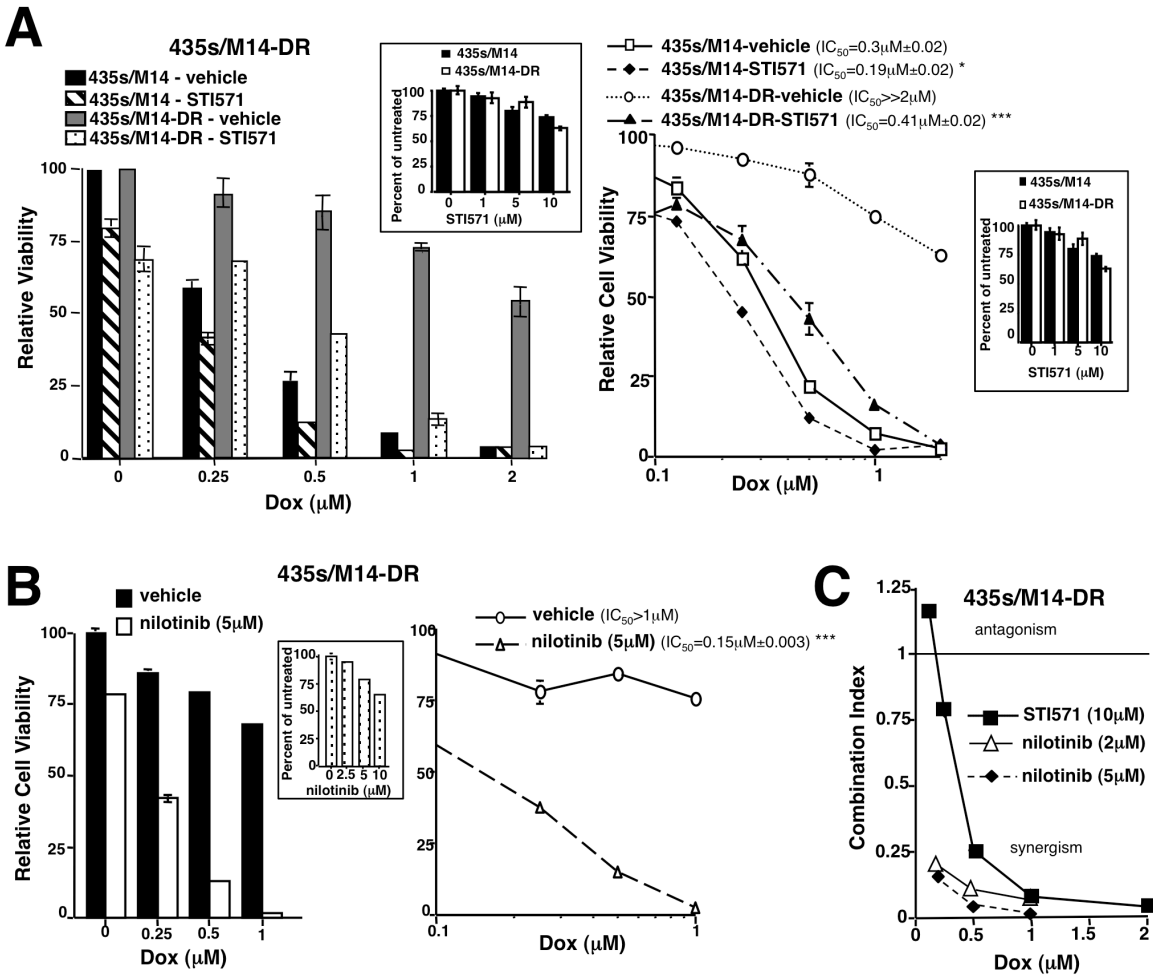

Figure 3.4. **c-Abl/Arg inhibitors dramatically synergize with doxorubicin to decrease highly resistant cell viability. (A, B)** Parental (435s/M14) and doxorubicin-resistant (435s/M14-DR) melanoma cells were plated in triplicate, treated with doxorubicin and STI571 (A) or nilotinib (B) for 72h, and viability assessed by CellTiter-Glo. Mean±SEM for 3 independent experiments (left). Representative dose response curve is shown (right). **p*<0.05, ****p*<0.001. **(C)** Graphical representation of combination indices obtained with CalcuSyn software (>1-antagonism; =1-additive; <1-synergism). Graph shown is representative of 3 independent experiments. Some error bars are too small for visualization.

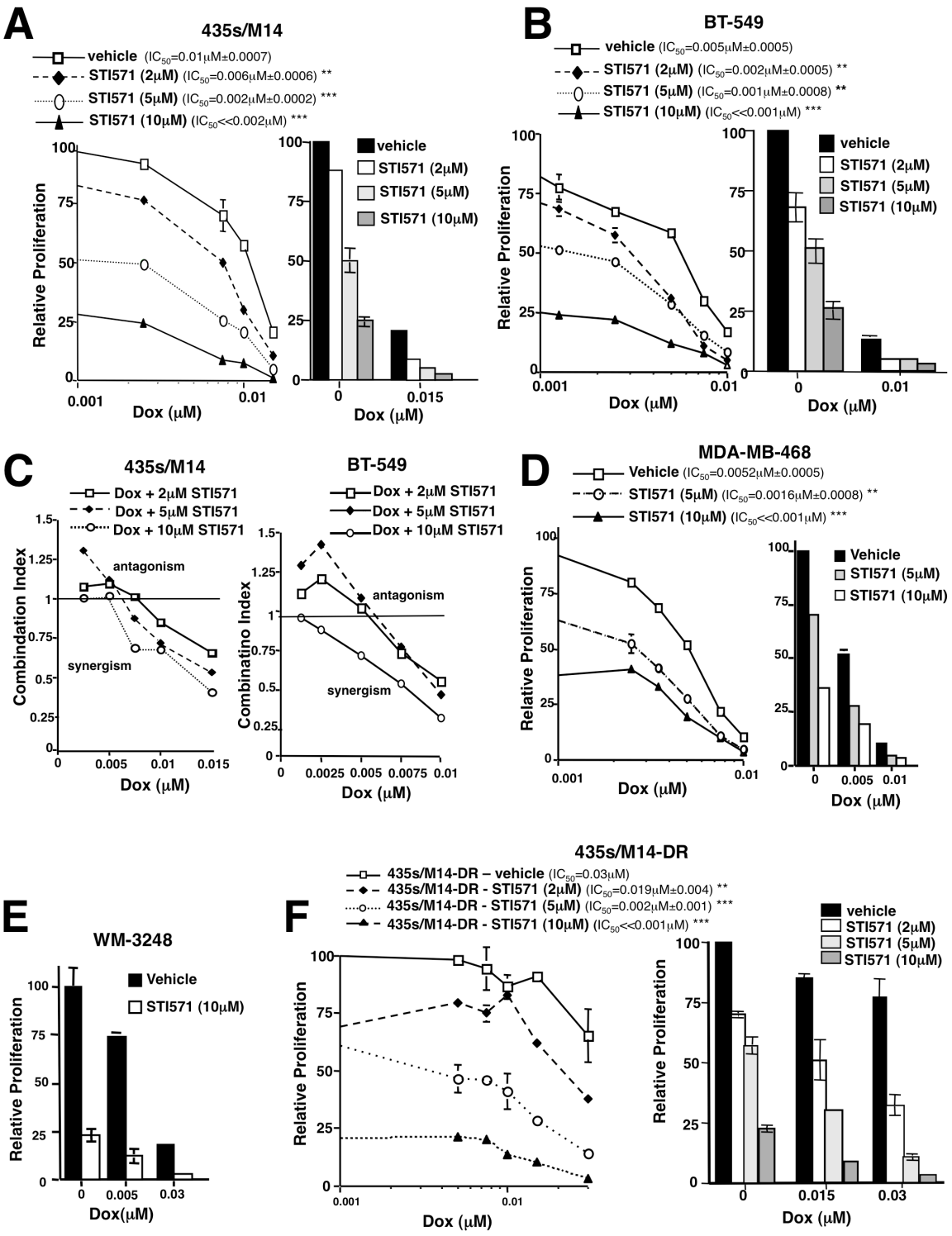
A
435s/M14
vehicle (IC50=0.01μM±0.0007)
STI571 (2μM) (IC50=0.006μM±0.0006) **
STI571 (5μM) (IC50=0.002μM±0.0002) ***
STI571 (10μM) (IC50<<0.002μM) ***
Relative Proliferation
Dox (μM)
vehicle
STI571 (2μM)
STI571 (5μM)
STI571 (10μM)
B
BT-549
vehicle (IC50=0.005μM±0.0005)
STI571 (2μM) (IC50=0.002μM±0.0005) **
STI571 (5μM) (IC50=0.001μM±0.0008) **
STI571 (10μM) (IC50<<0.001μM) ***
C
435s/M14
Dox + 2μM STI571
Dox + 5μM STI571
Dox + 10μM STI571
Combindation Index
antagonism
synergism
BT-549
Combinatino Index
D
MDA-MB-468
Vehicle (IC50=0.0052μM±0.0005)
STI571 (5μM) (IC50=0.0016μM±0.0008) **
STI571 (10μM) (IC50<<0.001μM) ***
E
WM-3248
Vehicle
STI571 (10μM)
Dox(μM)
F
435s/M14-DR
435s/M14-DR – vehicle (IC50=0.03μM)
435s/M14-DR - STI571 (2μM) (IC50=0.019μM±0.004) **
435s/M14-DR - STI571 (5μM) (IC50=0.002μM±0.001) ***
435s/M14-DR - STI571 (10μM) (IC50<<0.001μM) ***

Figure 3.5. c-Abl/Arg promote proliferation of breast cancer and melanoma cells in the presence of doxorubicin. (A) 435s/M14 and **(B)** BT-549 cells were plated in triplicate, treated with STI571 and/or doxorubicin for 72h, and proliferation assessed by tritiated thymidine assay. Representative dose response curves (left) and mean±SEM for 3 independent experiments (right) are shown. **(C)** Graphical representation of combination indices obtained with CalcuSyn software (>1-antagonism; =1-additive; <1-synergism). Graph shown is representative of 3 independent experiments. **(D)** MDA-MB-468 and **(E)** WM-3248 cells were plated in triplicate, treated with doxorubicin and/or STI571 for 72h, and proliferation assessed by tritiated thymidine assay. Graphs shown are representative experiments. (D) MDA-MB-468 - Dox (0.005μM)+STI571 (10μM) CI=1.1; Dox (0.01μM)+STI571 (10μM) CI=0.9; (E) WM3248 - Dox (0.005μM)+STI571 (10μM) CI=0.72; Dox (0.03μM)+STI571 (10μM) CI=0.56. **(F)** 435s/M14-DR cells were plated in triplicate, treated with doxorubicin and/or STI571 for 72h, and proliferation assessed by tritiated thymidine assay. Representative dose response curves (left) and mean±SEM for 3 independent experiments (right) are shown. Some error bars are too small for visualization. (E) Done in collaboration with J. Tepe. $^{**}p \leq 0.01$, $^{***}p < 0.001$.

using extremely low doxorubicin doses (30-60nM; Fig 3.6B). Next, we determined if the decrease in viability following doxorubicin+STI571 treatment was also due to an increase in apoptosis. To ascertain this, breast cancer (BT-549 and MDA-MB-468), melanoma (435s/M14 and WM3248), and acquired chemoresistant melanoma (435s/M14-DR) cells were treated with STI571+doxorubicin and assayed for caspase-3/7 activity and PARP cleavage. STI571 alone modestly, but significantly, induced caspase-3/7 activity in all cell lines tested (Figure 3.7A-D). In both breast cancer and melanoma cells, STI571 potentiated doxorubicin-mediated caspase-3/7 activity (Figure 3.7A, B). Whereas no significant apoptotic response to doxorubicin was observed in 435s/M14-DR cells, STI571+doxorubicin dramatically induced caspase-3/7 activity (Figure 3.7C). Intriguingly, MDA-MB-468 cells underwent apoptosis in response to doxorubicin, but experienced no further sensitization upon co-treatment with STI571 (Figure 3.7D), indicating that the potentiated decrease in MDA-MB-468 cell viability following STI571+doxorubicin treatment was primarily via inhibition of proliferation. We further demonstrated that STI571 enhanced doxorubicin-mediated apoptosis in 435s/M14, WM3248, and 435s/M14-DR melanoma cells via Annexin-V FACS analysis (Figure 3.8A) and PARP cleavage assays (Figure 3.8B-D). In conclusion, c-Abl/Arg promote chemoresistance to doxorubicin across multiple cell types and in highly resistant melanoma cells by promoting proliferation and inhibiting apoptosis.

3.4 Discussion

In this chapter, we demonstrate that c-Abl/Arg inhibitors synergize with doxorubicin to inhibit proliferation, induce a G2/M block, and dramatically promote apoptosis of melanoma, breast cancer, and advanced chemoresistant melanoma cells. Currently melanoma essentially represents an untreatable disease, with little to no improvement having been observed in one-year survival rates. It is highly resistant to currently used chemotherapeutics, leaving surgery as the only viable therapeutic option [88, 116]. Although doxorubicin is not routinely used in treatment of melanoma, it is frequently used in breast cancer therapy [101], and we present evidence demonstrating that c-Abl/Arg inhibition sensitizes melanoma cells to a therapeutically viable dose of doxorubicin, giving new life to a previously unsuccessful treatment option (Figure 3.2C-435s/M14, Dox+Nilotinib IC_{50}=0.16μM; Figure 3.1D-MDA-MB-468, Dox alone IC_{50}=0.1μM).

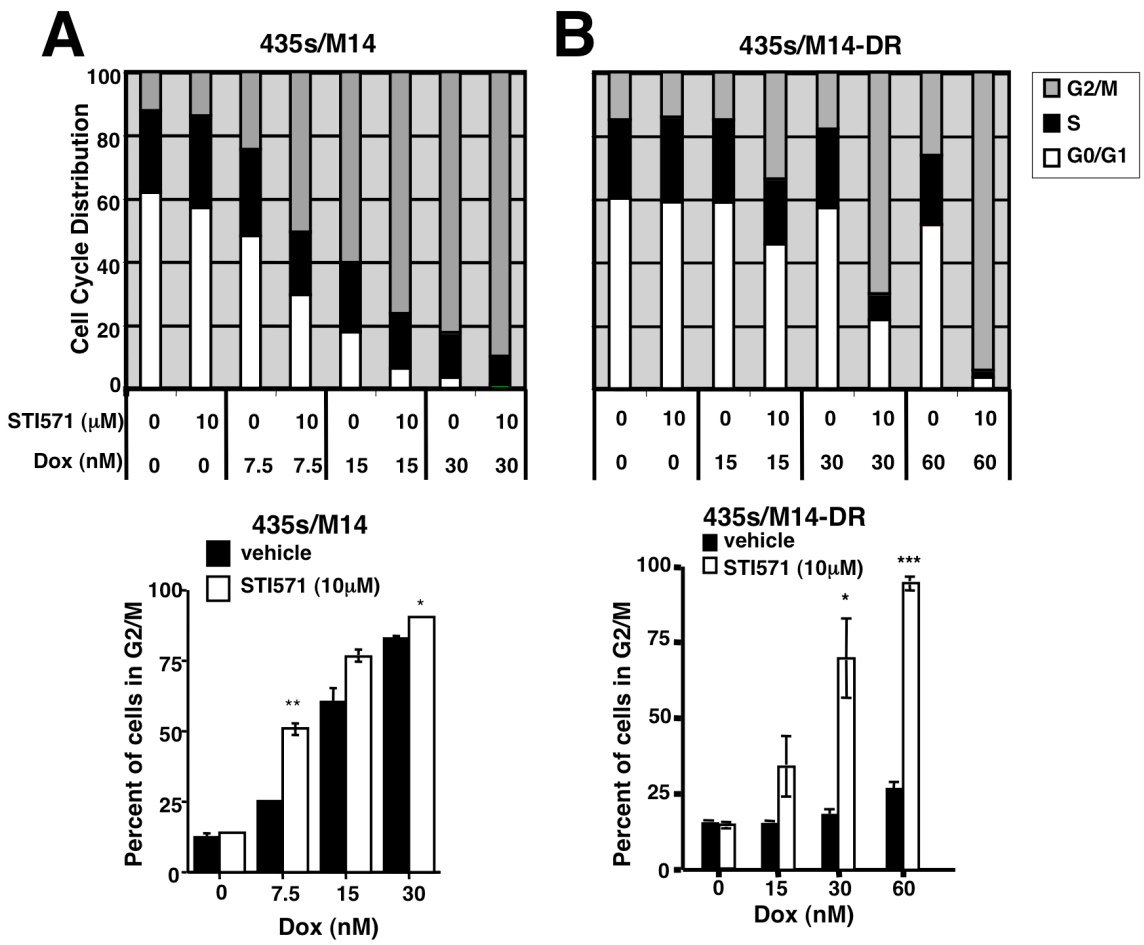

Figure 3.6. c-Abl/Arg prevent doxorubicin-induced G2/M arrest. (A, B) Asynchronous 435s/M14 (A) and 435s/M14-DR (B) cells were treated with STI571 and/or doxorubicin for 72h, and analyzed by FACS. Cell cycle distribution for a representative experiment is shown (top). Mean±SEM of 3 independent experiments (bottom). *$p \leq 0.05$, **$p \leq 0.01$, ***$p < 0.001$.

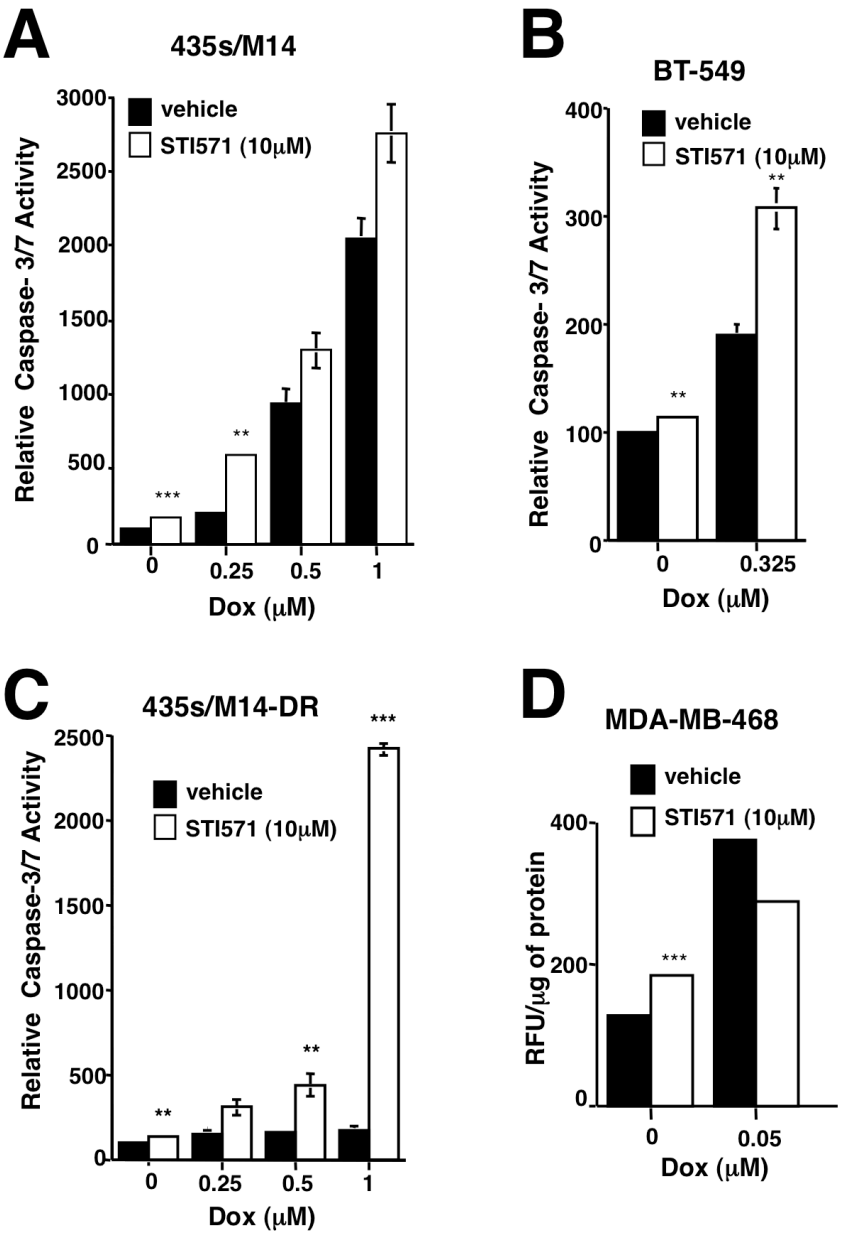

Figure 3.7. c-Abl/Arg prevent doxorubicin-induced apoptosis. Cells were treated with STI571 and/or doxorubicin (40h), attached and detached cells were lysed, and apoptosis assessed by fluorescent caspase-3/7 assay (Promega) **(A-D)**. Data shown are mean±SEM of 3 experiments. Some error bars are too small for visualization. $^{**}p \leq 0.01$, $^{***}p < 0.001$.

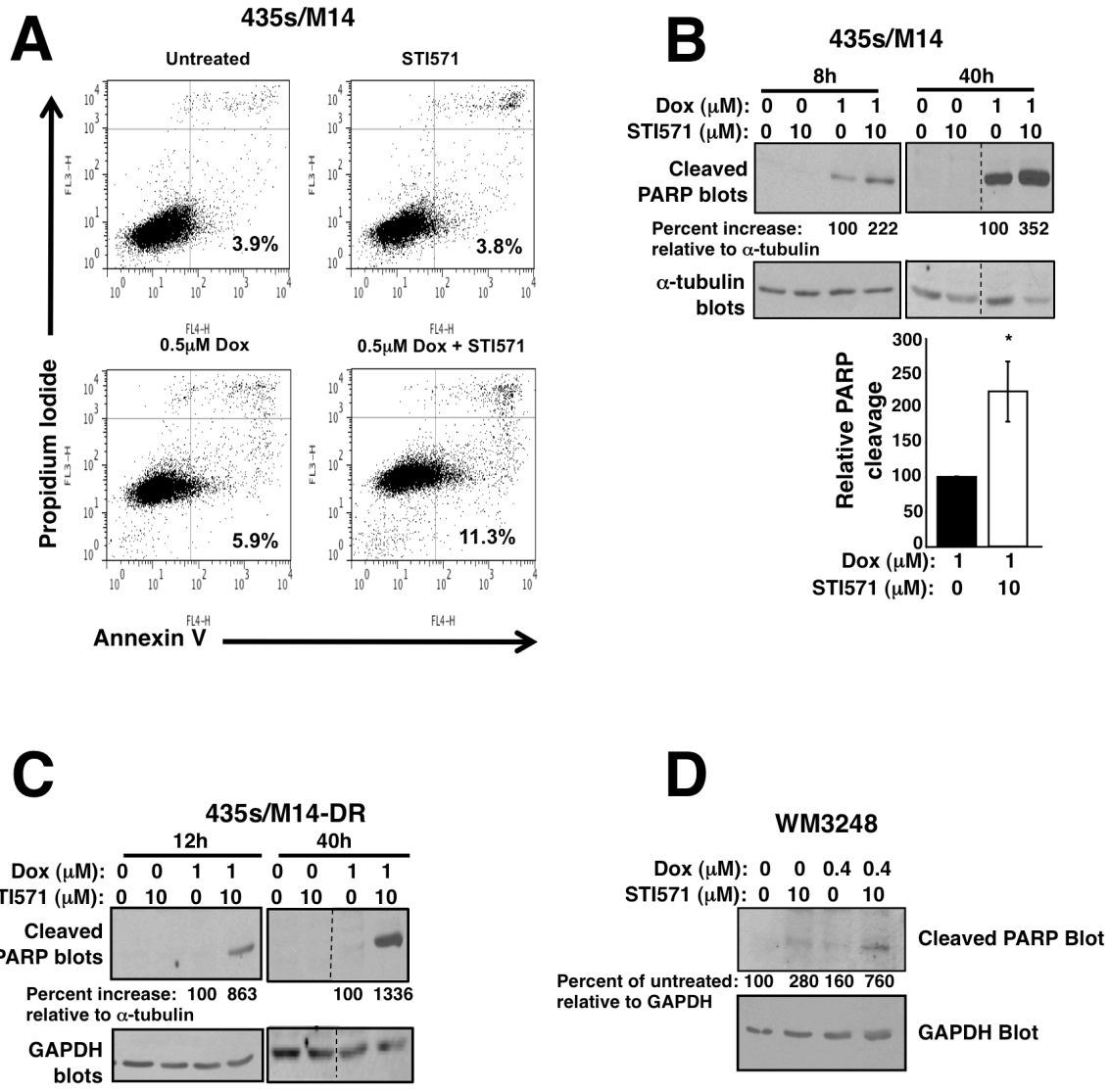

Figure 3.8. STI571+doxorubicin induces apoptosis in melanoma cells. Cells were treated with STI571 and/or doxorubicin (40h), unless indicated otherwise, attached and detached cells were lysed, and apoptosis assessed by Annexin-V FACS analysis **(A)**, and PARP cleavage **(B-D)**. Data are representative of 3 independent experiments (A-D). Mean±SEM of 3 experiments (B, right). (D) Done in collaboration with J. Tepe. *$p \leq 0.05$.

As mentioned in the previous chapter, silencing c-Abl and Arg in combination with doxorubicin is not experimentally feasible. Inhibition of c-Abl/Arg via siRNA dramatically inhibits cell proliferation, and since chemotherapy works by targeting rapidly proliferating cells and cells must be transfected prior to chemotherapeutic treatment, this dramatic reduction in cell proliferation prevents full activity of chemotherapeutic drugs. Despite this technical limitation, we confirmed that STI571 specifically inhibited c-Abl/Arg by overexpressing STI571-resistant mutant forms of those proteins (AblT/ArgT). In cells expressing STI571-resistant mutant forms of c-Abl/Arg, STI571 did not synergistically act with doxorubicin to potentiate further loss of cell viability.

It is also interesting that the loss of viability observed in MDA-MB-468 cells following doxorubicin+STI571 treatment (Figure 3.1D) is primarily due to cytostasis, since doxorubicin+STI571 halted cell proliferation (Figure 3.5D) without inducing apoptosis (Figure 3.7D). In contrast, STI571+doxorubicin dramatically induces apoptosis of all melanoma cell lines tested. Intriguingly, in the previous chapter, we observed that combining 5-fluoruracil+STI571 synergistically induced MDA-MB-468 cell apoptosis, but all other classes of chemotherapeutics tested in combination with STI571 preferentially halted MDA-MB-468 cell proliferation [180]. In that chapter, we postulated that “inhibition of STAT3 activation may be a common mechanism by which STI571 synergizes with chemotherapeutic agents to inhibit the proliferation of MDA-MB-468 cells” [180], and we further address this possibility in chapter 5.

We previously demonstrated that Abl family kinases drive G1→S cell cycle transition in 435s/M14 melanoma cells in response to growth factor stimulation [39]. Moreover, we now show that c-Abl and Arg are critically important in preventing doxorubicin-induced blockade of cell cycle progression at the G2/M checkpoint. The summation of our data demonstrates the critical role of c-Abl/Arg activity in cancer cell proliferation via their influence at multiple phases of the cell cycle. The mechanism by which c-Abl and Arg promote doxorubicin resistance will be addressed in future chapters. In conclusion, data presented here demonstrate that c-Abl/Arg inhibitors dramatically sensitize melanoma, breast cancer, and advanced chemoresistant melanoma cells to doxorubicin, halting proliferation and inducing apoptosis.

CHAPTER FOUR

STI571-MEDIATED CHEMOSENSITIZATION OF ACQUIRED CHEMORESISTANT MELANOMA IS PARTIALLY MEDIATED VIA ABCB1

4.1 Introduction

Significantly, we demonstrated in the previous chapter that STI571 dramatically sensitizes acquired chemoresistant melanoma cells to G2/M arrest and apoptosis in the presence of doxorubicin. The degree of sensitization that we observed is especially exciting when considering the degree of difficulty that clinicians experience in treating advanced chemoresistant metastatic melanoma. As mentioned earlier, there has been little improvement in one-year survival rates for patients with metastatic melanoma, while the number of newly diagnosed cases continues to increase faster than with any other cancer [88]. Melanomas possess extremely high resistance levels to all known chemotherapeutic agents, and cells intractable to treatment are highly metastatic [182]. Approximately 40% of patients will develop multidrug resistance, making this a tremendous hurdle for cancer therapy [189, 190]. Cells resistant to chemotherapy, such as doxorubicin, not only evade apoptosis, but also are more invasive than their parental counterparts [100]. To best treat cancer types endued with the propensity for developing resistance, therapeutic strategies must target multiple survival mechanisms.

Chemotherapeutic resistance occurs via upregulation of anti-apoptotic signaling pathways and expression of multi-drug resistance transporters [133, 182]. The ATP binding cassette (ABC) transporter family, a primary mechanism for cancer cell resistance, effluxes a wide variety of hydrophobic chemotherapeutic compounds [128]. ABCB1, in particular, confers the greatest degree of resistance to the widest array of drugs, including those central to many chemotherapeutic regimens (e.g. anthracyclines and taxanes) [128]. A recent retrospective study showed that melanoma metastases express significantly higher levels of ABCB1 than primary tumors, indicating that ABCB1 contributes to the aggressive nature of malignant melanoma [125], and another report demonstrated a functional link between ABCB1 expression and melanoma invasion [126]. Activation of PI3K and ERK pathways has been shown to induce ABCB1 upregulation [191, 192].

Understanding the mechanisms underlying melanoma drug resistance is critical for developing new therapies to treat resistant/disseminated disease. Herein, we identified a mechanism by which melanoma cells develop resistance to the

chemotherapeutic anthracycline, doxorubicin, by demonstrating that c-Abl/Arg mediate upregulation of ABCB1, and c-Abl/Arg inhibitors dramatically sensitize highly resistant melanoma cells to doxorubicin by inhibiting ABCB1 expression and function. These data indicate that, in addition to preventing metastatic disease [193], c-Abl/Arg inhibitors also are likely to reverse acquired chemotherapeutic resistance.

4.2 Materials and Methods

4.2.1 Reagents and Cell Lines

MDA-MB-435s cells were obtained from the University of North Carolina Tissue Culture Facility, and are a spindle-shaped, highly metastatic variant of MDA-MB-435 cells (Chapel Hill, NC). Genetic analysis confirmed that these cells are identical to melanoma M14, and therefore, are referred to as 435s/M14 [157, 193]. A drug-resistant variant of 435s/M14 (435s/M14-DR) was created via step-wise treatment with increasing concentrations of doxorubicin (using a maximum dose of 100nM) [185]. 435s/M14 and 435s/M14-DR cells were cultured in DMEM/10% FBS (fetal bovine serum), + insulin (10μg/ml). STI571 (Gleevec; imatinib mesylate) and nilotinib were obtained from Novartis (Basal, Switzerland). STI571 was dissolved in water (10mM) and stored at -80^{o}C, while nilotinib (10mM) was dissolved in DMSO, and stored at 4^{o}C. Doxorubicin, paclitaxel, camptothecin, 5-fluorouracil (5-FU), cisplatin, and verapamil were purchased from Sigma (St. Louis, MO). Rhodamine 123 was purchased from Invitrogen (Carlsbad, CA). Luciferin was obtained from Promega (Madison, WI). Silencer select ABCB1 siRNA was obtained from Ambion (Carlsbad, CA). α-tubulin and Arg antibodies were purchased from Santa Cruz Biotechnologies (Santa Cruz, CA). GAPDH and c-Abl (8E9) were obtained from BD Biosciences (Chicago, IL). Lamin A/C, ABCB1, ABCG2, and ABCC1 antibodies were from Milllipore (Temecula, CA). Western blots were performed as described in the manufacturers' protocols.

4.2.2 CellTiter-Glo Viability Assay (Promega; Madison, WI)

Cells were plated in 96-well plates in triplicate in 100μl of medium, refreshed with media containing drugs the following day when cells were 30-40% confluent, and harvested 72h later. CellTiter-Glo reagent (100μl) was added to each well, the plates were rocked for 2', incubated at room temperature for 10', 100μl was removed from each well and transferred to an opaque 96-well plate, and luminescence (total light emitted, 10"/well) measured with a Synergy 2 microplate reader (Biotek; Winooski, VT).

4.2.3 Drug efflux assays [194]

Subconfluent cells were incubated with either rhodamine 123 (0.5μg/ml) or doxorubicin (10μM) in the presence of verapamil (10μM) or STI571 (40μM) for 30', washed extensively and incubated with verapamil or STI571 for an additional 45', and analyzed by FACS to assess intracellular retention of rhodamine 123 or doxorubicin.

4.2.4 Cell Lysis and Western Blots

Cells were plated in 60mm dishes, treated the following day, and detached nad attached cells were lysed in RIPA buffer (50mM Tris pH 7.5, 150mM NaCl, 1% triton-X 100, 0.1% SDS, 1% sodium deoxycholate, 1mM PMSF, 1mM sodium orthovanadate, 25mM sodium fluoride, 10μg/ml leupeptin, aprotinin, pepstatin). Total protein was quantitated with a Lowry DC kit (Biorad; Hercules, CA), equal protein was loaded on SDS-PAGE gels, and blots were incubated with specified antibodies.

4.2.5 Subcellular Fractionation

Cells were plated in 60mm dishes, and cytoplasmic/membrane and nuclear fractions were isolated using the NE-PER kit (Pierce; Rockford, IL) according to the manufacturer's protocol.

4.2.6 Semi-quantitative RT-PCR

Cells were plated in 60mm dishes, refreshed with media containing drugs the following day when cells were 30-40% confluent, RNA extracted 48h later (RNeasy kit; Qiagen; Valencia, CA), digested with DNase I (Invitrogen), reverse-transcribed with Superscript Reverse Transcriptase and random primers (Invitrogen; Carlsbad, CA), and PCR performed using primers specific for c-Abl (10nM), and Arg (10nM). β-actin primers (10nM) were included in the PCR reaction as an internal control. PCR cycling parameters involved 27 cycles of 95^{o}C-1', 55^{o}C-1', 72^{o}C-1'. Aliquots were also taken at cycles 31 and 35 to check for linearity. Scanned photographs were quantified with ImageQuant (Molecular Dynamics, GE Healthcare, Piscataway, NJ) and specific bands normalized to β-actin internal control bands.

4.2.7 Statistics

Statistical analyses were performed using Sigma Stat for Windows (Systat Software, Inc.; San Jose, CA). Combination Index (CI) values were calculated with CalcuSyn software (Biosoft; Cambridge, UK) using single drug and drug combination dose response curves.

4.3 Results

4.3.1 ABCB1 is dramatically upregulated in 435s/M14-DR cells.

Chemotherapeutic resistance commonly develops due to upregulation of multi-drug resistance transporters, which efflux the chemotherapeutic agents, and transporter upregulation is observed in late stage, metastatic melanomas [80, 133, 195]. To determine whether an ABC transporter is upregulated in 435s/M14-DR cells, we tested whether the cells also are resistant to other chemotherapeutic agents from a variety of different classes. Interestingly, 435s/M14-DR cells were highly resistant to paclitaxel, and this resistance was abrogated by STI571 treatment (Figure 4.1A). However, 435s/M14-DR cells remained sensitive to camptothecin, 5-fluorouracil, and cisplatin (Figure 4.1A). Candidate transporters that efflux doxorubicin and paclitaxel include ABCB1, ABCG2, and ABCC1 [134]. 435s/M14-DR cells expressed dramatically elevated levels of ABCB1 protein compared to parental cells, whereas ABCC1 and ABCG2 were expressed at low levels in both cell lines (Figure 4.1B). Treatment of 435s/M14-DR cells with STI571 or transfection of cells with c-Abl but not Arg siRNA inhibited ABCB1 expression (Figure 4.1C), indicating that active c-Abl contributes to ABCB1 upregulation following acquired resistance to doxorubicin. Next, we tested whether the STI571-mediated decrease in ABCB1 expression influenced doxorubicin retention. Doxorubicin possesses intrinsic fluorescence, which allows for its detection by flow cytometry. Cells were treated with vehicle/STI571 for 72h, and then incubated with doxorubicin for 30' in the absence of STI571 in a doxorubicin efflux assay, and intracellular doxorubicin assessed in living cells. Less intracellular doxorubicin was observed in 435s/M14-DR cells as compared to parental cells, which do not overexpress ABCB1 (Figure 4.1D). Moreover, doxorubicin efflux in 435s/M14-DR cells was partially inhibited when cells were treated prior to the efflux assay with STI571 (Figure 4.1D). Since STI571 was not present during the efflux assay (i.e. during incubation with doxorubicin), and STI571 binding to ABC transporters is known to be a reversible process [148], these data

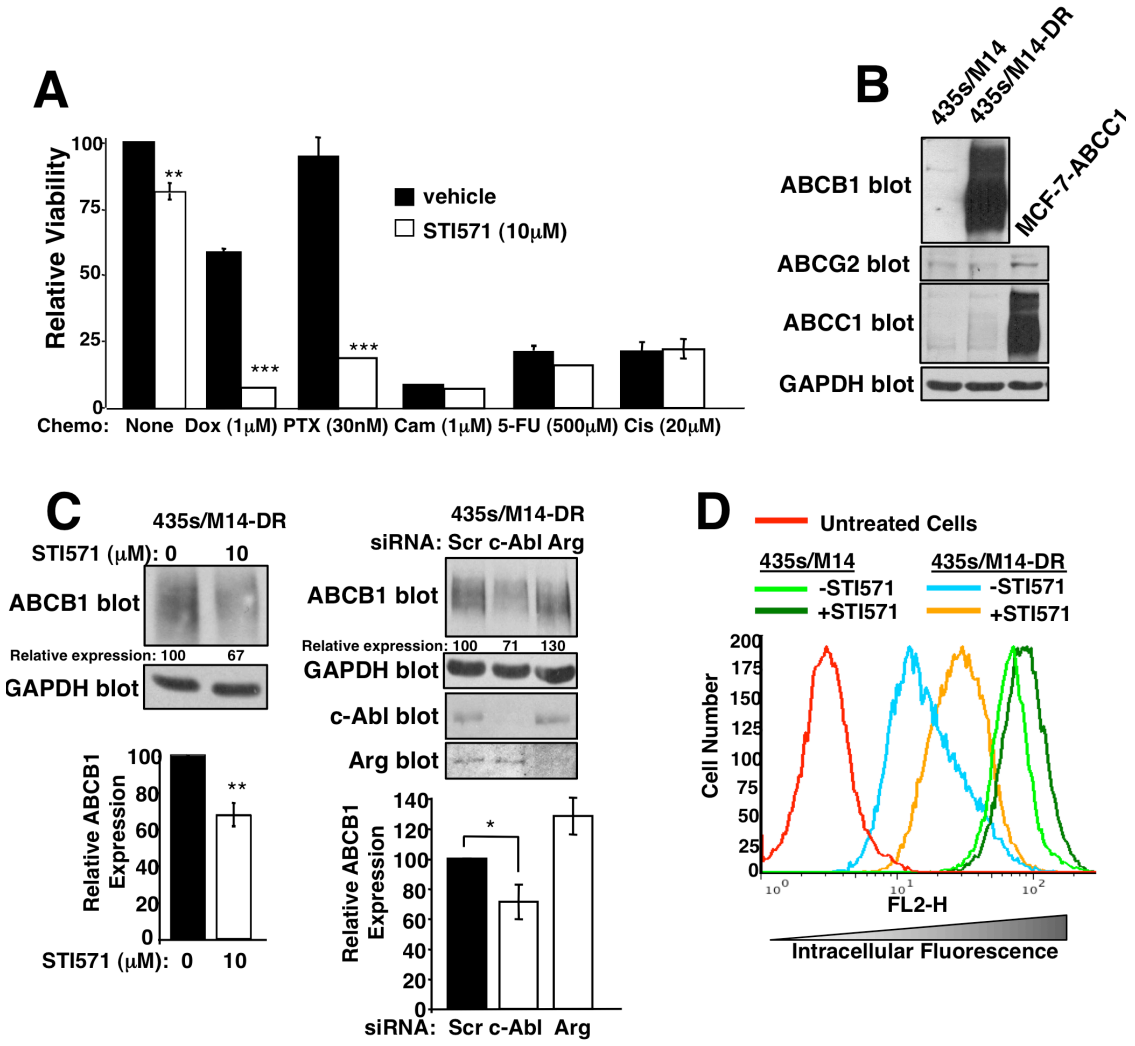

Figure 4.1. 435s/M14-DR cells are resistant to paclitaxel and doxorubicin, and express high levels of ABCB1. (A) Cells were plated in triplicate, treated for 72h with STI571 (10μM) and/or the indicated chemotherapeutic drugs, and viability assessed by CellTiter-Glo (Promega, Madison, WI). A representative experiment is shown. Some error bars are too small for visualization. PTX=paclitaxel, Cam=camptothecin, Cis=cisplatin, 5-FU=5-fluorouracil. **(B)** Lysates prepared in non-reducing conditions from untreated cells were analyzed by Western blot. Lysate from MCF-7 cells transfected with ABCC1 served as a positive control for ABCC1 expression. **(C)** Cells were treated with STI571 for 48h or transfected with siRNAs, and lysates analyzed for ABCB1 expression by Western blotting. Graphs are Mean±SEM from 3 independent experiments. *p<0.05,**p≤0.01. **(D)** Cells were treated with STI571 for 72h, washed extensively, treated with doxorubicin for 30' in the absence of STI571, and intracellular doxorubicin fluorescence assessed by FACS analysis.

indicate that c-Abl inhibits intracellular doxorubicin retention, in part, by increasing ABCB1 expression.

4.3.2 STI571 increases intracellular doxorubicin accumulation, in part, by inhibiting ABCB1 function.

STI571 has been shown to be a substrate and/or inhibitor of ABCB1 and ABCG2 in leukemic cells [148, 171-175, 196]. Therefore, STI571 also may mediate chemosensitization by directly inhibiting drug efflux. To confirm that ABCB1 mediates doxorubicin efflux in 435s/M14-DR cells and to ascertain whether STI571 specifically interferes with ABCB1-mediated efflux of doxorubicin, we performed a doxorubicin efflux assay in the absence or presence of STI571 and ABCB1 siRNA or the ABCB1 inhibitor (verapamil) and measured doxorubicin intracellular fluorescence. Silencing ABCB1 inhibited doxorubicin efflux (Figure 4.2A), and STI571 inhibited efflux of doxorubicin and the ABCB1 substrate, rhodamine 123, to a similar extent as verapamil (Figure 4.2B, C). Taken together, these studies demonstrate that STI571 directly inhibits ABCB1-mediated doxorubicin efflux in 435s/M14-DR melanoma cells, in addition to preventing ABCB1 upregulation.

Next, we assessed the functional impact of ABCB1 expression on chemoresistance of 435s/M14-DR cells by assessing the effect of silencing/inhibiting ABCB1 on cell viability. Silencing ABCB1 or verapamil treatment dramatically sensitized resistant cells to doxorubicin (Figure 4.3A, B). However, STI571 retained the ability to inhibit the viability of cells treated with verapamil/doxorubicin or ABCB1 siRNA/doxorubicin, indicating that inhibition of ABCB1 is not the only mechanism by which STI571 sensitizes 435s/M14-DR cells to doxorubicin (Figure 4.3A, B). In addition, unlike rhodamine 123, in the absence of pump inhibitors, doxorubicin is not completely effluxed from 435s/M14-DR cells (Figure 4.2C vs. Figure 4.2B). Therefore, since 435s/M14-DR cells continue to retain some doxorubicin, yet, are resistant to its effects, this indicates that transporter-independent pathways are likely to contribute to doxorubicin resistance. To test this hypothesis, we examined whether 435s/M14-DR cells continue to efflux doxorubicin following prolonged treatment with doxorubicin (72h; cell viability time point). Interestingly, doxorubicin was efficiently effluxed after 2h doxorubicin treatment; however, after 72h, high levels of doxorubicin were retained in 435s/M14-DR cells (Figure 4.3C), even though >80% of cells are alive at this time point

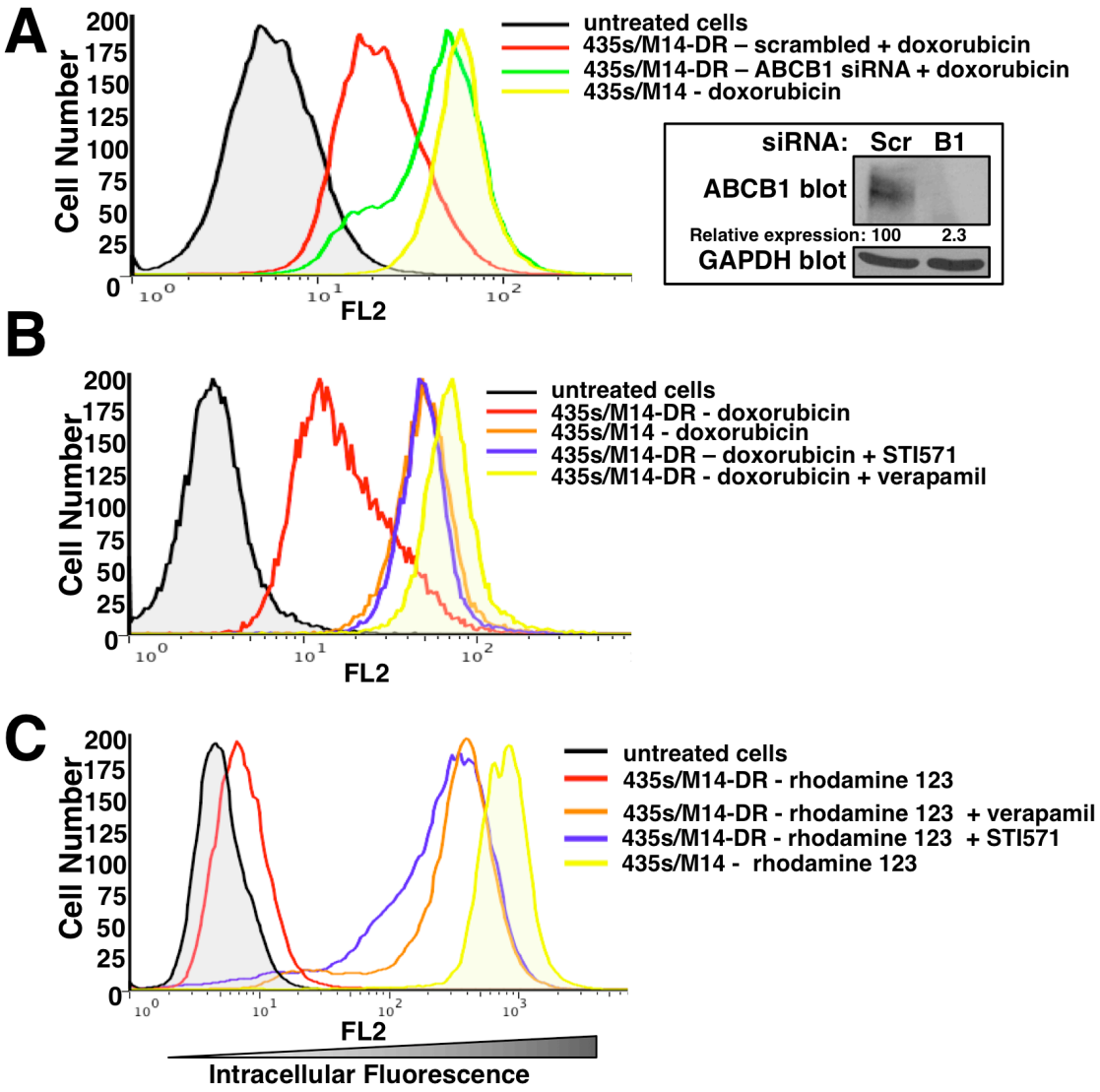

Figure 4.2. STI571 reverses doxorubicin-resistance, in part, by directly inhibiting ABCB1 function. **(A)** siRNA-transfected cells were treated with doxorubicin for 30', cells were washed, and intracellular doxorubicin fluorescence quantitated by FACS analysis. A representative Western blot demonstrating siRNA knockdown efficiency on the day of harvest is shown (right). **(B, C)** Cells were treated with either doxorubicin (10μM) **(B)** or rhodamine 123 (0.5μg/ml) **(C)** in the presence of the ABCB1 inhibitor, verapamil (10μM), or STI571 (40μM) for 30', washed and incubated with verapamil or STI571 for an additional 45', and rhodamine 123 or doxorubicin intracellular fluorescence assessed by FACS. Experiments shown are representative of 3 independent experiments.

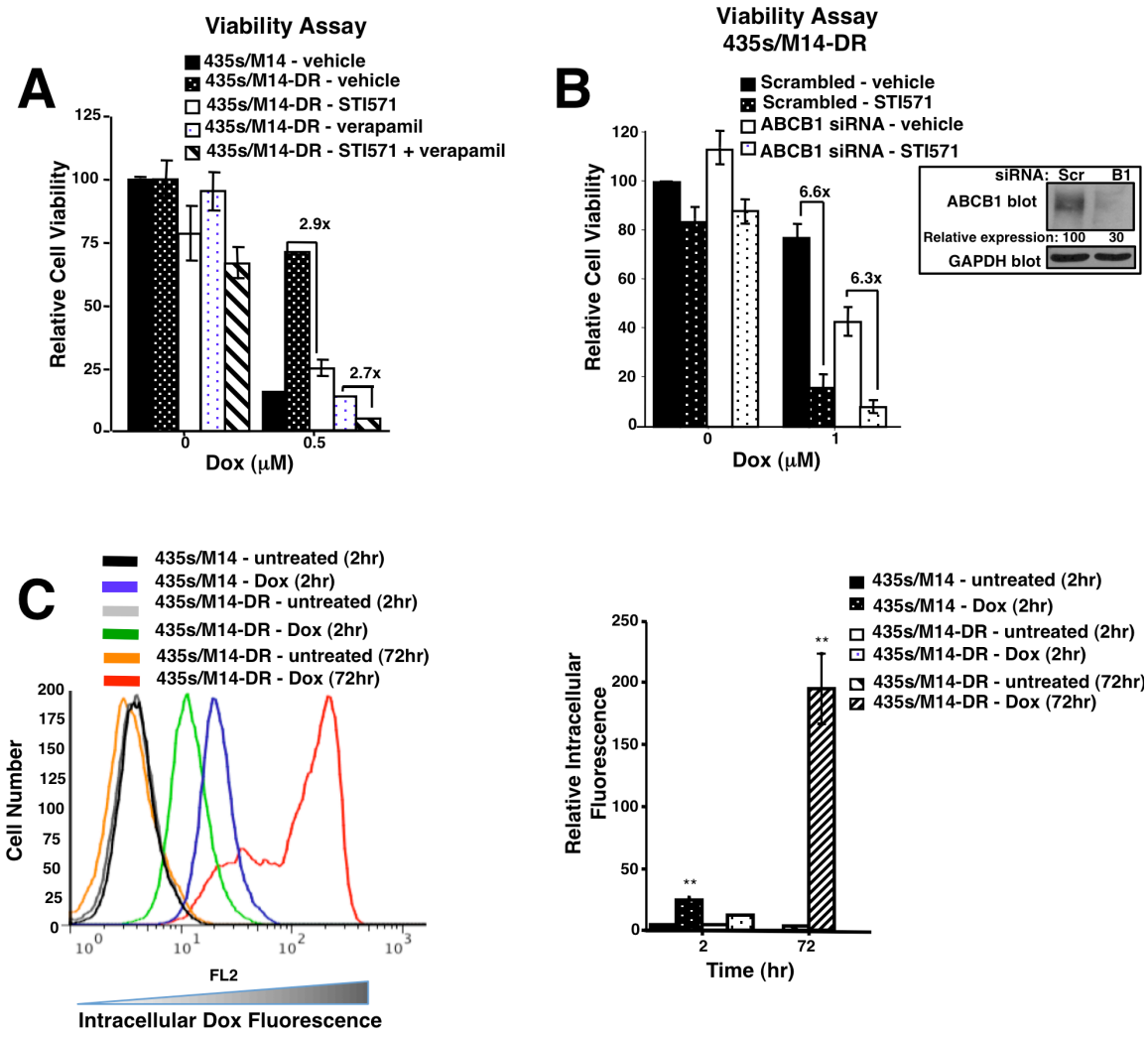

Figure 4.3. **Resistance to doxorubicin occurs via transporter-dependent and independent mechanisms.** **(A,B)** ABCB1 was inhibited with verapamil (10μM) **(A)** or silenced with siRNA **(B)**, cells were treated STI571 (10μM) and/or doxorubicin (0.5μM) for 72h, and cell viability assessed (CellTiter-Glo assay; Promega, Madison, WI). A representative Western blot demonstrating silencing efficiency on the day of harvest is shown **(B, right)**. Dox+STI571 CI=0.66±0.19; Dox+verapamil CI=0.14±0.04; Dox+STI571+verapamil CI=0.47±0.5. **(C)** Cells were treated with doxorubicin (1μM) for 2h or 72h, washed, and intracellular doxorubicin fluorescence assessed by FACS. Graphs are representative of 3 independent experiments **(A-C)**. **(C, right)** Mean±SEM from 3 independent experiments. Some error bars are too small for visualization. **$p \leq 0.01$.

(Figure 3.4A). Taken together, these data indicate that transporter-independent pathways also play a major role in resistance of 435s/M14-DR cells to doxorubicin.

4.4 Discussion

In this chapter, we demonstrate that STI571 directly inhibits ABCB1 function in melanoma cells and activated c-Abl contributes to acquired doxorubicin resistance by upregulating expression of ABCB1. c-Abl/Arg inhibitors have been identified as substrates of drug transporters in other cell types [134, 197]; however, this is the first demonstration that they inhibit ABCB1 in melanoma cells. In addition, we are the first to show that activation of c-Abl promotes expression of an ABC transporter, which indicates that STI571's effects on drug transport involve not only direct inhibition but also indirect modulation via expression regulation. These data are significant because they indicate that c-Abl plays an active role in promoting ABC transporter upregulation during acquired chemotherapeutic resistance. Intriguingly, ABCB1 also is known to efflux STI571 [148]; however, doxorubicin-resistant, ABCB1-expressing cells are actually more sensitive to STI571 than parental cells (Figure 3.4A). This may be due to the fact that c-Abl is more highly activated in resistant compared with parental cells (Figure 4.4A), since STI571 preferentially binds the active conformation of c-Abl/Arg [198]. c-Abl protein expression was decreased in a post-transcriptional manner, since no change was observed in mRNA levels (Figure 4.4A). In addition, more c-Abl was localized to the cytoplasm in the highly resistant cells relative to parental cells (Figure 4.4B), which is significant, since we previously demonstrated that activation of cytoplasmic c-Abl and Arg promotes cancer cell proliferation, anchorage-independent growth, invasion, and survival [38, 39, 193].

The ability of c-Abl/Arg inhibitors to not only sensitize highly resistant cells to doxorubicin, but also paclitaxel, indicates broad spectrum application of c-Abl/Arg inhibitors is warranted for any therapeutic regimen targeting drug-resistant cells possessing highly active c-Abl/Arg. c-Abl/Arg inhibitors have been shown to inhibit a number of ABC transport proteins (i.e., ABCB1, ABCG2) [174, 197], and, based on our data, the transporter-specific inhibitory function of drugs like STI571, coupled with inhibition of c-Abl/Arg signaling mechanisms, may indicate a high degree of therapeutic usefulness for patients whose tumors harbor highly active Abl family kinases.

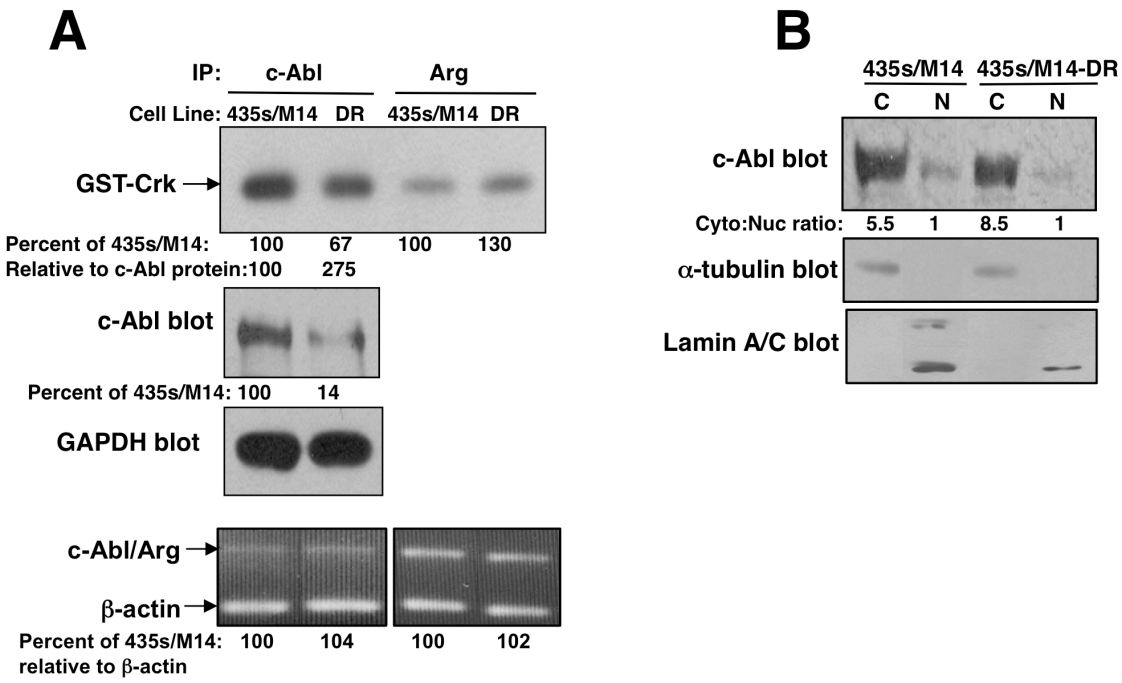

Figure 4.4. 435s/M14–DR cells contain highly active, predominantly cytoplasmic Abl family kinases. (A) c-Abl and Arg were immunoprecipitated from untreated cell lysates and analyzed by *in vitro* kinase assay using GST-Crk as a substrate (top), by Western blotting with indicated antibodies (middle), or RNA was extracted from untreated cells and semi-quantitative RT-PCR was performed with c-Abl- and Arg-specific primers (bottom). **(B)** Cells were fractionated into cytoplasmic/membrane and nuclear fractions using NE-PER (Pierce) and analyzed by Western blotting. All experiments were performed three times, and representative experiments are shown.

Although 435s/M14-DR cells, which have acquired resistance to doxorubicin, express high levels of ABCB1, and ABCB1 clearly effluxes doxorubicin, unlike rhodamine 123, another ABCB1 substrate, doxorubicin is not fully effluxed from these cells (Figure 4.2). This could be due to upregulation of another transporter that effluxes doxorubicin. Although we did not observe upregulation of ABCC1, ABCG2, or ABCC2, we cannot rule out upregulation of other transporters that efflux doxorubicin (Figure 4.1B; data not shown). However, we found that prolonged treatment (72h) with doxorubicin induces a significant accumulation of intracellular doxorubicin (Figure 4.3C) even though >80% of the cells are alive at this time point (Figure 3.4A). The enhanced intrinsic resistance of these cells, which allows them to thrive despite retaining drastically high levels of doxorubicin (in connection with our data demonstrating STI571 decreases cell viability to a greater degree than explained by silencing/inhibiting ABCB1), leads to our studies in future chapters focused on determining the c-Abl/Arg-mediated signaling pathway that promotes cellular resistance to chemotherapy.

In summary, our data demonstrate that c-Abl and Arg dramatically promote acquired chemoresistance in melanoma cells in part by inducing expression of an efflux pump (ABC transporter). These data have important clinical ramifications, as they indicate that c-Abl/Arg inhibitors not only may be effective for treating metastatic disease [193], but also are likely to be effective in reversing acquired chemoresistance.

CHAPTER FIVE

ABL FAMILY KINASES PROMOTE MELANOMA CHEMORESISTANCE VIA STAT3-MEDIATED INHIBITION OF NF-KB TRANSCRIPTIONAL REPRESSION AND A STAT3-MEDIATED HSP27/P38/AKT SURVIVAL PATHWAY

5.1 Introduction

Cancer therapy is severely limited by resistance to currently used treatments [116]. Tumor cells resistant to therapeutic intervention promote advanced disease and metastasis, which is responsible for 90% of all cancer-related deaths [199]. Slightly less than half of all cancers recur due to aberrant proliferation, invasion, and survival, and spread to secondary sites [190]. Thus, there is a great need to identify new drug combinations for treating patients with metastatic disease.

Cancer progression to metastasis is driven by aberrant kinase activation (i.e., PI3K/Akt, MAPK, and receptor tyrosine kinases) and induction of transcription factors such as NF-κB and STAT3, all of which have major roles in survival and chemoresistance [70, 114]. Inhibiting expression of the anti-apoptotic proteins, XIAP and cIAP1, targets of NF-κB, promotes chemotherapy-induced cell death [84, 130]. NF-κB signaling is also activated by STAT3 and PI3K/Akt and promotes cancer cell survival in the presence of chemotherapeutic agents [79-81]; however, recent evidence indicates that NF-κB promotes cell death upon stimulation with chemotherapeutics such as doxorubicin in some cell types [86, 87]. These studies demonstrated that doxorubicin induces apoptosis via p65/RelA-mediated transcriptional repression of anti-apoptotic genes [86, 87, 200, 201]. Understanding the dual nature of NF-κB and elucidating how it may be possible to convert this classically pro-survival protein into a tumor suppressor is an especially intriguing therapeutic option. Activation of the PI3K/Akt pathway is critical for chemoresistance and survival [60, 70, 71]; however, the mechanism by which Akt activation occurs in response to chemotherapeutic agents is unclear. Therefore, it is important to ascertain cell type-specific activators of Akt signaling in order to design drugs that can prevent aberrant activation in response to therapy.

Recently, we provided the first evidence that Abl family non-receptor tyrosine kinases (c-Abl, Arg) are activated in a subset of primary melanomas and in some melanoma cell lines, and promote many processes involved in melanoma progression such as proliferation, invasion, survival, and metastasis [50]. We further demonstrated that c-Abl promotes melanoma cell invasion in a STAT3-dependent manner [50]. Based

on our data in both breast cancer and melanoma cells demonstrating that activated c-Abl/Arg promote processes including proliferation and invasion [38, 39, 50], and survival in response to chemotherapeutic agents (chapters 2-4), we focused this chapter on the signaling mechanisms by which c-Abl/Arg promote chemoresistance. Understanding the mechanisms underlying drug resistance is critical for developing new therapies to treat resistant/disseminated disease. In this chapter, we identified novel signaling pathways by which cells develop resistance to the chemotherapeutic anthracycline, doxorubicin, by demonstrating that c-Abl/Arg: 1) modulate STAT3 to prevent NF-κB-mediated repression of anti-apoptotic targets, and 2) act via STAT3 to promote HSP27/p38/Akt activation. These data demonstrate not only that c-Abl/Arg inhibitors are likely to prevent chemotherapeutic resistance, but also outline the specific mechanism by which c-Abl and Arg promote survival in the presence of doxorubicin.

5.2 Materials and Methods

5.2.1 Cell Lines and Reagents

Cell lineage and culturing procedures were described in chapters 3 and 4. STAT3 cDNA (pRc/CMV-STAT3C; Addgene, Cambridge, MA) was donated by Dr. James Darnell. Vector and STAT3C-expressing cells were obtained by transfection, G418 selection (900μg/ml), and pooling clones. The 3X-NF-κB reporter construct was provided by Dr. Denis Guttridge (Ohio State University; Columbus, OH) [202]. Cells expressing GFP-tagged PI3K(E545K) (Addgene, Cambridge, MA) were obtained by transfection/G418+Puromycin selection, and flow sorting GFP-positive cells (University of Kentucky Flow Cytometry Facility). STI571 (Gleevec; imatinib mesylate) and nilotinib were obtained from Novartis (Basal, Switzerland). STI571 was dissolved in water (10mM) and stored at -80^{o}C. Doxorubicin was purchased from Sigma (St. Louis, MO). LY294002 was obtained from Cell Signaling Technology (Danvers, MA). Silencer select STAT3 and p65/RelA siRNAs were purchased from Ambion. PARP (poly(ADP-ribose) polymerase; sc-8007), α-tubulin, p65/RelA antibodies were purchased from Santa Cruz Biotechnologies (Santa Cruz, CA); GAPDH was obtained from BD Biosciences (Chicago, IL); Lamin A/C was obtained from Milllipore (Temecula, CA); β-Actin and FLAG (M2) antibodies from Sigma (St. Louis, MO); XIAP, cIAP1, and HSP27 antibodies were from R&D Systems (Minneapolis, MN); and STAT3, phospho-STAT3 (Y705), caspase-3 (8G10), phospho-Crk/CrkL (Y221/Y207), phospho-p38 (T180/T182), p38, Akt, and phospho-Akt (S473) antibodies were purchased from Cell Signaling Technology

(Danvers, MA). Western blots were performed as described in the manufacturers' protocols.

5.2.2 Viability and Apoptosis Assays

CellTiter-Glo Viability Assay (Promega; Madison, WI). Cells were plated in 96-well plates in triplicate in 100μl of medium, refreshed with media containing drugs the following day when cells were 30-40% confluent, and harvested 72h later. CellTiter-Glo reagent (100μl) was added to each well, the plates were rocked for 2', incubated at room temperature for 10', 100μl was removed from each well and transferred to an opaque 96-well plate, and luminescence (total light emitted, 10"/well) measured with a Synergy 2 microplate reader (Biotek; Winooski, VT). PARP and caspase-3 cleavage blots. Cells were plated in 60mm dishes, and treated with drugs the following day when cells were 30-40% confluent. After 40h, attached and detached cells were lysed in RIPA buffer (50mM Tris pH 7.5, 150mM NaCl, 1% Triton-X 100, 0.1% SDS, 1% sodium deoxycholate), protein was quantitated by Lowry DC (Bio-Rad; Hercules, CA), equal protein was loaded on SDS-PAGE gels, and blots were incubated with antibodies for PARP, caspase-3, and GAPDH.

5.2.3 Proliferation Assays

Tritiated thymidine assays [180]. Cells were plated in 24-well plates in triplicate, drug-treated the following day when cells were 30-40% confluent, and harvested after 72h. Cells were pulsed with tritiated thymidine (2.5 μCi; 2h), washed with PBS, incubated in 10% trichloroacetic acid, radioactivity was solubilized in 0.2N NaOH, and analyzed on a scintillation counter. Cell cycle analysis. Cells were plated in 100mm dishes, refreshed with media containing drugs the following day when cells were 30-40% confluent, and harvested after 72h. Cells were labeled with bromodeoxyuridine (BrdU, 10μM) for 1h at 37°C, trypsinized, washed and permeabilized with ethanol (70%), stained with fluorescein isothiocyanate (FITC)-conjugated anti-BrdU antibody and propidium iodide (PI; 5μg/ml), and analyzed by fluorescence-activated cell sorting (FACS) using Cell Quest software (BD Biosciences) and Modfit analysis (Verity Software House, Topsham, ME).

5.2.4 Semi-quantitative RT-PCR

Cells were plated in 60mm dishes, refreshed with media containing drugs the following day when cells were 30-40% confluent, RNA extracted 48h later (RNeasy kit; Qiagen; Valencia, CA), digested with DNase I (Invitrogen), reverse-transcribed with Superscript Reverse Transcriptase and random primers (Invitrogen; Carlsbad, CA), and PCR performed using primers specific for XIAP (10nM), cIAP1 (10nM). β-actin primers (10nM) were included in the PCR reaction as an internal control. PCR cycling parameters involved 27 cycles of 95^{o}C-1', 55^{o}C-1', 72^{o}C-1'. Aliquots were also taken at cycles 31 and 35 to check for linearity. Scanned photographs were quantified with ImageQuant (Molecular Dynamics, GE Healthcare, Piscataway, NJ) and specific bands normalized to β-actin internal control bands.

cIAP1 forward primer, 5'CAGCCTGAGCAGCTTGCAA3',
cIAP1 reverse primer, 5'CTTCTGAAGAACTTTCTCCAG3'
XIAP forward primer, 5'AGTGGTAGTCCTGTTTCAGCATCA3',
XIAP reverse primer, 5'AAAGATAGTCTGCATGTGTCTCAG3'
β-actin forward primer, 5'CCTTCCTGGGCATGGAGTCCT3',
β-actin reverse primer 5'GGAGCAATGTCTTTGATCTTC3'

5.2.5 Luciferase assays

Cells were transfected with 3X-NF-κB luciferase reporter and pcDNA3.1 plasmids (10:1 ratio), selected with G418 (900μg/ml), and clones were pooled. Cells expressing the reporter were plated in triplicate, treated with STI571 and/or doxorubicin for 24h, lysed in lysis buffer (Promega; Madison, WI), lysate was incubated with luciferin (Promega; Madison, WI) for 2", and luminescence resulting from luciferase activity measured with the Synergy 2 microplate reader (total light emitted, 10"/well).

5.2.6 Nuclear fractionation assays

Cells were plated in 60mm dishes, and nuclear fractions were isolated using the NE-PER kit (Pierce; Rockford, IL) as described in the manufacturer's protocol.

5.2.7 Statistics

Statistical analyses were performed using Sigma Stat for Windows (Systat Software, Inc.; San Jose, CA). Combination Index (CI) values were calculated with

CalcuSyn software (Biosoft; Cambridge, UK) using single drug and drug combination dose response curves.

5.3 Results

5.3.1 c-Abl/Arg promote survival in response to doxorubicin in a STAT3-dependent manner.

We focused our efforts on better understanding the signaling mechanisms by which c-Abl/Arg promote chemoresistance in melanoma. Progression of melanoma from radial growth phase to vertical growth phase depends on aberrant expression of transcription factors, such as STAT3 [114]. We previously showed that c-Abl/Arg induced STAT3 phosphorylation in melanoma and breast cancer cells [39, 50]. Therefore, we tested whether Abl family kinases mediated survival in the presence of chemotherapeutics in a STAT3-dependent manner. We demonstrated that inhibition of Abl family kinases induced caspase-3/7 activity in melanoma and breast cancer cells (Figure 2.1B) [188]; therefore, we first tested the relationship of STAT3 and c-Abl/Arg in absense of doxorubicin. We observed that stable expression of a constitutively active form of STAT3 (STAT3C) completely rescued STI571-mediated induction of caspase-3/7 activity (Figure 5.1A). Since c-Abl/Arg act via STAT3 to promote survival, we proceeded to assess the effect of doxorubicin+STI571 on STAT3 phosphorylation in parental and acquired chemoresistant melanoma cells. We observed a dramatic decrease in pSTAT3 (Figure 5.1B) that corresponded with significantly decreased cell viability (Figure 3.1A; 3.4A). Expression of STAT3C partially rescued the ability of STI571 to synergize with doxorubicin to decrease cell viability (Figure 5.2A) and promote G2/M arrest (Figure 5.2B, C). This indicates that c-Abl/Arg promote cell proliferation in the presence of doxorubicin in a STAT3-independent manner.

We next tested whether c-Abl/Arg promote resistance to doxorubicin-induced apoptosis via STAT3. We observed that STAT3C completely rescued the STI571-mediated increase in doxorubicin-induced apoptosis as detected by cleavage of PARP and caspase-3 (Figure 5.3A). Cleavage of PARP and caspase-3 was assessed after cells were treated with doxorubicin or doxorubicin+STI571. In pcDNA cells doxorubicin+STI571 enhanced cleavage of PARP and caspase-3 far greater than doxorubicin alone (Figure 5.3A). However, in cells stably expressing a constitutively active form of STAT3 (STAT3C) there is no corresponding increase in apoptosis with STI571+doxorubicin (Figure 5.3A). Additionally, treatment of STAT3 siRNA-transfected

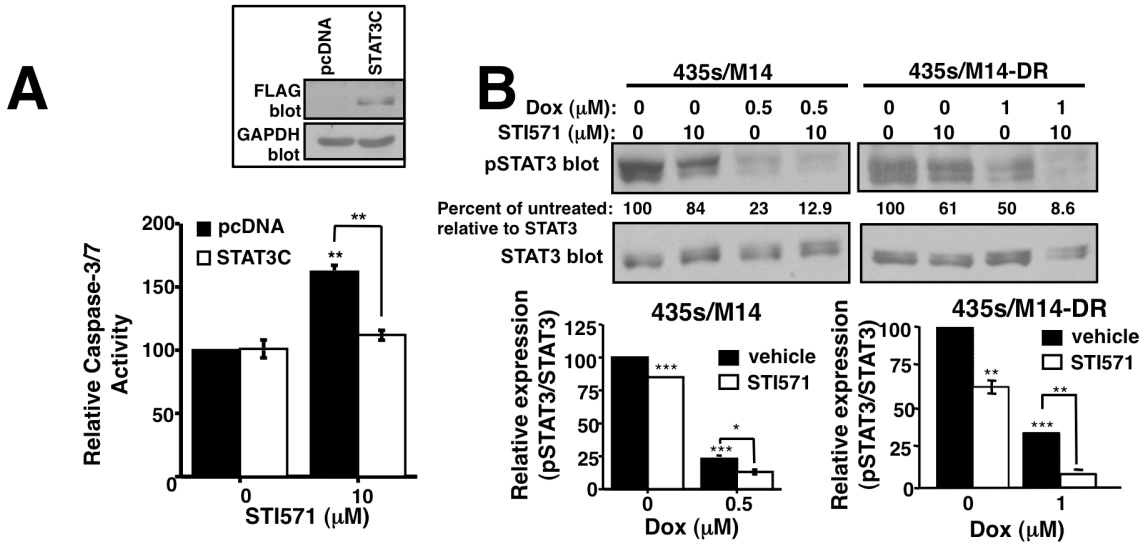

Figure 5.1. **c-Abl/Arg promote survival via STAT3 and regulate pSTAT3 in response to doxorubicin.** **(A)** 435s/M14 cells, stably transfected with pcDNA or STAT3C, were treated with STI571 (40h), attached and detached cells were lysed, caspase-3/7 activation assessed. Graph represents mean±SEM from 3 independent experiments. Representative Western blot demonstrating STAT3C expression is shown. **(B)** Parental (435s/M14) and doxorubicin-resistant (435s/M14-DR) cells were treated with STI571 and/or doxorubicin (40h), attached and detached cells were lysed, and blotted with the indicated antibodies. **p*<0.05,***p*≤0.01, ****p*<0.001.

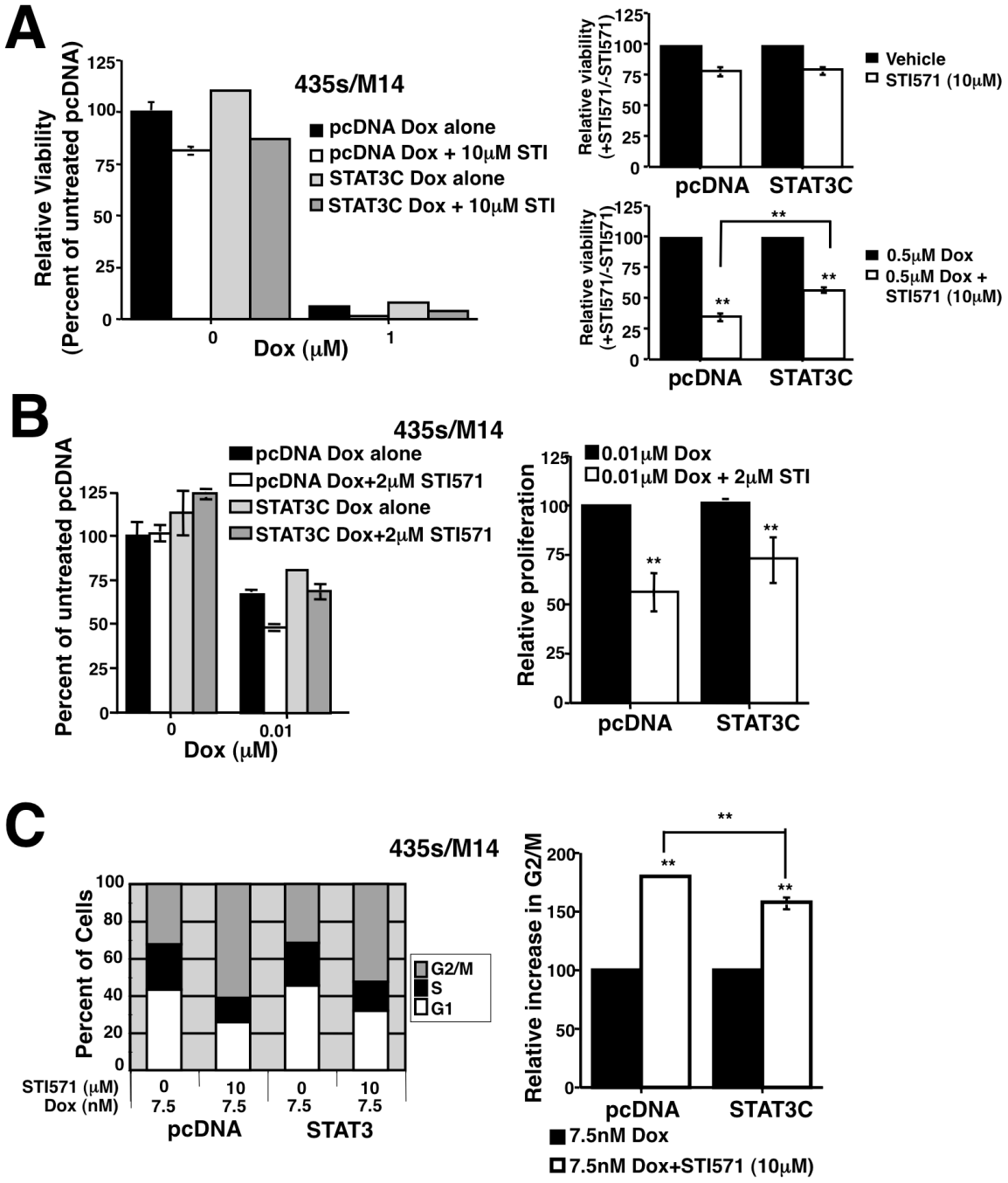

Figure 5.2. c-Abl/Arg promote proliferation in the presence of doxorubicin via a STAT3-independent mechanism. (A-C) pcDNA and STAT3C cells were treated with STI571 and/or doxorubicin for 72h, and analyzed by CellTiter-Glo viability assay (A), tritiated thymidine assay (B), or BrdU/PI FACS analysis (C). Graphs shown represent data from individual experiments (left) and mean±SEM for three independent experiments (right). ** $p \leq 0.01$.

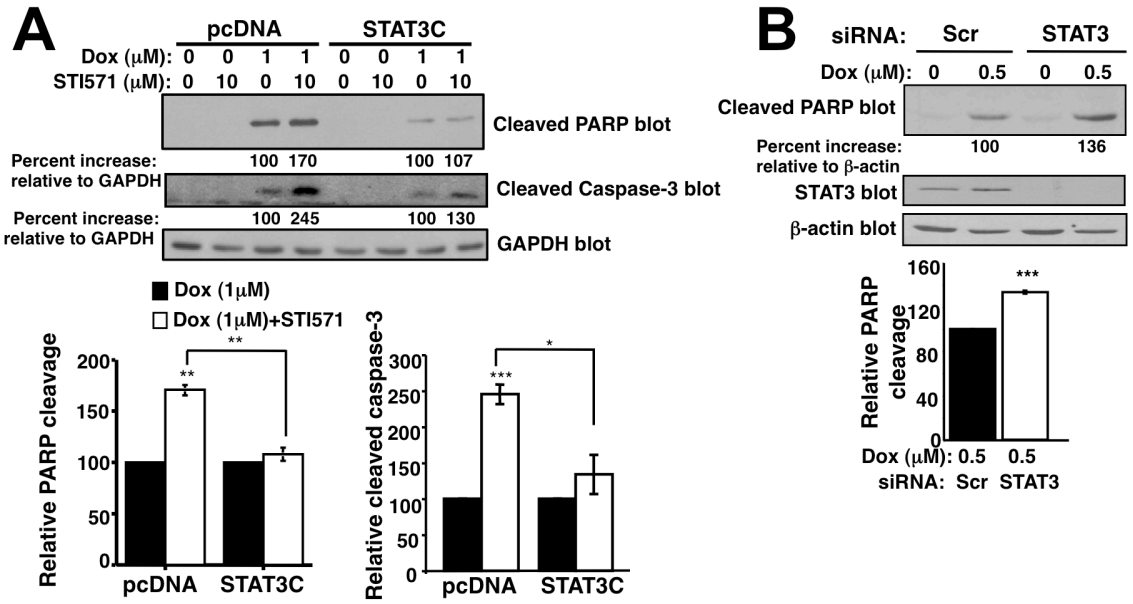

Figure 5.3. **c-Abl/Arg promote survival in response to doxorubicin in a STAT3-dependent manner. (A)** 435s/M14 cells transfected stably with pcDNA or STAT3C cells were treated with STI571 and/or doxorubicin for 40h followed by western blotting with indicated antibodies. **(B)** 435s/M14 cells were transfected with STAT3 siRNA, treated with doxorubicin (40h), and attached and detached cells were lysed, and blotted. Graphs are mean±SEM for three independent experiments. *$p<0.05$,**$p\leq0.01$, ***$p<0.001$.

cells with doxorubicin induced apoptosis (Figure 5.3B). These exciting data show that c-Abl/Arg prevent doxorubicin-induced apoptosis in a STAT3-dependent manner.

5.3.2 c-Abl/Arg→STAT3 prevents doxorubicin-mediated NF-κB transcriptional repression.

NF-κB promotes oncogenesis, increasing proliferation, survival, invasion, and metastasis by promoting the transcription of pro-proliferative, pro-invasive, and anti-apoptotic genes [203]. Recent data has shown that STAT3 promotes NF-κB transcriptional activity and acetylation of p65/RelA [78]. Based on our strong data demonstrating a link between c-Abl/Arg and STAT3, we next examined whether c-Abl/Arg regulated NF-κB signaling in these cells. We fractionated STI571-treated cells and observed that STI571 decreased nuclear localization of p65/RelA (Figure 5.4A). We also measured p65/RelA nuclear localization following treatment of cells with c-Abl/Arg-specific siRNAs, and we observed that c-Abl/Arg promote p65/RelA nuclear localization (Figure 5.4B). We tested whether c-Abl/Arg promote NF-κB transcriptional activity by creating a cell line that stably expressed a NF-κB promoter-regulated luciferase construct [202]. We demonstrated that STI571 decreased NF-κB activity both basally and following stimulus with TNFα (Figure 5.4C). Importantly, these data provide the first demonstration that c-Abl/Arg regulate NF-κB signaling in melanoma.

In some cell types, NF-κB promotes survival and resistance to doxorubicin; however, in other cells, doxorubicin kills cells by activating NF-κB and converting it into a repressor, which promotes apoptosis [75, 86, 87, 200]. To determeine how STI571+doxorubicin affected NF-κB activity, we fractionated parental 435s/M14 melanoma cells after treatment with STI571+doxorubicin and observed a dramatic increase in the doxorubicin-induced nuclear localization of p65/RelA by STI571 (Figure 5.5A). This coincided with an increase in p65/RelA phosphorylation at both 8h and 40h (Figure 5.5B, data not shown). In parental 435s/M14 cells, the increase in nuclear p65/RelA following doxorubicin+STI571 also coincided with decreased NF-κB transcriptional activity, as observed by a decrease in luciferase activity (Figure 5.5C, top). Intriguingly in contrast, doxorubicin treatment induced NF-κB transcriptional activity in 435s/M14-DR cells, and this was abrogated by cotreatment with STI571 (Figure 5.5C, bottom). This demonstrates that NF-κB signaling is regulated very differently in parental vs. acquired chemoresistant cells.

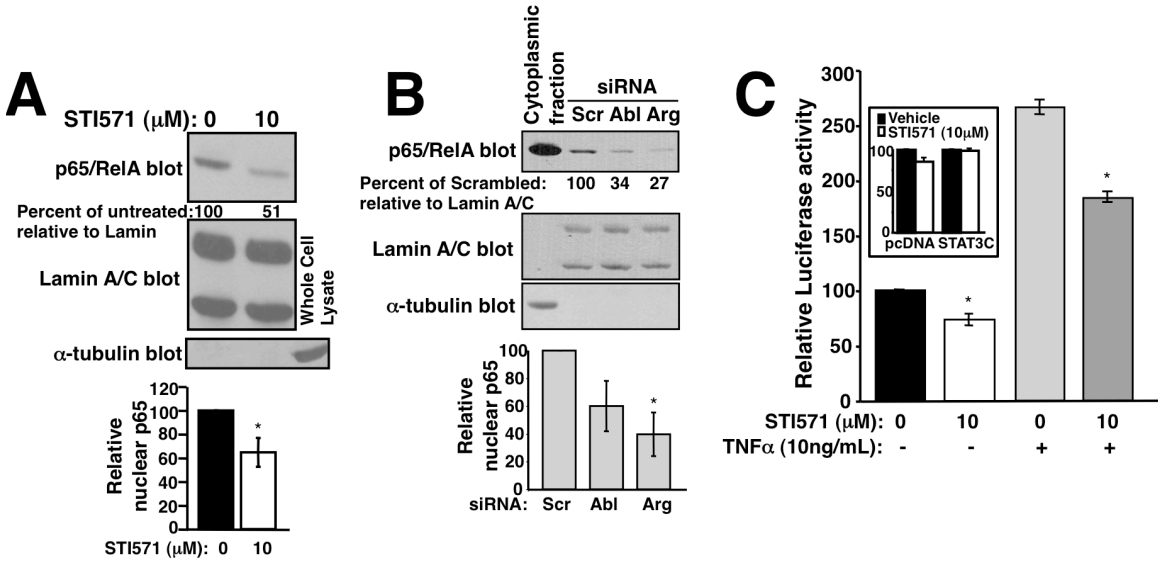

Figure 5.4. c-Abl/Arg promote NF-κB signaling in melanoma cells. (A, B) Cells were treated with STI571 for 40h (A), or c-Abl/Arg-specific siRNAs (B), fractionated using NE-PER (Pierce), and nuclear fractions were analyzed by Western blotting. Graphs represent mean±SEM from 3 independent experiments. **(C)** Cells stably expressing a 3X-NF-κB-luciferase reporter were plated in triplicate, treated with STI571 for 8h in the absense or presence of TNFα, and luciferase activity assessed in the lysate (Promega, Madison, WI). Mean±SEM for 3 independent experiments is shown. (B) Performed by W. Friend. *p<0.05.

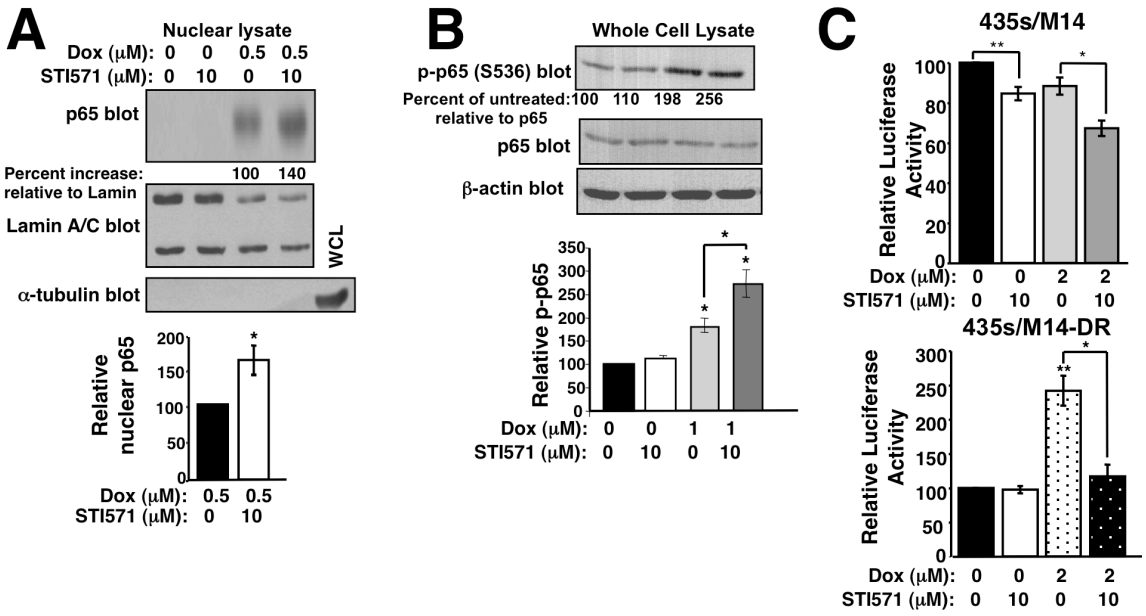

Figure 5.5. **c-Abl/Arg activation of STAT3 prevents doxorubicin-mediated NF-κB transcriptional repression. (A)** 435s/M14 cells were treated with STI571 and/or doxorubicin (8h), and nuclear fractions blotted with indicated antibodies. Graph represents mean±SEM from 3 independent experiments. **(B)** 435s/M14 cells were treated with STI571 and/or doxorubicin (8h), attached and detached cells were lysed, and blotted with indicated antibodies. Graph represents mean±SEM from 3 independent experiments. **(C)** Parental (435s/M14) and doxorubicin-resistant (435s/M14-DR) cells, stably expressing a 3X-NF-κB-luciferase reporter, were treated with STI571 and/or doxorubicin (8h), and luciferase activity assessed. Mean±SEM from 3 independent experiments performed in triplicate. *p<0.05, **p<0.01.

Next, we silenced p65/RelA with siRNA and observed that inhibition of p65/RelA decreased the effectiveness of doxorubicin to induce apoptosis, and, significantly, partially inhibited the dramatic induction of apoptosis observed by cotreatment with STI571 (Figure 5.6). We next wanted to assess whether c-Abl/Arg prevented doxorubicin-induced nuclear localization of p65/RelA in a manner dependent on STAT3. We first tested whether STAT3 affected nuclear localization of p65/RelA by silencing STAT3 since this should have the same effect as inhibiting c-Abl/Arg→STAT3 signaling with STI571. As observed with STI571, silencing STAT3 resulted in increased nuclear p65/RelA following doxorubicin treatment (Figure 5.7A). Constitutively active STAT3 (STAT3C) prevented the STI571+doxorubicin-induced nuclear localization of p65/RelA and, significantly, also prevented the decrease in NF-κB transcriptional activity observed with STI571+doxorubicin (Figure 5.7B, C). These data are significant because we are the first to demonstrate that c-Abl/Arg act via STAT3 to inhibit nuclear localization of p65/RelA and thereby relieve the doxorubicin-induced NF-κB-mediated transcriptional repression of anti-apoptotic genes. These data indicate that inhibition of c-Abl/Arg→STAT3 induces doxorubicin-mediated NF-κB transcriptional repression.

5.3.3 c-Abl/Arg promote cIAP1/XIAP transcription in the presence of doxorubicin in a STAT3-dependent manner.

Since c-Abl/Arg inhibit doxorubicin-mediated NF-κB transcriptional repression via STAT3, we sought to establish whether this resulted in expression changes of anti-apoptotic NF-κB targets. The anti-apoptotic proteins, cIAP1 and XIAP, targets of NF-κB, are overexpressed in melanomas, and prevent caspase activation in response to apoptotic stimuli [204-206]. We performed semi-quantitative RT-PCR and demonstrated that c-Abl/Arg promote transcription of cIAP1/XIAP in the presence of doxorubicin. Doxorubicin induced transcription of cIAP1/XIAP and c-Abl/Arg were required for cIAP1/XIAP transcription in the presence of doxorubicin, since transcript levels were dramatically lower following cotreatment with STI571 (Figure 5.8A, B). We confirmed this finding by Western blot and observed a decrease in expression of both of these anti-apoptotic proteins following treatment with STI571+doxorubicin at both 8 and 40 hours (Figure 5.8A, B; data not shown). In doxorubicin-resistant cells, doxorubicin treatment increased transcription of cIAP1, but had little effect on XIAP transcription or cIAP1/XIAP protein expression (Figure 5.9A, B). However, addition of STI571 dramatically reduced

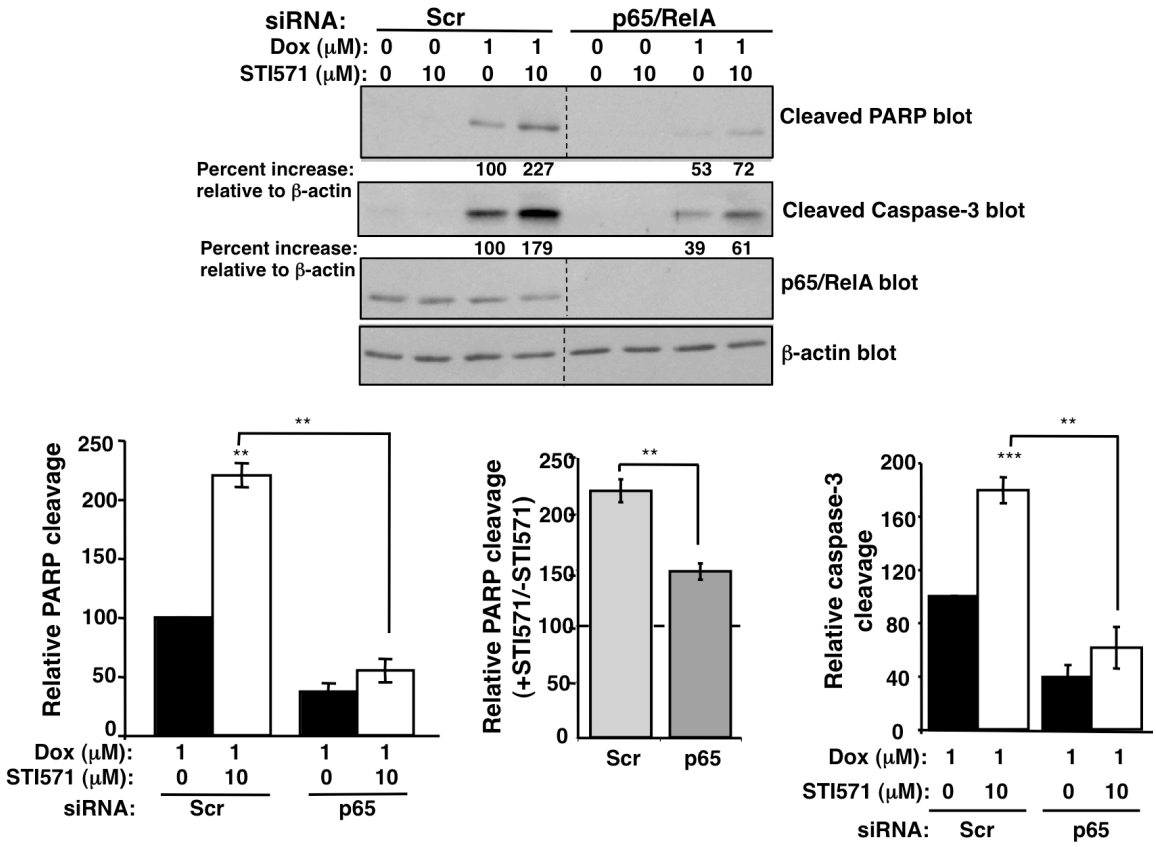

Figure 5.6. **p65/RelA is required for doxorubicin-mediated apoptosis.** 435s/M14 cells, transfected with p65/RelA siRNA, were treated with STI571 and/or doxorubicin (8h), and PARP and caspase-3 cleavage assessed. Mean±SEM from 3 independent experiments (left). Mean±SEM of fold differences between doxorubicin+STI571 and doxorubicin-treated samples (right). ** $p \leq 0.01$, *** $p < 0.001$.

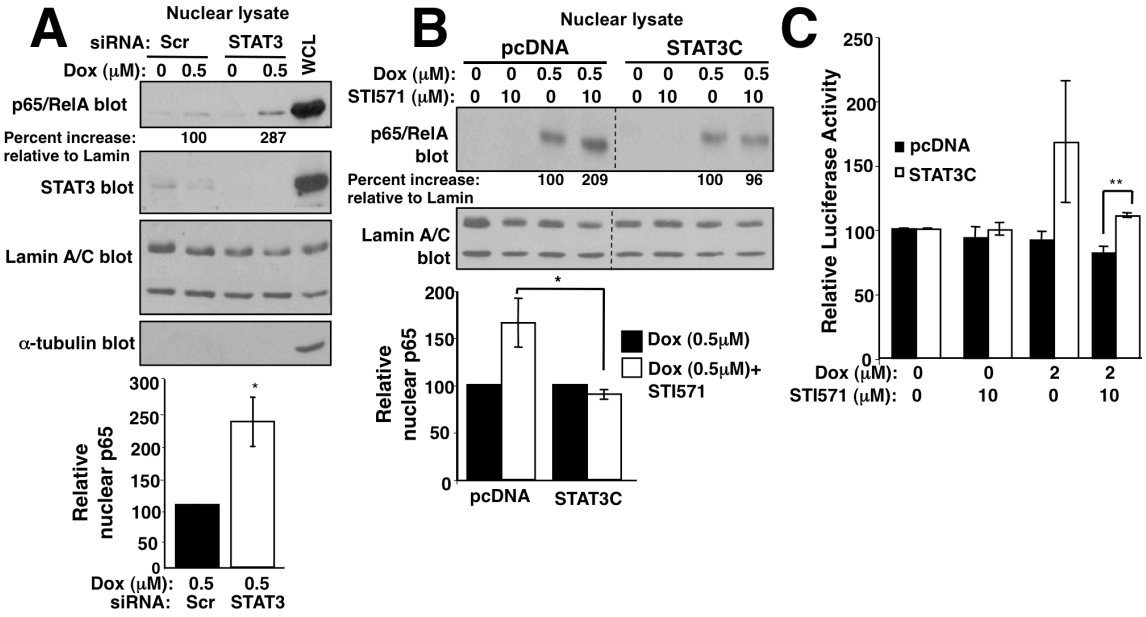

Figure 5.7. **c-Abl/Arg inhibit p65-mediated transcriptional repression in a STAT3-dependent manner. (A)** 435s/M14 cells, transfected with STAT3 siRNA, were treated with doxorubicin (8h), and nuclear fractions analyzed by Western blot. Graph represents mean±SEM from 3 independent experiments. **(B)** 435s/M14 cells stably expressing pcDNA or STAT3C were treated with STI571 and/or doxorubicin (8h), and nuclear fractions assessed by Western blot. Graph represents Mean±SEM of 3 independent experiments. **(C)** pcDNA and STAT3C-expressing cells, stably expressing a 3X-NF-κB-luciferase reporter, were treated with STI571 and/or doxorubicin (8h), and luciferase activity assessed. Mean±SEM from 3 independent experiments performed in triplicate. **p*<0.05, ***p*≤0.01.

cIAP1/XIAP protein expression at 12h and 40h time points (Figure 5.9A, B; data not shown), and inhibited transcription of cIAP1 (Figure 5.9A, B). Moreover, expression of STAT3C prevents the STI571+doxorubicin-mediated decrease in cIAP1/XIAP in parental cells, confirming the role of c-Abl/Arg→STAT3 in mediating expression of anti-apoptotic factors in the presence of doxorubicin (Figure 5.10). These data are significant because they confirm that STI571 not only prevents NF-κB activation following doxorubicin treatment, but also converts NF-κB into a transcriptional repressor, thereby inhibiting transcription of cIAP1/XIAP.

5.3.4 c-Abl/Arg promote survival to doxorubicin via HSP27/p38/Akt pathway.

c-Abl/Arg act via STAT3 to prevent NF-κB transcriptional repression in response to doxorubicin, promoting survival and chemoresistance of metastatic melanoma cells. However, c-Abl/Arg→STAT3 promote survival in the presence of doxorubicin via more than one signaling pathway since expression of constitutively active STAT3 (STAT3C) fully rescued STI571-mediated induction of apoptosis (Figure 5.3A) and STI571's potentiation of doxorubicin-mediated NF-κB transcriptional repression (Figure 5.7B, C), but silencing p65/RelA only partially abrogated STI571+doxorubicin-induced apoptosis (Figure 5.6). Therefore, we focused on the PI3K/Akt pathway, a major mediator of survival in melanoma cells and a signaling target of BCR-Abl in leukemic cells [70, 184, 207]. We observed increased phosphorylation of Akt in response to doxorubicin in both parental and doxorubicin-resistant cells, and induction of pAkt in response to doxorubicin is abrogated by addition of STI571 in parental, as well as doxorubicin-resistant, cells (Figure 5.11A, B). Likewise, we observed that doxorubicin activated Abl family kinases, as demonstrated by increased phosphorylation of the c-Abl/Arg substrate, Crk/CrkL (Figure 5.11A). To confirm that activation of Akt promoted survival, we inhibited PI3K using LY294002 and observed that Akt activation indeed promotes melanoma cell survival in response to doxorubicin (Figure 5.11C). The PI3K/Akt pathway promotes survival in response to a wide array of stimuli [62]. In response to neutrophil cell stress, Akt activation occurs via complex formation with HSP27 and activation by p38/MAPK [63, 64]; however, no report has previously described Akt activation by doxorubicin via the cell stress response pathway.

HSP27 expression promotes Akt activity in neutrophils in response to cell stress by forming a complex that brings p38/MAPK in proximity with Akt [64]. We observed that

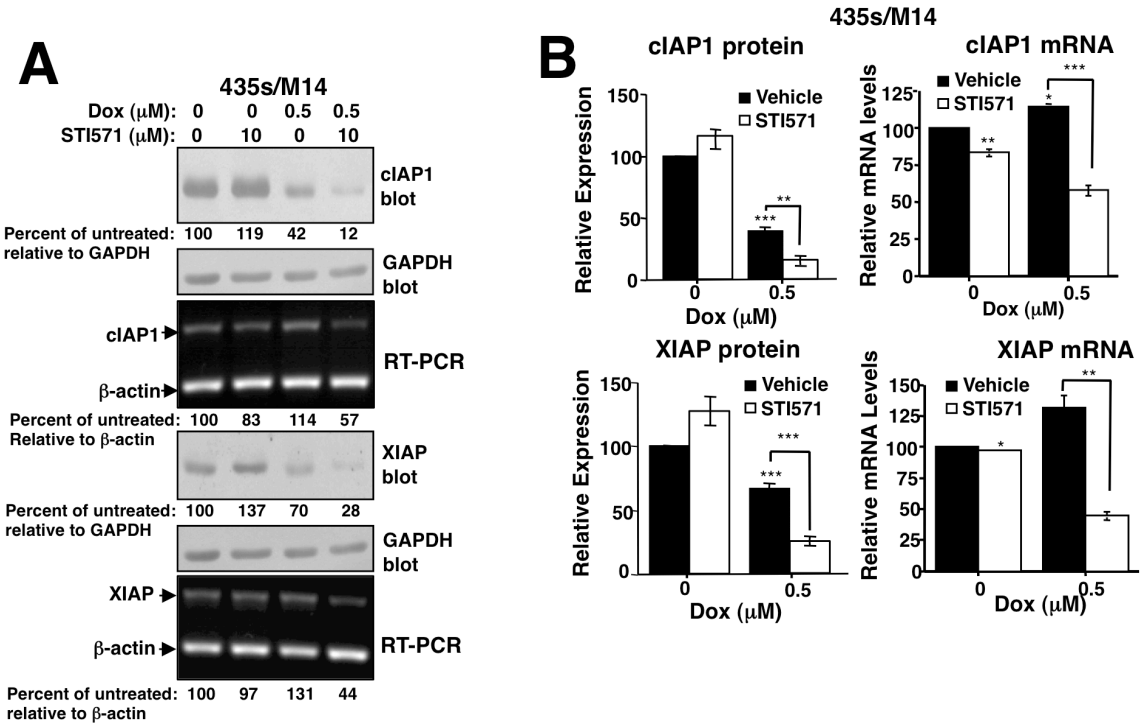

Figure 5.8. c-Abl/Arg promote cIAP1/XIAP expression in melanoma cells. (A) Cells were treated with STI571 and/or doxorubicin (40h-top, 24h-bottom), lysate analyzed by Western blot (top), and RNA subjected to semi-quantitative RT-PCR (bottom). **(B)** Graphical representation of semiquantitative RT-PCR (right) and Western blots (left). Mean±SEM for 3 independent experiments. *p<0.05, **$p\leq$0.01, ***p<0.001.

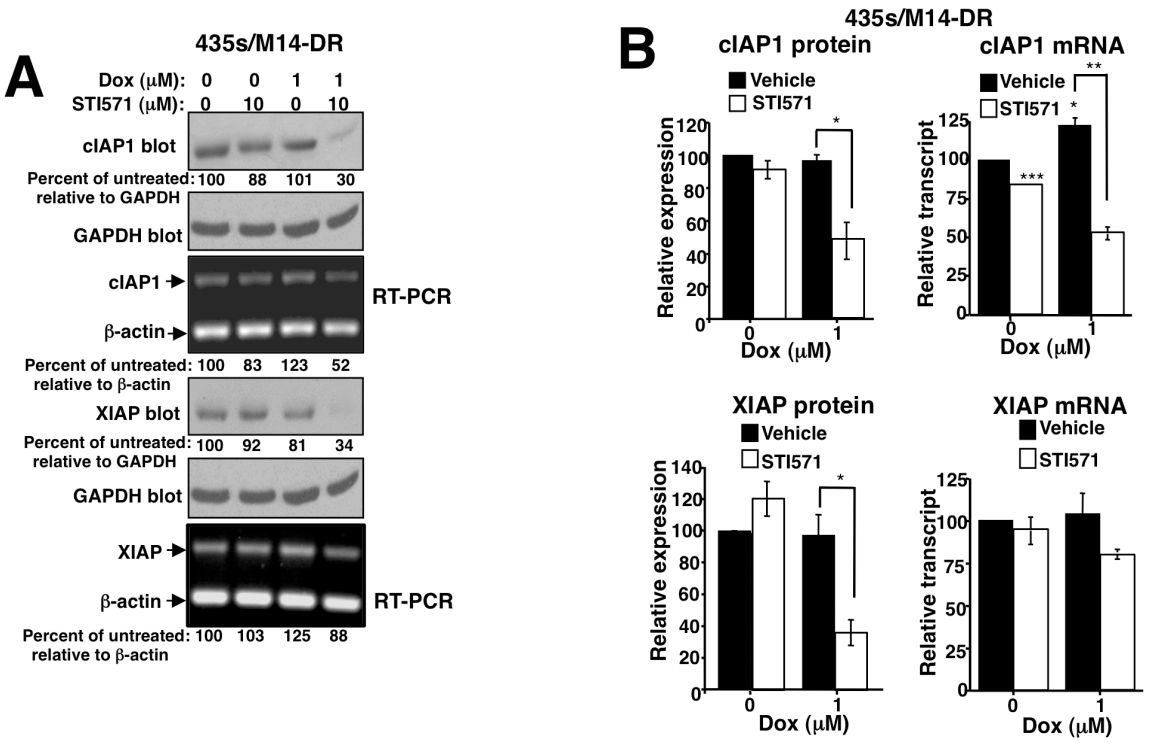

Figure 5.9. c-Abl/Arg promote cIAP1/XIAP expression in highly resistant melanoma cells. (A) Cells were treated with STI571 and/or doxorubicin (40h), lysate analyzed by Western blot (top), and RNA subjected to semi-quantitative RT-PCR (bottom). **(B)** Graphical representation of semiquantitative RT-PCR (right) and Western blots (left). Mean±SEM for 3 independent experiments. *p<0.05, **$p\leq$0.01, ***p<0.001.

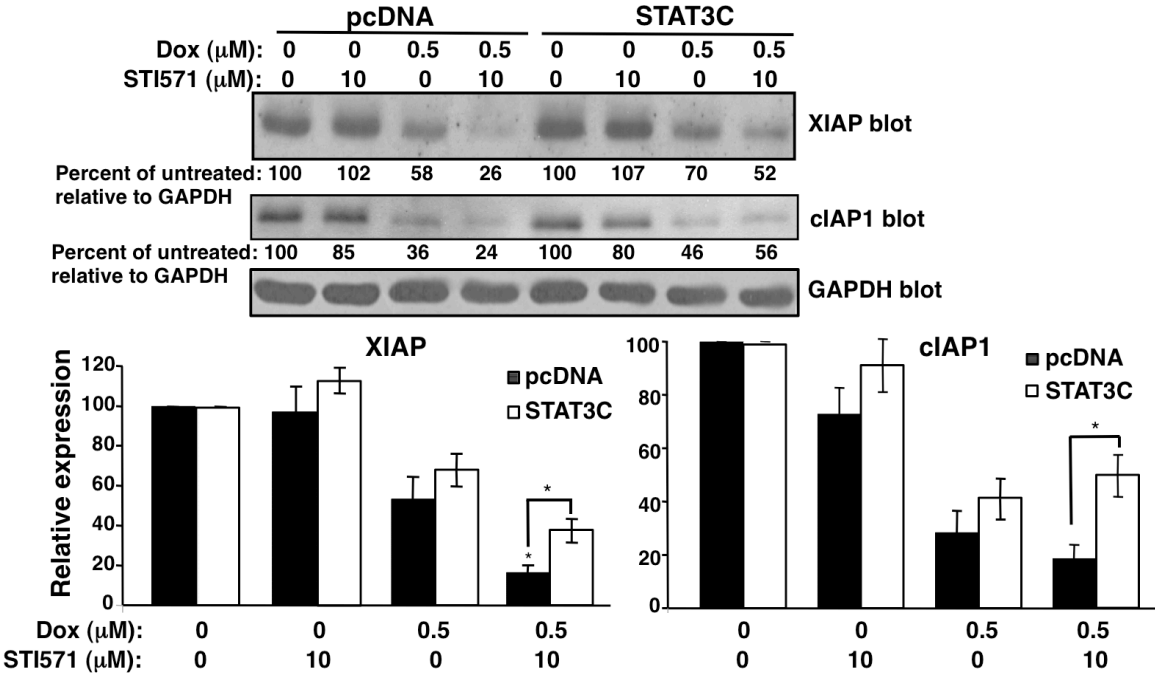

Figure 5.10. **c-Abl/Arg inhibit p65-mediated repression of NF-κB targets in a STAT3-dependent manner.** pcDNA and STAT3C-expressing cells were treated with STI571 and/or doxorubicin (40h), and lysate from attached and detached cells was assessed by Western blot. Mean±SEM from 3 independent experiments. *p<0.05.

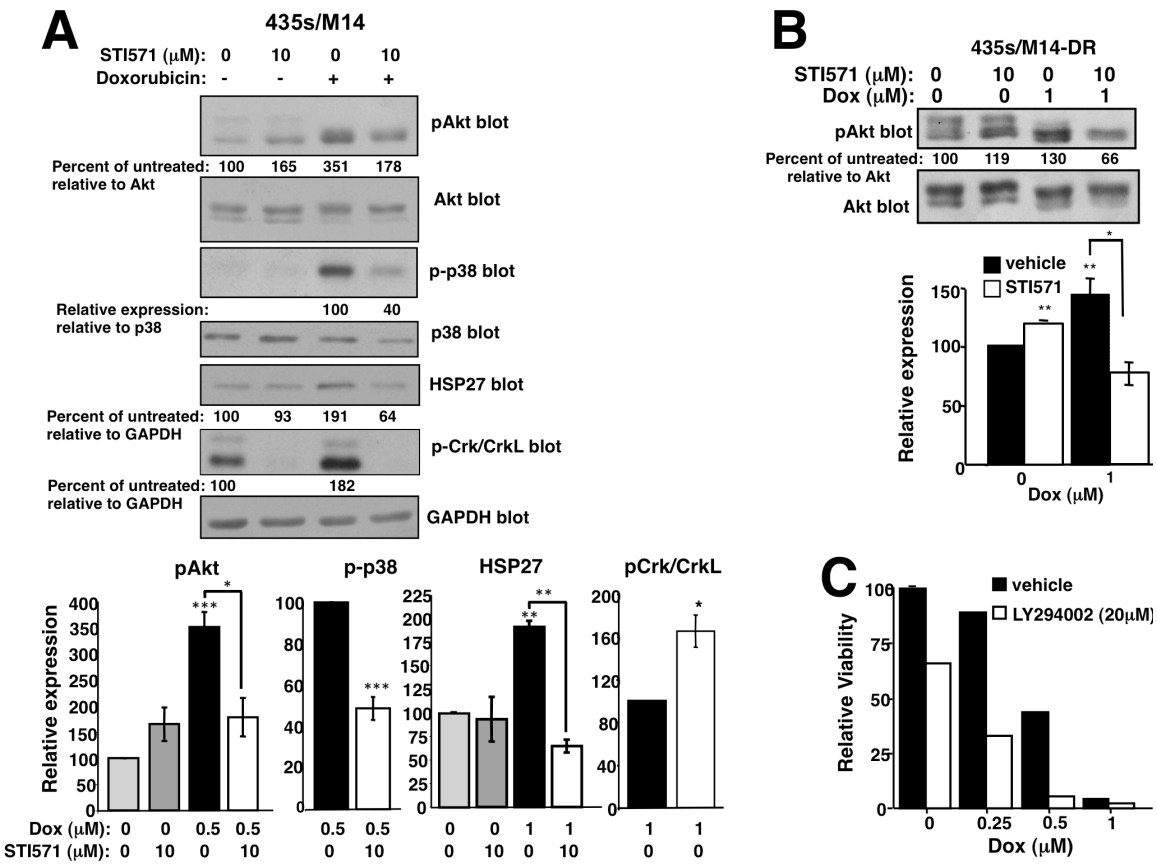

Figure 5.11. **c-Abl/Arg promote survival via Akt, p38, and HSP27. (A, B)** 435s/M14 (A) and 435s/M14-DR (B) cells were treated with STI571 in combination with doxorubicin (435s/M14-0.5μM, p38 and Akt; 1μM, HSP27 and pCrkL) for 40h, attached and detached cells were lysed, and assessed by Western blot with indicated antibodies. Graphs represent mean±SEM from 3 independent experiments. **(C)** 435s/M14 cells were treated with doxorubicin and LY294002 for 72h and viability assessed via CellTiter-Glo assay. Graph represents mean±SEM from 3 independent experiments. Some error bars are too small for visualization. *p<0.05, **$p\leq$0.01, ***$p\leq$0.001.

STI571+doxorubicin completely decreased HSP27 expression, correlating with decreased pAkt (Figure 5.11A). The same pattern of regulation that we observed with pAkt was also observed with p38/MAPK, in which STI571 completely prevented the doxorubicin-induced increase in p38/MAPK phosphorylation (Figure 5.11A). This is the first observation of c-Abl/Arg mediating stress-induced Akt activation in melanoma. We proceeded to determine the role of STAT3 in c-Abl/Arg-mediated activation of Akt. Constitutively active STAT3 (STAT3C) prevented the STI571-mediated decrease in HSP27, p38/MAPK, and Akt phosphorylation that we observed following doxorubicin treatment (Figure 5.12A). The role of STAT3 in regulating expression of these pro-survival proteins was confirmed with STAT3 siRNA. We discovered that doxorubicin treatment of STAT3 siRNA-transfected cells resulted in loss of HSP27 expression and decreased phosphorylation of p38/MAPK and Akt (Figure 5.12B), as previously observed with STI571+doxorubicin (Figure 5.11A). Significantly, this is the first demonstration that STAT3 mediates activation of Akt. We next examined whether c-Abl/Arg-mediated activation of Akt mediated cell survival in the presence of doxorubicin. Expression of a constitutively active form of the p110α catalytic subunit of PI3K (PI3K-E545K), which activates Akt, partially rescued STI571+doxorubicin-induced apoptosis (Figure 5.13). These data, together with our observations on NF-κB-mediated apoptosis, demonstrate that c-Abl and Arg promote survival in the presence of doxorubicin by activating STAT3. This leads to activation of a pro-survival signaling complex containing HSP27/p38/Akt and prevention of doxorubicin-mediated NF-κB transcriptional repression of pro-survival factors XIAP and cIAP1 (Figure 5.14).

5.4 Discussion

In this chapter, we showed that c-Abl/Arg regulate multiple survival pathways (i.e., STAT3, NF-κB, Akt) involved in doxorubicin resistance. Foremost, we demonstrate that c-Abl/Arg inhibit doxorubicin-mediated apoptosis via activation of STAT3. Furthermore, we demonstrated in this chapter that c-Abl/Arg→STAT3 signaling prevents doxorubicin-induced NF-κB-mediated transcriptional repression of anti-apoptotic genes. We also identified a novel melanoma survival pathway, in which c-Abl/Arg→STAT3 promotes cell survival via activation of HSP27/p38/Akt signaling. This expands on our previous data demonstrating that melanoma cell invasion occurs via c-Abl/Arg→STAT3 signaling [50], and illustrates the critical nature of these proteins in melanoma progression.

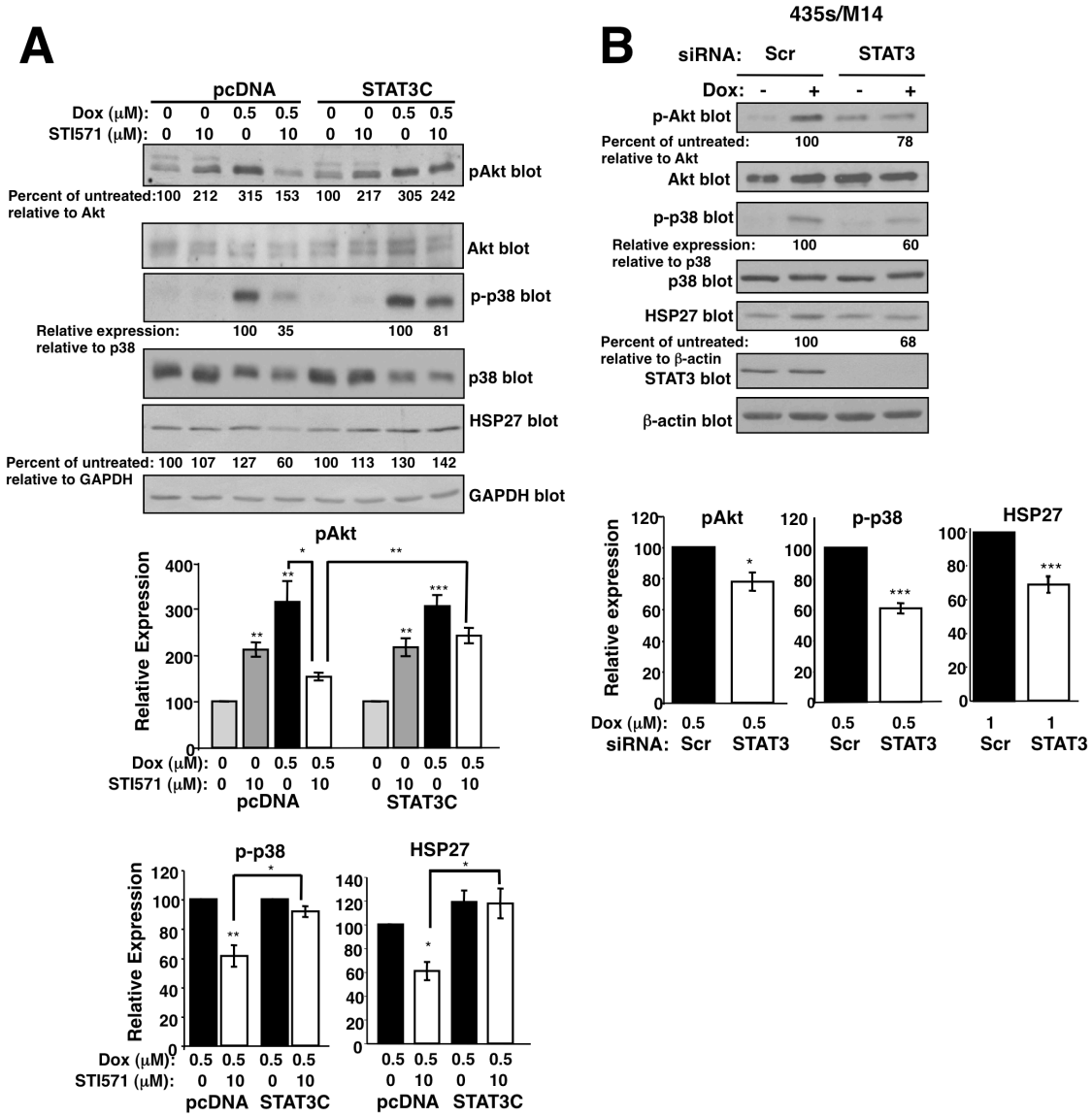

Figure 5.12. **c-Abl/Arg promote chemoresistance by activating a STAT3/HSP27/p38/Akt survival pathway. (A)** pcDNA and STAT3C-expressing cells were treated with STI571 and treated with doxorubicin for 40h, and lysate from attached and detached cells blotted with the indicated antibodies. Graphs represent mean±SEM from 3 independent experiments. **(B)** STAT3 was silenced with siRNA in combination with doxorubicin (0.5μM, p38 and Akt; 1μM, HSP27) for 40h, attached and detached cells were lysed, and assessed by Western blot with indicated antibodies. Graphs represent mean±SEM from 3 independent experiments. **p*<0.05, ***p*≤0.01, ****p*<0.001.

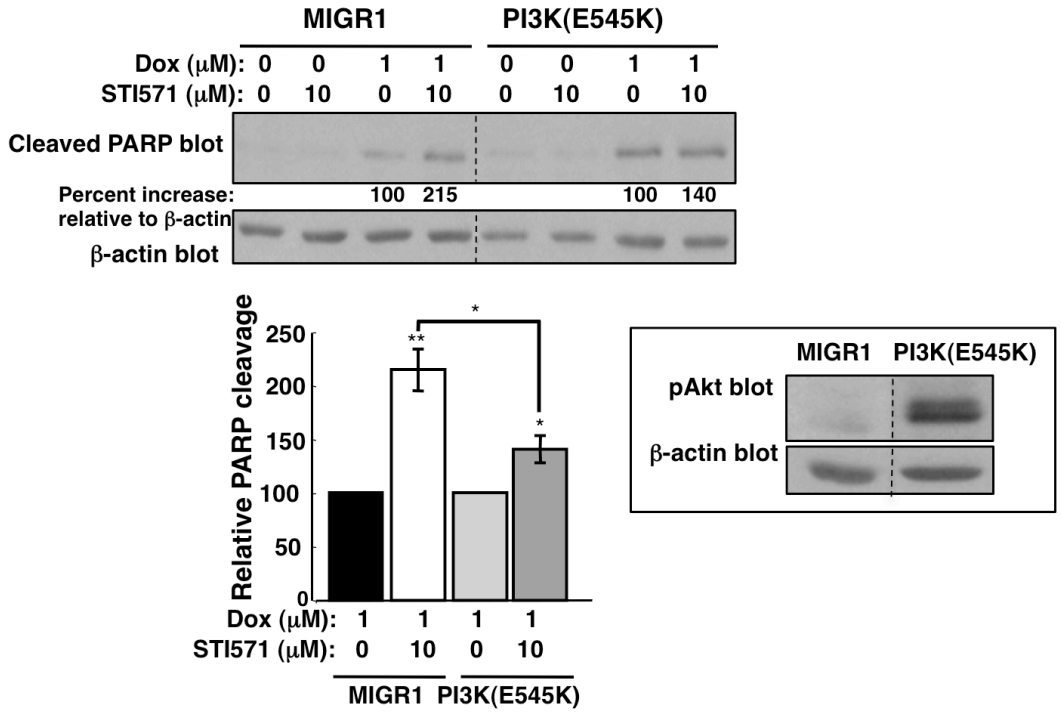

Figure 5.13. Constitutive activation of Akt partially rescues STI571+doxorubicin-induced apoptosis. 435s/M14 cells expressing vector or constitutively active PI3K(E545K) were treated with STI571 and/or doxorubicin (8h) and PARP cleavage assessed. Graph represents mean±SEM from 3 independent experiments. A representative Western blot demonstrating Akt activation in cells expressing PI3K(E545K) is shown. *$p<0.05$, **$p\leq0.01$.

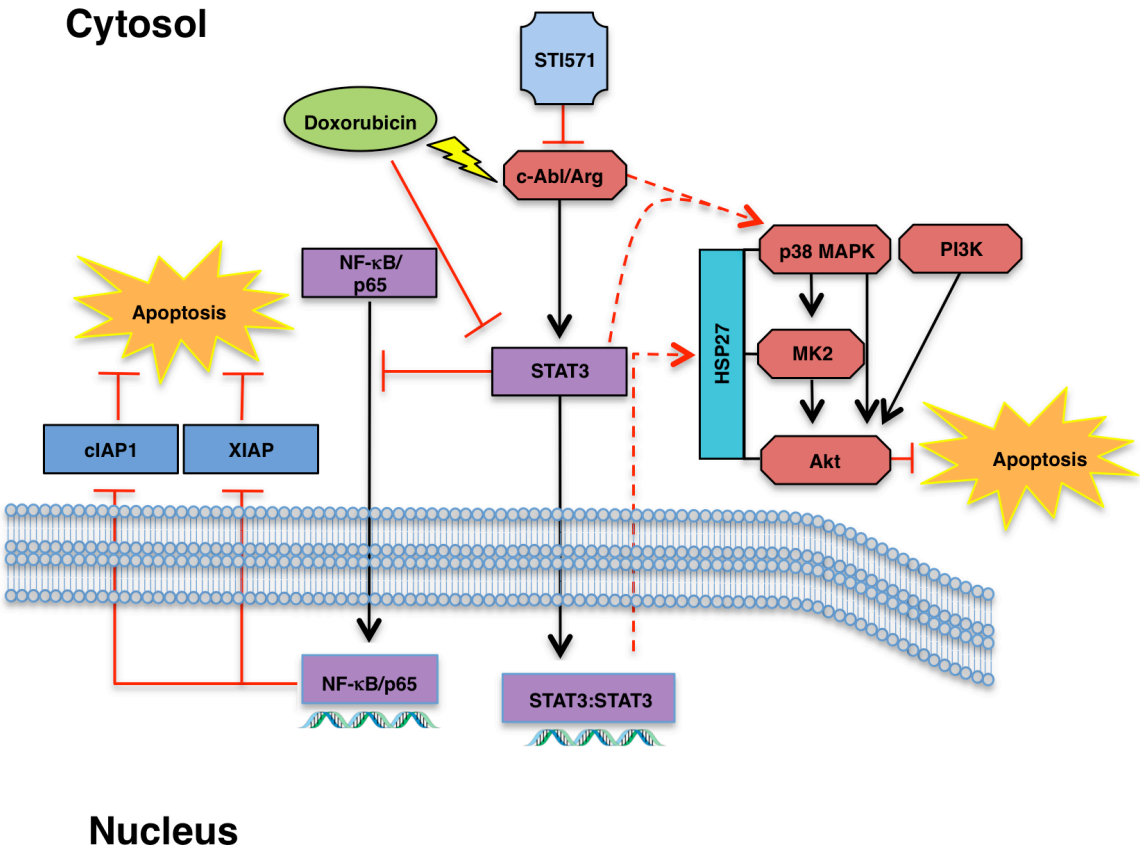

Figure. 5.14. Mechanisms by which c-Abl/Arg drive doxorubicin resistance. c-Abl/Arg activation of STAT3 prevents doxorubicin-mediated phosphorylation and translocation of NF-κB into the nucleus and NF-κB-mediated transcription of anti-apoptotic genes such as cIAP1/XIAP. c-Abl/Arg activation of STAT3 also promotes activation of a HSP27/p38/Akt survival pathway. Designed in collaboration with Hope Johnson (Markey Cancer Research Communications Office).

The role of NF-κB in doxorubicin-induced cell death is controversial as doxorubicin induces NF-κB anti-apoptotic activity in some cell types, and in others it inhibits NF-κB anti-apoptotic signaling by converting it into a transcriptional repressor [75, 86]. It is unclear why NF-κB responds differently to pro-apoptotic stimuli, such as doxorubicin, in different cell types, and the manner in which NF-κB transcriptionally represses anti-apoptotic targets is also controversial since reports differ on the mechanism by which this occurs [86, 87]. Some reports indicate that phophorylation and acetylation of p65/RelA is required for NF-κB-mediated transcriptional repression [86], while others report that DNA binding and transcriptional repression of anti-apoptotic genes occurs in the absense of p65/RelA phosphorylation and acetylation [87].

STAT3 modulates the activity of NF-κB, and, in the absence of doxorubicin, STAT3 promotes phosphorylation and acetylation of NF-κB and thereby increases its transcriptional activity in cancer cells [78], but there is a lack of clarity regarding the mechanism by which NF-κB mediates transcriptional repression of anti-apoptotic genes. We now present evidence that the response of the NF-κB pathway to doxorubicin occurs in a manner dependent on the expression level of pSTAT3 and phosphorylation of p65/RelA coincides with enhanced transcriptional repression. A fundamental discrepancy in how NF-κB responds to doxorubicin between two related cell types (435s/M14 and 435s/M14-DR cells) corresponds with dramatic differences in pSTAT3 expression, offering insight into the mechanism governing NF-κB activity in response to doxorubicin. Doxorubicin promotes phosphorylation of p65/RelA; however, in parental cells there is no induction of transcriptional activity. In fact, the addition of STI571 effectively inhibits pSTAT3 (Figure 5.1B), further enhances phosphorylation of p65/RelA (Figure 5.5C), and dramatically enhances NF-κB-mediated transcriptional repression of anti-apoptotic targets in parental cells treated with doxorubicin (Figure 5.8). Expression of constitutively active STAT3 (STAT3C) prevents STI571-mediated nuclear localization of p65/RelA (Figure 5.7B), the corresponding decrease in transcriptional activity (Figure 5.7C), and downregulation of anti-apoptotic NF-κB targets (Figure 5.10). Therefore, c-Abl and Arg inhibit NF-κB transcriptional repression of apoptotic genes in a STAT3-dependent manner; thereby, promoting cell survival in the presence of doxorubicin.

In contrast with our observations in parental cells, doxorubicin dramatically increased NF-κB transcriptional activity in cells with acquired chemoresistance, which retain much higher levels of pSTAT3 than parental cells. In parental cells, doxorubicin

decreases pSTAT3 levels, but in 435s/M14-DR cells, doxorubicin has much less effect on STAT3 phosphorylation (Figure 5.1B) and, doxorubicin activates NF-κB transcriptional activity (Figure 5.5C). This increase in NF-κB activity in melanoma cells possessing acquired resistance perfectly mirrors the observed increase in NF-κB transcriptional activity observed when cells expressing constitutively active STAT3 (STAT3C) are treated with doxorubicin (Figure 5.7C), indicating that STAT3 modulates whether NF-κB acts as a transcriptional repressor or transcriptional activator in the presence of doxorubicin. Interestingly, STI571 treatment not only prevented doxorubicin-mediated upregulation of NF-κB targets, but significantly inhibited expression of NF-κB targets (cIAP1, XIAP) at protein and transcriptional levels, indicating that inhibition of c-Abl/Arg converts NF-κB from a transcriptional activator to a transcriptional repressor in the presence of doxorubicin in resistant cells. In summary, we demonstrate that modulation of NF-κB by c-Abl/Arg requires STAT3, indicating that STAT3 expression predicates whether NF-κB will act as a transcriptional repressor or transcriptional activator in the presence of doxorubicin. Future experiments delineating the mechanism by which c-Abl/Arg→STAT3 directly modulates NF-κB transcriptional activity are currently in progress. These data are highly significant because they functionally demonstrate that inhibition of c-Abl/Arg can convert a master survival regulator, NF-κB, from a pro-survival into a pro-apoptotic factor, thereby making conventional chemotherapeutic drugs more effective for treating metastatic disease, and this knowledge could potentially lead to the development of agents that specifically convert NF-κB into a transcriptional repressor of anti-apoptotic targets in cancer cells.

In addition to promoting activation of NF-κB, doxorubicin also increases phosphorylation of the survival factor, Akt, in a c-Abl/Arg-dependent manner. Doxorubicin induced loss of an upper phospho-Akt band, and increased expression of a lower phospho-Akt band. This may be due to band collapse of the upper into the lower form such as by dephosphorylation or deglycosylation, or doxorubicin may inhibit phosphorylation of a specific Akt isoform and increase phosphorylation of a different isoform. Future experiments are in progress to elucidate the Akt isoform or post-translational modification responsible for promoting c-Abl/Arg-mediated doxorubicin resistance.

Interestingly, induction of ABCB1 expression has been linked to activation of PI3K/Akt signaling [191, 192]. Thus, our observation that c-Abl/Arg upregulate Akt in

response to doxorubicin treatment, suggests that c-Abl may promote ABCB1 expression via Akt. Intriguingly, we found that prolonged treatment (72h) with doxorubicin induces a significant accumulation of intracellular doxorubicin (Figure 4.3C) even though >80% of the cells are alive at this time point (Figure 3.4A). Moreover, doxorubicin treatment, of acquired chemoresistant cells, induces changes in signal transduction pathways (i.e., Akt, NF-κB, STAT3), which indicates that these cells still respond to doxorubicin despite expressing high levels of ABCB1 (Figure 5.1B; 5.5C; 5.11B). Taken together, these data indicate that drug transport is only partially responsible for the high-level doxorubicin resistance observed, and c-Abl/Arg-dependent upregulation of anti-apoptotic and pro-proliferative signaling pathways also contribute to acquired doxorubicin resistance. These data have important clinical ramifications, as they identify underlying resistance mechanisms within advanced chemoresistant cells which may be targeted by c-Abl/Arg inhibitors to better treat metastatic disease and reverse breast cancer and melanoma chemoresistance.

We have proven that c-Abl/Arg inhibition dramatically sensitizes breast cancer and melanoma cells to doxorubicin, halting proliferation and inducing apoptosis. We now present a model outlining the signaling network by which c-Abl/Arg→STAT3 promote resistance to doxorubicin-induced apoptosis (Figure 5.14). As described in this chapter, STAT3C completely prevents STI571-mediated induction of apoptosis; however, only partially rescues the STI571-potentiated decrease in cell proliferation. The mechanism by which STI571+doxorubicin halts cell proliferation is the subject of chapter 6.

CHAPTER SIX

ABL FAMILY KINASES PROMOTE PROLIFERATION VIA STAT3-INDEPENDENT MODULATION OF THE MEK/ERK PATHWAY

6.1 Introduction

The MAPK (mitogen-activated protein kinase) signaling pathway is made up of a series of serine/threonine kinases, and is critical to cancer cell progression [70]. Canonical activation of this pathway occurs via growth factor receptor-mediated stimulation, which phosphorylates adaptor proteins (i.e., Grb-2), allowing them to bind guanine exchange factors (i.e., SOS), and thereby activate Ras [208]. Ras/Raf-dependent activation of MEK (mitogen-activated protein kinase kinase) and ERK (extracellular signal-regulated kinase) promotes cell cycle progression and survival; therefore, this pathway is currently under intense therapeutic scrutiny, with B-Raf inhibitors generating especially strong clinical data [117]. ERK signaling can promote or inhibit proliferation depending on the amplitude of activation and duration of the signal, whereas MEK/ERK inhibition sensitizes other cells to doxorubicin-induced cell death [209, 210].

STI571 increases pERK1/2 in BCR-Abl$^+$ CML cells [162], and treatment w/ a MEK1/2 inhibitor sensitizes CML cells to STI571-dependent apoptosis [163]. Intrinsic resistance of malignant melanomas to DNA damage-inducing therapies has also been tied to activation of PI3K/Akt and B-Raf/ERK signaling pathways [68, 117]. Co-targeting these pathways has been a major therapeutic focus for melanoma treatment [72]. Studies have demonstrated that inhibition of MEK/ERK signaling reduced melanoma cell growth *in vitro* [72]; however, mounting evidence shows that enhanced ERK activation in mutant B-Raf cells decreases cell proliferation [211]. In these cells, Akt3 promotes cancer cell proliferation by phosphorylating and negatively regulating B-Raf, slightly reducing its activation of MEK/ERK, since overstimulation of B-Raf/MEK/ERK induces cytostasis [211].

It is critical to understand the mechanisms that promote chemoresistance so that new therapies can be devised to better target aggressive cancers. To this end, we have previously demonstrated that c-Abl/Arg promote proliferation and survival of breast cancer and melanoma cells [39, 50], and have specifically shown in chapter 5 that c-Abl/Arg inhibit doxorubicin-mediated apoptosis in a STAT3-dependent manner. STI571, a c-Abl/Arg inhibitor, synergizes with doxorubicin to dramatically halt cell proliferation by

promoting G2/M arrest (Figure 3.5; 3.6); however, this occurs in a STAT3-independent manner (Figure 5.2). MEK/ERK signaling promotes proliferation and survival [70]; therefore, we sought to elucidate whether c-Abl/Arg regulate ERK signaling in response to doxorubicin. We show that activation of the MEK/ERK pathway occurs coordinately with STI571+doxorubicin-mediated inhibition of cell cycle progression and cell proliferation; however, inhibition of MAPK signaling dramatically sensitized cells to STI571 and STI571+doxorubicin. We also postulate a model that sheds light on the role of MAPK signaling in chemoresistant cell growth and survival.

6.2 Materials and Methods

6.2.1 Reagents and Cell Lines

MDA-MB-435s cells were obtained from the University of North Carolina Tissue Culture Facility, and are a spindle-shaped, highly metastatic variant of MDA-MB-435 cells (Chapel Hill, NC). Genetic analysis confirmed that these cells are identical to melanoma M14, and therefore, are referred to as 435s/M14 [50]. A drug-resistant variant of 435s/M14 (435s/M14-DR) was created via step-wise treatment with increasing concentrations of doxorubicin (using a maximum dose of 100nM) [185]. 435s/M14 and 435s/M14-DR cells were cultured in DMEM/10% FBS (fetal bovine serum), + insulin (10μg/ml). BT-549 breast cancer cells were cultured in DMEM/10% FBS. MDA-MB-468 breast cancer cells were cultured in MEM/10% FBS, + sodium pyruvate (10μg/ml). STI571 (Gleevec; imatinib mesylate) was obtained from Novartis (Basal, Switzerland), dissolved in water (10mM), and stored at -80^{o}C. Doxorubicin was obtained from Sigma (St. Louis, MO) and dissolved in water. U0126 was obtained from Cell Signaling Technology (Danvers, MA) and dissolved in DMSO. ERK1/2 (sc-94) was purchased from Santa Cruz Biotechnologies (Santa Cruz, CA, USA) and phospho-ERK1/2 antibody was obtained from Promega (Madison, WI). Western blots were performed as described in the manufacturers' protocols.

6.2.2 Cell Lysis and Western Blots

Cells were plated in 60mm dishes, treated the following day, and detached nad attached cells were lysed in RIPA buffer (50mM Tris pH 7.5, 150mM NaCl, 1% triton-X 100, 0.1% SDS, 1% sodium deoxycholate, 1mM PMSF, 1mM sodium orthovanadate, 25mM sodium fluoride, 10μg/ml leupeptin, aprotinin, pepstatin). Total protein was

quantitated with a Lowry DC kit (Biorad; Hercules, CA), equal protein was loaded on SDS-PAGE gels, and blots were incubated with specified antibodies.

6.2.3 CellTiter-Glo (CTG) assay (Promega; Madison, WI)

Cells were plated in triplicate in 96-well plates, refreshed with media containing drugs the next day when cells were 30-40% confluent, and harvested 72h (for doxorubicin+STI571+U0126), or 96h (for STI571+U0126), later with an equal volume of CTG reagent. Plates were rocked for 2m, half of the volume was transferred to an opaque 96-well plate, and total light emitted was measured 10m later using a Synergy 2 microplate reader (Biotek; Winooski, VT).

6.3 Results

6.3.1 Inhibition of Abl family kinases induces ERK activation.

Aggressive tumor cells co-opt a multitude of proliferation and survival pathways during progression to metastasis [199]. MEK/ERK signaling is one of the most frequently deregulated pathways in cancer cell progression due to its ability to promote proliferation and survival [212]. Our previous observations indicate a role for the MAPK pathway in c-Abl/Arg-mediated signaling within breast cancer and melanoma cells [39, 180]. We have demonstrated that inhibition of c-Abl/Arg by siRNA and STI571 treatment induces ERK activation, specifically ERK1, dramatically in 435s/M14 melanoma cells [39]. This occurred as early as 2-4h after STI571 treatment, indicating a direct, rather than compensatory, mechanism [39]. Likewise, STI571-mediated induction of ERK1/2 activity was observed in multiple breast cancer cell lines possessing highly active c-Abl/Arg [180]. Similar to our observations, treatment of BCR-Abl$^+$ CML cells with STI571 increases ERK1/2 activity [162]. We have previously demonstrated that Abl family kinases promote cell proliferation, G1→S transition, and survival [39]. Therefore, to determine whether STI571-mediated upregulation of ERK1/2 activity is required for STI571-dependent inhibition of proliferation and loss of cell viability, we treated cells with STI571 and U0126, a MEK1/2 inhibitor, alone and in combination and observed a dramatic decrease in cell viability in 435s/M14 melanoma and BT-549 and MDA-MB-468 breast cancer cells (Figure 6.1A-C). This indicates that inhibition of ERK1/2 activity promotes cell death and dramatically sensitizes cells to STI571.

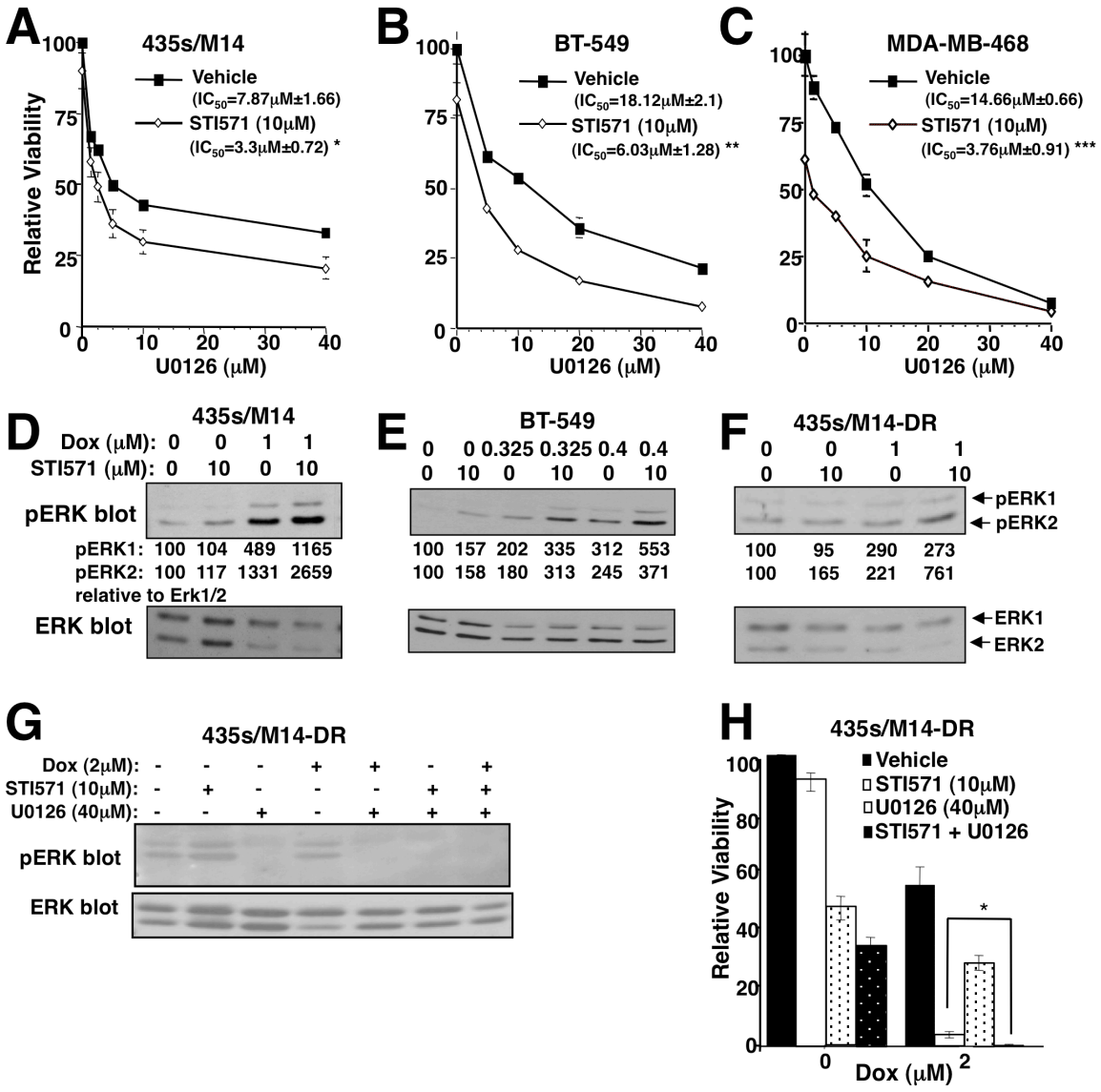
A
435s/M14
Vehicle
(IC50=7.87μM±1.66)
STI571 (10μM)
(IC50=3.3μM±0.72) *
Relative Viability
U0126 (μM)
B
BT-549
Vehicle
(IC50=18.12μM±2.1)
STI571 (10μM)
(IC50=6.03μM±1.28) **
U0126 (μM)
C
MDA-MB-468
Vehicle
(IC50=14.66μM±0.66)
STI571 (10μM)
(IC50=3.76μM±0.91) ***
U0126 (μM)
D
435s/M14
Dox (μM): 0 0 1 1
STI571 (μM): 0 10 0 10
pERK blot
pERK1: 100 104 489 1165
pERK2: 100 117 1331 2659
relative to Erk1/2
ERK blot
E
BT-549
0 0 0.325 0.325 0.4 0.4
0 10 0 10 0 10
100 157 202 335 312 553
100 158 180 313 245 371
F
435s/M14-DR
0 0 1 1
0 10 0 10
pERK1
pERK2
100 95 290 273
100 165 221 761
ERK1
ERK2
G
435s/M14-DR
Dox (2μM): - - - + + - +
STI571 (10μM): - + - - - + +
U0126 (40μM): - - + - + + +
pERK blot
ERK blot
H
435s/M14-DR
Vehicle
STI571 (10μM)
U0126 (40μM)
STI571 + U0126
Relative Viability
Dox (μM)

Fig. 6.1. Inhibition of MEK/ERK signaling sensitizes cells to STI571 and doxorubicin+STI571. (A-C) Cells were plated in triplicate, treated with STI571 and/or U0126 for 96h, and viability assessed by CellTiter-Glo assay (Promega, Madison, WI). Mean±SEM for 3 independent experiments. Some error bars are too small for visualization. (D-F) Cells were treated with STI571 and/or doxorubicin for 40h, attached and detached cells were lysed, and analyzed by Western blotting with indicated antibodies. Experiments shown are representative of 3 independent experiments. (G,H) Cells were treated with STI571, U0126, and/or doxorubicin for 72h, and analyzed by Western blotting (G) and CellTiter-Glo assay (H). Mean±SEM for 3 independent experiments. Combination indices (CI) were determined for mean±SEM of 3 independent experiments (<1=synergistic; 1=additive; >1=antagonistic). Dox+STI571 CI=0.24±0.15; Dox+U0126 CI=0.38±0.18; U0126+STI571 CI=0.72±0.14; Dox+U0126+STI571 CI=0.14±0.1. (G,H) Done in collaboration with W. Friend. *p<0.05; **p<0.01; ***p<0.001.

6.3.2 Addition of STI571 and doxorubicin dramatically induces ERK activity in breast cancer and melanoma cells.

We demonstrated in chapters 3 and 5 that STI571, a c-Abl/Arg inhibitor, synergizes with doxorubicin to dramatically halt cell proliferation by promoting G2/M arrest in a STAT3-independent manner (Figure 3.5; 3.6; 5.2). Therefore, we sought to elucidate whether the anti-proliferative effects of STI571+doxorubicin occured via regulation of ERK signaling. Similar to our observations with STI571 alone, we previously provided evidence of a potentiated induction of ERK1/2 activity in breast cancer cells treated with combinations of STI571 and camptothecin, 5-fluorouracil, or cisplatin, and this coincided with inhibition of cell proliferation [180]. Cotreatment of BT-549 breast cancer and 435s/M14 melanoma cells with doxorubicin+STI571 dramatically induced ERK1/2 activity at doses that resulted in loss of cell viability, proliferation, and induction of apoptosis (Figure 6.1D, E; 3.1A, B), and this effect was observed as early as 4h post-treatment (data not shown).

6.3.3 Inhibition of MAPK signaling sensitizes doxorubicin-resistant cells to undergo apoptosis.

ERK signaling can promote or inhibit proliferation depending on the amplitude of activation and duration of the signal [209, 210]. Sustained ERK activation induces cell cycle arrest and apoptosis in some cell types in response to doxorubicin, whereas MEK/ERK inhibition sensitizes other cells to doxorubicin-induced cell death [209, 210]. Interestingly, doxorubicin treatment of advanced chemoresistant cells only modestly increased ERK phosphorylation, and STI571 treatment dramatically potentiated doxorubicin-induced ERK2 phosphorylation at 4h and 40h time points (Figure 6.1F, data not shown). Based on these results, it is possible that inhibition of Abl family kinases may activate ERK1/2 by deregulating a negative feedback mechanism, or inducing a cytoprotective stress response pathway. To test whether ERK upregulation mediates apoptosis or survival, we inhibited ERK1/2 activation by treating cells with a MEK inhibitor (U0126) (Figure 6.1G). Significantly, U0126 treatment of 435s/M14-DR cells sensitized cells to doxorubicin, STI571, and doxorubicin+STI571 treatment (Figure 6.1H), indicating that inhibition of ERK2 activity abrogated acquired chemoresistant melanoma cell survival.

6.4 Discussion

The Ras/Raf/MEK/ERK pathway promotes doxorubicin resistance [80]; however, sustained activation of this pathway following doxorubicin treatment can lead to cell cycle arrest [209]. To help resolve how ERK1/2 activity promotes or inhibits cell proliferation we present a model of ERK1/2's actions as a molecular rheostat (i.e., a resistor in a biological circuit) within the confines of Ohm's Law. We believe this model harmonizes all known aspects of ERK signaling in carcinoma cells. To bypass cell senescence and promote tumorigenic growth, cancer cells have upregulated mechanisms to fine tune activation of the ERK pathway [211]. Cancer cells continue to proliferate under these conditions; however, disruption of these cellular regulators of ERK activity give rise to aberrantly high ERK activity, once again initiating the cellular senescence protocol [211]. Aberrantly high ERK1/2 activity promotes cytostasis; however, cells can overcome this stimulation and recapture control of ERK activity as we observed with 435s/M14-DR cells (Figure 6.1F). In summary, our data, viewed through the model we propose, illustrates that aberrantly high ERK1/2 activity potentially induces cytostasis; however, shutting off this signaling pathway seemingly shifts the fate of a cell toward apoptosis (Figure 6.2A; 6.1H).

Viewed in context of Ohm's Law, stimulation of a circuit possessing low resistance (moderate ERK activation) with a set amount of voltage (growth promoting signals) corresponds to a set output of current (proliferation); however with increased resistance (more ERK activation), the same amount of voltage (growth promoting signals) now correspond to less current output (proliferation) (Figure 6.2B) [213]. As with most cellular signaling events, a number of factors are likely to determine the response of cells to insults and/or stimuli. We have previously demonstrated in breast cancer cells that cell type-specific differences in signaling pathway modulation governs the response of cells to combination treatments of STI571 and chemotherapeutic drugs [180]. Complete inhibition of ERK1/2 activity trumps the cytostatic response induced by highly activated ERK1/2. We postulate that just as voltage flows through a circuit, with resistance building only slightly as the output current increases, increasing ERK activity promotes cell growth; however, once a threshold level of activation is reached, increasing ERK activity further results in cytostasis (Figure 6.2A). This corresponds to Ohm's Law since dramatic increases in resistance within a circuit lead to less current output [213]. Moreover, inhibition of ERK activity fully sensitizes cells to undergo apoptosis (Figure 6.1H), just as a failed resistor prevents current flow due to the loss of

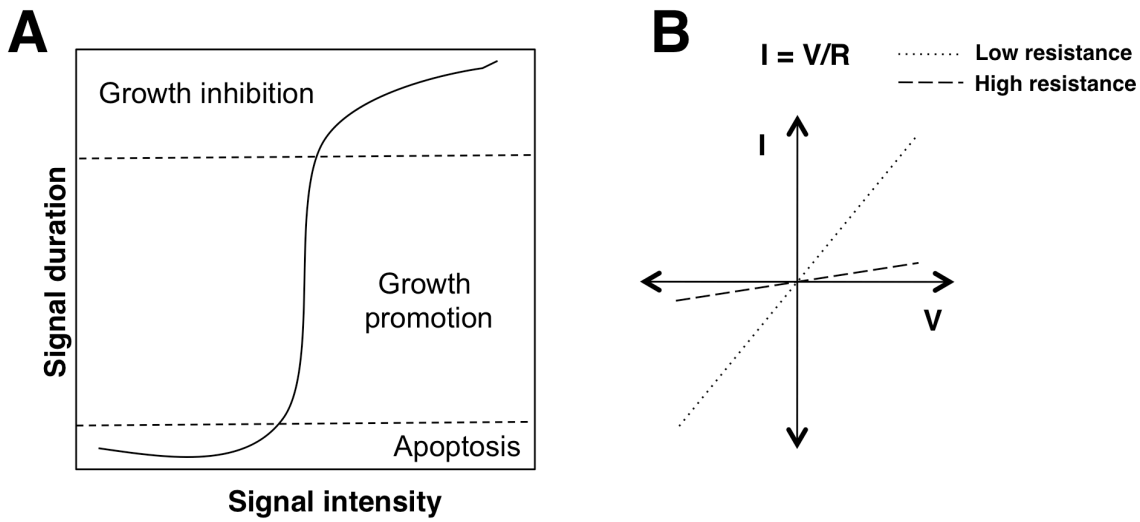

Fig. 6.2. Model illustrating that the extent of ERK activation determines cell proliferation/apoptosis. (A) As the signal intensity and/or signal duration of ERK activity increases, a threshold level of growth-promoting ERK activation is surpassed and cytostasis is induced. **(B)** Based on Ohm's Law, a circuit with high resistance yields much lower current output than a circuit with low/moderate resistance when presented with the same amount of voltage. I=current; V=voltage; R=resistance.

conductive material, resulting in infinite resistance [213]. In line with our hypothesis, other reports have established that Akt regulates ERK activity to promote growth, and inhibition of Akt leads to increased ERK activity and cytostasis [211].

ERK phosphorylation can promote chemoresistance or inhibit proliferation depending on signal duration, amplitude, and cellular context [80]. 435s/M14 and 435s/M14-DR melanoma cells possess mutant B-Raf and wildtype PTEN [214], and in this cellular context, activation of Akt results in B-Raf phosphorylation, which limits B-Raf activity and thereby limits overstimulation of ERK activity [211]. BT-549 and MDA-MB-468 cells possess mutant PTEN, suggesting that activated Akt may induce ERK activation, irrespective of B-Raf status, in these cells as well [214, 215]. In all cell types tested in this chapter, ERK activity is regulated to circumvent cytostasis and drive proliferation and survival. Here, we show that doxorubicin induces upregulation of ERK1/2 in breast cancer and melanoma cells, and inhibition of c-Abl/Arg with STI571 potentiates this upregulation. Interestingly, ERK activation is regulated differently in cells possessing acquired chemoresistance. Unlike ERK2, ERK1 is not further upregulated in response to STI571+doxorubicin. Others have demonstrated that ERK2, but not ERK1, promotes resistance to anti-cancer therapy [216]. Likewise, ERK1, but not ERK2, was shown to inhibit Ras-dependent proliferation [217]. In order to evade anti-apoptotic insults, these acquired chemoresistant melanoma cells may have downregulated ERK1 activity, which explains why only ERK2 remains sensitive to STI571+doxorubicin (Figure 6.1F). However, the inhibition of c-Abl/Arg critically sensitizes these acquired chemoresistant cells to doxorubicin-mediated decrease in cell viability, and coordinately overstimulates ERK2 activity (Figure 3.4A; 6.1F).

Based on current literature, and the model we propose, one cannot differentiate the effect that ERK activation has on proliferation vs. apoptosis based on data derived from use of MEK/ERK inhibitors. ERK activation results in two completely opposite physiological outcomes depending on the intensity and duration of activation [209, 210] (Figure 6.2A). Our model reconciles seemingly conflicting data regarding ERK activation, and explains how STI571+doxorubicin treatment halts cell proliferation. Moreover, our data are particularly exciting since we demonstrate that despite the benefit of arresting cancer cell growth, if the desired outcome is inhibition of cancer cell viability, then ERK inhibitors combined with doxorubicin and c-Abl/Arg inhibitors may be a highly effective combination for treating acquired resistance.

CHAPTER SEVEN
SUMMARY AND FUTURE DIRECTIONS

7.1 Summary

Chemoresistance presents a tremendous hurdle in cancer therapy and the discovery of novel therapeutic targets that specifically impinge on the viability of resistant cells is cancer type and cell type-specific in nearly all cases. Highly refractory cells are typically the most aggressive and invasive forms of disease [80, 195]. Receptor and non-receptor tyrosine kinases are overwhelmingly involved across all cancer types in the dissemination and amplification of growth promoting signals [218]. Our data demonstrate that the non-receptor tyrosine kinases, c-Abl and Arg, are highly active in response to growth factors (i.e., EGFR, Her2, IGF-1R), and c-Abl and Arg are integrally involved in promoting proliferation, survival to nutrient deprivation, invasion, and metastasis, properties indicative of highly advanced, metastatic disease [38, 39, 50].

Our current work has identified Abl family kinases as critical mediators of chemoresistance in breast cancer and melanoma cells. Inhibition of c-Abl/Arg sensitizes a panel of breast cancer cell lines to halt proliferation and undergo apoptosis in response to a variety of chemotherapeutic agents. c-Abl/Arg inhibitors, likewise, dramatically synergize with doxorubicin to arrest melanoma cells in G2/M phase of the cell cycle, and induce apoptosis in melanoma and breast cancer cells; therefore, c-Abl and Arg promote proliferation and survival in the presence of chemotherapy in both breast cancer and melanoma cells. We also discovered that c-Abl promotes ABCB1 expression in acquired chemoresistant melanoma cells, and inhibitors of c-Abl/Arg dramatically sensitize advanced chemoresistant cells to doxorubicin via inhibition of ABCB1 transporter activity and c-Abl and Arg-mediated signaling pathways. In the presence of doxorubicin, c-Abl and Arg act via STAT3 to prevent NF-κB-mediated transcriptional repression of anti-apoptotic genes, and upregulate an HSP27/p38/Akt pro-survival signaling pathway in melanoma cells leading to enhanced survival. These data are of particular importance due to the highly resistant nature of melanoma and the clinical frustration resulting from the inability to halt advanced disease progression.

7.2 Future Directions

7.2.1 CHAPTER TWO: ABL FAMILY KINASES PROMOTE BREAST CANCER CHEMORESISTANCE

We demonstrated that the c-Abl/Arg inhibitor, STI571, was highly effective at sensitizing breast cancer cells to a variety of chemotherapeutic drugs. Our data illustrate the cell type-specific nature wherein these combinations are most effective. We observed that STI571 synergizes with camptothecin in MDA-MB-231 cells, cisplatin in BT-549 cells, and paclitaxel, 5-FU, and cisplatin in MDA-MB-468 cells. The significance of these studies would be greatly enhanced by extension of our *in vitro* data to xenograft mouse studies. We have observed markedly enhanced efficacy *in vivo* with use of nilotinib rather than STI571 [50], so future *in vivo* studies will focus on combining nilotinib with chemotherapy. Mammary fat pad injections in nude mice would allow us to monitor primary tumor regression in chemotherapy-treated mice vs. mice cotreated with nilotinib and chemotherapy. Combinations that would be especially interesting to test are cisplatin and nilotinib in BT-549 xenografts and 5-FU and nilotinib in MDA-MB-468 xenografts due to the dramatic induction of apoptosis observed *in vitro* in these cells with these drug combinations. Considering our recent evidence demonstrating that c-Abl/Arg promote melanoma metastasis [50], the data presented in chapter 2 suggest that inhibition of c-Abl/Arg could synergize with chemotherapeutics to significantly prevent the metastatic spread of breast cancer as well; therefore, separate studies within this aim will be carried out in which treatment with nilotinib and/or chemotherapy will be administered upon removal of primary tumors and lungs of all animals will be monitored using IVIS imaging (University of Kentucky DLAR).

Potential biomarkers identified from our signaling studies could help identify which therapy may yield the best prognosis in specific subsets of patients. We identified Akt, NF-κB, and ERK signaling pathways as major downstream targets of c-Abl/Arg in breast cancer cells. Future experiments will confirm these signaling molecules as potential mediators of c-Abl/Arg signaling. First, silencing these genes with siRNAs will confirm that inhibition of these pathways promotes cell death in the presence of chemotherapeutics. Second, BT-549 cells were sensitized to STI571+cisplatin via inhibition of Akt signaling; therefore, a constitutively active form of PI3K (PI3K(E545K)) will be expressed in these cells, resulting in dramatic activation of Akt signaling, which should prevent synergism of STI571 and cisplatin if cells are sensitized to this therapy due to Akt inhibition. Also, increased levels of the NF-κB inhibitory molecule, IκB, were

observed following STI571+camptothecin treatment in MDA-MB-231 cells. We will silence IκB, which should activate NF-κB signaling, and determine whether this prevents the dramatic decrease in cell proliferation observed with STI571+camptothecin treatment. We also found in MDA-MB-468 cells that low concentrations of 5-FU were antagonistic with STI571; however, cells were sensitized to higher concentrations of 5-FU when combined with STI571. STI571 has been shown to interact with certain ABC transporters [148]; therefore, we could identify if STI571 sensitizes MDA-MB-468 cells to 5-FU by inhibiting efflux of 5-FU via a drug transporter (i.e., ABCG2).

We present evidence that Abl family kinases are functionally involved in promoting breast cancer cell proliferation in the presence of chemotherapeutics from a variety of different classes. Cell proliferation is promoted via complex regulation of cell cycle components allowing for aberrant progression through the cell cycle [219, 220]. We demonstrated that Abl kinases promote G1→S progression in breast cancer cells, and activate STAT3 [39]. STAT3 activates c-Myc, which inhibits p27 and activates cyclin D1/cyclin dependent kinase 4 (cdk4) complexes [54, 55, 221]. These steps are critical for cell cycle transition, and can promote cell cycle reentry after DNA repair processes halt cycling cells [3, 222]. To determine if c-Abl/Arg promote proliferation via cyclin D1 and c-Myc, protein expression of cyclin D1 and c-Myc will be measured following treatment with STI571 and various chemotherapeutics. Since we observed that c-Abl/Arg→STAT3 regulate chemoresistance, we will elucidate whether cyclin D1 and c-Myc are regulated in a STAT3-dependent manner by treating STAT3 siRNA-transfected cells with anti-proliferative chemotherapeutics described in chapter 2 and monitoring expression changes of these proteins. Further studies focused on testing the mechanism by which Abl family kinases promote proliferation and survival in the presence of breast cancer chemotherapeutics will test whether constitutive activation of cyclin D1 and c-Myc rescues the inhibition of proliferation observed with STI571+chemotherapy treatment. These data could lead to insights regarding the mechanism by which c-Abl/Arg promote breast cancer cell proliferation in response to chemotherapeutic agents.

7.2.2 CHAPTER THREE: ABL FAMILY KINASES PROMOTE CHEMORESISTANCE TO DOXORUBICIN

We definitively demonstrated that c-Abl and Arg promote doxorubicin resistance in invasive melanoma and breast cancer cells. c-Abl and Arg are specifically targeted by STI571, and inhibition of these kinases sensitizes cells to doxorubicin-mediated cell

cycle arrest in G2/M phase and induction of apoptosis. As noted in the discussion regarding chapter 2, we are likewise focused on transitioning our exciting data describing synergistic interactions of c-Abl/Arg inhibitors and doxorubicin to *in vivo* studies. We observed that STI571 synergizes with doxorubicin to kill BT-549, WM-3248, 435s/M14, and 435s/M14-DR cells and the significance of these data would be strengthened further by xenograft mouse studies. As mentioned in the discussion regarding chapter 2, we have observed greater efficacy *in vivo* with use of nilotinib rather than STI571 [50], so future *in vivo* studies will focus on combining nilotinib with doxorubicin. Subcutaneous injections to the flanks of nude mice will be done to form primary melanoma tumors so that tumor regression in doxorubicin-treated mice vs. mice cotreated with nilotinib and doxorubicin can be studied. We previously demonstrated that c-Abl/Arg promote melanoma metastasis [50]; therefore, future studies will focus on whether inhibition of c-Abl/Arg synergizes with doxorubicin to significantly prevent metastatic spread of melanoma. Extended use of doxorubicin is restricted due to cardiac toxicity [223]. The c-Abl/Arg inhibitor, STI571, may induce cardiomyopathy; however, this remains controversial [224]. We have demonstrated that STI571 sensitizes melanoma cells to doxorubicin, dramatically lowering its IC_{50}. Since STI571 allows for lower levels of doxorubicin to be used for therapy, as compared to doxorubicin alone, we will determine whether STI571+doxorubicin decreases cardiomyopathy as compared to relative high dose treatment of doxorubicin. This will be quantitated by monitoring the weights of the animals during the course of the experiment and H/E (hematoxylin/eosin) staining sections of the hearts of euthanized mice. Further analysis of ventricular hypertrophy markers (i.e., ANP, BNP) will be assessed via semi-quantitative RT-PCR.

We demonstrated that c-Abl/Arg prevent doxorubicin-induced apoptosis, and that c-Abl/Arg inhibitors dramatically sensitize cells to undergo apoptosis. Apoptosis, whether mediated by the intrinsic or extrinsic pathway, is initiated via a plethora of stimuli [204]. Future experiments will determine if STI571 sensitizes cells to doxorubicin by inducing an ER (endoplasmic reticulum) stress response. ER stress occurs via increased Ca^{2+} signaling and accumulation of misfolded proteins [225]. We have demonstrated c-Abl/Arg-mediated induction of HSP27, a chaperone responsible for the correct folding of misfolded proteins [226], in the presence of doxorubicin (Figure 5.11A) and preliminary data from an R&D Apoptosis Array showed that STI571 dramatically decreased cytochrome c expression (J.T. Sims, unpublished observation), indicating potential deregulation of mitochondria and Ca^{2+} repositories. Abl family kinases have been shown

to modulate Ca^{2+} levels in cells, and STI571-mediated apoptosis of CML cells occurs via ER stress [225, 227]. This evidence suggests a role for STI571 in cellular regulation of Ca^{2+} and modulation of ER stress. We will determine if STI571+doxorubicin-mediated apoptosis results from an ER stress response by first characterizing cellular levels of GRP78 and CHOP, which are known ER stress-regulated proteins [228, 229]. CHOP promotes apoptosis via ER stress response [228]; therefore, we will determine whether silencing this gene prevents synergistic induction of apoptosis following STI571+doxorubicin. In addition, we will quantify the effects that c-Abl/Arg have on cellular Ca^{2+} homeostasis in the presence of doxorubicin using a fluorescent dye, Fura-2, which binds free intracellular calcium [230]. These data will be critical as we seek a fuller understanding of how c-Abl and Arg promote survival and chemoresistance.

7.2.3 CHAPTER FOUR: STI571-MEDIATED CHEMOSENSITIZATION OF DRUG-RESISTANT MELANOMA PARTIALLY MEDIATED VIA ABCB1

We have shown that Abl family kinases promote chemoresistance. One mechanism by which this occurs is via c-Abl-mediated induction of ABCB1 expression. c-Abl/Arg inhibitors, such as STI571, inhibit ABCB1-mediated efflux of doxorubicin and thereby dramatically sensitize advanced chemoresistant cells to undergo apoptosis and halt proliferation. Therefore, STI571-mediated inhibition of drug transport involves not only direct inhibition of transporter activity, but also indirect modulation via regulation of transporter expression. These data are significant because they indicate that c-Abl plays an active role in promoting ABC transporter upregulation during acquired chemotherapeutic resistance. Interestingly, ABCB1 expression and efflux activity is induced in leukemic cells via PI3K/Akt/FOXO3a signaling [231]. Thus, our observation that c-Abl/Arg activate Akt in response to doxorubicin treatment, suggests that c-Abl may promote ABCB1 expression via Akt. We will determine if c-Abl/Arg→Akt activates FOXO3a and determine whether doxorubicin-induced upregulation of ABCB1 occurs via this mechanism. Future experiments will also address whether decreased expression of ABCB1 observed in response to silencing c-Abl expression with siRNA specifically decreases the cells' ability to efflux doxorubicin.

Interestingly, Ejlertesen and colleagues found that sensitivity to doxorubicin/anthracyclines depends on Her2, Top2A, and TIMP1 expression [232]. Top2A (topoisomerase 2A) is a direct target of doxorubicin and therefore is recognized as a determinant of cellular response to doxorubicin [232]. We have demonstrated that

Her2 activates Abl family kinases and that activation of Abl family kinases in these cells promotes chemoresistance [38, 180]. Significantly, we recently discovered that 435s/M14-DR cells highly express TIMP1 as compared to parental cells, and STI571-mediated inhibition of c-Abl/Arg dramatically decreases TIMP1 transcription in these cells (J.T. Sims and S. Ganguly, unpublished observations). These data could lead to a greater understanding of c-Abl/Arg-mediated resistance mechanisms in solid tumor cells in light of the recently recognized role for TIMP1-mediated survival via PI3K/Akt signaling [233].

Drugs that regulate reactive oxygen species (ROS) formation have been shown to induce melanoma cell apoptosis [234], and the ability of cells to combat this insult correlates with disease progression [235]. Upregulation of survival pathways, like those regulated by NF-κB, promote cell survival in the presence of increased ROS [236, 237]. ROS are eliminated from cells via controlled elimination processes by peroxiredoxin, glutathione peroxidase, and catalase [238], and doxorubicin, which produces ROS, induces catalase expression [239]. In other cell types, c-Abl/Arg operate as part of the oxidative stress response to phosphorylate and activate catalase [238, 240]. Using the R&D Apoptosis Array, we found that 435s/M14-DR cells, which contain increased c-Abl/Arg activity (Figure 4.4), possess dramatically elevated levels of catalase as compared with parental cells, and STI571+doxorubicin dramatically decreases catalase expression in these cells (J.T. Sims, unpublished observation). 435s/M14-DR cells initially efflux doxorubicin efficiently; however, with prolonged treatment, doxorubicin accumulates within these cells. Despite enhanced levels of intracellular doxorubicin, which is known to induce ROS, these acquired chemoresistant cells remain viable. A potential mechanism of resistance to the ROS-inducing effects of doxorubicin may be via c-Abl/Arg-mediated upregulation of catalase. Catalase expression and activity in response to Abl family kinases will be tested [241]. The identification of a potential connection between c-Abl/Arg and catalase in acquired chemoresistant cells could yield significant insights for the cancer field regarding potential mechanisms of resistance.

Future studies are focused on understanding the molecular mechanisms by which this acquired chemoresistant cell population, containing very highly active c-Abl/Arg, promotes cell survival and resistance. Studies aimed at characterizing the 435s/M14-DR cells show that these doxorubicin-resistant cells proliferate at a higher rate than parental cells in serum-deprived conditions (J.T. Sims, unpublished observation). Cancer stem cells (CSCs) are highly resistant to chemotherapeutic agents [242]. CSCs

make up a small subset of dedifferentiated, highly refractory cells within a tumor that are able to survive commonly used chemotherapeutics and result in residual disease [243-245]. We demonstrated that a small subset of highly resistant cells derived from serial treatment of 435s/M14 melanoma cells with doxorubicin is exquisitely sensitive to STI571, and we hypothesize that these cells may possess CSC qualities allowing for the outgrowth of a highly refractory cell population. Preliminary data demonstrate no alteration of the CSC markers, CD24/CD44, relative to parental cells (J.W. Friend, unpublished observation), but the melanoma stem cell markers CD133 and ALDH were not tested [244]. If 435s/M14-DR cells possess a stem cell phenotype then our discovery that these highly resistant cells preferentially express a greater degree of highly active, cytoplasmically localized c-Abl/Arg as compared to parental cells will be extremely important for therapeutically targeting this highly refractory subset of cancer cells and provide rationale for new CSC-based therapies.

7.2.4 CHAPTER FIVE: ABL FAMILY KINASES PROMOTE MELANOMA CHEMORESISTANCE VIA STAT3-MEDIATED INHIBITION OF NF-KB TRANSCRIPTIONAL REPRESSION AND A STAT3-MEDIATED HSP27/P38/AKT SURVIVAL PATHWAY

We previously showed that c-Abl promotes melanoma invasion via a STAT3-dependent mechanism [50]. Moreover, we now demonstrate that c-Abl and Arg promote resistance to apoptosis via activation of STAT3. Understanding the c-Abl/Arg→STAT3-mediated regulation of IAP molecules is imperative for combating chemoresistance. One mechanism by which cIAP1/XIAP are negatively regulated is via interaction with Smac/DIABLO [83]. Other reports have shown that high IAP expression and low Smac/DIABLO expression could lead to doxorubicin resistance in multiple myeloma cells [83]. Preliminary data from an R&D Apoptosis Array demonstrate a strong correlation between increased Smac/DIABLO and decreased cIAP1 protein expression in cells treated with STI571+doxorubicin (J.T. Sims, unpublished observation). Thus, a possible mechanism by which c-Abl and Arg enhance IAP protein expression and prevent caspase-dependent apoptosis may involve downregulation of Smac/DIABLO.

Mounting evidence has recently demonstrated a clear pro-apoptotic role for the NF-κB pathway [246]; however, the mechanism by which NF-κB mediates apoptosis is unclear and perhaps could differ based on cell type and/or stimuli [86, 87]. We have demonstrated that inhibition of c-Abl/Arg→STAT3 signaling promotes doxorubicin-

mediated conversion of p65/RelA into a transcriptional repressor of anti-apoptotic genes. We confirm previous reports suggesting that post-translational modification of p65/RelA in response to chemotherapeutic agents promotes transcriptional repression by means of our observation that phosphorylation of p65/RelA coincides with decreased transcriptional activity and loss of cIAP1 and XIAP expression (Figure 5.5B,C; 5.8) [247]. We provide further clarity regarding the conversion of NF-κB into a transcriptional repressor by demonstrating that c-Abl/Arg act via STAT3 to prevent doxorubicin-induced transcriptional repression of NF-κB targets, and propose that STAT3 expression levels dictate whether p65/RelA will respond to doxorubicin in a pro- or anti-apoptotic manner. The interaction of p65/RelA with HDACs has been shown in other cell types to be dependent on p65/RelA phosphorylation [86, 247]. We hypothesize that c-Abl/Arg→STAT3 prevents the binding of histone deacetylases (HDACs) to p65/RelA by modulating the phosphorylation status of p65/RelA. Therefore, our observation that c-Abl/Arg→STAT3 decreases phosphorylation and promotes cytoplasmic retention of p65/RelA in response to doxorubicin provides insight into mechanism of NF-κB regulation in these cells (Figure 5.7B).

We will test whether the phosphorylation and acetylation of NF-κB is dependent on STAT3. We also will extend our findings regarding the STI571-mediated conversion of NF-κB from a pro-survival factor to a transcriptional repressor to other melanoma and breast cancer cell lines. We will first test whether silencing p65/RelA decreases doxorubicin-mediated cell death and prevents STI571+doxorubicin potentiation of apoptosis in a number of melanoma and breast cancer cell lines. Following these studies, assessment of transcriptional activity will be done using our stable luciferase-based promoter system as described in chapter 5.

Akt is activated in ~70% of melanomas [184], which makes our observation of c-Abl/Arg→Akt signaling critical to understanding and preventing melanoma chemoresistance. We have demonstrated that Abl family kinases are activated by doxorubicin to promote HSP27/p38/Akt activation. The mechanism by which c-Abl/Arg are activated by doxorubicin is unknown. Intriguingly, in certain cell types, DNA-PK is activated by DNA damage and acts in a PDK2-like manner to activate Akt via phosphorylation on S473 [68]. Studies have demonstrated that DNA-PK directly phosphorylates c-Abl and that stimulation of DNA-PK via incubation with sonicated DNA resulted in enhanced c-Abl-dependent phosphorylation of the Abl substrate, GST-Crk [248]. Moreover, it would also be interesting to test whether DNA-PK may activate c-Abl

in melanoma cells in response to doxorubicin, resulting in activation of Akt via complex formation with p38 and HSP27. Our observations that c-Abl/Arg promote HSP27/p38/Akt signaling in a STAT3-dependent manner provides evidence of novel c-Abl/Arg-mediated signaling pathways in solid tumor cells, and also demonstrates that doxorubicin-induced Akt activation via HSP27/p38 occurs not only in neutrophils, but also in solid tumor cells. To confirm direct regulation of Akt via p38 and HSP27, siRNA-mediated inhibition of both p38 and HSP27 will be performed and the decrease in doxorubin-induced Akt phosphorylation will be assessed. To verify that c-Abl/Arg promote complex formation of HSP27/p38/Akt in response to doxorubicin, Akt, p38, and HSP27 will be immunoprecipitated in lysates from untreated, doxorubicin-treated, and STI571+doxorubicin-treated samples. The interaction of these proteins in response to these various treatments will offer insight into the c-Abl/Arg-mediated resistance mechanism.

The identification of signaling molecules modulated by c-Abl/Arg provides a number of therapeutic targets that can be used as biomarkers to determine if tumors are likely to respond to c-Abl/Arg inhibitors in combination with chemotherapeutic drug treatment. Since c-Abl/Arg are integral to advanced melanoma progression and metastasis [50], we will also determine if c-Abl/Arg regulate melanoma specific biomarkers. One such marker of particular interest is GRIN2A, the gene that encodes NMDA receptors, which is mutated in 33% of melanomas [249]. GRIN2A can activate Akt [250], and associates with Src family kinases, PTK2B [251, 252], and, intriguingly, Abl family kinases interact with NMDA receptors (i.e., glutamate receptor) in neurons [253]. This work is of particular significance if we determine that c-Abl/Arg regulate biomarkers such as GRIN2A, since this would aid in the selection of patient populations who may be good candidates for c-Abl/Arg inhibitor therapy. The proper identification of advanced chemoresistant tumors that possess elevated levels of these tumor-promoting signaling molecules will lead to effective use of targeted agents in treatment regimen possibly rendered ineffective in the past. Our current work has identified potential biomarkers (STAT3, Akt, p38, HSP27) that could provide rationale for the selection of patients who may be candidates for combination treatment with c-Abl/Arg inhibitors. The extension of our findings to established biomarkers, such as GRIN2A, would aid in this effort as well.

7.2.5 CHAPTER SIX: ABL FAMILY KINASES PROMOTE PROLIFERATION VIA STAT3-INDEPENDENT MODULATION OF THE MEK/ERK PATHWAY

Inhibition of MEK/ERK signaling sensitizes acquired chemoresistant cells to STI571/doxorubicin treatment. To better understand the mechanism by which U0126 synergizes with STI571 and doxorubicin to kill resistant cells, we will express activated ERK and determine whether this limits STI571+doxorubicin-induced G2/M arrest and apoptosis in 435s/M14-DR cells. There are potential issues related to this experiment since enhanced activation of ERK can also stimulate cytostasis of cancer cells [211]. We will modulate expression of ERK1/2 via siRNA and tet-inducible expression vectors, and determine whether expression of either isoform is more responsible for the observed effects in resistant cells. This is of particular importance because we observed downregulated ERK1 activation in STI571+doxorubicin-treated 435s/M14-DR cells as compared to parental cells. Others have demonstrated that MAPK signaling is downregulated in doxorubicin-resistant cells [254].

Preliminary data indicate that STI571 prevents ERK1/2 activation in WM3248 cells grown in serum-deprived conditions (S. Ganguly, unpublished observation). WM3248 cells possess wildtype B-Raf and mutant PTEN; therefore, regulation of ERK signaling in these cells may be via another mechanism rather than c-Abl/Arg→Akt signaling since these cells possess activated Akt. To further test the reason for this discrepancy, we will use a tet-inducible system to regulate expression of activated ERK1/2 and thereby determine whether activation of ERK1/2 prevents the STI571+doxorubicin-mediated decrease in WM3248 cell proliferation. Understanding the mechanism by which STI571 prevents breast cancer and melanoma cell proliferation is especially important in relation to inhibition of disease progression, and these studies will shed light on that potential mechanism.

7.3 Studies in Progress

Our work has identified Abl family kinases as causative agents in solid tumor progression (i.e., breast cancer, melanoma, glioblastoma) [38, 44, 50]. Others have also demonstrated a role of c-Abl and Arg in breast cancer [41-43, 255], gastric carcinomas [45], hepatocellular carcinoma [256], and lung cancer [19, 257]. Some recent evidence has demonstrated a potential role of c-Abl in prostate cancer motility [48]. We propose future experiments that will elucidate whether c-Abl/Arg are activated in invasive/metastatic prostate cancer and promote prostate cancer progression and

survival. We have discovered that Abl family kinases are indeed highly activated in invasive/metastatic prostate cancer cells, and their activation strongly correlates with the invasive/metastatic capability of each cell line (Figure 7.1A). Prostate cancer, the most frequently diagnosed noncutaneous form of cancer, is difficult to treat if not detected early, and refinement of biomarkers for this cancer can potentially result in dramatically improved patient prognosis [258]. Recent evidence by Kyprianou and colleagues suggests that Talin, a high molecular weight cytoskeletal protein overexpressed in prostate cancer, is a causative prognostic marker of disease progression to metastasis [259]. Talin promotes proliferation, survival, invasion through the endothelial cell layer, and metastasis via activation of integrin and Akt signaling pathways [260]. Talin is critical for focal adhesion formation and cell motility, and is a known substrate of c-Abl [261]. It was recently shown in PC3 cells that HSP90 stabilizes c-Abl, thereby promoting WASF3-mediated cell motility, and that PDGF-stimulated nuclear localization of β-catenin occurs via c-Abl [48, 49]. Others have shown that STI571 sensitized PC3, but not LNCAP, cells to UV, but the mechanism and reason for the discrepancy between cell types is unknown [262]. PC3 cells are more aggressive and are androgen-independent, whereas LNCAP cells are androgen-dependent and much less aggressive [263], and we have previously demonstrated that Abl family kinase activation is enhanced in the most aggressive/invasive breast cancer cell lines [38].

Here we present novel data demonstrating that Abl family kinases are dramatically activated in invasive/metastatic prostate cancer cells (Figure 7.1A). Importantly, DU145 cells, which are highly invasive and hormone-insensitive, also possessed dramatically enhanced c-Abl/Arg activities (Figure 7.1A). Talin expression, similar to our observation with Abl family kinase activity, also increases with disease stage [259]. We also observed that overexpression of Talin in PC3 cells markedly increased c-Abl/Arg activity (Figure 7.1B); however, silencing Talin expression in DU145 cells did not dramatically alter c-Abl/Arg activities (Figure 7.2A). Studies focused on the functional interplay of these two proteins could potentially reveal critical information regarding prostate cancer progression and motility.

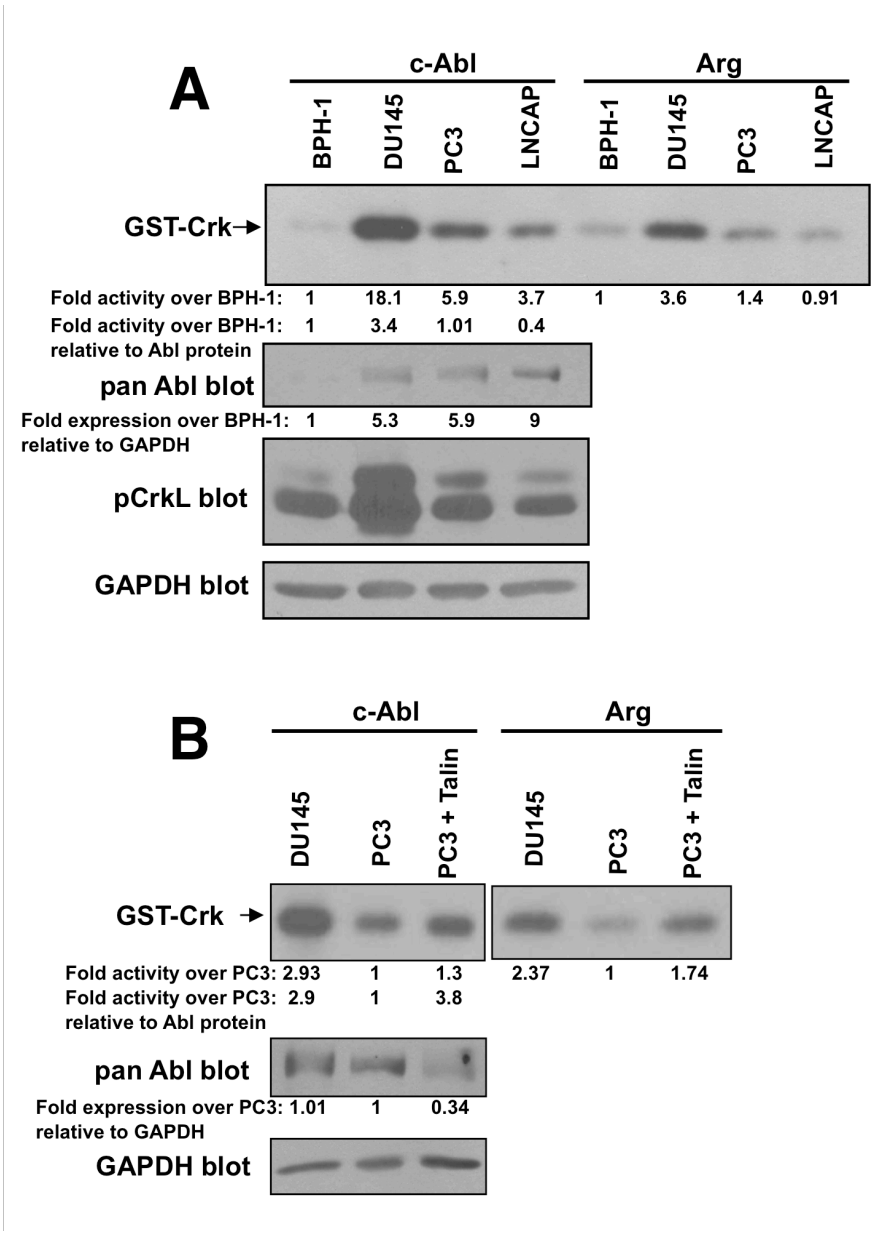

Figure 7.1. Expression and activation of Abl kinases in prostate cancer cell lines. **(A)** c-Abl and Arg kinase activities were assessed in serum-starved prostate cancer cell lines by *in vitro* kinase assay (top). Western blotting was performed for Abl protein expression or using a phospho-specific antibody to CrkL. **(B)** c-Abl and Arg kinase activities were assessed in serum-starved prostate cancer cell lines by *in vitro* kinase assay and Abl protein expression determined by Western blotting. Blots are representative of 3 independent experiments. Relative protein levels were quantitated by analyzing blots with ImageQuant software.

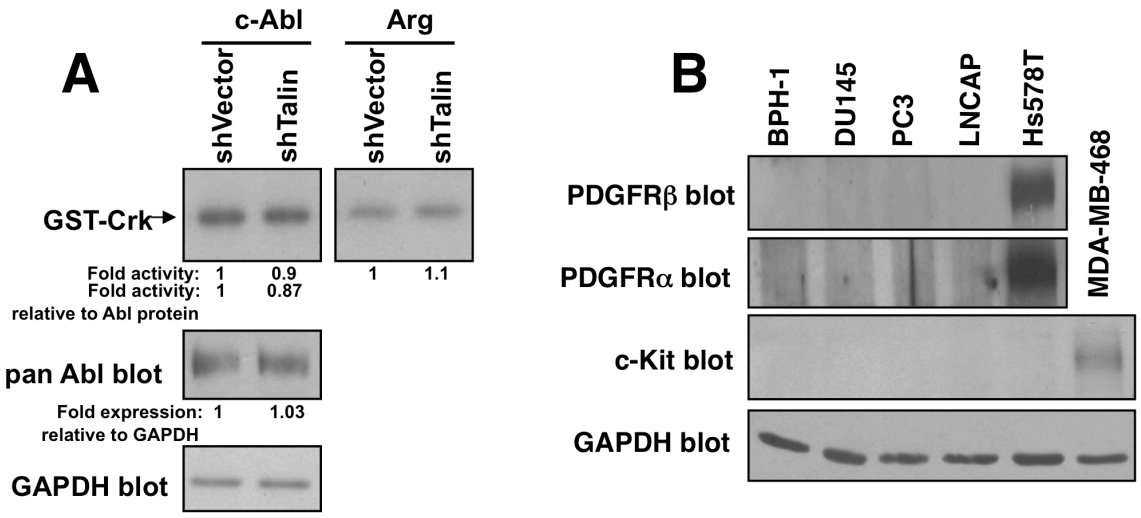

Figure 7.2. Silencing Talin does not inhibit the activity of Abl family kinases. (A) c-Abl and Arg kinase activities were assessed in serum-starved DU145 shVector and shTalin cells by *in vitro* kinase assay. **(B)** Expression of PDGFRα and β in prostate cancer cell lines. Lysates from serum-starved prostate cancer cell lines were probed with antibodies to both PDGFRα and β. Blots are representative of 3 independent experiments.

Future experiments will focus on elucidating the functional relationship between Abl family kinases and Talin in prostate cancer cells and how these proteins regulate diverse signaling pathways to promote cell migration/motility and prostate cancer progression to metastasis. Experiments are currently underway focused on whether c-Abl/Arg and Talin interact to promote prostate cell viability and motility, and preliminary results indicate that co-inhibition of Abl family kinases and Talin synergistically prevents prostate cell motility and dramatically decreases cell viability (data not shown). Importantly, two other primary potential targets of c-Abl/Arg inhibitors (i.e., c-Kit, PDGFR) are not expressed in these cells (Figure 7.2B). These preliminary studies represent a potentially exciting foray into the study of c-Abl and Arg in prostate cancer progression.

References

1. Pendergast, A.M., *The Abl family kinases: mechanisms of regulation and signaling.* Adv Cancer Res, 2002. **85**: p. 51-100.
2. Sirvent, A., C. Benistant, and S. Roche, *Cytoplasmic signalling by the c-Abl tyrosine kinase in normal and cancer cells.* Biol Cell, 2008. **100**(11): p. 617-31.
3. Furstoss, O., et al., *c-Abl is an effector of Src for growth factor-induced c-myc expression and DNA synthesis.* EMBO J, 2002. **21**(4): p. 514-24.
4. Lin, J. and R. Arlinghaus, *Activated c-Abl tyrosine kinase in malignant solid tumors.* Oncogene, 2008. **27**(32): p. 4385-91.
5. Colicelli, J., *ABL tyrosine kinases: evolution of function, regulation, and specificity.* Sci Signal, 2010. **3**(139): p. re6.
6. Van Etten, R.A., P. Jackson, and D. Baltimore, *The mouse type IV c-abl gene product is a nuclear protein, and activation of transforming ability is associated with cytoplasmic localization.* Cell, 1989. **58**(4): p. 669-78.
7. Wen, S.T., P.K. Jackson, and R.A. Van Etten, *The cytostatic function of c-Abl is controlled by multiple nuclear localization signals and requires the p53 and Rb tumor suppressor gene products.* EMBO J, 1996. **15**(7): p. 1583-95.
8. Taagepera, S., et al., *Nuclear-cytoplasmic shuttling of C-ABL tyrosine kinase.* Proc Natl Acad Sci U S A, 1998. **95**(13): p. 7457-62.
9. Van Etten, R.A., *Cycling, stressed-out and nervous: cellular functions of c-Abl.* Trends Cell Biol, 1999. **9**(5): p. 179-86.
10. Wang, J.Y., *Regulation of cell death by the Abl tyrosine kinase.* Oncogene, 2000. **19**(49): p. 5643-50.
11. Bradley, W.D. and A.J. Koleske, *Regulation of cell migration and morphogenesis by Abl-family kinases: emerging mechanisms and physiological contexts.* J Cell Sci, 2009. **122**(Pt 19): p. 3441-54.
12. Hantschel, O., et al., *A myristoyl/phosphotyrosine switch regulates c-Abl.* Cell, 2003. **112**(6): p. 845-57.
13. Nagar, B., et al., *Structural basis for the autoinhibition of c-Abl tyrosine kinase.* Cell, 2003. **112**(6): p. 859-71.
14. Welch, P.J. and J.Y. Wang, *A C-terminal protein-binding domain in the retinoblastoma protein regulates nuclear c-Abl tyrosine kinase in the cell cycle.* Cell, 1993. **75**(4): p. 779-90.
15. Wen, S.T. and R.A. Van Etten, *The PAG gene product, a stress-induced protein with antioxidant properties, is an Abl SH3-binding protein and a physiological inhibitor of c-Abl tyrosine kinase activity.* Genes Dev, 1997. **11**(19): p. 2456-67.
16. Plattner, R., et al., *A new link between the c-Abl tyrosine kinase and phosphoinositide signalling through PLC-[gamma]1.* Nat Cell Biol, 2003. **5**(4): p. 309-319.
17. Van Etten, R.A., *c-Abl regulation: a tail of two lipids.* Curr Biol, 2003. **13**(15): p. R608-10.
18. Zhu, J. and S.K. Shore, *c-ABL tyrosine kinase activity is regulated by association with a novel SH3-domain-binding protein.* Mol Cell Biol, 1996. **16**(12): p. 7054-62.
19. Lin, J., et al., *Oncogenic activation of c-Abl in non-small cell lung cancer cells lacking FUS1 expression: inhibition of c-Abl by the tumor suppressor gene product Fus1.* Oncogene, 2007. **26**(49): p. 6989-96.
20. He, X., et al., *Proliferating cell nuclear antigen destabilizes c-Abl tyrosine kinase and regulates cell apoptosis in response to DNA damage.* Apoptosis, 2009. **14**(3): p. 268-75.

21. Pendergast, A.M., *BCR-ABL protein domain, function, and signaling.* , in *Chronic myeloid leukemia: biology and treatment*, R. Hehlmann, Editor. 2001, Martin Dunitz, Lt: London. p. 19-39.
22. Salgia, R., et al., *BCR/ABL induces multiple abnormalities of cytoskeletal function.* Journal of Clinical Investigations, 1997. **100**(1): p. 46-57.
23. Skorski, T., et al., *The SH3 domain contributes to BCR/ABL-dependent leukemogenesis in vivo: Role in adhesion, invasion and homing.* Blood, 1998. **91**(2): p. 406-418.
24. Nowell, P.C. and D.A. Hungerford, *Chromosome studies on normal and leukemic human leukocytes.* J Natl Cancer Inst, 1960. **25**: p. 85-109.
25. Advani, A.S. and A.M. Pendergast, *Bcr-Abl variants: biological and clinical aspects.* Leuk Res, 2002. **26**(8): p. 713-20.
26. Ernst, T., et al., *Identification of FOXP1 and SNX2 as novel ABL1 fusion partners in acute lymphoblastic leukaemia.* Br J Haematol, 2011. **153**(1): p. 43-6.
27. Pendergast, A.M., *BCR-ABL protein domain, function, and signaling*, in *Chronic Myeloid Leukaemia: Biology and Treatment*, A.M. Carella, et al., Editors. 2001, Martin Dunitz, Lt.: London. p. 19-39.
28. Scheijen, B. and J.D. Griffin, *Tyrosine kinase oncogenes in normal hematopoiesis and hematological disease.* Oncogene, 2002. **21**: p. 3314-3333.
29. De Braekeleer, E., et al., *ABL1 fusion genes in hematological malignancies: a review.* Eur J Haematol, 2011. **86**(5): p. 361-71.
30. Druker, B.J., et al., *Efficacy and safety of a specific inhibitor of the BCR-ABL tyrosine kinase in chronic myeloid leukemia.* N Engl J Med, 2001. **344**(14): p. 1031-7.
31. Deininger, M.W., *Nilotinib.* Clin Cancer Res, 2008. **14**(13): p. 4027-31.
32. Druker, B.J., et al., *Effects of a selective inhibitor of the Abl tyrosine kinase on the growth of Bcr-Abl positive cells.* Nat Med, 1996. **2**(5): p. 561-6.
33. Quintas-Cardama, A., H. Kantarjian, and J. Cortes, *Flying under the radar: the new wave of BCR-ABL inhibitors.* Nat Rev Drug Discov, 2007. **6**(10): p. 834-48.
34. Weisberg, E., et al., *Characterization of AMN107, a selective inhibitor of native and mutant Bcr-Abl.* Cancer Cell, 2005. **7**(2): p. 129-41.
35. Manley, P.W., et al., *Extended kinase profile and properties of the protein kinase inhibitor nilotinib.* Biochim Biophys Acta, 2010. **1804**(3): p. 445-53.
36. Day, E., et al., *Inhibition of collagen-induced discoidin domain receptor 1 and 2 activation by imatinib, nilotinib and dasatinib.* Eur J Pharmacol, 2008. **599**(1-3): p. 44-53.
37. Plattner, R., et al., *c-Abl is activated by growth factors and Src family kinases and has a role in the cellular response to PDGF.* Genes Dev, 1999. **13**(18): p. 2400-11.
38. Srinivasan, D. and R. Plattner, *Activation of Abl tyrosine kinases promotes invasion of aggressive breast cancer cells.* Cancer Res, 2006. **66**(11): p. 5648-55.
39. Srinivasan, D., J.T. Sims, and R. Plattner, *Aggressive breast cancer cells are dependent on activated Abl kinases for proliferation, anchorage-independent growth and survival.* Oncogene, 2008. **27**(8): p. 1095-105.
40. Plattner, R., et al., *A New Link Between the c-Abl Tyrosine Kinase and Phosphoinositide Signaling via PLC-γ1.* Nat Cell Biol, 2003. **5**(4): p. 309-19.
41. Sirvent, A., et al., *The tyrosine kinase Abl is required for Src-transforming activity in mouse fibroblasts and human breast cancer cells.* Oncogene, 2007. **26**(52): p. 7313-23.

42. Smith-Pearson, P.S., et al., *Abl kinases are required for invadopodia formation and chemokine-induced invasion.* J Biol Chem, 2010. **285**(51): p. 40201-11.
43. Mader, C.C., et al., *An EGFR-Src-Arg-cortactin pathway mediates functional maturation of invadopodia and breast cancer cell invasion.* Cancer Res, 2011. **71**(5): p. 1730-41.
44. Srinivasan, D., D.M. Kaetzel, and R. Plattner, *Reciprocal regulation of Abl and receptor tyrosine kinases.* Cell Signal, 2009. **21**(7): p. 1143-50.
45. Furlan, A., et al., *Abl interconnects oncogenic Met and p53 core pathways in cancer cells.* Cell Death Differ, 2011. **18**(10): p. 1608-16.
46. O'Neill, A.J., et al., *Abl expression in human fetal and adult tissues, tumours, and tumour microvessels.* J Pathol, 1997. **183**(3): p. 325-9.
47. Singer, C.F., et al., *Expression of tyrosine kinases in human malignancies as potential targets for kinase-specific inhibitors.* Endocr Relat Cancer, 2004. **11**(4): p. 861-9.
48. Teng, Y., et al., *HSP90 and HSP70 are essential for stabilization and activation of the WASF3 metastasis promoting protein.* J Biol Chem, 2012.
49. Iqbal, S., et al., *PDGF Upregulates Mcl-1 Through Activation of beta-Catenin and HIF-1alpha-Dependent Signaling in Human Prostate Cancer Cells.* PLoS One, 2012. **7**(1): p. e30764.
50. Ganguly, S.S., et al., *c-Abl and Arg are activated in human primary melanomas, promote melanoma cell invasion via distinct pathways, and drive metastatic progression.* Oncogene, 2011.
51. Aggarwal, B.B., et al., *Signal transducer and activator of transcription-3, inflammation, and cancer: how intimate is the relationship?* Ann N Y Acad Sci, 2009. **1171**: p. 59-76.
52. Levy, D.E. and J.E. Darnell, Jr., *Stats: transcriptional control and biological impact.* Nat Rev Mol Cell Biol, 2002. **3**(9): p. 651-62.
53. Bromberg, J. and J.E. Darnell, Jr., *The role of STATs in transcriptional control and their impact on cellular function.* Oncogene, 2000. **19**(21): p. 2468-73.
54. Bromberg, J., *Stat proteins and oncogenesis.* J Clin Invest, 2002. **109**(9): p. 1139-42.
55. Menssen, A. and H. Hermeking, *Characterization of the c-MYC-regulated transcriptome by SAGE: identification and analysis of c-MYC target genes.* Proc Natl Acad Sci U S A, 2002. **99**(9): p. 6274-9.
56. Yang, W., et al., *Repression of transcription of the p27(Kip1) cyclin-dependent kinase inhibitor gene by c-Myc.* Oncogene, 2001. **20**(14): p. 1688-702.
57. Kucab, J.E., et al., *Celecoxib analogues disrupt Akt signaling, which is commonly activated in primary breast tumours.* Breast Cancer Res, 2005. **7**(5): p. R796-807.
58. Luo, J., B.D. Manning, and L.C. Cantley, *Targeting the PI3K-Akt pathway in human cancer: rationale and promise.* Cancer Cell, 2003. **4**(4): p. 257-62.
59. Comer, F.I. and C.A. Parent, *PI 3-kinases and PTEN: how opposites chemoattract.* Cell, 2002. **109**(5): p. 541-4.
60. Carnero, A., et al., *The PTEN/PI3K/AKT signalling pathway in cancer, therapeutic implications.* Curr Cancer Drug Targets, 2008. **8**(3): p. 187-98.
61. Blume-Jensen, P. and T. Hunter, *Oncogenic kinase signalling.* Nature, 2001. **411**(6835): p. 355-65.
62. Dowling, R.J., et al., *Dissecting the role of mTOR: lessons from mTOR inhibitors.* Biochim Biophys Acta, 2010. **1804**(3): p. 433-9.

63. Rane, M.J., et al., *p38 Kinase-dependent MAPKAPK-2 activation functions as 3-phosphoinositide-dependent kinase-2 for Akt in human neutrophils.* J Biol Chem, 2001. **276**(5): p. 3517-23.
64. Rane, M.J., et al., *Heat shock protein 27 controls apoptosis by regulating Akt activation.* J Biol Chem, 2003. **278**(30): p. 27828-35.
65. Zheng, C., et al., *MAPK-activated protein kinase-2 (MK2)-mediated formation and phosphorylation-regulated dissociation of the signal complex consisting of p38, MK2, Akt, and Hsp27.* J Biol Chem, 2006. **281**(48): p. 37215-26.
66. Wu, R., et al., *Hsp27 regulates Akt activation and polymorphonuclear leukocyte apoptosis by scaffolding MK2 to Akt signal complex.* J Biol Chem, 2007. **282**(30): p. 21598-608.
67. Shi, G.X., L. Jin, and D.A. Andres, *A rit GTPase-p38 mitogen-activated protein kinase survival pathway confers resistance to cellular stress.* Mol Cell Biol, 2011. **31**(10): p. 1938-48.
68. Bozulic, L., et al., *PKBalpha/Akt1 acts downstream of DNA-PK in the DNA double-strand break response and promotes survival.* Mol Cell, 2008. **30**(2): p. 203-13.
69. Song, H., et al., *Stat3 modulates heat shock 27kDa protein expression in breast epithelial cells.* Biochem Biophys Res Commun, 2004. **314**(1): p. 143-50.
70. Steelman, L.S., et al., *JAK/STAT, Raf/MEK/ERK, PI3K/Akt and BCR-ABL in cell cycle progression and leukemogenesis.* Leukemia, 2004. **18**(2): p. 189-218.
71. Yuan, Z.Q., et al., *AKT2 inhibition of cisplatin-induced JNK/p38 and Bax activation by phosphorylation of ASK1: implication of AKT2 in chemoresistance.* J Biol Chem, 2003. **278**(26): p. 23432-40.
72. Smalley, K.S., et al., *Multiple signaling pathways must be targeted to overcome drug resistance in cell lines derived from melanoma metastases.* Mol Cancer Ther, 2006. **5**(5): p. 1136-44.
73. Biswas, D.K., et al., *NF-kappa B activation in human breast cancer specimens and its role in cell proliferation and apoptosis.* Proc Natl Acad Sci U S A, 2004. **101**(27): p. 10137-42.
74. Wang, X., et al., *Oestrogen signalling inhibits invasive phenotype by repressing RelB and its target BCL2.* Nat Cell Biol, 2007. **9**(4): p. 470-8.
75. Li, F. and G. Sethi, *Targeting transcription factor NF-kappaB to overcome chemoresistance and radioresistance in cancer therapy.* Biochim Biophys Acta, 2010. **1805**(2): p. 167-80.
76. Chaturvedi, M.M., et al., *NF-kappaB addiction and its role in cancer: 'one size does not fit all'.* Oncogene, 2011. **30**(14): p. 1615-30.
77. Gupta, S.C., et al., *Inhibiting NF-kappaB activation by small molecules as a therapeutic strategy.* Biochim Biophys Acta, 2010. **1799**(10-12): p. 775-87.
78. Lee, H., et al., *Persistently activated Stat3 maintains constitutive NF-kappaB activity in tumors.* Cancer Cell, 2009. **15**(4): p. 283-93.
79. Cusack, J.C., R. Liu, and A.S. Baldwin, *NF- kappa B and chemoresistance: potentiation of cancer drugs via inhibition of NF- kappa B.* Drug Resist Updat, 1999. **2**(4): p. 271-273.
80. McCubrey, J.A., et al., *Roles of the RAF/MEK/ERK and PI3K/PTEN/AKT pathways in malignant transformation and drug resistance.* Adv Enzyme Regul, 2006. **46**: p. 249-79.
81. Grivennikov, S.I. and M. Karin, *Dangerous liaisons: STAT3 and NF-kappaB collaboration and crosstalk in cancer.* Cytokine Growth Factor Rev, 2010. **21**(1): p. 11-9.

82. Hayden, M.S. and S. Ghosh, *Shared principles in NF-kappaB signaling.* Cell, 2008. **132**(3): p. 344-62.
83. Abe, S., et al., *Rapid induction of IAP family proteins and Smac/DIABLO expression after proapoptotic stimulation with doxorubicin in RPMI 8226 multiple myeloma cells.* Exp Mol Pathol, 2007. **83**(3): p. 405-12.
84. Arnt, C.R., et al., *Synthetic Smac/DIABLO peptides enhance the effects of chemotherapeutic agents by binding XIAP and cIAP1 in situ.* J Biol Chem, 2002. **277**(46): p. 44236-43.
85. Gangadharan, C., M. Thoh, and S.K. Manna, *Inhibition of constitutive activity of nuclear transcription factor kappaB sensitizes doxorubicin-resistant cells to apoptosis.* J Cell Biochem, 2009. **107**(2): p. 203-13.
86. Campbell, K.J., S. Rocha, and N.D. Perkins, *Active repression of antiapoptotic gene expression by RelA(p65) NF-kappa B.* Mol Cell, 2004. **13**(6): p. 853-65.
87. Ho, W.C., K.M. Dickson, and P.A. Barker, *Nuclear factor-kappaB induced by doxorubicin is deficient in phosphorylation and acetylation and represses nuclear factor-kappaB-dependent transcription in cancer cells.* Cancer Res, 2005. **65**(10): p. 4273-81.
88. Jemal, A., et al., *Cancer statistics, 2008.* CA Cancer J Clin, 2008. **58**(2): p. 71-96.
89. Hanahan, D. and R.A. Weinberg, *The hallmarks of cancer.* Cell, 2000. **100**(1): p. 57-70.
90. Thiery, J.P., *Epithelial-mesenchymal transitions in tumour progression.* Nat Rev Cancer, 2002. **2**(6): p. 442-54.
91. van Diest, P.J., E. van der Wall, and J.P. Baak, *Prognostic value of proliferation in invasive breast cancer: a review.* J Clin Pathol, 2004. **57**(7): p. 675-81.
92. van Diest, P.J., E. van der Wall, and J.P.A. Baak, *Prognostic value of proliferation in invasive breast cancer: a review*. 2004. p. 675-681.
93. Buettner, R., L.B. Mora, and R. Jove, *Activated STAT signaling in human tumors provides novel molecular targets for therapeutic intervention.* Clin Cancer Res, 2002. **8**(4): p. 945-54.
94. Santen, R.J., et al., *The role of mitogen-activated protein (MAP) kinase in breast cancer.* J Steroid Biochem Mol Biol, 2002. **80**(2): p. 239-56.
95. Morgensztern, D. and H.L. McLeod, *PI3K/Akt/mTOR pathway as a target for cancer therapy.* Anticancer Drugs, 2005. **16**(8): p. 797-803.
96. Hynes, N.E., *Tyrosine kinase signalling in breast cancer.* Breast Cancer Res, 2000. **2**(3): p. 154-7.
97. Diaz, N., et al., *Activation of stat3 in primary tumors from high-risk breast cancer patients is associated with elevated levels of activated SRC and survivin expression.* Clin Cancer Res, 2006. **12**(1): p. 20-8.
98. Berishaj, M., et al., *Stat3 is tyrosine-phosphorylated through the interleukin-6/glycoprotein 130/Janus kinase pathway in breast cancer.* Breast Cancer Res, 2007. **9**(3): p. R32.
99. Real, P.J., et al., *Resistance to chemotherapy via Stat3-dependent overexpression of Bcl-2 in metastatic breast cancer cells.* Oncogene, 2002. **21**(50): p. 7611-8.
100. Glynn, S.A., et al., *A new superinvasive in vitro phenotype induced by selection of human breast carcinoma cells with the chemotherapeutic drugs paclitaxel and doxorubicin.* Br J Cancer, 2004. **91**(10): p. 1800-7.
101. Goodman, L.S., et al., *Goodman & Gilman's the pharmacological basis of therapeutics*. 10th ed. 2001, New York: McGraw-Hill, Medical Pub. Division. xxvii, 2148 p., [1] folded leaf of plate.

102. Lankelma, J., et al., *Doxorubicin gradients in human breast cancer.* Clin Cancer Res, 1999. **5**(7): p. 1703-7.
103. Liu, K., et al., *Regulation of E2F1 by BRCT domain-containing protein TopBP1.* Mol Cell Biol, 2003. **23**(9): p. 3287-304.
104. Gewirtz, D.A., *A critical evaluation of the mechanisms of action proposed for the antitumor effects of the anthracycline antibiotics adriamycin and daunorubicin.* Biochem Pharmacol, 1999. **57**(7): p. 727-41.
105. Lee, T.K., T.C. Lau, and I.O. Ng, *Doxorubicin-induced apoptosis and chemosensitivity in hepatoma cell lines.* Cancer Chemother Pharmacol, 2002. **49**(1): p. 78-86.
106. Ashwell, S. and S. Zabludoff, *DNA damage detection and repair pathways--recent advances with inhibitors of checkpoint kinases in cancer therapy.* Clin Cancer Res, 2008. **14**(13): p. 4032-7.
107. Frei, E.a.K.H.A., *Combination chemotherapy, dose, and schedule*, in *Cancer Medicine*, J.F. Holland, Bast, R.C., Morton, D.L., Frei, E., Kufe, D.W., and Weichselbaum, R.R., Editor. 1997, Williams & Williams: Baltimore. p. 817-837.
108. Agrawal, A., et al., *Overview of tyrosine kinase inhibitors in clinical breast cancer.* Endocr Relat Cancer, 2005. **12 Suppl 1**: p. S135-44.
109. Berwick, M., E. Erdei, and J. Hay, *Melanoma epidemiology and public health.* Dermatol Clin, 2009. **27**(2): p. 205-14, viii.
110. Kabbarah, O. and L. Chin, *Revealing the genomic heterogeneity of melanoma.* Cancer Cell, 2005. **8**(6): p. 439-41.
111. Zaidi, M.R., C.P. Day, and G. Merlino, *From UVs to metastases: modeling melanoma initiation and progression in the mouse.* J Invest Dermatol, 2008. **128**(10): p. 2381-91.
112. Shepherd, C., I. Puzanov, and J.A. Sosman, *B-RAF inhibitors: an evolving role in the therapy of malignant melanoma.* Curr Oncol Rep, 2010. **12**(3): p. 146-52.
113. Govindarajan, B., et al., *Overexpression of Akt converts radial growth melanoma to vertical growth melanoma.* J Clin Invest, 2007. **117**(3): p. 719-29.
114. Melnikova, V.O. and M. Bar-Eli, *Transcriptional control of the melanoma malignant phenotype.* Cancer Biol Ther, 2008. **7**(7): p. 997-1003.
115. McGary, E.C., D.C. Lev, and M. Bar-Eli, *Cellular adhesion pathways and metastatic potential of human melanoma.* Cancer Biol Ther, 2002. **1**(5): p. 459-65.
116. Mouawad, R., et al., *Treatment for metastatic malignant melanoma: old drugs and new strategies.* Crit Rev Oncol Hematol, 2010. **74**(1): p. 27-39.
117. Hocker, T.L., M.K. Singh, and H. Tsao, *Melanoma genetics and therapeutic approaches in the 21st century: moving from the benchside to the bedside.* J Invest Dermatol, 2008. **128**(11): p. 2575-95.
118. Held, L., et al., *Oncogenetics of melanoma: basis for molecular diagnostics and therapy.* J Dtsch Dermatol Ges, 2011.
119. Davies, H., et al., *Mutations of the BRAF gene in human cancer.* Nature, 2002. **417**(6892): p. 949-54.
120. Tsai, J., et al., *Discovery of a selective inhibitor of oncogenic B-Raf kinase with potent antimelanoma activity.* Proc Natl Acad Sci U S A, 2008. **105**(8): p. 3041-6.
121. Nazarian, R., et al., *Melanomas acquire resistance to B-RAF(V600E) inhibition by RTK or N-RAS upregulation.* Nature, 2010. **468**(7326): p. 973-7.
122. Flaherty, K.T., et al., *Inhibition of mutated, activated BRAF in metastatic melanoma.* N Engl J Med, 2010. **363**(9): p. 809-19.

123. Smalley, K.S., V.K. Sondak, and J.S. Weber, *c-KIT signaling as the driving oncogenic event in sub-groups of melanomas.* Histol Histopathol, 2009. **24**(5): p. 643-50.
124. Satzger, I., et al., *Anal mucosal melanoma with KIT-activating mutation and response to imatinib therapy--case report and review of the literature.* Dermatology, 2010. **220**(1): p. 77-81.
125. Walsh, N., et al., *Membrane transport proteins in human melanoma: associations with tumour aggressiveness and metastasis.* Br J Cancer, 2010. **102**(7): p. 1157-62.
126. Colone, M., et al., *The multidrug transporter P-glycoprotein: a mediator of melanoma invasion?* J Invest Dermatol, 2008. **128**(4): p. 957-71.
127. Hodi, F.S., et al., *Improved survival with ipilimumab in patients with metastatic melanoma.* N Engl J Med, 2010. **363**(8): p. 711-23.
128. Szakacs, G., et al., *Targeting multidrug resistance in cancer.* Nat Rev Drug Discov, 2006. **5**(3): p. 219-34.
129. Ghobrial, I.M., T.E. Witzig, and A.A. Adjei, *Targeting Apoptosis Pathways in Cancer Therapy*. 2005. p. 178-194.
130. Wright, C.W. and C.S. Duckett, *Reawakening the cellular death program in neoplasia through the therapeutic blockade of IAP function.* J Clin Invest, 2005. **115**(10): p. 2673-8.
131. Hsieh, F.C., G. Cheng, and J. Lin, *Evaluation of potential Stat3-regulated genes in human breast cancer.* Biochem Biophys Res Commun, 2005. **335**(2): p. 292-9.
132. Lopes, R.B., et al., *Expression of the IAP protein family is dysregulated in pancreatic cancer cells and is important for resistance to chemotherapy.* Int J Cancer, 2007. **120**(11): p. 2344-52.
133. Chen, K.G. and M.M. Gottesman, *How Melanoma Cells Evade Chemotherapy*. From Melanocytes to Melanoma, ed. V.J. Hearing and S.P.L. Leong. 2006, Totowa, NJ: Humana Press Inc.
134. Sissung, T.M., et al., *Pharmacogenetics of membrane transporters: an update on current approaches.* Mol Biotechnol, 2010. **44**(2): p. 152-67.
135. Gillet, J.P., T. Efferth, and J. Remacle, *Chemotherapy-induced resistance by ATP-binding cassette transporter genes.* Biochim Biophys Acta, 2007. **1775**(2): p. 237-62.
136. Schinkel, A.H. and J.W. Jonker, *Mammalian drug efflux transporters of the ATP binding cassette (ABC) family: an overview.* Adv Drug Deliv Rev, 2003. **55**(1): p. 3-29.
137. Staud, F. and P. Pavek, *Breast cancer resistance protein (BCRP/ABCG2).* Int J Biochem Cell Biol, 2005. **37**(4): p. 720-5.
138. Ambudkar, S.V., et al., *P-glycoprotein: from genomics to mechanism.* Oncogene, 2003. **22**(47): p. 7468-85.
139. Doyle, L.A., et al., *A multidrug resistance transporter from human MCF-7 breast cancer cells.* Proc Natl Acad Sci U S A, 1998. **95**(26): p. 15665-70.
140. Xu, J., et al., *Characterization of oligomeric human half-ABC transporter ATP-binding cassette G2.* J Biol Chem, 2004. **279**(19): p. 19781-9.
141. Deeley, R.G. and S.P. Cole, *Substrate recognition and transport by multidrug resistance protein 1 (ABCC1).* FEBS Lett, 2006. **580**(4): p. 1103-11.
142. Elliott, A.M. and M.A. Al-Hajj, *ABCB8 mediates doxorubicin resistance in melanoma cells by protecting the mitochondrial genome.* Mol Cancer Res, 2009. **7**(1): p. 79-87.
143. Frank, N.Y., et al., *ABCB5-mediated doxorubicin transport and chemoresistance in human malignant melanoma.* Cancer Res, 2005. **65**(10): p. 4320-33.

144. Molinari, A., et al., *Induction of P-glycoprotein expression on the plasma membrane of human melanoma cells.* Anticancer Res, 2000. **20**(4): p. 2691-6.
145. Hirschmann-Jax, C., et al., *A distinct "side population" of cells with high drug efflux capacity in human tumor cells.* Proc Natl Acad Sci U S A, 2004. **101**(39): p. 14228-33.
146. Nakanishi, T., et al., *Complex interaction of BCRP/ABCG2 and imatinib in BCR-ABL-expressing cells: BCRP-mediated resistance to imatinib is attenuated by imatinib-induced reduction of BCRP expression.* Blood, 2006. **108**(2): p. 678-84.
147. Hui, R.C., et al., *Doxorubicin activates FOXO3a to induce the expression of multidrug resistance gene ABCB1 (MDR1) in K562 leukemic cells.* Mol Cancer Ther, 2008. **7**(3): p. 670-8.
148. Burger, H. and K. Nooter, *Pharmacokinetic resistance to imatinib mesylate: role of the ABC drug pumps ABCG2 (BCRP) and ABCB1 (MDR1) in the oral bioavailability of imatinib.* Cell Cycle, 2004. **3**(12): p. 1502-5.
149. Rabindran, S.K., et al., *Reversal of a novel multidrug resistance mechanism in human colon carcinoma cells by fumitremorgin C.* Cancer Res, 1998. **58**(24): p. 5850-8.
150. Allen, J.D., et al., *Potent and specific inhibition of the breast cancer resistance protein multidrug transporter in vitro and in mouse intestine by a novel analogue of fumitremorgin C.* Mol Cancer Ther, 2002. **1**(6): p. 417-25.
151. Guo, B., et al., *Potent killing of paclitaxel- and doxorubicin-resistant breast cancer cells by calphostin C accompanied by cytoplasmic vacuolization.* Breast Cancer Res Treat, 2003. **82**(2): p. 125-41.
152. Jemal, A., et al., *Cancer statistics, 2007.* CA Cancer J Clin, 2007. **57**(1): p. 43-66.
153. Rowinsky, E.K., *The development and clinical utility of the taxane class of antimicrotubule chemotherapy agents.* Annu Rev Med, 1997. **48**: p. 353-74.
154. Pommier, Y., *Topoisomerase I inhibitors: camptothecins and beyond.* Nat Rev Cancer, 2006. **6**(10): p. 789-802.
155. Longley, D.B., D.P. Harkin, and P.G. Johnston, *5-fluorouracil: mechanisms of action and clinical strategies.* Nat Rev Cancer, 2003. **3**(5): p. 330-8.
156. Meriggi, F., B. Di Biasi, and A. Zaniboni, *The Renaissance of platinum-based chemotherapy for metastatic breast cancer.* J Chemother, 2008. **20**(5): p. 551-60.
157. Rae, J.M., et al., *MDA-MB-435 cells are derived from M14 melanoma cells--a loss for breast cancer, but a boon for melanoma research.* Breast Cancer Res Treat, 2007. **104**(1): p. 13-9.
158. Burkle, A., *Poly(ADP-ribose). The most elaborate metabolite of NAD+.* FEBS J, 2005. **272**(18): p. 4576-89.
159. Yu, H. and R. Jove, *The STATs of cancer--new molecular targets come of age.* Nat Rev Cancer, 2004. **4**(2): p. 97-105.
160. Cogswell, P.C., et al., *Selective activation of NF-kappa B subunits in human breast cancer: potential roles for NF-kappa B2/p52 and for Bcl-3.* Oncogene, 2000. **19**(9): p. 1123-31.
161. Liu, Z.G., et al., *Three distinct signalling responses by murine fibroblasts to genotoxic stress.* Nature, 1996. **384**(6606): p. 273-6.
162. Chu, S., et al., *BCR/ABL kinase inhibition by imatinib mesylate enhances MAP kinase activity in chronic myelogenous leukemia CD34+ cells.* Blood, 2004. **103**(8): p. 3167-74.
163. Yu, C., et al., *Pharmacologic mitogen-activated protein/extracellular signal-regulated kinase kinase/mitogen-activated protein kinase inhibitors interact synergistically with STI571 to induce apoptosis in Bcr/Abl-expressing human leukemia cells.* Cancer Res, 2002. **62**(1): p. 188-99.

164. Traynor, J., *Basic and clinical pharmacology Edited by B. G. Katzung, 3rd ed. Prentice/Hall International, 1987, pound26.25.* J Pharm Biomed Anal, 1988. **6**(5): p. 527-527.
165. Burton, E.A., R. Plattner, and A.M. Pendergast, *Abl tyrosine kinases are required for infection by Shigella flexneri.* EMBO J, 2003. **22**(20): p. 5471-9.
166. Decaudin, D., et al., *In vivo efficacy of STI571 in xenografted human small cell lung cancer alone or combined with chemotherapy.* Int J Cancer, 2005. **113**(5): p. 849-56.
167. Wang-Rodriguez, J., et al., *STI-571 (Gleevec) potentiates the effect of cisplatin in inhibiting the proliferation of head and neck squamous cell carcinoma in vitro.* Laryngoscope, 2006. **116**(8): p. 1409-16.
168. Zhang, P., et al., *Gleevec (STI-571) inhibits lung cancer cell growth (A549) and potentiates the cisplatin effect in vitro.* Mol Cancer, 2003. **2**: p. 1.
169. Mundhenke, C., et al., *Novel treatment of ovarian cancer cell lines with Imatinib mesylate combined with Paclitaxel and Carboplatin leads to receptor-mediated antiproliferative effects.* J Cancer Res Clin Oncol, 2008. **134**(12): p. 1397-405.
170. Bellone, G., et al., *Inhibition of cell survival and invasive potential of colorectal carcinoma cells by the tyrosine kinase inhibitor STI571.* Cancer Biol Ther, 2004. **3**(4): p. 385-92.
171. Mahon, F.X., et al., *MDR1 gene overexpression confers resistance to imatinib mesylate in leukemia cell line models.* Blood, 2003. **101**(6): p. 2368-73.
172. Burger, H., et al., *Chronic imatinib mesylate exposure leads to reduced intracellular drug accumulation by induction of the ABCG2 (BCRP) and ABCB1 (MDR1) drug transport pumps.* Cancer Biol Ther, 2005. **4**(7): p. 747-52.
173. Burger, H., et al., *Imatinib mesylate (STI571) is a substrate for the breast cancer resistance protein (BCRP)/ABCG2 drug pump.* Blood, 2004. **104**(9): p. 2940-2.
174. Houghton, P.J., et al., *Imatinib mesylate is a potent inhibitor of the ABCG2 (BCRP) transporter and reverses resistance to topotecan and SN-38 in vitro.* Cancer Res, 2004. **64**(7): p. 2333-7.
175. Liu, W., et al., *The tyrosine kinase inhibitor imatinib mesylate enhances the efficacy of photodynamic therapy by inhibiting ABCG2.* Clin Cancer Res, 2007. **13**(8): p. 2463-70.
176. Yuan, J.H., et al., *Breast cancer resistance protein expression and 5-fluorouracil resistance.* Biomed Environ Sci, 2008. **21**(4): p. 290-5.
177. Pratt, S., et al., *The multidrug resistance protein 5 (ABCC5) confers resistance to 5-fluorouracil and transports its monophosphorylated metabolites.* Mol Cancer Ther, 2005. **4**(5): p. 855-63.
178. Stockmans, G., et al., *Triple-negative breast cancer.* Curr Opin Oncol, 2008. **20**(6): p. 614-20.
179. Mersin, H., et al., *The prognostic importance of triple negative breast carcinoma.* Breast, 2008. **17**(4): p. 341-6.
180. Sims, J.T., et al., *STI571 sensitizes breast cancer cells to 5-fluorouracil, cisplatin and camptothecin in a cell type-specific manner.* Biochem Pharmacol, 2009. **78**(3): p. 249-60.
181. Cobleigh, M.A., *Other options in the treatment of advanced breast cancer.* Semin Oncol, 2011. **38 Suppl 2**: p. S11-6.
182. Soengas, M.S. and S.W. Lowe, *Apoptosis and melanoma chemoresistance.* Oncogene, 2003. **22**(20): p. 3138-51.
183. Bradbury, P.A. and M.R. Middleton, *DNA repair pathways in drug resistance in melanoma.* Anticancer Drugs, 2004. **15**(5): p. 421-6.

184. Robertson, G.P., *Functional and therapeutic significance of Akt deregulation in malignant melanoma.* Cancer Metastasis Rev, 2005. **24**(2): p. 273-85.
185. Shen, D.W., et al., *Multiple drug-resistant human KB carcinoma cells independently selected for high-level resistance to colchicine, adriamycin, or vinblastine show changes in expression of specific proteins.* J Biol Chem, 1986. **261**(17): p. 7762-70.
186. Gorre, M.E., et al., *Clinical resistance to STI-571 cancer therapy caused by BCR-ABL gene mutation or amplification.* Science, 2001. **293**(5531): p. 876-80.
187. Ricci, C., et al., *Mutation in the ATP-binding pocket of the ABL kinase domain in an STI571-resistant BCR/ABL-positive cell line.* Cancer Res, 2002. **62**(21): p. 5995-8.
188. Sims, J.T. and R. Plattner, *MTT assays cannot be utilized to study the effects of STI571/Gleevec on the viability of solid tumor cell lines.* Cancer Chemother Pharmacol, 2009. **64**(3): p. 629-33.
189. Burgess, D.J., et al., *Topoisomerase levels determine chemotherapy response in vitro and in vivo.* Proc Natl Acad Sci U S A, 2008. **105**(26): p. 9053-8.
190. Higgins, C.F., *Multiple molecular mechanisms for multidrug resistance transporters.* Nature, 2007. **446**(7137): p. 749-57.
191. Kuo, M.T., et al., *Induction of human MDR1 gene expression by 2-acetylaminofluorene is mediated by effectors of the phosphoinositide 3-kinase pathway that activate NF-kappaB signaling.* Oncogene, 2002. **21**(13): p. 1945-54.
192. Katayama, K., et al., *Inhibition of the mitogen-activated protein kinase pathway results in the down-regulation of P-glycoprotein.* Mol Cancer Ther, 2007. **6**(7): p. 2092-102.
193. Ganguly, S.S., et al., *c-Abl and Arg are activated in human primary melanomas, promote melanoma cell invasion via distinct pathways, and drive metastatic progression.* Oncogene, 2011. **in press (Epub Sept. 5, 2011)**.
194. Lee, J.S., et al., *Rhodamine efflux patterns predict P-glycoprotein substrates in the National Cancer Institute drug screen.* Mol Pharmacol, 1994. **46**(4): p. 627-38.
195. Fletcher, J.I., et al., *ABC transporters in cancer: more than just drug efflux pumps.* Nat Rev Cancer, 2010. **10**(2): p. 147-56.
196. Ozvegy-Laczka, C., et al., *High-affinity interaction of tyrosine kinase inhibitors with the ABCG2 multidrug transporter.* Mol Pharmacol, 2004. **65**(6): p. 1485-95.
197. Tiwari, A.K., et al., *Nilotinib (AMN107, Tasigna) reverses multidrug resistance by inhibiting the activity of the ABCB1/Pgp and ABCG2/BCRP/MXR transporters.* Biochem Pharmacol, 2009. **78**(2): p. 153-61.
198. Nagar, B., et al., *Structural basis for the autoinhibition of c-Abl tyrosine kinase.* Cell, 2003. **112**: p. 859-871.
199. Bogenrieder, T. and M. Herlyn, *Axis of evil: molecular mechanisms of cancer metastasis.* Oncogene, 2003. **22**(42): p. 6524-36.
200. Ashikawa, K., et al., *Evidence that activation of nuclear factor-kappaB is essential for the cytotoxic effects of doxorubicin and its analogues.* Biochem Pharmacol, 2004. **67**(2): p. 353-64.
201. Bian, X., et al., *NF-kappa B activation mediates doxorubicin-induced cell death in N-type neuroblastoma cells.* J Biol Chem, 2001. **276**(52): p. 48921-9.
202. Dahlman, J.M., et al., *The RelA/p65 subunit of NF-kappaB specifically regulates cyclin D1 protein stability: implications for cell cycle withdrawal and skeletal myogenesis.* J Cell Biochem, 2009. **106**(1): p. 42-51.

203. Basseres, D.S. and A.S. Baldwin, *Nuclear factor-kappaB and inhibitor of kappaB kinase pathways in oncogenic initiation and progression.* Oncogene, 2006. **25**(51): p. 6817-30.
204. Ghobrial, I.M., T.E. Witzig, and A.A. Adjei, *Targeting apoptosis pathways in cancer therapy.* CA Cancer J Clin, 2005. **55**(3): p. 178-94.
205. Chen, N., et al., *Caspases and inhibitor of apoptosis proteins in cutaneous and mucosal melanoma: expression profile and clinicopathologic significance.* Hum Pathol, 2009. **40**(7): p. 950-6.
206. Emanuel, P.O., et al., *Immunohistochemical detection of XIAP in melanoma.* J Cutan Pathol, 2008. **35**(3): p. 292-7.
207. Madhunapantula, S.V. and G.P. Robertson, *The PTEN-AKT3 signaling cascade as a therapeutic target in melanoma.* Pigment Cell Melanoma Res, 2009. **22**(4): p. 400-19.
208. Malumbres, M. and A. Pellicer, *RAS pathways to cell cycle control and cell transformation.* Front Biosci, 1998. **3**: p. d887-912.
209. Tang, D., et al., *ERK activation mediates cell cycle arrest and apoptosis after DNA damage independently of p53.* J Biol Chem, 2002. **277**(15): p. 12710-7.
210. Choi, J., et al., *The effect of doxorubicin on MEK-ERK signaling predicts its efficacy in HCC.* J Surg Res, 2008. **150**(2): p. 219-26.
211. Cheung, M., et al., *Akt3 and mutant V600E B-Raf cooperate to promote early melanoma development.* Cancer Res, 2008. **68**(9): p. 3429-39.
212. Lopez-Bergami, P., *The role of mitogen- and stress-activated protein kinase pathways in melanoma.* Pigment Cell Melanoma Res, 2011. **24**(5): p. 902-21.
213. Kuphaldt, T.R., *Lessons In Electric Circuits*. 5th ed. Vol. 1. 2006.
214. Hollestelle, A., et al., *Phosphatidylinositol-3-OH kinase or RAS pathway mutations in human breast cancer cell lines.* Mol Cancer Res, 2007. **5**(2): p. 195-201.
215. Aksamitiene, E., et al., *PI3K/Akt-sensitive MEK-independent compensatory circuit of ERK activation in ER-positive PI3K-mutant T47D breast cancer cells.* Cell Signal, 2010. **22**(9): p. 1369-78.
216. Normanno, N., et al., *Breast cancer cells with acquired resistance to the EGFR tyrosine kinase inhibitor gefitinib show persistent activation of MAPK signaling.* Breast Cancer Res Treat, 2008. **112**(1): p. 25-33.
217. Vantaggiato, C., et al., *ERK1 and ERK2 mitogen-activated protein kinases affect Ras-dependent cell signaling differentially.* J Biol, 2006. **5**(5): p. 14.
218. Craven, R.J., H. Lightfoot, and W.G. Cance, *A decade of tyrosine kinases: from gene discovery to therapeutics.* Surgical Oncology, 2003. **12**(1): p. 39-49.
219. Sutherland, R.L. and E.A. Musgrove, *Cyclins and Breast Cancer.* Journal of Mammary Gland Biology and Neoplasia, 2004. **9**(1): p. 95-104.
220. Barbacid, M., et al., *Cell cycle and cancer: genetic analysis of the role of cyclin-dependent kinases.* Cold Spring Harb Symp Quant Biol, 2005. **70**: p. 233-40.
221. Vlach, J., et al., *Growth arrest by the cyclin-dependent kinase inhibitor p27Kip1 is abrogated by c-Myc.* EMBO J, 1996. **15**(23): p. 6595-604.
222. Mitchell, K.O. and W.S. El-Deiry, *Overexpression of c-Myc inhibits p21WAF1/CIP1 expression and induces S-phase entry in 12-O-tetradecanoylphorbol-13-acetate (TPA)-sensitive human cancer cells.* Cell Growth Differ, 1999. **10**(4): p. 223-30.
223. Gianni, L., E. Salvatorelli, and G. Minotti, *Anthracycline cardiotoxicity in breast cancer patients: synergism with trastuzumab and taxanes.* Cardiovasc Toxicol, 2007. **7**(2): p. 67-71.

224. Schellings, M.W., B. Lowenberg, and Y.M. Pinto, *Another look at imatinib mesylate.* N Engl J Med, 2007. **356**(11): p. 1183; author reply 1183.
225. Pattacini, L., et al., *Endoplasmic reticulum stress initiates apoptotic death induced by STI571 inhibition of p210 bcr-abl tyrosine kinase.* Leuk Res, 2004. **28**(2): p. 191-202.
226. Jego, G., et al., *Targeting heat shock proteins in cancer.* Cancer Lett, 2010.
227. Vichalkovski, A., et al., *Tyrosine kinase modulation of protein kinase C activity regulates G protein-linked Ca2+ signaling in leukemic hematopoietic cells.* Cell Calcium, 2006. **39**(6): p. 517-28.
228. Tabas, I. and D. Ron, *Integrating the mechanisms of apoptosis induced by endoplasmic reticulum stress.* Nat Cell Biol, 2011. **13**(3): p. 184-90.
229. Jiang, C.C., et al., *Human melanoma cells under endoplasmic reticulum stress acquire resistance to microtubule-targeting drugs through XBP-1-mediated activation of Akt.* Neoplasia, 2009. **11**(5): p. 436-47.
230. Grynkiewicz, G., M. Poenie, and R.Y. Tsien, *A new generation of Ca2+ indicators with greatly improved fluorescence properties.* J Biol Chem, 1985. **260**(6): p. 3440-50.
231. Hui, R.C., et al., *The forkhead transcription factor FOXO3a increases phosphoinositide-3 kinase/Akt activity in drug-resistant leukemic cells through induction of PIK3CA expression.* Mol Cell Biol, 2008. **28**(19): p. 5886-98.
232. Ejlertsen, B., et al., *HER2, TOP2A, and TIMP-1 and responsiveness to adjuvant anthracycline-containing chemotherapy in high-risk breast cancer patients.* J Clin Oncol, 2010. **28**(6): p. 984-90.
233. Sorensen, N.M., et al., *TIMP-1 is significantly associated with objective response and survival in metastatic colorectal cancer patients receiving combination of irinotecan, 5-fluorouracil, and folinic acid.* Clin Cancer Res, 2007. **13**(14): p. 4117-22.
234. Chang, S.P., et al., *Imatinib mesylate induction of ROS-dependent apoptosis in melanoma B16F0 cells.* J Dermatol Sci, 2011. **62**(3): p. 183-91.
235. Cui, X., *Reactive Oxygen Species: The Achilles' Heel of Cancer Cells?* Antioxid Redox Signal, 2012.
236. Morgan, M.J. and Z.G. Liu, *Crosstalk of reactive oxygen species and NF-kappaB signaling.* Cell Res, 2011. **21**(1): p. 103-15.
237. Zhou, L.Z., A.P. Johnson, and T.A. Rando, *NF kappa B and AP-1 mediate transcriptional responses to oxidative stress in skeletal muscle cells.* Free Radic Biol Med, 2001. **31**(11): p. 1405-16.
238. Rhee, S.G., et al., *Controlled elimination of intracellular H(2)O(2): regulation of peroxiredoxin, catalase, and glutathione peroxidase via post-translational modification.* Antioxid Redox Signal, 2005. **7**(5-6): p. 619-26.
239. Fang, J., H. Nakamura, and A.K. Iyer, *Tumor-targeted induction of oxystress for cancer therapy.* J Drug Target, 2007. **15**(7-8): p. 475-86.
240. Cao, C., Y. Leng, and D. Kufe, *Catalase activity is regulated by c-Abl and Arg in the oxidative stress response.* J Biol Chem, 2003. **278**(32): p. 29667-75.
241. Beers, R.F., Jr. and I.W. Sizer, *A spectrophotometric method for measuring the breakdown of hydrogen peroxide by catalase.* J Biol Chem, 1952. **195**(1): p. 133-40.
242. Engelmann, K., H. Shen, and O.J. Finn, *MCF7 side population cells with characteristics of cancer stem/progenitor cells express the tumor antigen MUC1.* Cancer Res, 2008. **68**(7): p. 2419-26.

243. Fillmore, C.M. and C. Kuperwasser, *Human breast cancer cell lines contain stem-like cells that self-renew, give rise to phenotypically diverse progeny and survive chemotherapy.* Breast Cancer Res, 2008. **10**(2): p. R25.
244. Zabierowski, S.E. and M. Herlyn, *Melanoma stem cells: the dark seed of melanoma.* J Clin Oncol, 2008. **26**(17): p. 2890-4.
245. Fang, D., et al., *A tumorigenic subpopulation with stem cell properties in melanomas.* Cancer Res, 2005. **65**(20): p. 9328-37.
246. Radhakrishnan, S.K. and S. Kamalakaran, *Pro-apoptotic role of NF-kappaB: implications for cancer therapy.* Biochim Biophys Acta, 2006. **1766**(1): p. 53-62.
247. Campbell, K.J. and N.D. Perkins, *Post-translational modification of RelA(p65) NF-kappaB.* Biochem Soc Trans, 2004. **32**(Pt 6): p. 1087-9.
248. Kharbanda, S., et al., *Functional interaction between DNA-PK and c-Abl in response to DNA damage.* Nature, 1997. **386**(6626): p. 732-5.
249. Wei, X., et al., *Exome sequencing identifies GRIN2A as frequently mutated in melanoma.* Nat Genet, 2011. **43**(5): p. 442-6.
250. Carter, C.J., *Multiple genes and factors associated with bipolar disorder converge on growth factor and stress activated kinase pathways controlling translation initiation: implications for oligodendrocyte viability.* Neurochem Int, 2007. **50**(3): p. 461-90.
251. Ma, J. and G.Y. Zhang, *Lithium reduced N-methyl-D-aspartate receptor subunit 2A tyrosine phosphorylation and its interactions with Src and Fyn mediated by PSD-95 in rat hippocampus following cerebral ischemia.* Neurosci Lett, 2003. **348**(3): p. 185-9.
252. Seabold, G.K., et al., *Interaction of the tyrosine kinase Pyk2 with the N-methyl-D-aspartate receptor complex via the Src homology 3 domains of PSD-95 and SAP102.* J Biol Chem, 2003. **278**(17): p. 15040-8.
253. Beazely, M.A., M. Weerapura, and J.F. MacDonald, *Abelson tyrosine kinase links PDGFbeta receptor activation to cytoskeletal regulation of NMDA receptors in CA1 hippocampal neurons.* Mol Brain, 2008. **1**: p. 20.
254. Smith, L., et al., *The analysis of doxorubicin resistance in human breast cancer cells using antibody microarrays.* Mol Cancer Ther, 2006. **5**(8): p. 2115-20.
255. Li, X., et al., *c-Abl and Arg tyrosine kinases regulate lysosomal degradation of the oncoprotein Galectin-3.* Cell Death Differ, 2010. **17**(8): p. 1277-87.
256. Yoon, C.H., et al., *Claudin-1 acts through c-Abl-protein kinase Cdelta (PKCdelta) signaling and has a causal role in the acquisition of invasive capacity in human liver cells.* J Biol Chem, 2010. **285**(1): p. 226-33.
257. Yogalingam, G. and A.M. Pendergast, *Abl kinases regulate autophagy by promoting the trafficking and function of lysosomal components.* J Biol Chem, 2008. **283**(51): p. 35941-53.
258. Madu, C.O. and Y. Lu, *Novel diagnostic biomarkers for prostate cancer.* J Cancer, 2010. **1**: p. 150-77.
259. Desiniotis, A. and N. Kyprianou, *Significance of talin in cancer progression and metastasis.* Int Rev Cell Mol Biol, 2011. **289**: p. 117-47.
260. Sakamoto, S., et al., *Talin1 promotes tumor invasion and metastasis via focal adhesion signaling and anoikis resistance.* Cancer Res, 2010. **70**(5): p. 1885-95.
261. Cui, L., et al., *c-Abl kinase is required for beta 2 integrin-mediated neutrophil adhesion.* J Immunol, 2009. **182**(5): p. 3233-42.
262. Xu, Y., et al., *RelB-dependent differential radiosensitization effect of STI571 on prostate cancer cells.* Mol Cancer Ther, 2010. **9**(4): p. 803-12.
263. Tai, S., et al., *PC3 is a cell line characteristic of prostatic small cell carcinoma.* Prostate, 2011. **71**(15): p. 1668-79.

VITA

Name: Jonathan T. Sims
Date of Birth: August 2, 1982
Place of Birth: Newbern, TN, USA

Education:

2000-2002	A.A.	Florida College (General Studies)
2002-2004	B.S.	Western Kentucky University (Recombinant Genetics; Chemistry)

Honors, Awards and Society Memberships:

2000-2002	Florida College Scholars Academic Scholarship
2000-2002	Florida College Crest Club Undergraduate Science Society membership
2002-2004	Western Kentucky University Association of Undergraduate Geneticists membership
2002-2004	Western Kentucky University Chemistry Club membership
2003	KBRIN Undergraduate Summer Research Fellowship
2005-2007	American Chemical Society (ACS) membership
2007-2008	Ohio Valley Society of Toxicology membership
2007-2008	American Association for the Advancement of Science (AAAS) membership
2007-2008	Department of Molecular and Biomedical Pharmacology Graduate Student Representative
2008	Certificate in Business Administration, University of Kentucky Gatton College of Business & Economics
2008-present	Delta Epsilon Iota Honor Society membership
2009-present	American Association for Cancer Research (AACR) membership

Positions:

01/03-05/04	Undergraduate Research Assistant under Donald Slocum, Ph.D., Department of Chemistry, Western Kentucky University, Bowling Green, KY
06/03-08/03	Summer Research Assistant under Jason A. Chesney, M.D., Ph.D., Molecular Targets Group, Brown Cancer Center, University of Louisville, Louisville, KY
08/03-12/04	Undergraduate Research Assistant under Rodney A. King, Ph.D., Department of Biology, Western Kentucky University, Bowling Green, KY
01/05-08/05	Research Assistant under Jason A. Carlyon, Ph.D., Department of Microbiology, Immunology, and Molecular Genetics, University of Kentucky, Lexington, KY
05/06-04/12	Graduate Research Assistant under Rina Plattner, Ph.D., Department of Molecular and Biomedical Pharmacology, University of Kentucky, Lexington, KY

Poster Presentations:

1. **Sims, J.**, Clem, A.L., Telang, S., Chesney, J. “Virus detection and identification using

random multiplex (RT)-PCR with 3'-locked random primers." Kentucky Biomedical Research Infrastructure Network (KBRIN) Summer Internship Research Symposium, Louisville, KY, July 2003.

2. **Sims J.**, McLaughlin, M.R., Balaa, M.F., King, R. "Isolation of salmonella bacteriophages from swine effluent lagoons." Kentucky Academy of Science (KAS) 90th Annual Meeting, Murray, KY, November 2004.
3. **Sims J.T.** and Plattner R. "Abl kinases as potential therapeutic targets in breast cancer." University of Kentucky Graduate Student Interdisciplinary Conference, Lexington, KY, April 2007.
4. **Sims J.T.,** Ganguly, S., Fiore, L, Holler, C., Park, E.S., Plattner, R. "STI571 sensitizes breast cancer cells to 5-Fluorouracil, Cisplatin, and Camptothecin in a cell type-specific manner." American Association for Cancer Research (AACR) 100th Annual Meeting, Denver, CO, April 2009.
5. **Sims J.T.,** Ganguly, S., Fiore, L, Holler, C., Park, E.S., Plattner, R. "STI571 sensitizes breast cancer cells to 5-Fluorouracil, Cisplatin, and Camptothecin in a cell type-specific manner." Markey Cancer Research Day, Lexington, KY, April 2010.

Peer-Reviewed Publications:

1. McLaughlin, M.R., Balaa, M.F., **Sims, J.**, King, R. (2006) Isolation of salmonella bacteriophages from swine effluent lagoons. **Journal of Environmental Quality**, Feb 2;35(2):522-8.
2. Reneer, D.V., Kearns, S.A., Yago, T., **Sims, J.**, Cummings, R.D., McEver, R.P., Carlyon, J.A. (2006) Characterization of a sialic acid- and P-selectin glycoprotein ligand-1-independent adhesin activity in the granulocytotropic bacterium Anaplasma phagocytophilum. **Cellular Microbiology,** Dec;8(12):1972-84
3. Clem, A.L., **Sims, J.**, Telang, S., Eaton, J.W., Chesney, J. (2007) Virus detection and identification using random multiplex (RT)-PCR with 3'-locked random primers. **Virology Journal,** Jun 28;4:65.
4. Srinivasan, D., **Sims, J.T.**, Plattner R. (2008) Deregulated Abl Kinases Promote Proliferation, Anchorage-Independent Growth and Survival of Aggressive Breast Cancer Cells. **Oncogene,** 14;27(8):1095-105.
5. **Sims, J.T.**, and R. Plattner. (2009) MTT assays cannot be utilized to study the effects of STI571/Gleevec on the viability of solid tumor cell lines. **Cancer Chemotherapy and Pharmacology,** Aug;64(3):629-33.
6. **Sims, J.T.**, Ganguly, S., Fiore, L., Holler, C., Park, E.S., Plattner, R. (2009) STI571 (Gleevec) sensitizes breast cancer cells to 5-Fluorouracil, Cisplatin, and Camptothecin in a cell type-specific manner**. Biochemical Pharmacology,** Aug 1;78(3):249-60.
7. Zhao, H., Ou-Yang, F., Chen I., Hou, M., Yuan, S.F., Chang, H., Lee, Y., Plattner R., Waltz, S., Ho, S., **Sims, J.**, Wang, S. (2010) Enhanced resistance to tamoxifen by the c-ABL proto-oncogene in breast cancer. **Neoplasia**, Mar;12(3):214-23.
8. Huang, B., Troese, M.J., Ye, S., **Sims, J.T.**, Galloway, N.L., Borjesson, D., Carlyon, J.A. (2010) *Anaplasma phagocytophilum* APH1387 is expressed throughout bacterial intracellular development and localizes to the pathogen-occupied vacuolar membrane. **Infect Immun**, May;78(5):1864-73.
9. Huang, B., Troese, M.J., Howe, D., Ye, S., **Sims, J.T.**, Heinzen,R., Borjesson, D., Carlyon, J.A. (2010) *Anaplasma phagocytophilum* APH_0032 is expressed late during infection and localizes to the pathogen-occupied vacuolar membrane. **Microb Pathog,** Nov;49(5):273-84.
10. Ganguly, S., Fiore L.S., **Sims, J.T.**, Friend, J.W., Srinivasan, D., Cibull, M.L., Wang, C., Novak, M., Kaetzel, D.M., Plattner, R. (2011) c-Abl and Arg are activated in

human primary melanomas, promote melanoma cell invasion via distinct pathways, and drive metastatic progression. **Oncogene**, Sep 5. [Epub ahead of print].
11. **Sims, J.T.**, Friend, J.W., Bennett, H., Tepe, J.T., Plattner, R. (2012) c-Abl/Arg drive doxorubicin resistance by preventing NF-κB-mediated transcriptional repression of anti-apoptotic genes, activating a novel HSP27/p38/Akt survival pathway, and upregulating ABCB1. In Preparation.